



University of Strathclyde

Department of Pure and Applied Chemistry

Application of Bioisosteres to Modulate Molecular Properties in Medicinal Chemistry

Thesis submitted to the University of Strathclyde in fulfilment of the
requirements for the degree of Doctor of Philosophy

Nicholas Measom

2017

Declaration of copyright

This thesis is the result of the author's original research. It has been composed by the author and has not been previously submitted for examination which has led to the award of a degree.

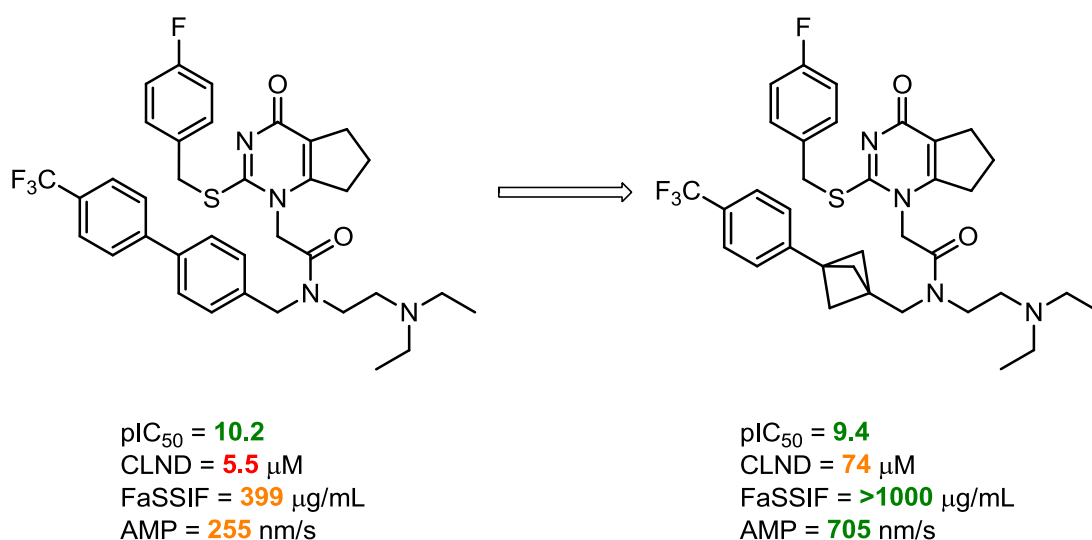
The copyright of this thesis belongs to GSK in accordance with the author's contract of engagement with GSK under the terms of the United Kingdom Copyright Acts. Due acknowledgement must always be made of the use of any material contained in, or derived from, this thesis.

Signed:

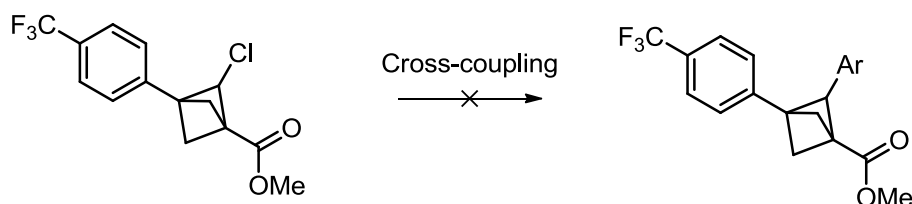
Date:

Abstract

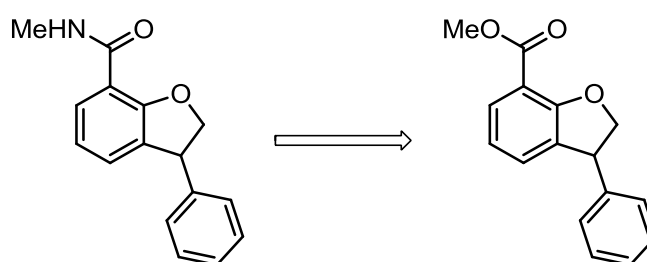
This research describes the use of bioisosteres within two medicinal chemistry programmes. Firstly, a bicyclo[1.1.1]pentane (BCP) was investigated as a phenyl group replacement in an attempt to improve the physicochemical profiles of two Lp-PLA₂ inhibitors. Installation of the BCP unit was accomplished through a challenging 10-step synthesis in reasonable yields. The physicochemical profiles of both inhibitors were enhanced with high potency maintained when one BCP inhibitor was compared to its parent.



With the enhancement in physicochemical profiles the application of the BCP unit to alternative systems was desired. To this end, the synthetic route to the BCP was investigated in order to allow access to a variety of functionality across the BCP moiety. Electron deficient aromatic systems proved to be the most suitable analogues to the route investigated with significant challenges encountered on alternative templates. Additionally, isolation of the mono-chlorinated BCP stimulated interest in potential cross-coupling reactions to generate novel BCP systems. An extensive investigation provided no desired cross-coupled product with ring opening of the BCP providing a considerable challenge.



Bioisosteres were also investigated in the context of BET inhibition. Utilising an ester as a bioisosteric amide group allowed investigation of a soft-drug approach to BET inhibitors. Replacement of a methyl amide with an ester allowed retention of potency at the target with the introduction of a metabolically labile group to facilitate site selective inhibition.



The lability of the ester group was investigated in a human whole blood assay to investigate the half-lives of the compounds, in which it was shown that the ester functionality was unstable. This provided good evidence to support the soft-drug approach in BET inhibition. Further elaboration of the initial hit led to an unforeseen reduction in potency which was rationalised as a conformational bias against the optimum geometry for binding.

Human Biological Samples Statement

The human biological samples were sourced ethically and their research use was in accord with the terms of the informed consents

Permissions to reprint or modify diagrams

In all cases where a diagram has been reprinted or modified from a copyright protected source for use in this thesis the appropriate permission has been obtained. Each figure or table from a copyright protected source is accompanied by the appropriate accreditation text as defined in the legal licence for use. The accreditation text format is different for each copyright holder.

Acknowledgements

I would firstly like to thank my academic supervisor, Dr. Craig Jamieson, from the University of Strathclyde for his support throughout my PhD. Not only has his expertise been invaluable to my studies but his dedication and willingness to provide support and guidance has allowed me to flourish over the course of my PhD, for which I will be eternally grateful. I would also like to acknowledge my internal examiner Dr. Glenn Burley for his critical analysis and review of my work which has allowed me to develop my writing and presentation skills.

I would like to give a special thank you to Dr. David Hirst, my GSK supervisor for the majority of my PhD. His help and support has been invaluable to me. I am extremely grateful for his dedication, patience, and understanding. He has provided me with so much help throughout my PhD and it is very important to me that I convey my deepest gratitude for all his efforts, especially as I probably haven't been the easiest person to deal with at times.

I would also like to thank Dr. Vipulkumar Patel for providing me with the opportunity to work within the Flexible Discovery Unit at GSK. His unique style has allowed me to flourish within the department, in which he has also provided me with many development opportunities both professionally and personally. His support for my personal development is much appreciated.

There are so many people across GSK and the University of Strathclyde that I would like to thank. Everyone has been so helpful and willing to provide me with their time and support. Special mentions go to Peter Campbell for helping me during my placement in Strathclyde; Sean Lynn for his teaching and continued support with NMR assignments; Dr. Eric Manas for his help with molecular modelling and Don Somers for running the X-ray crystallography.

I would like to say thank you to Prof. Harry Kelly and Prof. William Kerr for the opportunity to undertake my PhD under the collaborative GSK/UoS PhD scheme. I am very grateful to Prof. Patrick Vallance for funding such a scheme. The last three years have been incredibly worthwhile.

I would like to thank Thomas Clohessy and Storm Hart for making my PhD an unforgettable experience. I am so glad we have been able to support each other through the good times and the bad.

Finally, I would like to thank my Mum and Dad. Without their unwavering support I would not have been able to get where I am today. I am extremely grateful for everything they have done for me and I hope I have been able to make them proud.

Abbreviations

ABL – Abelson murine leukaemia viral oncogene homolog

ACAT – Acyl-coenzyme A acyl transferase

ACHN – Azobis(cyclohexanecarbonitrile)

ACS – Acute coronary syndrome

AD – Alzheimer's disease

AIBN – Azobisisobutyronitrile

AMP – Artificial membrane permeability

BBB – Blood-brain barrier

BCP – Bicyclo[1.1.1]pentane

BET – Bromodomain and extra-terminal domain

Brd – Bromodomain

CAD – Coronary artery disease

Caco-2 – Colonic adenocarcinoma 2

CCK – Cholecystokinin

CHD – Coronary heart disease

CLND – Chemiluminescent nitrogen detection

CNS – Central nervous system

COE – Cyclooctene

CVD – Cardiovascular disease

DavePhos – 2-Dicyclohexylphosphino-2'-(*N,N*-dimethylamino)biphenyl

dba – Dibenzylideneacetone

DEG – Diethylene glycol

DIBAL-H – Diisobutylaluminium hydride

Diglyme – Diethylene glycol dimethyl ether

DIPEA - *N,N*-diisopropylethylamine

DMF – *N,N*-dimethylformamide

DMPK – Drug metabolism and pharmacokinetics

DMSO – Dimethylsulfoxide

DNA – Deoxyribonucleic acid

dppf – 1,1'-Ferrocenediyl-bis(diphenylphosphine)

EF/WM – Executive function/working memory

EHT – Extended Hückel theory

F% – Bioavailability

FaSSIF – Fasted stated simulated intestinal fluid

FDA – Food and drug administration

FGI – Functional group interconversion

GBVI – Generalised Born/volume integral implicit

GI – Gastrointestinal

GSK3 – Glycogen synthase kinase 3

HBA – H-bond acceptor

HBD – H-bond donor

HCV – Hepatitis C virus

HE – Hantzsch ester

HFIP – 1,1,1,3,3,3-Hexafluoroisopropanol

HHEP – Human hepatocytes

HIV – Human immunodeficiency virus

HLM – Human liver microsomes

HRMS – High resolution mass spectrometry

HSA – Human serum albumin

HTS – High throughput screening

IgG – Immunoglobulin G

IL-8 – Interleukin 8

INF- γ – Interferon γ

JohnPhos – (2-Biphenyl)di-*tert*-butylphosphine

KIE – Kinetic isotope effect

LCMS – Liquid Chromatography mass spectrometry

LE – Ligand efficiency

Lp-PLA₂ – Lipoprotein-associated phospholipase A2

LPC – Lysophosphatidylcholine

LPS – Lipopolysaccharide

MCP-1 – Monocyte chemoattractant protein 1

mCPBA – *meta*-Chloroperbenzoic acid

M-CSF – Macrophage colony-stimulating factor

MDAP – Mass directed automated purification

mGluR – Metabotropic glutamate receptor

MI – Myocardial infarction

MLM – Mouse liver microsomes

MOE – Molecular operating environment

MW – Molecular weight

NF- κ B – Nuclear factor kappa B

NMR – Nuclear magnetic resonance

NS5B – Non-structural 5B

PAH – Pulmonary arterial hypertension

PAF – Platelet activating factor

PAF-AH – Platelet-activating factor acetylhydrolase

PBS – Phosphate-buffered saline

PC – Phosphatidylcholine

PCE – Perchloroethylene

PFI – Property forecast index

PLA₂ – Phospholipase A₂

PSA – Polar surface area

PTM – Post-translational modifications

RNA – Ribonucleic acid

RuPhos – 2-Dicyclohexylphosphino-2',6'-diisopropoxybiphenyl

SAHA – Suberanolhydroxamic acid

STAB – Sodium triacetoxyborohydride

T3P[®] - Propyl phosphonic anhydride solution

TBD – 1,5,7-triazabicyclo[4.4.0]dec-5-ene

TBME – *tert*-Butyl methyl ether

TFA – Trifluoroacetic acid

TFE – 2,2,2-Trifluoroethanol

Th17 – T-helper cell 17

THF – Tetrahydrofuran

TLC – Thin layer chromatography

TMS – Tetramethylsilane

TTMSS – Tris(trimethylsilyl)silane

UV – Ultraviolet

VCAM-1 – Vascular cell adhesion molecule 1

XantPhos – 4,5-Bis(diphenylphosphino)-9,9-dimethylxanthene

XPhos – 2-Dicyclohexylphosphino-2',4',6'-triisopropylbiphenyl

Contents

1.0 Targeting atherosclerosis	1
1.1 Atherosclerosis.....	2
1.2 Lp-PLA ₂	3
1.3 Lp-PLA ₂ inhibitors.....	7
1.4 Darapladib and rilapladib properties.....	9
1.5 Physicochemical properties and attrition.....	11
2.0 Bioisosterism	18
2.1 Early work.....	19
2.2 Bioisosteres.....	20
2.3 Deuterium as an isostere for hydrogen.....	21
2.4 Fluorine as an isostere for hydrogen.....	23
2.5 Bioisosteres for carbon and alkyl moieties.....	26
2.6 Carbonyl mimetics.....	30
2.7 Carboxylic acids.....	36
2.8 Heterocycles.....	41
2.9 Phenyl group mimetics.....	46
2.10 Bicyclo[1.1.1]pentane (BCP).....	50
2.11 Synthesis of BCP.....	55
2.12 Aims: application of the BCP to Lp-PLA ₂ inhibitors.....	61
3.0 Results and discussion	66

3.1 Synthesis of BCP analogues of Lp-PLA ₂ inhibitors.....	67
3.2 Comparison of BCP analogues to progenitor compounds.....	85
3.3 Substrate scope.....	88
3.4 Cross coupling.....	107
3.5 Conclusion.....	118
4.0 Bioisosteres in modulating stability.....	120
4.1 Soft-drugs.....	121
4.2 Bromodomain (Brd) and extra-terminal domain (BET) proteins.....	127
4.3 Aims.....	134
5.0 Bioisosteres as acetyl-lysine mimetics.....	135
5.1 Application to BET inhibitors.....	136
5.2 Conclusion.....	165
6.0 General Experimental.....	168
7.0 Experimental.....	172
7.1 Lp-PLA ₂ experimental.....	173
7.2 BET experimental.....	220
8.0 Assay protocols.....	269
9.0 References.....	273
10.0 Appendix.....	286

1.0 Targeting atherosclerosis

1.1 Atherosclerosis

Atherosclerosis is the build-up of waxy plaque on the inner arteries and has been implicated in myocardial infarction (MI) and stroke.¹ The process of atherogenesis involves a complex interplay between the bloodstream and arterial wall components.² This was originally thought to be caused by bland lipid storage in the arterial wall, however, more recently it was discovered that this lipid build up goes hand-in-hand with an inflammatory response.² In normal endothelial tissue white blood cells do not bind.² However, after build up of lipids within the arterial wall the endothelial cells start to express adhesion molecules such as vascular cell adhesion molecule-1 (VCAM-1).² VCAM-1 is able to bind white blood cells and recruit them to the arterial wall at sites of lipid build up (Figure 1A).² Monocytes and T-cells can then be transferred across the endothelium by a variety of chemoattractant proteins specific to each cell type, such as monocyte chemoattractant protein-1 (MCP-1).^{2,3} Once these blood-derived inflammatory cells reside within the arterial wall they participate and propagate a local inflammatory response. These cells release free radicals and inflammatory cytokines such as interferon- γ (INF- γ) and lymphotoxin. This creates localised oxidative stress in which free radicals oxidise lipids, the products of which increase vascular inflammation (Figure 1B).¹ As the inflammatory response continues, macrophages can accumulate and, in the presence of a macrophage colony-stimulating factor (M-CSF), can cause the blood monocytes to differentiate into foam cells. This leads to lesions and fatty streaks on the arterial walls called atheroma. The macrophages within the atheroma produce proteolytic enzymes which degrade the fibrous collagen cap of the arterial wall.² The reduction in cap size and strength leaves these plaques susceptible to rupturing. Disruption of the atherosclerotic plaques can lead to blockage of vital blood vessels, acute MI or stroke (Figure 1C).¹ The enzyme lipoprotein-associated phospholipase A₂ (Lp-PLA₂), also known as platelet-activating factor acetylhydrolase (PAF-AH), has been extensively studied as a potential therapeutic target for the treatment of atherosclerosis.¹

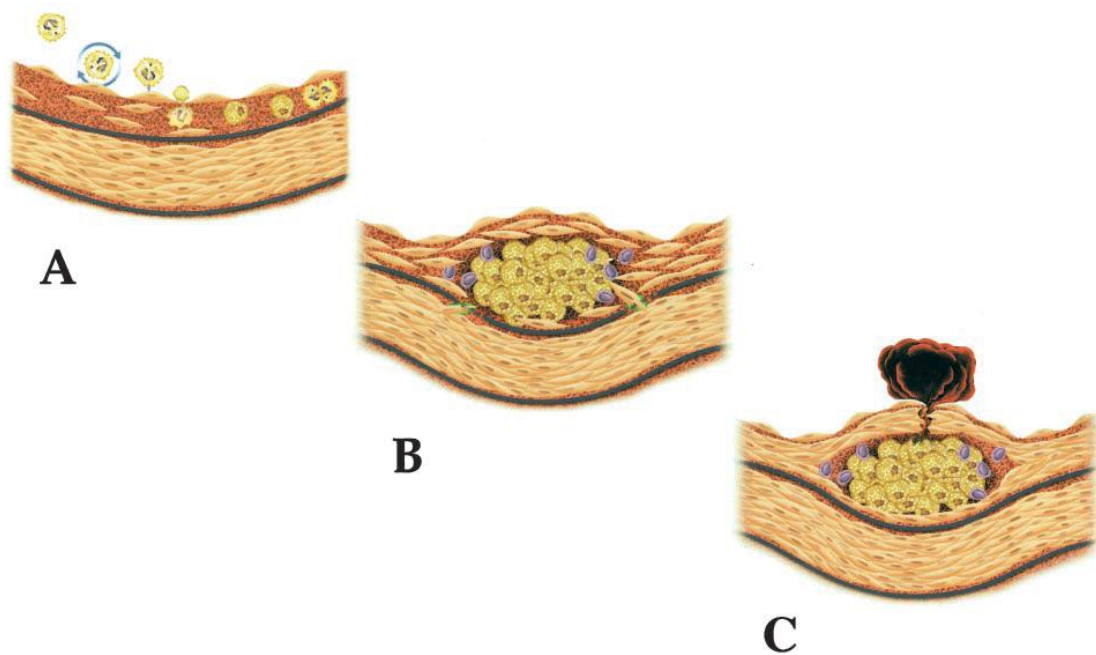


Figure 1 - Atherosclerotic plaque build up² Figure reproduced from *Inflammation and Atherosclerosis*, Libby P., Ridker P. M., Maseri A., *Circulation*, 2002, 105, 1135-1143 with permission from Wolters Kluwer Health Inc

1.2 Lp-PLA₂

Lp-PLA₂ is a member of the PLA₂ super-family of which there are fifteen separate groups and several sub-groups.⁴ The PLA₂ family are assigned to groups based upon their sequence, molecular weight, disulfide bonding pattern, requirement for Ca²⁺ and other features.^{1,4} As such, Lp-PLA₂ is classified by its sequence, size, calcium independence and substrate specificity as a member of the VIIA PLA₂ or PLA₂G7 group.^{4,5} The crystal structure of the isolated Lp-PLA₂ enzyme has been solved to confirm the presence of an α/β hydrolase fold consistent with neutral lipases and esterases, with a classic serine/histidine/aspartate catalytic triad (Figure 2), using diethyl 4-nitrophenyl phosphate (paraoxon) as a covalent ligand.⁶ The crystal structure, which was solved to 1.5 Å resolution, shows that the active site is open and lacks a lid region (Figure 3).⁶ This open conformation may account for the ability of the enzyme to hydrolyse a range of phospholipids with different *sn*-2 (hydroxyl of second carbon in glycerol) acyl chains. The substrates available to the enzyme include short- and medium-length *sn*-2 fatty acyl chains, however this chain length restriction is relaxed if the *sn*-2 acyl chain contains polar functionality.^{7,8} This might be accounted for by the polar chain extending out into solvent rather than into the

hydrophobic pocket of the enzyme due to the open conformation of the active site.

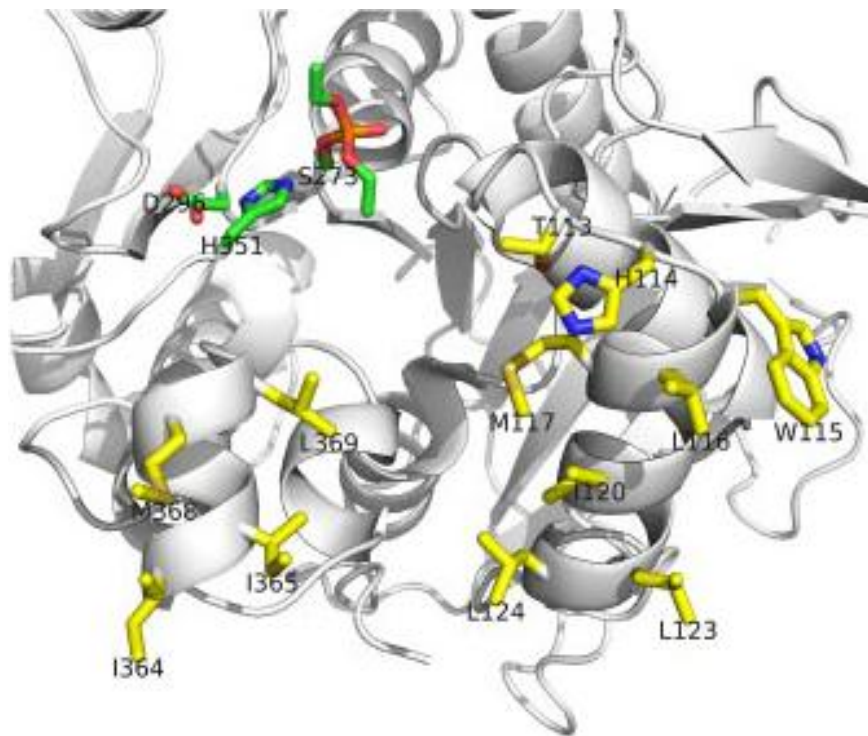


Figure 2 - Lp-PLA₂ crystal structure with covalently bound paraoxon in the active site⁶

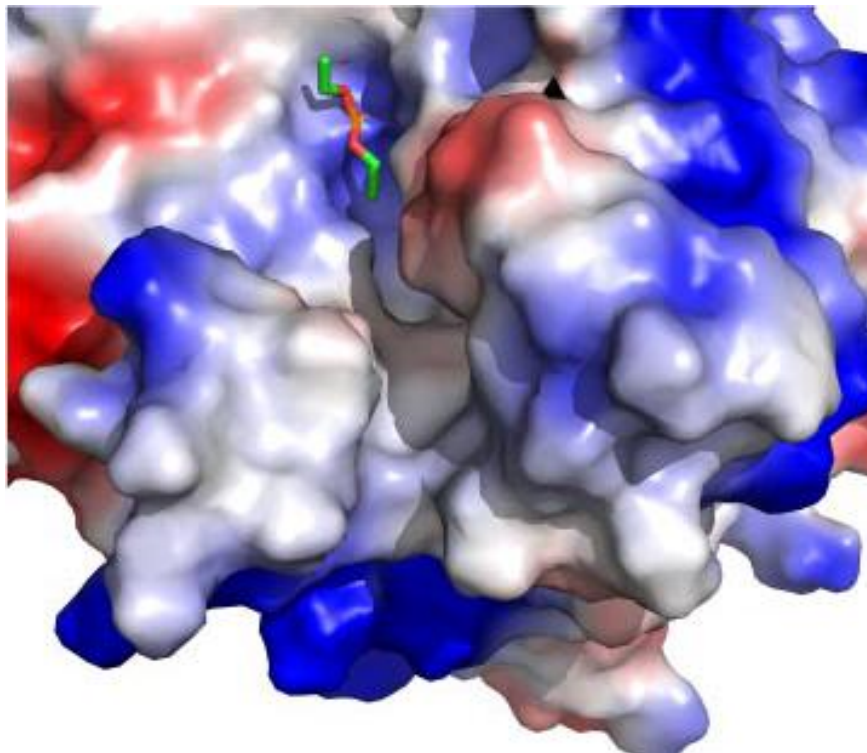
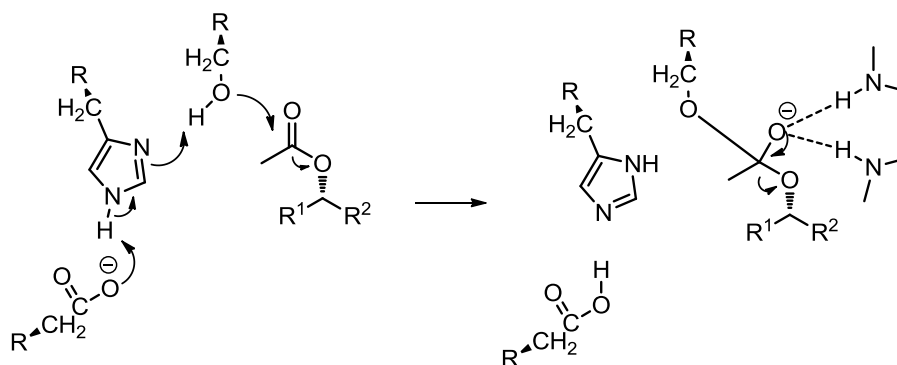


Figure 3 - Lp-PLA₂ crystal structure showing surface of active site with covalently bound paraoxon⁶



Scheme 1 - Enzyme activity: catalytic triad

The catalytic activity of Lp-PLA₂ is primarily driven by 3 key residues; Ser273, His351 and Asp296 collectively known as the catalytic triad (Scheme 1). The serine residue attacks the bound phospholipid with two backbone amide residues, which form what is known as the oxyanion hole, stabilising the tetrahedral intermediate *via* hydrogen bonding. The nucleophilicity of the serine residue is increased by the “proton shuttle” that exists between the histidine and aspartate residues.

Lp-PLA₂, produced primarily by macrophages,⁹ hydrolyses platelet-activating factor (PAF) (Figure 4) and glycerophospholipids with short, truncated or oxidised fatty acyl groups at the *sn*-2 position of glycerol.^{4,5,10-12} It circulates through the bloodstream in the active form as a complex with low and high density lipoproteins.¹³

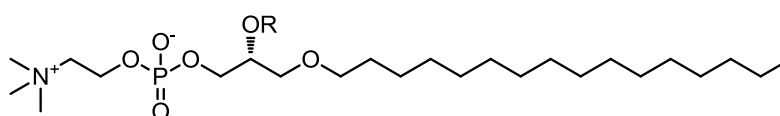


Figure 4 – R = Ac Platelet activating factor (PAF) 1.2.1, R = H LPC 1.2.2

Hydrolysis of PAF and other similar substrates by Lp-PLA₂ generates pro-inflammatory mediators such as lysophosphatidylcholine (LPC) and oxidised non-esterified fatty acids. LPC can induce apoptosis but also impairs dead cell removal and thus leads to necrosis.^{1,14}

Extensive epidemiological and genetic studies have been conducted to elucidate the role of Lp-PLA₂ and its association with atherosclerosis.^{1,15} A comprehensive epidemiological study, of 79,036 participants across 32 different studies, in healthy patients suggested that the activity levels of Lp-PLA₂ are not a useful predictor of

future coronary heart disease (CHD).¹⁶ Further studies investigating Lp-PLA₂ activity combined with levels of oxidised phospholipids indicated only a weak potentiation of the risk of cardiovascular events.^{17,18} Additionally, in patients suffering from acute coronary syndrome, no discernible correlation between Lp-PLA₂ activity and future ischemic events was observed.¹⁹ However, in patients with stable cardiovascular disease (CVD) a correlation was observed. Several studies indicated that increased Lp-PLA₂ mass predicts future cardiovascular events.^{20–23} However, Lp-PLA₂ is carried in the bloodstream with lipoproteins and these are themselves common risk factors for future cardiovascular events. A comprehensive study of over 35,000 patients demonstrated that an increase in Lp-PLA₂ activity or concentration correlated to the increased risk of CHD or ischemic stroke with the models adjusted for the common risk factors including lipoproteins.¹⁶ A summary of the epidemiological evidence suggests that increased Lp-PLA₂ concentration increases the risk of MI, ischemic stroke and cardiac death in patients with stable CVD, therefore making the target of therapeutic interest in this patient cohort.¹

Genetic studies have also elucidated an association between Lp-PLA₂ and CHD. A missense mutation (G>T) at position 994 in the PLA2G7 gene produces a substitution of a valine for a phenylalanine (Val279Phe) near the active site of the enzyme.²⁴ Homozygous carriers of this variant display no Lp-PLA₂ activity and heterozygous carriers display 50% activity compared with the wild type allele.^{24,25} Studies, predominantly in Asian individuals, demonstrated that the Val279Phe allele shows an increased risk for atherosclerosis, coronary artery disease (CAD), stroke and MI.^{26–30} As this mutation occurs between the active site residues Ser273 and Asp296, it is postulated that this effects the protein folding in a way that disrupts the active site conformation thereby removing activity. However, there are two studies within Korean individuals that suggest that the Val279Phe mutation lowers the risk of CVD.^{31,32} Despite conflicting reports, the considerable evidence linking Lp-PLA₂ with CVD has led to continued interest in this enzyme as a therapeutic target.¹

1.3 Lp-PLA₂ inhibitors

Despite the somewhat contradictory evidence associating Lp-PLA₂ to atherosclerosis, the high unmet medical need has led to the development of a range of potential therapeutic agents that inhibit Lp-PLA₂. Darapladib^{33,34} and rilapladib are examples of such compounds (Figure 5).

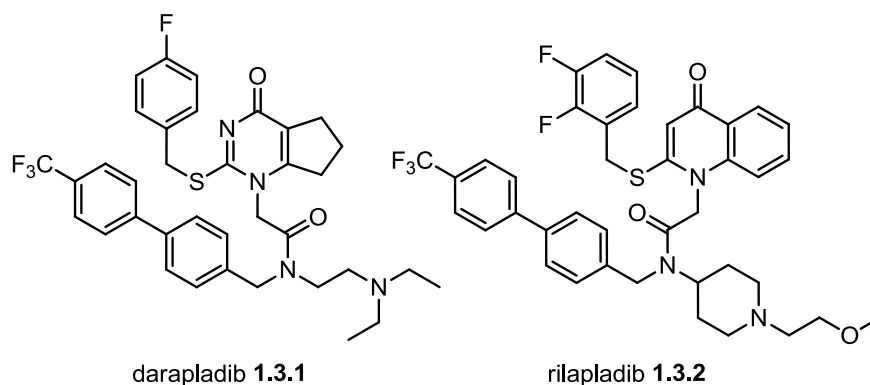


Figure 5 - Darapladib and rilapladib

Darapladib is the most extensively studied Lp-PLA₂ inhibitor and was progressed into phase III clinical trials. *In vivo* studies have repeatedly shown darapladib inhibits hydrolysis of Lp-PLA₂ substrates, such as PAF and others,³⁴ in rats, dogs, rabbits and pigs.³⁴ Pre-clinical studies in hypercholesterolemic pigs demonstrated a reduction in lesions, necrotic core area, and medial destruction upon treatment with darapladib. It also induced down regulation of inflammatory gene expression as well as a reduction in the pro-inflammatory cytokine MCP-1, which in turn led to a reduction in plaque macrophage content.³⁵ Other observed *in vivo* effects of darapladib include reduced content of lyso-PCs within atherosclerotic lesions;³⁶ however, no reduction of truncated oxidised PC species, which are known substrates of Lp-PLA₂ has been observed.³⁶ In a phase II study of patients with stable CHD, darapladib led to sustained inhibition of Lp-PLA₂ over 12 week treatment.³⁷ It resulted in an average of 59% reduction in Lp-PLA₂ activity and stopped the expansion of the plaque's necrotic core.³⁵ Additionally, across all phase II studies no major safety concerns were highlighted with only minor side effects of diarrhoea and malodour noted.^{37,38}

These *in vitro* and *in vivo* data supported progression of darapladib into two phase III trials for both stable and unstable coronary disease, the first of which was completed in 2014. The two and a half year investigation involved 13,026 patients in a double

blind study, the objective of which was to evaluate darapladib's efficacy and safety in patients after an acute coronary syndrome (ACS) event.³⁹ This investigation concluded that there was no significant reduction in the risk of major coronary events and therefore unfortunately this study did not reach its primary end point. It was also noted that patients within the darapladib test group reported an odour-related concern as well as an increase in reports of diarrhoea compared to the placebo.³⁹ A recent press release relating to darapladib's second phase III trial in over 30,000 patients indicated no significant reduction in adverse cardiovascular events compared to placebo.⁴⁰

The structurally related compound rilapladib has also been developed as an Lp-PLA₂ inhibitor, however, in this case it has been examined in the context of Alzheimer's disease (AD).⁴¹ Darapladib had previously been shown in a diabetic mellitus and hypocholesterolaemic pig model to reduce the extent of immunoglobulin G (IgG) brain parenchyma penetration.⁴² This indicated a reduction in blood-brain barrier (BBB) leakage and also lowered the amount of brain amyloid β peptide deposition. Both of these indicators suggest that it is possible to reduce the production of pro-inflammatory mediators at the BBB. This should result in reduced levels of neuroinflammation and central nervous system (CNS) amyloid β concentrations, leading to reduction in plaques responsible for the onset of AD. A 24 week study was therefore conducted to evaluate rilapladib in this context.⁴¹ The study concluded that rilapladib was well tolerated in terms of its safety and that there was a significant difference in executive function/working memory (EF/WM) between placebo and rilapladib.⁴¹

1.4 Darapladib and rilapladib properties

Unsurprisingly, comparison of the available X-ray data indicates darapladib and rilapladib bind to Lp-PLA₂ in similar manner, with the exocyclic carbonyl mimicking the ester functionality of the enzyme's natural substrates e.g. PAF (Figure 6).

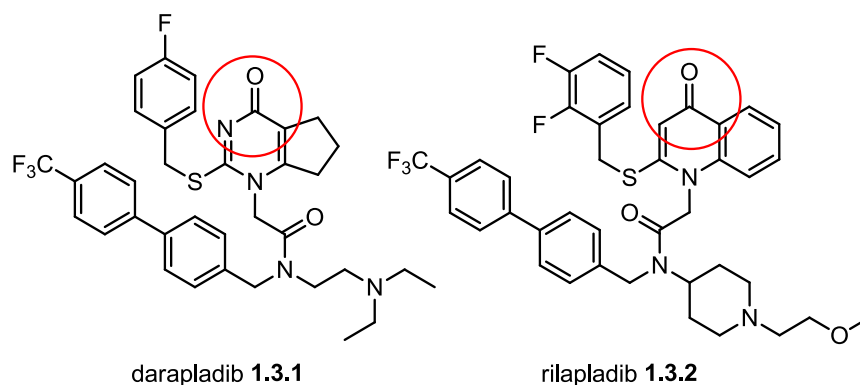


Figure 6 - Key binding motif highlighted on darapladib and rilapladib

This blocks the active site in the region in which the Ser273, His351 and Asp296 form the catalytic triad and the backbone amide NHs of a Leu153 and Phe274 help to bind the substrate. The remaining functionality occupies hydrophobic pockets adjacent to the active site made up of a variety of Leu, Phe and Trp residues.⁴³ This is confirmed by the X-ray crystal structure of darapladib bound within the active site of the Lp-PLA₂ enzyme (Figure 7).⁴³

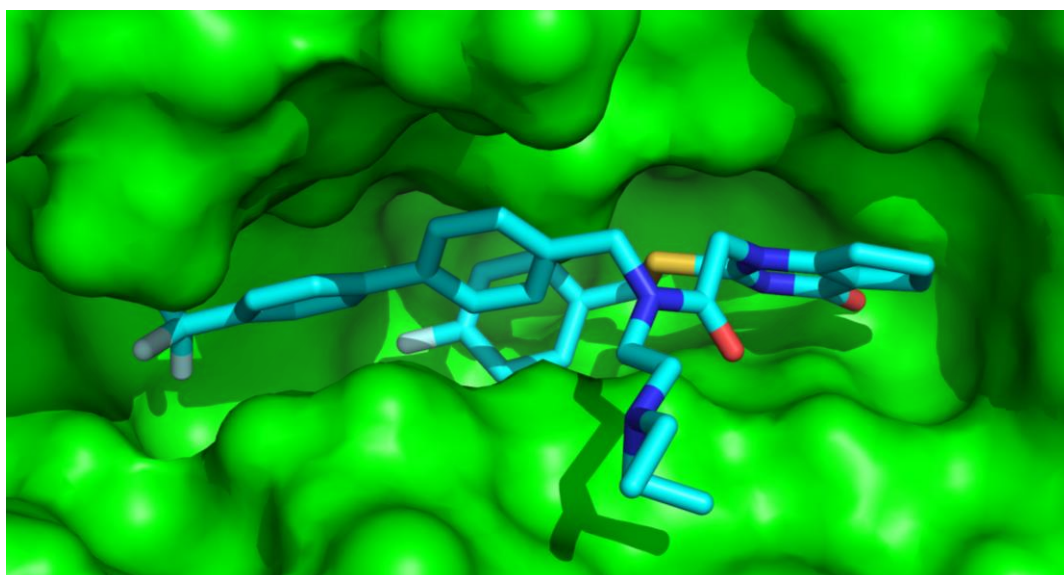


Figure 7 - X-ray crystal structure of darapladib bound to Lp-PLA₂

Darapladib shows excellent potency against Lp-PLA₂ in *in vitro* assays with a pIC₅₀ of 10.2.³⁴ It has good artificial membrane permeability (AMP) of 255 nm/s, probably as a result of its highly lipophilic nature and its basic centre. Its kinetic solubility (CLND) is poor; however it displays modest thermodynamic solubility (FaSSIF) (Table 1). Similarly rilapladib displays excellent Lp-PLA₂ potency with a pIC₅₀ of 9.6.

Table 1 - Summary of darapladib and rilapladib data

	Darapladib	Rilapladib
pIC₅₀	10.2	9.6 ⁴⁴
CLND (μM)	5.5	<1
FaSSIF (μg/mL)	183, 399 [#]	203
ChromLog D_{7.4}	6.6	6.74
AMP (nm/s)	255	160
Molecular weight	666.77	735.81
PFI	10.6	11.74

[#]Two batches tested

Despite their high potency, both inhibitors exhibit sub-optimal physicochemical profiles. They have high molecular weights, low aqueous solubility and high property forecast indices (PFI).⁴⁵ This leaves both molecules in an undesirable physicochemical space that is frequently associated with increased risk of attrition (*vide infra*).

Therefore, there remains an unmet need to identify analogues of these potent Lp-PLA₂ inhibitors with improved physicochemical properties, which is the focus of this chapter. The specific parameters of interest to the current study are detailed in the following section.

1.5 Physicochemical properties and attrition

Physicochemical properties, such as solubility and permeability, are key parameters when investigating drug molecules.^{46,47} Not only does a drug require potency at the target of interest, it must cross a number of environments to reach that target. For a drug that is orally dosed, these include the gut, in which the pH varies between 1.2 and 8; digestive enzymes which metabolise xenobiotics; and the small intestine wall through which the drug must permeate.⁴⁸ Once in the blood stream it then has to resist further metabolism in the liver and finally reach the target of interest to cause a biological effect.⁴⁸

Medicinal chemists must therefore consider numerous parameters beyond simple potency when designing a potential drug molecule. Firstly, a compound of interest has to be soluble. Aqueous solubility is important because this can affect absorption within the gastrointestinal (GI) tract. An undissolved compound is unlikely to permeate and therefore will pass through the GI tract and be excreted, leading to poor bioavailability. Furthermore, a molecule must be sufficiently permeable to permeate across the intestinal wall *via* diffusion or be actively carried across the membrane by active transporters. Additionally, permeability is important when access to intracellular targets is required. Upon absorption, the compound must survive liver metabolism to be able to reach its site of action intact.

In order to predict the ability of a molecule to reach its site of action *in vivo*, medicinal chemists use a range of measures. In the early discovery phase, solubility can be measured using a high throughput chemiluminescent nitrogen detection (CLND) method. This is measured from stock dimethylsulfoxide (DMSO) solutions and gives a kinetic measure of solubility.

More advanced molecules can be tested in FaSSIF to investigate thermodynamic solubility. This utilises a buffer containing sodium taurocholate, lecithin, maleic acid, and sodium chloride aiming to mimic intestinal fluid to give a more accurate representation of the biological system.

Partitioning a compound between solutions of *n*-octanol and water will provide an insight into the lipophilicity of a compound, and allows us to calculate a distribution

coefficient (log D). Log D can be utilised to investigate the distribution of compound at a certain pH. The pH of human blood is approximately 7.4 so this tends to be used to predict solubility within this environment. However, it is also useful to examine more extreme pHs to assess the relative lipophilicity in different compartments; gastric fluid for example has a pH of approximately 2. Octanol/water distribution coefficients are time consuming to measure, therefore a high throughput chromatographic method known as ChromLog D_{7.4} has been developed.⁴⁵

Additional parameters examined include permeability, which can be correlated to absorption. This can be predicted by examining the passive diffusion of compound across an artificial phospholipid membrane.

Metabolic stability is also important to ensure the compound can survive for a reasonable period within the body without degradation to inactive or toxic by-products. This can be estimated using an *in vitro* human liver microsomal assay, involving the metabolism of compound with a variety of enzymes present in the liver and measuring the concentration of parent drug after a period of time.

These parameters in combination make up the physicochemical profile of a drug molecule. These data can be used to make predictions about the potential issues associated with drug metabolism and pharmacokinetics (DMPK) moving forward. In addition to measured properties, a range of computationally derived factors are also of interest, particularly at the compound design stage.

A seminal paper by Lipinski *et al.* investigated the properties of over 2,000 compounds, from the World Drug Index, in order to ascertain a general profile of oral drug-likeness.⁴⁹ This investigation looked at a range of properties including: calculated log P (clog P), molecular weight (MW), and number of H-bond donors/acceptors.⁴⁹ From this analysis, Lipinski observed that approximately 90% of the compounds in this set lay within a specific range for each parameter:⁴⁹

- 1) ≤ 5 H-bond donors (HBD)
- 2) ≤ 10 H-bond acceptors (HBA)
- 3) ≤ 500 MW
- 4) ≤ 5 clog P

These guidelines are collectively known as the “rule of 5” and are now commonly used throughout the medicinal chemistry community as predictors of oral exposure; molecules which obey these rules have a greater chance of exhibiting a good pharmacokinetic profile, and thus being successful in the clinic.^{48,49}

A similar analysis has been conducted by Veber and co-workers.^{48,50} This investigation considered 1,100 drug candidates at GlaxoSmithKline and showed that oral bioavailability in rat was related to both the number of rotatable bonds within a molecule and the total polar surface area (PSA), such that good bioavailability can be achieved if:^{48,50,51}

5) ≤ 13 rotatable bonds

6) $\leq 140 \text{ \AA}^2$ PSA

Additionally, Bhal *et al.* examined log P as a descriptor versus log D.⁵² This analysis provided evidence to suggest that log D was a better measure since it takes into account the distribution of the ionised and un-ionised states of the compound at biologically relevant pHs.⁵²

Since Lipinski’s seminal work, pharmaceutical companies have developed their own rules to guide medicinal chemists in the design of molecules in good oral “drug-like” physicochemical space. Pfizer has developed both the 3/75 rule and also the golden triangle.^{53,54} The 3/75 rule was derived from an investigation of 245 compounds in which it was discovered that compounds with a log P greater than 3 and a topological PSA less than 75 \AA^2 were 2.5 times more likely to be toxic.⁵⁴ Eli Lilly reported a similar trend with log P in a study of over 400 compounds, however, found no correlation between topographical PSA and toxicology.⁵⁵ Leeson *et al.* have also noted similar trends in an examination of over 2,000 compounds.⁴⁷ These data suggest that the more lipophilic a compound the more likely it is to exhibit toxicological side effects.

The golden triangle was also developed as a visualisation technique to aid medicinal chemists in achieving metabolically stable, permeable drug molecules.⁵³ This technique utilises a plot of MW versus log D with a baseline from log D -2 to 5 at a MW of 200 with an apex at log D approximately 1.5 at a MW of 450 .⁵³ With a

“golden triangle” superimposed which has an apex at Log D equal to 1.5 and MW of 450. Compounds whose MW and Log D fall within this triangle, have a greater chance of having suitable permeability and clearance profiles (Figure 8).⁵³

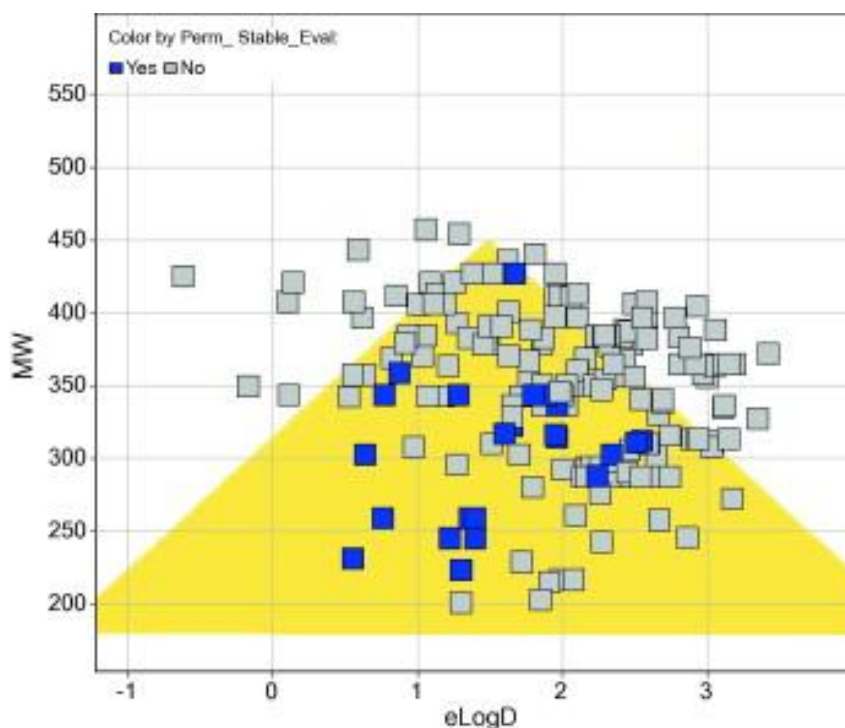


Figure 8 - Pfizer golden triangle Reprinted from *Using the Golden Triangle to optimize clearance and oral absorption*, Johnson T. W., Dress K. R., Edwards M., *Bioorg. Med. Chem. Lett.*, 2009, 19, 5560-5564, Copyright 2009 with permission from Elsevier

It is noteworthy that some compounds within the desired region can fail in the clearance or permeability assays.⁵³ Explanations for this include metabolic soft spots within the molecule having an impact on clearance or some Lipinski rules being broken; such as the number of HBDS/HBAs leading to non-permeable compounds.⁵³

Within our laboratories, we have also developed a numerical visualisation to predict developability of compounds. This PFI is calculated as ChromLog $D_{7.4}$ plus the number of aromatic rings.⁴⁵ Significant analysis has been undertaken by Young *et al.* and the data indicate that to maximise the chance of identifying a soluble, metabolically stable and permeable compound requires a compromise, with permeability and solubility inherently working against each other (Table 2).⁴⁵ It is also noteworthy that increased lipophilicity can impact promiscuity, with undesired off-target interactions with cytochrome P450 enzymes potentially leading to toxic effects.⁴⁵

Table 2 - Percentages of compounds achieving defined target values in the various developability assays categorised by PFI or iPFI⁴⁵ Reprinted from *Getting physical in drug discovery II: the impact of chromatographic hydrophobicity measurements and aromaticity*, Young R. J., Green D. V. S., Luscombe C. N., Hill A. P., *Drug Discov. Today*, 2011, 16, 822-830, Copyright 2011 with permission from Elsevier

Assay / target value	PFI = mChrom log D _{pH7.4} + #Ar								
	<3	3-4	4-5	5-6	6-7	7-8	8-9	9-10	>10
Solubility >200 μM	89	83	72	58	33	13	5	3	2
%HSA <95%	88	80	74	64	50	30	17	8	4
2C9 pIC₅₀ <5	97	90	83	68	48	32	23	22	38
2C19 pIC₅₀ <5	97	95	91	82	67	52	42	42	56
3A4 pIC₅₀ <5	92	83	80	75	67	60	58	61	66
Cl_{int} <3 ml/min/kg	79	76	68	61	54	42	41	39	52
Papp >200 nm/s	20	30	46	65	74	77	65	50	33
	iPFI = mChrom log P + #Ar								
hERG pIC₅₀ <5 (+1 charge)	86	93	88	70	54	36	29	21	11
Promiscuity <5 hits with pIC ₅₀ >5	85	78	74	65	49	30	20	13	7

HSA = Human serum albumin

The PFI measure also demonstrates the utility of controlling the number of aromatic rings in a molecule. This is a concept that has gained traction in recent years following on from the influential paper by Lovering *et al.* discussing “escaping from flatland”.⁵⁶ This investigation looked at the fraction of sp³ carbons as a measure of chemical saturation, which was then related to successful compound progression through the drug discovery process.⁵⁶ This analysis found that compounds were more likely to reach the latter stages of drug development if they contained more sp³ character.⁵⁶ Additionally, they noted a similar correlation between the number of chiral centres in a molecule and progression.⁵⁶ Increased saturation not only provides access to more chemical space but increases solubility and an improved selectivity profile.⁵⁶

Significant analysis of drug attrition has been conducted over the years and used to develop these concepts. Analyses of “drug-like” molecules reported before 1983 and 1983-2002 revealed a trend.⁵¹ It was clear that compounds made in the latter period had a tendency to fall outside the guidelines proposed by Lipinski and others.⁵¹ Since this study, the trend has continued; an analysis by Tyrchan *et al.* carried out on bioactive molecules disclosed between 2003 and 2007, showed an average increase in clog P from 2.7 to 4.1 and an increase in mean MW of 92.⁵⁷ This comprehensive

study also demonstrated that as compounds are progressed from the bioactive hit stage to clinical candidate and ultimately to drug molecule, the average physicochemical properties improve (Table 3).⁵⁷

Table 3 - Average properties of marketed drugs, clinical candidates and bioactive hit compounds⁵⁷
Reprinted from Physicochemical property profiles of marketed drugs, clinical candidates and bioactive compounds, Tyrchan C., Blomberg N., Engkvist O., Kogej T., Muresan S., Bioorg. Med. Chem. Lett., 2009, 19, 6943-6947, Copyright 2009 with permission from Elsevier

Property	Mean	Median
Marketed drugs (n = 976)		
cLog P	2.74	2.83
MW	335.5	318.5
PSA	64.7	59.1
Rotatable bonds	5.6	5
HBD	1.5	1
HBA	3.9	4
Clinical candidates (n = 6607)		
cLog P	3.39	3.47
MW	415.1	402.5
PSA	86.7	77.7
Rotatable bonds	7.5	7
HBD	1.9	2
HBA	5.3	5
Bioactive compounds (n = 1,184,611)		
cLog P	4.04	4.09
MW	455.0	450.5
PSA	87.5	81.5
Rotatable bonds	8.2	8
HBD	1.9	2
HBA	5.4	5

Potential explanations for this discrepancy between hit/lead compounds and marketed drugs include:⁵⁸

- 1) The biological targets studied are less tractable

- 2) Search for novelty through synthesising larger compounds
- 3) High throughput screening (HTS) generates more lipophilic starting points
- 4) Use of parallel or combinatorial synthetic chemistry leading to higher MW compounds
- 5) Organisational culture and strategy

A more recent study on drug attrition rates published in 2015 demonstrates that the discovery chemistry culture is changing. Termination of compounds due to sub-optimal pharmacokinetics was reduced by approximately 9% in the period 2006-2010 compared to 2000-2005.⁵⁹ This is possibly due to the pioneering work by Lipinski, Young, Leeson, Lovering, and others discussed previously. These have influenced organisational shifts towards improving the overall profile of molecules rather than focusing on potency at all costs.

With physicochemical properties being key to a drug candidate's success, methods of improving these important parameters are of considerable interest. Bioisosteres are one such method in which functional groups can be exchanged for similar functionality to enhance particular properties, and this concept is further explored in the subsequent section.

2.0 Bioisosterism

2.1 Early work

Isosterism is a concept that has been around for approximately 100 years, with the idea being formulated in 1919 by Langmuir.⁶⁰ He suggested that compounds having the same number of atoms and the same total number of electrons may arrange themselves in the same manner and can be classed as isosteric.⁶⁰ These compounds should therefore show similarities in physical properties.⁶⁰ This concept was further developed by Erlenmeyer in the 1930s. Erlenmeyer *et al.* investigated the difference between O, NH and CH₂ groups as well as phenyl versus thienyl. He demonstrated that antibodies were unable to distinguish between these functional groups in artificial antigens.^{61–63} It was not until 1950 that the term bioisosterism was coined. Friedman defined bioisosterism as compounds that exhibit similar biological effects but with different isomeric structures.⁶⁴ This idea therefore depends more on the context in which these isosteres are applied and less on their underlying physical properties, which is an extension of Langmuir's original definition, although the two are clearly connected. Bioisosterism therefore is separate but related to isosterism. More recently Burger proposed a broader definition of bioisosteres as: "Compounds or groups that possess near-equal molecular shapes and volumes, approximately the same distribution of electrons, and which exhibit similar physical properties."⁶⁵

With bioisosterism focusing on the biological activity of compounds, the design space of such groups can be wide. Different structural changes between bioisosteres can have a marked effect on size, shape, electronic distribution, polarisability, dipole, polarity, lipophilicity and pK_a.⁶³ All of these nuances have the potential to provide a beneficial or detrimental impact upon the biological activity of a compound. However, bioisoteric replacements have the potential to modify a variety of physicochemical parameters utilised in a medicinal chemistry setting. Bioisosteres are now key tools for a medicinal chemist, enhancing their ability to not only modify potency but also key parameters such as selectivity, metabolic stability, toxicity, physicochemical profile, and also intellectual property. The medicinal chemistry literature is now replete with examples of bioisosteres and their effects in many different drug-like molecules.⁶³

2.2 Bioisosteres

Bioisosteres can be classified into two groups: classical and non-classical. Classical bioisosteres encompass simple structural changes of mono-, di-, or trivalent atoms or groups as well as ring equivalents (Table 4).^{63,66} Non-classical bioisosteres are more structurally diverse exhibiting different steric and electronic parameters.^{63,66}

Table 4 - Classical bioisosteres⁶³ Adapted with permission from: *J. Med. Chem.*, 2011, 54, 2529-2591, Copyright 2011 American Chemical Society

Classical bioisosteres	
Monovalent	D and H F and H NH and OH RSH and ROH F, OH, NH ₂ , and CH ₃ Cl, Br, SH, and OH C and Si
Bivalent in which two bonds are affected	C=C, C=N, C=O, and C=S -CH ₂ -, -NH-, -O-, -S- RCOR', RCONHR', RCOOR', and RCOSR'
Trivalent in which three bonds are affected	R ₃ CH, R ₃ N R ₄ C, R ₄ N ⁺ , R ₄ Si Alkene, imine -CH=CH-, -S- -CH= and -N=C

2.3 Deuterium as an isostere for hydrogen

Substitution of a hydrogen with a deuterium atom represents the simplest form of bioisosterism. The only physical difference between deuterium and hydrogen is the extra neutron in the deuterium nucleus. However, this small change can translate into significant effects that can be exploited. For example, deuterium is slightly less lipophilic than hydrogen;^{67,68} the carbon deuterium bond length is slightly shorter and therefore stronger than the carbon hydrogen bond; and deuterium incorporation can increase basicity.^{69–72} As such, deuterium has been used by medicinal chemists to modulate compound metabolism,^{63,73,74} toxicity^{75,76} and to slow epimerisation.^{63,77}

Deuterium has commonly been used to investigate the mechanism of the metabolism of drug molecules. This is exemplified by the use of the kinetic isotope effect (KIE) to elucidate the rate determining step involved in a given metabolic pathway.^{74,75} These effects have now been translated into drug molecules to modulate their metabolism. An example of the incorporation of deuterium in a drug molecule has been reported by Auspex Pharmaceuticals. The original compound venlafaxine (Figure 9) is a dual serotonin/norepinephrine reuptake inhibitor which is used to treat depression.

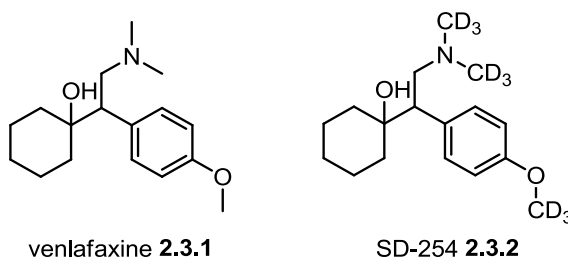


Figure 9 - Venlafaxine and deuterated analogue SD-254

The metabolic liabilities of this compound included O- and N-demethylation. Auspex therefore investigated incorporation of deuterium at these sites of metabolism. Subsequently, they produced SD-254 (Figure 9), which demonstrated a 50% reduced rate of metabolism *in vitro*. Early clinical studies of this compound have demonstrated increased exposure of the parent drug and reduced concentrations of the previously observed metabolites.⁶³ A further example of such deuterium incorporation includes the deuterated analogue of antidepressant paroxetine

developed by Concert Pharmaceuticals (Figure 10).^{78,79} Interestingly, deuteration in this case increases the rate of metabolism compared to parent compound.⁷⁹

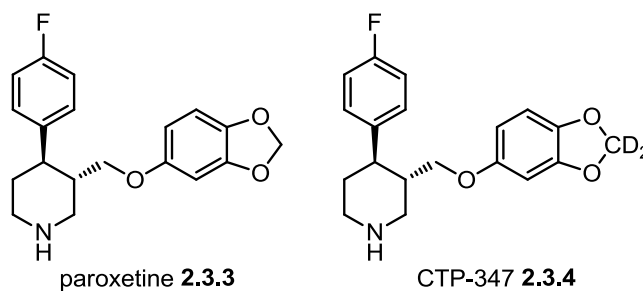
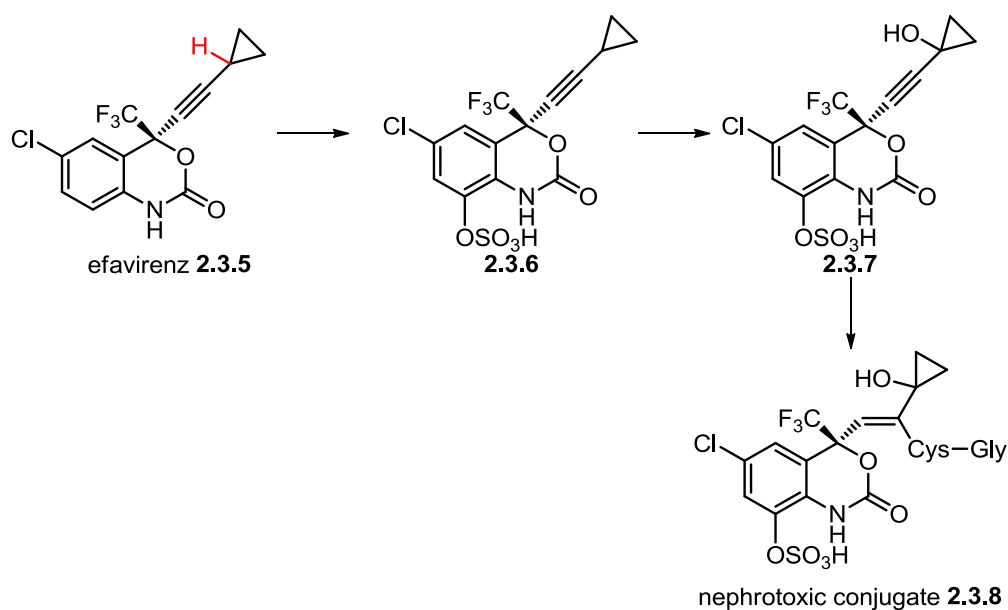


Figure 10 - Paroxetine and deuterated analogue CTP-347

Deuterium can also be used to inhibit the production of toxic metabolites. Efavirenz (Scheme 2) is a human immunodeficiency virus (HIV) 1 non-nucleoside reverse transcriptase inhibitor.⁷⁶ This compound is metabolised *via* a pathway that creates a glutathione derived nephrotoxic conjugate **2.3.8** (Scheme 2).⁷⁶



Scheme 2 - Metabolic pathway of efavirenz Reprinted from *The Species-Dependent Metabolism of Efavirenz Produces a Nephrotoxic Glutathione Conjugate in Rats*, Mutlib A. E., Gerson R. J., Meunier P. C., Haley P. J., Chen H., Gan L. S., Davies M. H., Gemzik B., Christ D. D., Krahn D. F., Markwalder J. A., Seitz S. P., Robertson R. T., Miwa G. T., *Toxicology and Applied Pharmacology*, 2000, 169, 102-113, Copyright 2000 with permission from Elsevier

Deuteration of the propargylic site (marked in red) impedes the oxidation to the alcohol functionality.^{63,76} This in turn reduces production of the nephrotoxin which is confirmed by diminished quantities in the urine.^{63,76}

2.4 Fluorine as an isostere for hydrogen

Another small atom, fluorine, can be a useful bioisostere for hydrogen. In a survey of compounds developed by Roche, lipophilicity was found to increase with fluorine incorporation.^{63,80} However, in some instances, particularly when fluorine was proximal to an oxygen, the lipophilicity was lowered. This effect is not understood but potential explanations include overall molecule polarity leading to an increase in solvation, or the strong electron-withdrawing nature of the fluorine polarising the carbon-oxygen bond leading to stronger H-bonding. In addition, fluorine forms the strongest known bonds to carbon (108 kcal/mol) and also has the ability to strengthen adjacent C-F, C-O and C-C bonds. Consequently, fluorine can generally be considered as biologically inert.⁶³ These properties allow modulation of metabolism^{80,81} and basicity^{82,83} as well as influencing structural conformation,⁸⁴ permeability^{85,86} and potency.⁸⁷⁻⁹⁰

Ezetimibe (Figure 12), developed by Schering-Plough, utilises fluorine to modulate metabolism.⁸¹ The original clinical candidate molecule **2.4.1** was initially developed as an acyl-coenzyme A cholesterol acyltransferase (ACAT) inhibitor,⁹¹ however, it was discovered that metabolites of this compound were producing the *in vivo* activity acting as cholesterol absorption inhibitors.⁸¹ An extensive investigation into these metabolites identified the metabolic weak spots of **2.4.1** and also elucidated which of those sites produced a beneficial effect (Figure 11).

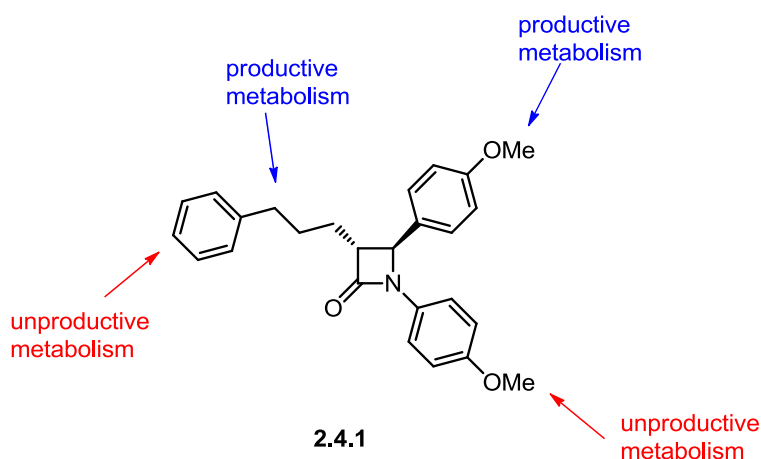
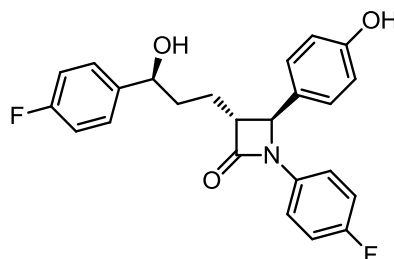


Figure 11 - Sites of metabolism of 2.4.1

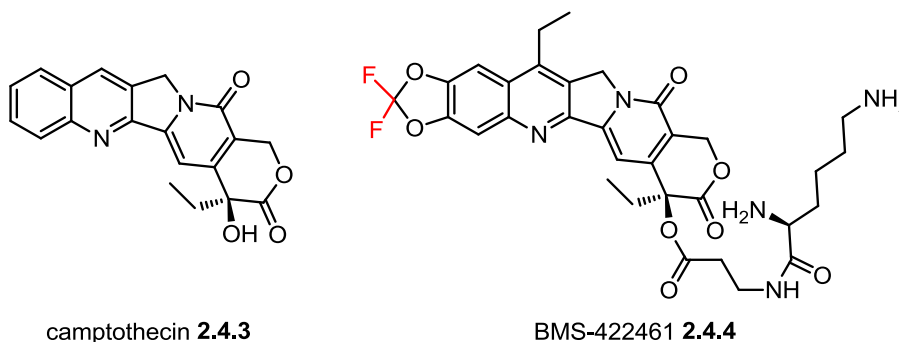
Subsequent blocking with fluorine of the metabolically labile sites which did not result in an active metabolite while incorporating the functionality of the beneficial metabolites produced ezetimibe ($IC_{50} = 0.14 - 0.26 \mu M$), a potent cholesterol absorption inhibitor (Figure 12).^{81,92}



ezetimibe 2.4.2

Figure 12 – Cholesterol absorption inhibitor ezetimibe⁸¹

A further example of the use of fluorine to modulate metabolism includes the pro-drug BMS-422461 (active drug $IC_{50} = 0.0015 \mu M$);⁹³ an analogue of camptothecin ($IC_{50} = 0.0171 \mu M$),⁹³ which is a known cytotoxic quinoline alkaloid developed by Bristol-Myers-Squibb (Figure 13).⁹⁴ A methylene group (highlighted site) is susceptible to metabolism by cytochrome P450 enzymes. Incorporation of the more stable geminal-difluoro group mitigates this risk.



camptothecin 2.4.3

BMS-422461 2.4.4

Figure 13 - Camptothecin⁹⁴ and pro-drug BMS-422461⁹³

In addition to tuning metabolism, the effect of replacing hydrogen with fluorine to improve potency is well established.⁸⁷⁻⁹⁰ In a series of antibacterial gyrase inhibitors, incorporation of an aryl fluorine substituent (highlighted position Figure 14 2.4.5) improved potency up to 7- fold as well as increasing cell penetration, reducing plasma protein binding and improving the pharmacokinetic profile.

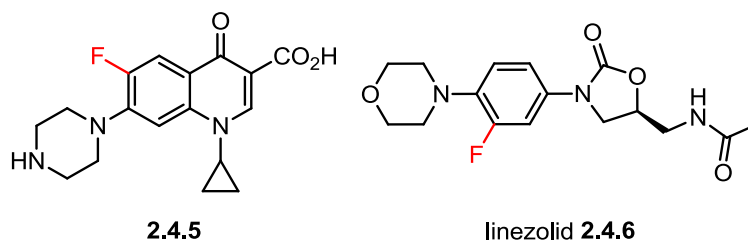
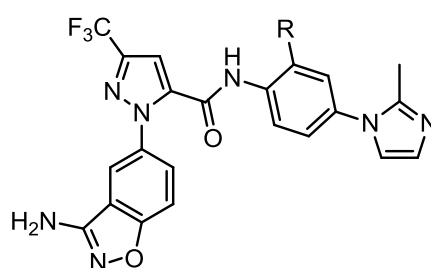


Figure 14 - Antibacterial gyrase inhibitor 2.4.5 and oxazolidinone antibacterial linezolid

This effect has also been demonstrated in an alternative series which led to the marketed antibacterial linezolid.⁹⁰

As mentioned above, fluorine has also been used to improve permeability. This bioisosteric replacement with fluorine has been used in two series of factor Xa inhibitors, a key protein involved in coagulation.^{85,86} The highlighted example shows an approximately 9-fold increase in permeability into human colonic adenocarcinoma (Caco-2) cells (Table 5).

Table 5 - Caco-2 permeability for anilide based factor Xa inhibitors^{63,86} Reprinted with permission from: *J. Med. Chem.*, 2005, 48, 1729-1744, Copyright 2005 American Chemical Society



R	Permeability (nm/s)
CN (2.4.7)	<1
H (2.4.8)	8.2
F (2.4.9)	74.1

This increase is attributed to an internal electrostatic interaction between the fluorine and the adjacent NH of the amide, which in effect masks this potential H-bond donor.

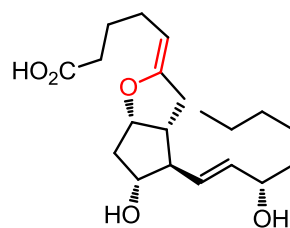
2.5 Bioisosteres for carbon and alkyl moieties

Bioisosteres of carbon and alkyl moieties are sought after because of the inherent lipophilicity of the parent group. Simple substitution of a methylene group with oxygen or sulfur can therefore be desirable to deliver improvements (albeit often minor) in the physicochemical profiles or potentially having an impact on the bond lengths and conformations of the drug molecules, thus affecting potency (Table 6).

Table 6 - Properties of CH₂ vs O vs S⁶³ Adapted with permission from: *J. Med. Chem.*, 2011, 54, 2529-2591, Copyright 2011 American Chemical Society

Property	R-CH ₂ -X-CH ₂ -R		
	X = CH ₂	X = O	X = S
C-X bond length (Å)	1.54	1.43	1.81
CXC bond angle (°) 	109.5	111	99
C...C distance (Å)	2.51	2.37	2.87
Van der Waals radius of X (Å)	2.0	1.40	1.85
Log P	3.39	0.77	1.95
Electronegativity	2.27	3.51	2.32
Contribution to van der Waals volume (cm ³ /mol)	10.2	3.7	10.8

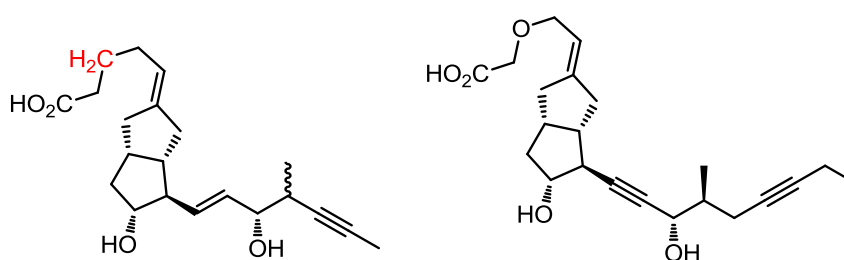
Bioisosteric switching between oxygen and carbon has been applied in the context of a prostacyclin mimetic. Prostacyclin is a known vasodilator but is unstable due to the sensitive enol ether functionality (Figure 15).^{63,95,96}



prostacyclin 2.5.1

Figure 15 - Prostacyclin with sensitive enol ether highlighted

Replacing oxygen for a methylene at this position removes this metabolically labile site. Further optimisation around prostacyclin afforded iloprost with a modified β -side chain (Figure 16).⁹⁶



iloprost 2.5.2

cicaprost 2.5.3

Figure 16 – Prostacyclin mimetics Iloprost and cicaprost

Iloprost demonstrated a comparable profile to the naturally produced prostacyclin with an increased half-life of 20-30 minutes, compared to 42 seconds.^{95,96} Oxidation β to the carboxylic acid moiety was identified as a metabolic liability (Figure 16).⁹⁶ This methylene unit was subsequently switched for the bioisosteric oxygen to block this instability. Further manipulation of the β -side chain generated cicaprost; which proved to be at least 5-fold more effective than iloprost as a vasodilator; with an additional 2- to 3- fold extension in half life.⁹⁶ This example particularly highlights the interchangeable nature of bioisosteres, with simple switches having large effects on metabolism.

Addition of oxygen can not only be used to block metabolism but can also act as an effective method of improving potency. A non-prostacyclin derived agonist of the prostacyclin receptor effectively demonstrates this (Table 7).⁹⁷

Table 7 - Non-prostacyclin derived inhibitors⁶³ Reprinted with permission from: *J. Med. Chem.*, 1992, 35, 3483-3497, Copyright 1992 American Chemical Society

Compound	X	Y	Z	Inhibition of blood platelet aggregation EC ₅₀ (μM)
2.5.4	CH ₂	O	CH ₂	1.2
2.5.5	CH ₂	CH ₂	CH ₂	16
2.5.6	CH ₂	Trans CH=CH		0.66
2.5.7	O	O	CH ₂	1.2
2.5.8	O	CH ₂	CH ₂	>80
2.5.9	O	Trans CH=CH		14

These data clearly show that a *trans*-alkene and methylene provide the most active compounds.^{63,97} However, it is worth noting the bioisosteric O **2.5.7** shows a marked increase in potency compared to **2.5.8**, although this is slightly lower than the optimal *trans*-alkene. This has been rationalised by the ability of the *trans*-alkene and the oxygen atom to conformationally bias the carboxylic acid moiety to the desired planar orientation, due to delocalisation into the phenyl ring system. The methylene analogue situates the carboxylic acid perpendicular to this as a result of a steric clash (Figure 17).^{63,97}

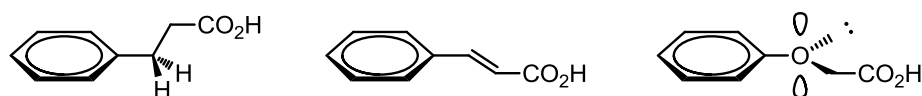
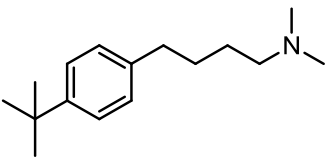
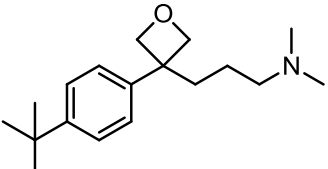
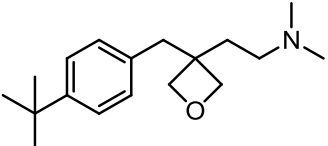
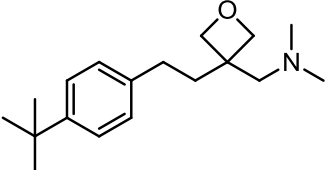


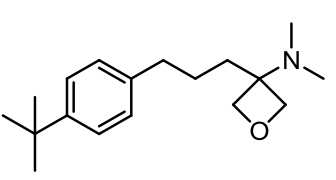
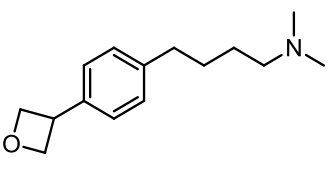
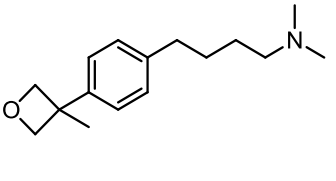
Figure 17 - Optimal geometries of 2.5.8, 2.5.9 and 2.5.7 Adapted with permission from: *J. Med. Chem.*, 2011, 54, 2529-2591, Copyright 2011 American Chemical Society

Interestingly, **2.5.6** and **2.5.9** show the opposite trend in potency with the conformational preference for a bend in the molecule at the X position. These trends have also been observed in a series of prostaglandin EP₃ receptor antagonists.⁹⁸

Geminal-dimethyl substituents are commonly used in drug molecules to restrict conformation or block metabolic sites.⁶³ However, these generally result in a notable increase in lipophilicity.⁶³ Oxetanes can be used as a bioisostere of these moieties with the benefit of being essentially liponeutral (having no effect on overall lipophilicity).⁹⁹⁻¹⁰¹ A systematic investigation into the influence of the oxetane ring on physicochemical properties has been conducted using **2.5.10** as a model compound (Table 8).⁹⁹⁻¹⁰¹

Table 8 - systematic analysis of 2.5.10 oxetane incorporation *Table reproduced from Oxetanes as Promising Modules in Drug Discovery, Wuitschik G., Rogers-Evans M., Müller K., Fischer H., Wagner B., Schuler F., Polonchuk L., Carreira E. M., Angew. Chem. Int. Ed., 2006, 45, 7736-7739 with permission from John Wiley & Sons*

	Structure	pK _a	Sol. (µg/mL)	Cl _{int} (HLM)*	Cl _{int} (MLM)*	Log D (Log P)
2.5.10		9.9	<1	16	417	1.8 (4.3)
2.5.11		9.6	270	0	147	1.7 (3.9)
2.5.12		9.2	4100	6	13	1.7 (3.5)
2.5.13		8.0	25	42	383	3.3 (4.0)

2.5.14		7.2	57	13	580	3.3 (3.6)
2.5.15		9.9	4000	2	27	-0.1 (2.4)
2.5.16		9.9	4400	0	43	0.8 (3.3)

*Units = $\mu\text{L}/\text{min}/\text{mg}$

These data show the potential beneficial effects the incorporation of an oxetane can have. In all cases the oxetane provides an improvement in solubility compared to the CH_2 but the effect is much more pronounced when replacing a dimethyl (**2.5.16**) or *tert*-butyl group (**2.5.15**).⁹⁹⁻¹⁰¹ As discussed previously, the Log D value also shows significant improvement between the parent **2.5.10** and oxetane derivatives **2.5.15** and **2.5.16**. Intrinsic clearance data in both human liver microsomes (HLM) and mouse liver microsomes (MLM) show an improvement, suggesting enhanced metabolic stability when employing oxetane systems.⁹⁹⁻¹⁰¹

2.6 Carbonyl mimetics

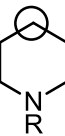
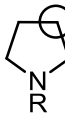
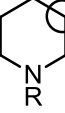
Oxetanes can also be considered as carbonyl mimetics. Ketones and aldehydes are generally too reactive to be feasible within a drug molecule, pertaining to their inherent ability to undergo redox processes *in vivo*. Oxetanes however, are more stable but possess a similar shape and ability to accept H-bonds, therefore have the capacity to act as mimetics (Figure 18).

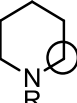
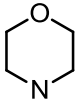


Figure 18 - Carbonyl and oxetane shapes

A comprehensive examination of some elaborate oxetane containing systems has been conducted by the Carreira group; investigating cyclic ketones, amides and morpholine replacements (Table 9).

Table 9 - Physicochemical and biochemical properties of oxetane, carbonyl and gem-dimethyl moieties¹⁰²
 Table reproduced from *Spirocyclic Oxetanes: Synthesis and Properties*, Wuitschik G., Rogers-Evans M., Buckl A., Bernasconi M., Märki M., Godel T., Fischer H., Wagner B., Parrila I., Schuler F., Schneider J., Alker A., Schweizer B., Müller K., Carreira E. M., *Angew. Chem. Int. Ed.*, 2008, 47, 4512-4515 with permission from John Wiley & Sons

Compound		Log D ^a (log P)	Solubility (µg/mL)	Cl _{int} ^b (HLM/MLM)	pK _a
	<i>gem</i> -Me ₂ (2.6.1)	0.8 (3.1)	290	0/16	9.6
	Oxetane (2.6.2)	0.5 (1.2)	24000	3/7	8.0
	Carbonyl ^c (2.6.3)	n.d.	n.d.	n.d.	n.d.
	<i>gem</i> -Me ₂ (2.6.4)	2.3 (4.4)	220	23/31	9.5
	Oxetane (2.6.5)	1.0 (2.0)	1400	6/22	8.3
	Carbonyl (2.6.6)	1.2 (1.6)	4000	120/88	7.5
	<i>gem</i> -Me ₂ (2.6.7)	1.4 (3.7)	40	10/39	9.7
	Oxetane (2.6.8)	0.7 (1.5)	730	2/27	8.1
	Carbonyl (2.6.9)	-0.1 (-0.1)	4100	100/580	6.1
	<i>gem</i> -Me ₂ (2.6.10)	2.3 (4.3)	13	31/89	9.4
	Oxetane (2.6.11)	1.7 (2.3)	2000	16/55	7.9
	Carbonyl (2.6.12)	0.1 (0.5)	2100	120/120	7.6
	<i>gem</i> -Me ₂ (2.6.13)	0.1 (2.8)	380	7/14	10.1

	Oxetane (2.6.14)	1.3 (1.3)	1400	21/26	6.2
	Carbonyl (2.6.15)	1.1 (1.1)	2100	5/190	–
	<i>gem</i> -Me ₂ (2.6.16)	0.9 (3.5)	41	0/13	10.0
	Oxetane (2.6.17)	1.9 (1.9)	2100	31/74	6.3
	Carbonyl (2.6.18)	1.2 (1.2)	1500	5/16	–
	<i>gem</i> -Me ₂ (2.6.19)	1.1 (3.9)	30	0/18	10.2
	Oxetane (2.6.20)	2.2 (2.4)	750	19/230	7.0
	Carbonyl (2.6.21)	1.6 (1.6)	6200	8/39	–
	(2.6.22)	1.6 (1.8)	>2600	15/41	7.1
	n = 1 (2.6.23)	0.9 (3.1)	450	8/18	9.6
	n = 2 (2.6.24)	0.2 (2.5)	580	6/18	9.7
	n = 3 (2.6.25)	–0.1 (2.1)	2500	0/11	9.5
	(2.6.26)	1.5 (1.6)	8000	9/8	7.0

R = piperonyl, [a] measured at pH 7.4 [b] = $\mu\text{L}/\text{min}/\text{mg}$ [c] = not measured due to compound instability

The general trends indicate the oxetane moiety is well suited to function as a carbonyl mimetic, exhibiting good solubility and lower clearance. The spirocyclic 2-oxa-6-azaspiro[3.3]heptane (**2.6.2**) also functions as an excellent bioisostere of the morpholine group (**2.6.26**) with comparable data across all measures.

Carbonyl bioisosteres have been extensively reported in the literature primarily due to the number of different groups that contain such functionality. Ketones, esters and amides are all potentially interchangeable with their selection having a wide impact on physicochemical and biochemical parameters (Figure 19).¹⁰³ Sulfoxides, sulfones and sulfoximines offer an alternative due to their tetrahedral nature. In certain circumstances this can be beneficial to the positioning of oxygen atom(s) in a prime vector for binding to a biological target (Figure 19).⁶³

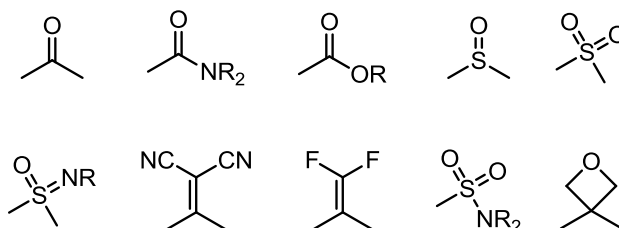


Figure 19 - Carbonyl bioisosteres^{63,103}

A sulfone has been utilised as a ketone mimetic in a series of Hepatitis C virus (HCV) non-structural protein 5B (NS5B) polymerase inhibitors.¹⁰⁴ A collaboration between Tibotec and Johnson & Johnson utilised structure-based design to propose **2.6.28** as a viable mimetic for **2.6.27** (Figure 20).¹⁰⁴

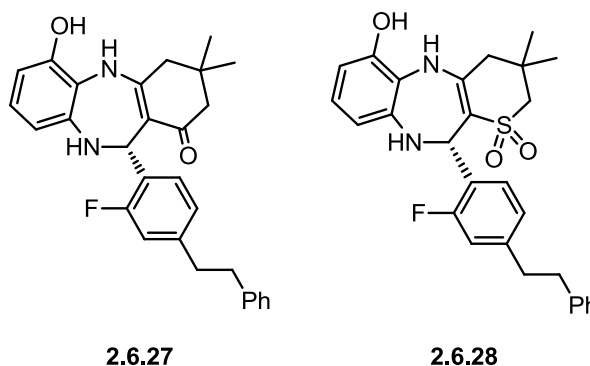


Figure 20 - HCV NS5B inhibitors **2.6.27** and **2.6.28**¹⁰⁴

X-ray crystal structures indicated the potential for a second hydrogen bonding interaction, which could be accessed *via* a tetrahedral sulfone.^{63,104} Sulfone analogue **2.6.28** did indeed exhibit an approximately 20-fold improvement in binding relative to its ketone analogue **2.6.27**.¹⁰⁴

As mentioned previously, amide and ester functionalities are interchangeable with a variety of other functional groups (Figure 19). The significant investigation into

bioisosteres for amides and esters has provided many suitable mimetics, with a myriad of different structural motifs reported (Figure 21).^{63,103,105,106}

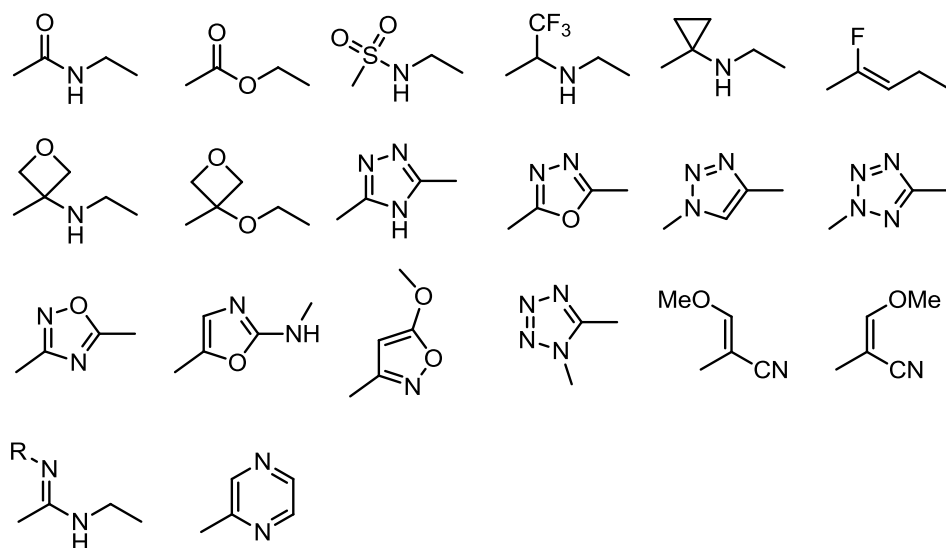


Figure 21 - Amide and ester bioisosteres

The trifluoroethylamine moiety as a replacement for an amide has been exploited in the context of a cathepsin K inhibitor, despite the deleterious effect on the physicochemical profile, particular in terms of Log P.¹⁰⁷ Balacatib is a potent, reversible covalent inhibitor of capthesin K, however it has poor selectivity over the related capthesins B, L and S (Figure 22).^{107,108}

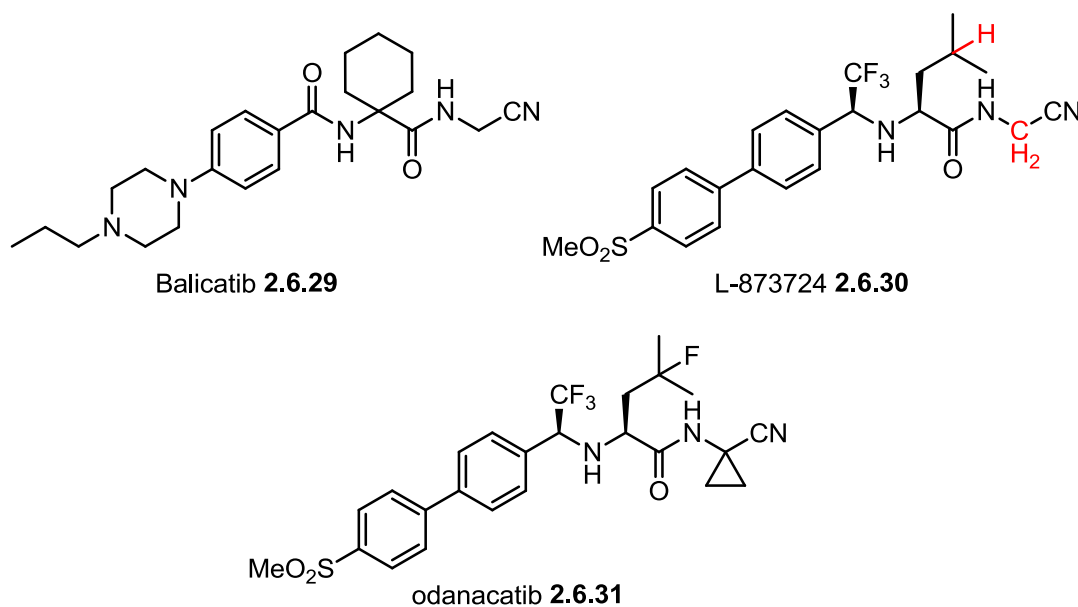


Figure 22 - Cathepsin K inhibitors^{107,108}

The bioisosteric replacement of the carbonyl with a trifluoromethyl group led to increased selectivity over the other cathepsins. Further modifications to the structure led to L-873724 which displayed superior selectivity and potency. However, this compound was not progressed due to metabolic instability (Figure 22). Blocking of the metabolically labile sites with cyclopropyl and fluorine groups led to odanacatib (Figure 22).¹⁰⁸ This exhibits excellent selectivity, bioavailability and metabolic stability, and was progressed into clinical development as a treatment for postmenopausal osteoporosis (Table 10).¹⁰⁸

Table 10 - Potency data for cathepsin K inhibitors¹⁰⁸ Reprinted from *The discovery of odanacatib (MK-0822), a selective inhibitor of cathepsin K*, Gauthier J. Y., Charet N., Cromlish W., Desmarais S., Duong L. T., Falguyret J-P. Kimmel D. B., Lamontagne S., Léger S., LeRiche T., Li C. S., Massé F., McKay D. J., Nicoll-Griffith D. A., et al., *Bioorg. Med. Chem. Lett.*, 2008, 18, 923-928, Copyright 2008 with permission from Elsevier

Compound	IC ₅₀ (nM)			
	Cathepsin K	Cathepsin B	Cathepsin L	Cathepsin S
Balicatib (2.6.29)	22	61	48	2900
L-873724 (2.6.30)	3	4807	1221	95
Odanacatib (2.6.31)	5	1050	4843	45

Heterocycles have also been investigated as replacements for esters and amides. A comprehensive study by Saunders *et al.* demonstrated the applicability of a wide range of five-membered heterocycles to act as ester bioisosteres, focusing on a muscarinic cholinergic receptor agonist (Figure 23).¹⁰⁵

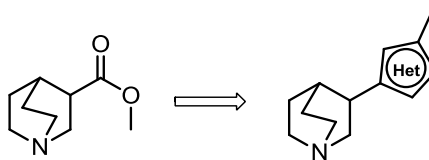


Figure 23 - Muscarinic cholinergic receptor agonists

In this investigation, replacing the ester for certain heterocycles, such as an oxadiazole maintained or increased agonist activity.¹⁰⁵ Interestingly, incorporation of some heterocycles switched the mode of action to antagonist, these included a furan, oxazole and isoxazole.¹⁰⁵ The alternative hydrogen bonding vectors accessible by these heterocycles was used to rationalise this effect.¹⁰⁵ This is another example where minor differences in selected bioisosteres can have a significant impact on its pharmacological properties.

2.7 Carboxylic acids

Similarly to amides and esters, carboxylic acids are a common functionality in drug design, with their propensity to establish strong ionic and hydrogen bonding interactions with drug targets. However, some inherent properties create certain issues, in particular, they can be metabolically unstable and pose toxicity risks.^{63,103} Furthermore, their high polarity and hydrophilicity present possible permeability issues, particularly across the BBB.^{63,103,109} Possible carboxylic acid mimetics have been extensively studied, again with a wide variety of different structural motifs being investigated (Figure 24).^{63,103,109}

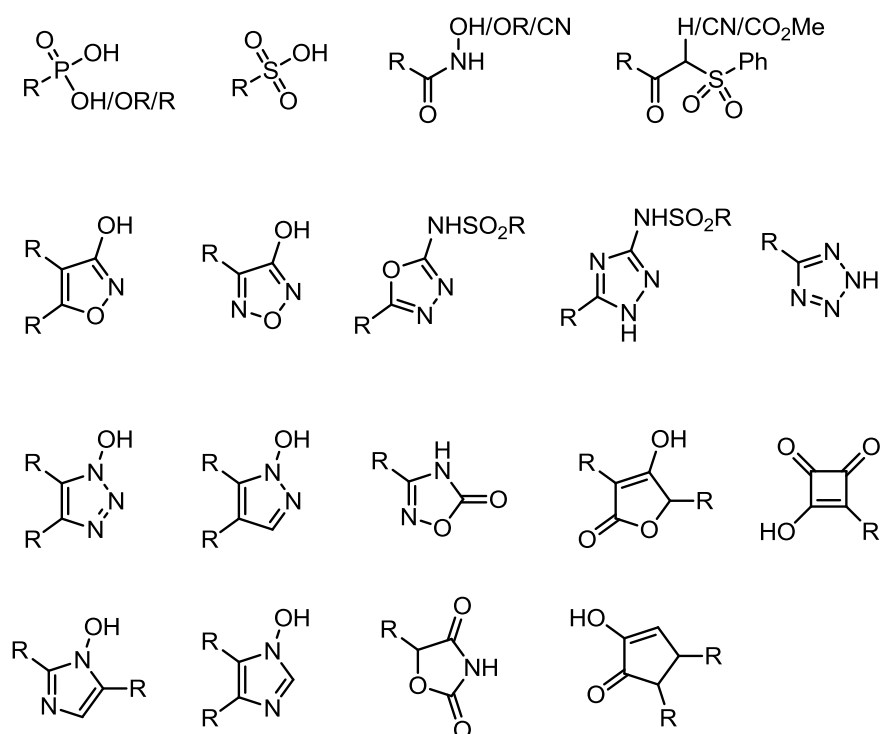
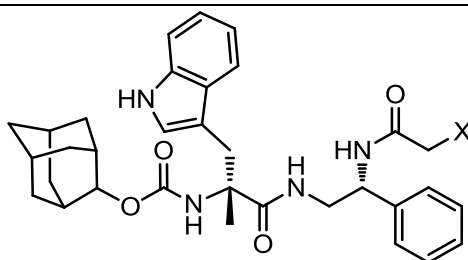
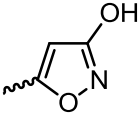


Figure 24 - Carboxylic acid bioisosteres^{63,103}

The properties of these structural motifs play an important role. Often they are used to impart more lipophilicity to aid permeability, however, it is crucial to have the correct charge distribution and geometry to allow the isostere to maintain the same interactions as the original carboxylic acid.¹⁰⁹ This effect is exemplified in a series of cholecystokinin-B (CCK-B) receptor antagonists (Table 11). The planar heterocyclic isostere **2.7.3** exhibits comparable potency and pK_a compared to the parent acid **2.7.1** (with the caveat that there is a slight drop in selectivity). However, generally the non-planar bioisosteres display a drop in potency.¹¹⁰

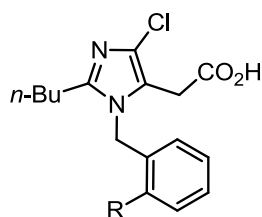
Table 11 - Comparison of CCK-B receptor antagonists *Table reproduced from Carboxylic Acid (Bio)isosteres in Drug Design, Ballatore C., Huryn D. M., Smith A. B., ChemMedChem, 2013, 8, 385-395 with permission from John Wiley & Sons*



Compound	X	CCK-B IC ₅₀ (nM)	CCK-A IC ₅₀ (nM)	pK _a
2.7.1	CH ₂ COOH	1.7	4500	5.6
2.7.2	CH ₂ SO ₃ Na	1.3	1010	<1
2.7.3		2.6	1700	6.5
2.7.4	CH ₂ P(O)(OH) ₂	23	2700	3.4, 7.8
2.7.5	CH ₂ P(O)(OH)Me	23	4400	3.7

Further heterocyclic alternatives were investigated, but all had diminished selectivity despite maintaining high CCK-B activity.¹¹⁰

One such heterocyclic acid bioisostere which has been used extensively in a variety of medicinal chemistry programmes is the tetrazole. One particular example of note are antagonists of the angiotensin II receptor, which is involved in vasoconstriction. The project was initiated based on three weak imidazole-based antagonists (Figure 25).¹¹¹

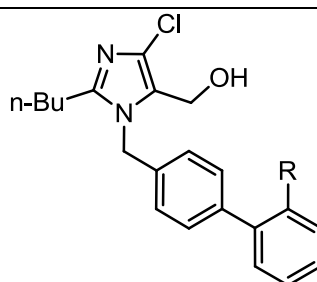


R = NO₂ **2.7.6**, Cl **2.7.7**, H **2.7.8**

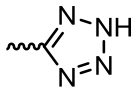
Figure 25 - Weak angiotensin II antagonists

Significant investigation of this template led to **2.7.9** which had an IC₅₀ of 0.23 μM.¹¹¹⁻¹¹³ This formed the basis for an investigation into a variety of other carboxylic acid bioisosteres (Table 12).¹¹³ Subsequently, tetrazole **2.7.14** was identified as an extremely potent, orally bioavailable candidate and progressed to market as losartan.¹¹⁴

Table 12 - Carboxylic acid bioisostere investigation in angiotensin II antagonists^{109,113} Reprinted with permission from: *J. Med. Chem.*, 1991, 34, 2525-2547, Copyright 1991 American Chemical Society



Compound	R	pK _a (estimated)	IC ₅₀ (μM)	Dose <i>iv</i> (mg/kg)	Dose <i>po</i> (mg/kg)
2.7.9	COOH	5	0.23	3	11
2.7.10	CONHOH	10.5	4.1	3	>30
2.7.11	CONHOCH ₃	10.9	2.9	10	Inactive
2.7.12	CONHSO ₂ Ph	8.4	0.14	>3	30
2.7.13	NHSO ₂ CF ₃	4.5	0.083	10	100

2.7.14 (losartan)		5-6	0.019	0.80	0.59
------------------------------------	---	-----	-------	------	------

Another example of the utility of a tetrazole as a carboxylic acid derivative is present in a cysteinyl leukotriene D₄ receptor antagonist. Initially, Fisons Ltd produced FPL-55712, which showed good potency, however, its poor bioavailability and short half life prevented progression to clinical trials.¹¹⁵ Further development in this area came from ICI Pharmaceuticals and Lilly Research Labs, both of which produced **2.7.15**.^{115,116} Lilly took this concept further and identified the tetrazole **2.7.16** as a significant improvement to the acid **2.7.15** with excellent oral activity (Figure 26). This was subsequently developed as an anti-asthmatic medication, tomelukast.¹¹⁷

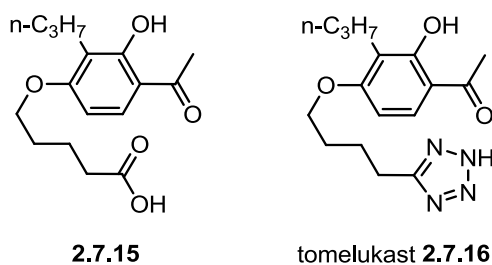


Figure 26 - LTD₄ receptor antagonists^{115,117}

Further examples of more unusual heterocycles being used as carboxylic acid mimetics include a squaric acid derivative in *N*-methyl-D-aspartate antagonist **2.7.17**;¹¹⁸ a difluorophenol in aldose reductase inhibitor **2.7.18**;¹¹⁹ and cyclopentane-1,2-diones in thromboxane A₂ receptor antagonists **2.7.19** (Figure 27).¹²⁰

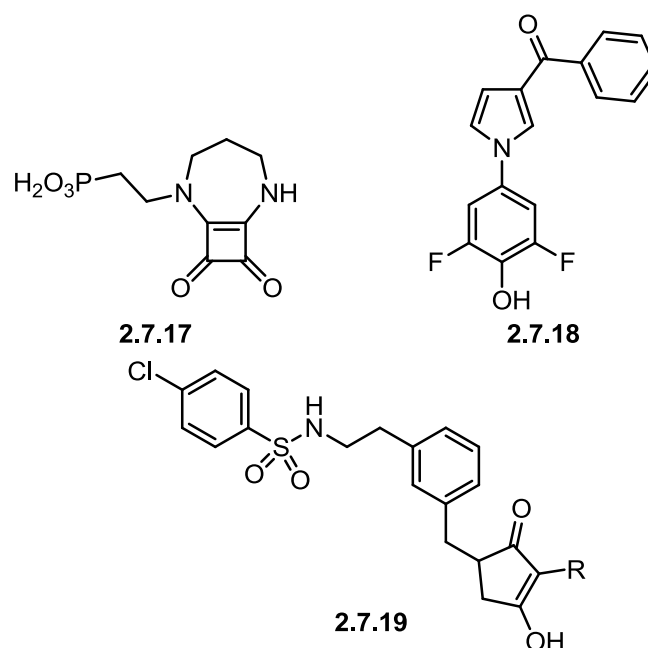


Figure 27 – Alternative heterocyclic examples of carboxylic acid bioisosteres

2.8 Heterocycles

With a multitude of heterocycles being employed as mimetics for a raft of other functional groups, heterocycles can themselves have a whole host of bioisosteres. Heterocycles are ubiquitous in drug design, being common scaffolds and often providing important structural functionality. The range of size, shape, electronic, and physical properties they provide allow the projection of substituents along a number of vectors as well as creating important drug-target interactions. The key functionality stems from their H-bond donor and acceptor abilities; electron withdrawing or donating effects; and potential π -interactions.

Examples of heterocycle bioisosterism are ubiquitous within the medicinal chemistry literature. One such example used pyridine as a pyrimidine substitute within a cathepsin S inhibitor. The pyrimidine based compound **2.8.1** had an IC_{50} of 6 nM and 40 nM against cathepsin S and K, respectively (Figure 28).¹²¹

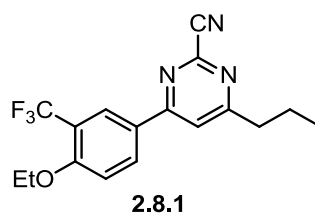
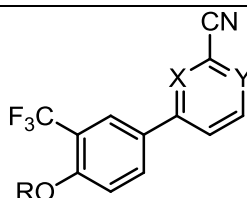


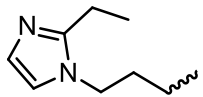
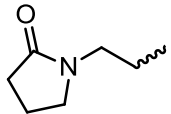
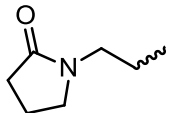
Figure 28 - Cathepsin S and K inhibitor 2.8.1

There was concern that this compound could potentially cause irreversible binding to glutathione, which in turn could lead to unwanted toxicity. Consequently, pyridines were investigated as pyrimidine replacements to reduce this risk.

Table 13 - Exploration of cathepsin inhibitors¹²¹ Reprinted from 4-(3-Trifluoromethylphenyl)-pyrimidine-2-carbonitrile as cathepsin S inhibitors: N3, not N1 is critically important, Cai J., Fradera X., van Zeeland M., Dempster M., Cameron K. S., Bennett D. J., Robinson J., Popplestone L., Baugh M., Westwood P., Bruin J., Hamilton W., Kinghorn E., Long C., Uitdehaag J. C. M., *Bioorg. Med. Chem. Lett.*, 2010, 20, 4507-4510, Copyright 2010 with permission from Elsevier



Compound	R	X	Y	IC ₅₀ Cat S (nM)	IC ₅₀ Cat K (nM)
2.8.2	Et	N	N	6	40
2.8.3	Et	N	CH	1660	>10000
2.8.4		N	N	1.3	13
2.8.5		N	CH	58	1660
2.8.6		CH	N	Inactive	Inactive
2.8.7		N	CH	31	3090

2.8.8		CH	N	Inactive	Inactive
2.8.9		N	CH	29	>10000
2.8.10		CH	N	Inactive	Inactive

It is evident from the data that the positioning of the nitrogen is key to activity, with all compounds being inactive in the absence of a nitrogen at position X (Table 13).¹²¹ Pyridine compound **2.8.3** demonstrates a loss in activity from the lead compound **2.8.1** but extension into the hydrophobic pocket of the enzyme allows this potency to be regained, as exhibited by **2.8.5**, **2.8.7** and **2.8.9**.¹²¹ Additionally, it was noted that compound **2.8.5** was the only example that had activity in human cells, with this explained by a lysosome penetration effect.¹²¹ This investigation highlights the utility of exchanging a particular heterocycle to modulate against a toxicity risk. Furthermore, it examines the ability of three separate heterocycles (**2.8.5**, **2.8.7** and **2.8.9**) to increase potency in a lipophilic region. Each shows comparable potency at cathepsin S but different potencies at cathepsin K, potentially leading to a highly selective molecule. It also demonstrates the importance of the overall molecular physicochemical properties with only **2.8.5** providing efficacy in a cell model.

A further significant example of the importance of heterocycle selection in medicinal chemistry is found in a series of glycogen synthase kinase 3 (GSK3) inhibitors, with conformational analysis being crucial to understanding the binding mode of the compounds.¹²²

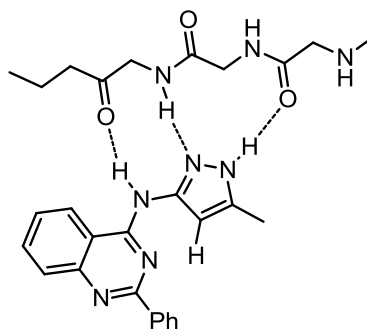
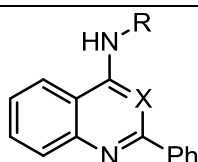


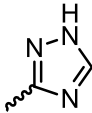
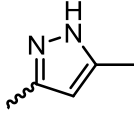
Figure 29 - Binding mode of 2.8.11 in GSK3^{63,122} Reprinted with permission from: *J. Med. Chem.*, 2011, 54, 2529-2591, Copyright 2011 American Chemical Society

The binding mode of **2.8.11**, was confirmed by X-ray crystallography and shown to involve three hydrogen bonding interactions with the enzyme (Figure 29).¹²² However, rationalisation of the data for other five-membered heterocycles proved challenging (Table 14).^{63,122}

Table 14 - Potency data of GSK3 inhibitors^{63,122} Reprinted with permission from: *J. Med. Chem.*, 2005, 48, 1278-1281, Copyright 2005 American Chemical Society



Compound	X	R	GSK3 K _i (nM)
2.8.11	N		24
2.8.12	N		>2000
2.8.13	N		110
2.8.14	N		23000

2.8.15	N		250
2.8.16	CH		2500

Compound **2.8.13** loses potency due to the lack of the methyl group, which creates a hydrophobic interaction.^{63,122} The isoxazole **2.8.12** potency was diminished due to the loss of a HBD, however the other heterocycles still possess a HBD to form such interactions.^{63,122} Conformational analysis of these heterocycles was required to give insight into the reduced activity observed.

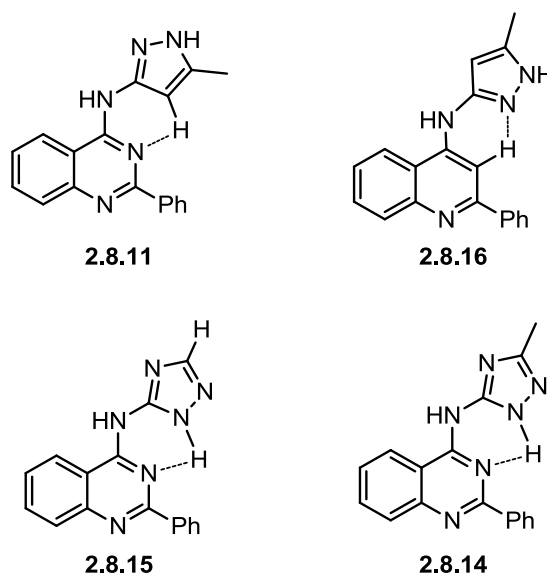


Figure 30 - Major conformational preferences for GSK3 inhibitors^{63,122} Reprinted with permission from: *J. Med. Chem.*, 2005, 48, 1278-1281, Copyright 2005 American Chemical Society

Figure 30 shows the major conformational preferences of the individual inhibitors in question. Compound **2.8.11** is the most potent with each of the individual hydrogen bond donors and acceptors perfectly positioned.^{63,122} Removing the nitrogen from the pyrimidine ring (**2.8.16**) causes a conformational shift in which the pyrazole ring rotates.^{63,122} This creates an intramolecular interaction between the pyrazole nitrogen and the CH of the core ring system.^{63,122} However, this removes one HBD and HBA whilst also twisting the methyl into a sub-optimal position for binding (**2.8.16**).^{63,122}

Triazole **2.8.15** also creates an internal hydrogen bond, nonetheless there is still one HBD and HBA available,^{63,122} therefore it retains modest potency.^{63,122} The addition of the methyl group to this triazole (**2.8.14**) then creates a steric clash as noted in the case of **2.8.16**, which causes a reduction in potency.^{63,122} This analysis demonstrates the varied effects heterocycles can have on conformation and therefore on drug-target interactions.^{63,122}

2.9 Phenyl group mimetics

Classically, phenyl group bioisosteres are aromatic heterocycles. Incorporation of heteroatoms into the phenyl structure often results in improvement of the physicochemical profile, whilst having minimal effect on any target binding interactions. They also have the potential to block metabolism and can have a beneficial impact on potency due to additional hydrogen bonding interactions *via* the heteroatoms.

One such example of blocking metabolism involves HIV-1 attachment inhibitors.¹²³ Indole **2.9.1** is a highly potent antiviral agent, however, metabolism of this compound can produce the toxic quinone **2.9.2** (Figure 31).^{63,123,124} Substitution of an aromatic methine for a nitrogen gives BMS-488043 **2.9.3**. Substitution of an aromatic methine for a nitrogen gives BMS-488043 which upon metabolism would give the amide **2.9.4**, a non-toxic metabolite (Figure 31).^{63,123,124} BMS-488043 also offers improved solubility and was subsequently progressed into clinical trials.¹²⁵

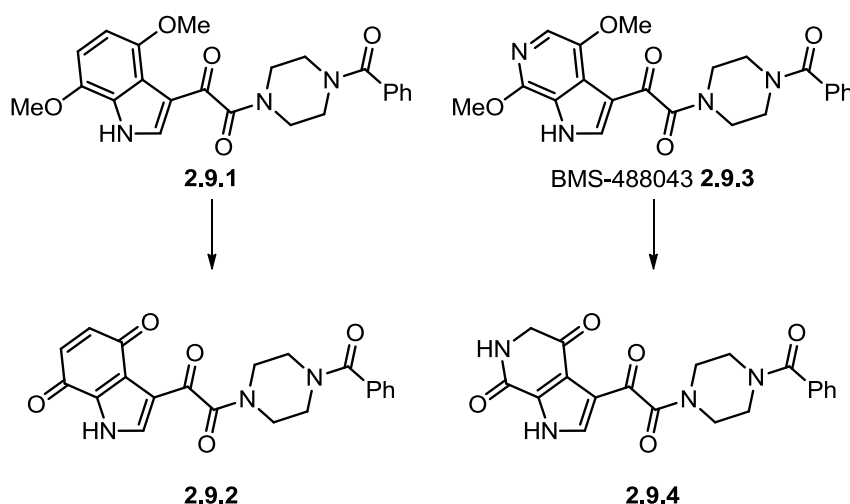


Figure 31 - HIV-1 attachment inhibitors and their metabolites^{63,123}

Further examples of heterocycles being incorporated for this purpose include modification of a phenol to prevent metabolism to a catechol, which can in turn form further quinone derived toxic metabolites (Figure 32).^{63,126} This heterocycle incorporation also improves upon the physicochemical profile of the molecules in question, demonstrated in a series of respiratory syncytial virus fusion inhibitors.^{63,126}

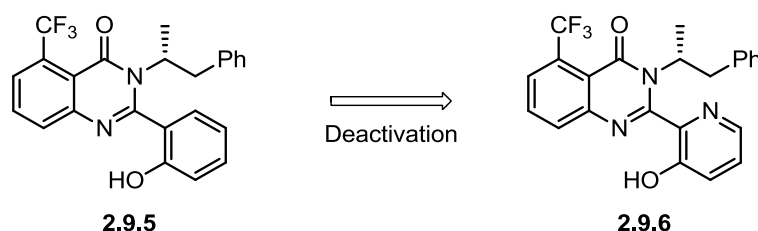


Figure 32 - Deactivation of phenol to prevent catechol formation¹²⁷

Less planar alternatives to aromatics have also been sought, with a particular aim to increase sp^3 character of lead compounds thereby “escaping from flatland”.⁵⁶ Saturated ring systems are therefore attractive as potential phenyl bioisosteres. However, when such replacements are applied issues can arise with the alternative vectors that saturated ring systems provide. Depending on the situation, this can be inherently beneficial, potentially allowing access to different regions of the target in question.

Having stated this, there are a paucity of direct saturated replacements for a phenyl ring that provide the correct geometry. For example, a cyclopropyl group has been used as an effective replacement of a phenyl within a factor Xa inhibitor. The prior literature identified compound **2.9.7** as an effective inhibitor ($K_i = 0.3$ nM), however, further exploration was conducted around the biphenyl moiety in order to identify compounds with improved potency, and *in vitro* and *in vivo* profiles (Figure 33).¹²⁸

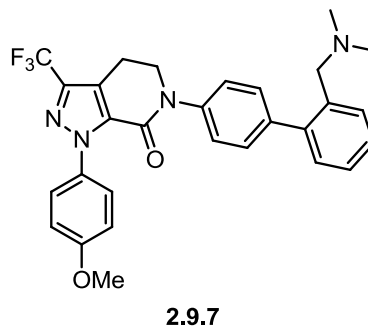
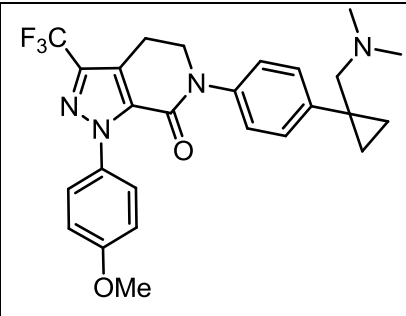
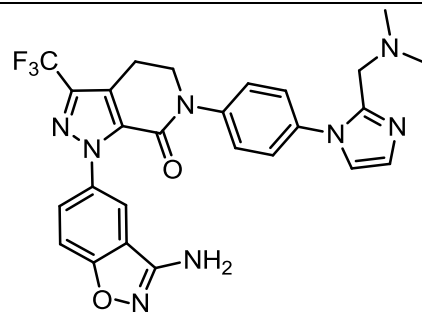


Figure 33 - Factor Xa inhibitor

Modelling of the cyclopropyl unit as a replacement for the terminal phenyl of the biphenyl segment suggested that the amine substituent would be orientated in a similar direction.¹²⁸ Compound **2.9.8** was subsequently tested and demonstrated superior potency to the parent compound as well as the related inhibitor razaxaban, which progressed to phase II trials.^{86,128}

Table 15 - Comparison of 2.9.8 and razaxaban *Reprinted from Achieving structural diversity using the perpendicular conformation of alpha-substituted phenylcyclopropanes to mimic the bioactive conformation of ortho-substituted biphenyl P4 moieties: Discovery of novel, highly potent inhibitors of factor Xa, Qiao J.X., Cheney D. L., Alexander R. S., Smallwood A. M., King S. R., He K., Rendina A. R., Luetgen J. M., Knabb R. M., Wexler R. R., Lam P. Y. S., Bioorg. Med. Chem. Lett., 2008, 18, 4118-4123, Copyright 2008 with permission from Elsevier*

	 2.9.8	 razaxaban 2.9.9
FXa K_i (nM)	0.035	0.19
Permeability (nm/s)	85	56
HLM t_{1/2} (min)	110	36
Cl (L/kg/h)	1.2	1.1
V_{dss} (L/kg)	15	5.3
t_{1/2} (h)	12	3.4
F%	53	84

Inhibitor **2.9.8** also displayed an enhanced physicochemical profile with increased stability, half-life, and permeability, whilst exhibiting lower bioavailability (F%) (Table 15). Based on this, it can be concluded that the cyclopropyl group is an effective *ortho*-phenyl isostere.

Among other saturated ring systems which have been considered as phenyl isosteres, cubanes are an alternative which offer the ability to explore the *para*-position of a phenyl group with a similar distance between the distal carbons (Figure 34).¹²⁹

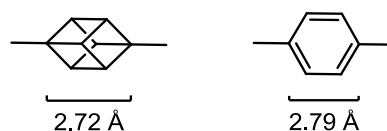


Figure 34 - Similarities between cubane and phenyl *Figure reproduced from Validating Eaton's Hypothesis: Cubane as a Benzene Bioisostere, Chalmers B. A., Xing H., Houston S., Clark C., Ghassabian S., Kuo A., Cao B., Reitsma A., Murray C-E. P., Stok J. E., Boyle G. M., Pierce C. J., Littler S. W., Winkler D. A., Bernhardt P. V., Pasay C., De Voss J. J., McCarthy J., Parsons P.G., Walter G. H., Smith M. T., Cooper H. M., Nilsson S. K., Tsanaktsidis J., Savage G. P., Williams C. M., Angew. Chem. Int. Ed., 2016, 55, 3580-3585 with permission from John Wiley & Sons*

Chalmers *et al.* investigated five clinical or agrochemical molecules, including suberanilohydroxamic acid (SAHA), leteprinin and benzocaine, with cubane bioisosteres inserted (Figure 35).¹²⁹

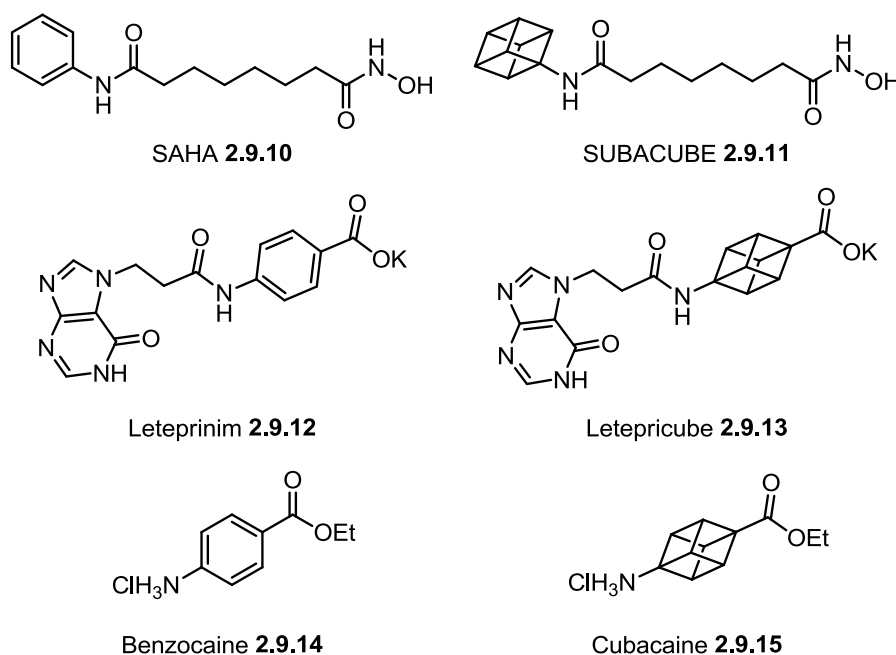


Figure 35 - Parent compound and their cubane derivative¹²⁹

Of the five cubane derivatives investigated, only one lost activity compared to its parent with two displaying increased bioactivity.¹²⁹ One such example was letepricube which displayed an increased suppression of neuronal differentiation compared to the parent neurotrophic drug leteprinin.¹²⁹ SUBACUBE and SAHA exhibited similar tumour suppression in both a cell based assay and mouse model for T-cell lymphoma.¹²⁹ Cubacaine also showed equal activity as an anesthetic in a rat model compared to its parent.¹²⁹

These examples demonstrate the successful use of a cubane as a phenyl surrogate, mostly in conjunction with a *para*-substitution pattern; however a cubane is

substantially more sterically encumbered than its phenyl equivalent and adds extra MW. Accordingly, efforts have been made to identify polycyclic systems related to cubanes which could provide the same vectors in terms of orienting substituents but without the attendant negative effects on physicochemical properties. One such framework which is of emerging interest is the bicyclo[1.1.1]pentane (BCP) moiety.

2.10 Bicyclo[1.1.1]pentane (BCP)

To date, the use of the BCP structure as a phenyl bioisostere has been reported in a limited number of examples. Firstly, Pellicciari *et al.* investigated the BCP within a metabotropic glutamate receptor (mGluR) 1 antagonist.^{130–132} This investigation built upon the work of Watkins *et al.* who discovered carboxyphenylglycines were mGluR antagonists (Figure 36).¹³³

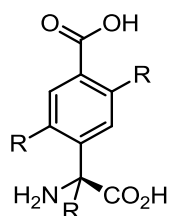


Figure 36 - General structure of mGluR antagonists

From this small subset, Pellicciari compared the phenyl **2.10.1** against the BCP **2.10.2** and cubane **2.10.3** moieties (Figure 37).^{130–132}

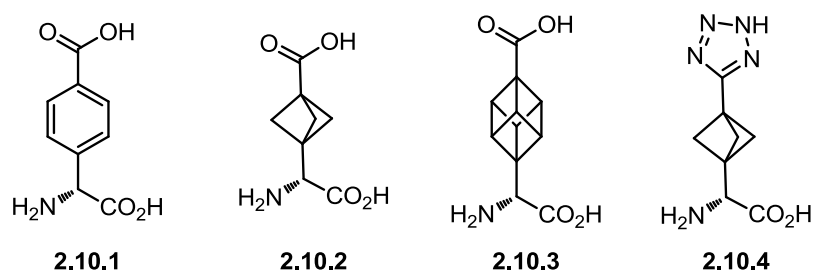


Figure 37 - mGluR antagonists

They showed that the BCP was a suitable replacement for the phenyl group displaying slightly enhanced potency, **2.10.2** IC₅₀ = 25 μM compared to **2.10.1** IC₅₀ = 44 μM. Interestingly, cubane **2.10.3**, which provides a similar distance across the rings, showed diminished potency, possibly due to the increased steric bulk it imparts (Figure 38).¹³¹ Tetrazole **2.10.4**, a known carboxylic acid replacement, was also

investigated in an attempt to mimic the distance across a phenyl ring and acid, however this also displayed reduced potency which was attributed to a change in the pK_a (Figure 38).^{131,132}

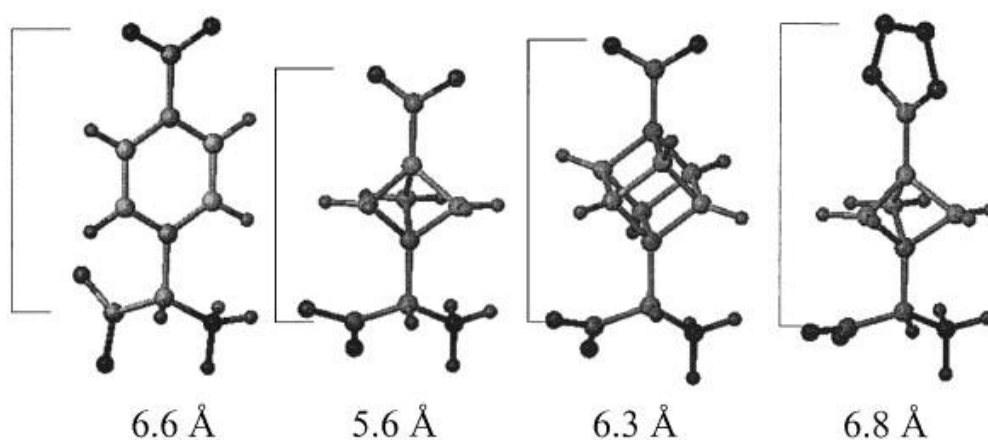
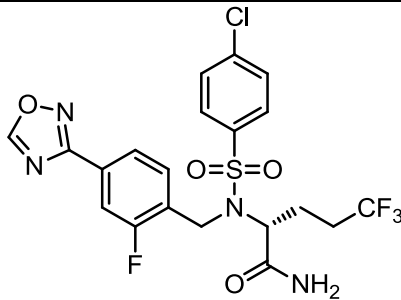
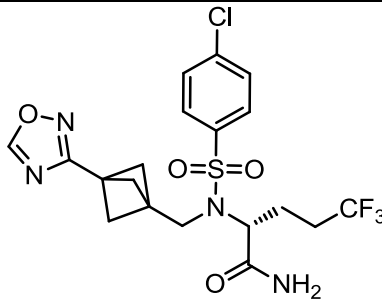


Figure 38 - Comparison of distances between pharmacophoric groups in 2.10.1, 2.10.2, 2.10.3 and 2.10.4¹³¹
Reprinted from Synthesis and biological evaluation of 2-(3'-(1H-tetrazol-5-yl)bicyclo[1.1.1]pent-1-yl)glycine (S-TBPG), a novel mGlu1 receptor antagonist, Costantino G., Maltoni K., Marinozzi M., Camaioni E., Prezeau L., Pin J-P., Pellicciari R., Bioorg. Med. Chem., 2001, 9, 221-227, Copyright 2001 with permission from Elsevier

However, this report only focused on the potency differences between the isosteres. More recently, evaluations of the physicochemical differences imparted by the BCP moiety were investigated, when Stepan and co-workers examined BCP as a phenyl ring bioisostere in a γ -secretase inhibitor **2.10.5** (Table 16).¹³⁴

Table 16 - Comparison of γ -secretase inhibitors 2.10.5 and 2.10.6¹³⁴ Reprinted with permission from: *J. Med. Chem.*, 2012, 55, 3414-3424, Copyright 2012 American Chemical Society

	 2.10.5	 2.10.6
IC₅₀ (nM)	0.225	0.178
Selectivity	350	178
Human hepatocytes (HHEP) CI	15.0	<3.80
($\mu\text{L}/\text{min}/\text{million cells}$)		
HLM CI (mL/min/kg)	<16.2	<8.17
Permeability (nm/s)	55.2	193
ELog D_{7.4}	4.70	3.80
Kinetic solubility (pH 6.5, μM)	0.60	216
Thermodynamic solubility (pH 6.5, μM)	1.70	19.7
Thermodynamic solubility (pH 7.4, μM)	0.90	29.4

Potency was maintained with the BCP analogue, albeit accompanied by a slight reduction in selectivity.¹³⁴ Permeability as well as solubility was improved, with an additional reduction in lipophilicity observed.¹³⁴ It is also noteworthy that the metabolic stability also improved, which was surprising considering the intrinsic ring strain of the system.¹³⁴ These data show the utility of the BCP as a phenyl bioisostere with an overall enhancement of the physicochemical profile.¹³⁴ These improvements can potentially be attributed to the disruption of planarity and increased 3-

dimensional character of the inhibitor **2.10.6**.¹³⁴ These inhibitors have also been explored in an *in vivo* model in which **2.10.6** demonstrated an improved oral absorption profile with good efficacy.¹³⁴

Further to this work, Stepan *et al.* have very recently published their findings when incorporating the BCP or a cubane into the imatinib template (Figure 39); an Abelson murine leukaemia viral oncogene homolog (ABL) 1 kinase inhibitor used to treat leukaemia.^{135,136}

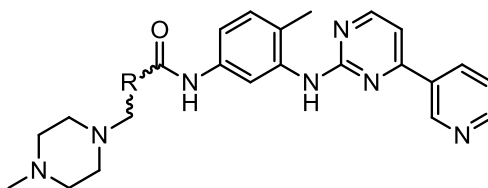
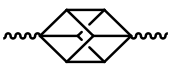


Figure 39- Imatinib template

The data show that the phenyl replacements improve the physicochemical profile with lower lipophilicity and increased solubility being exhibited by both the cubane **2.10.9** and BCP **2.10.8** analogues.¹³⁵ BCP **2.10.8** showed enhanced metabolic stability compared to both imatinib and cubane **2.10.9**, however the potency of both replacements was noticeably diminished (Table 17).¹³⁵

Table 17 - Comparison of imatinib, 2.10.8 and 2.10.9¹³⁵ *Table reproduced from Synthesis and Biopharmaceutical Evaluation of Imatinib Analogues Featuring Unusual Structural Motifs, Nicolaou K. C., Vourloumis D., Totokotsopoulos S., Papakyriakou A., Karsunky H., Fernando H., Gavriluk J., Webb D., Stepan A. F., ChemMedChem, 2015, 11, 31-37 with permission from John Wiley & Sons*

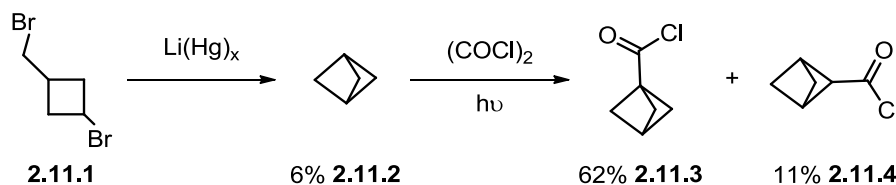
R	 imatinib 2.10.7	 2.10.8	 2.10.9
Potency (μM)	0.371	>30	>1
Fsp³	0.24	0.43	0.48
clog P	4.53	1.93	1.46
log D_{7.4}	2.45	1.51	1.67
Thermodynamic solubility (pH 7.4, μM)	30.7	2680	356
Permeability (nm/s)	82.8	65.5	94.4
HLM Cl (mL/min/kg)	18.7	<16.6	37.0
HHEP Cl (μL/min/million cells)	14.7	6.72	21.1

The significant drop in potency is potentially due to the loss of a key hydrophobic interactions within the binding site.¹³⁵ These data indicate that although the physicochemical profile should be improved, care must still be taken in selecting an aromatic group to be replaced with a bioisostere, and ideally will be informed through the use of biostructural data.

Based on the above, it was hypothesised that the BCP could be applied as a phenyl bioisostere in a lead optimisation programme of interest in our laboratory. Darapladib, an Lp-PLA₂ inhibitor discussed previously, has reached phase III clinical trials but nonetheless, it exhibits a sub-optimal physicochemical profile. As such, the previous literature in the synthesis of BCPs was examined with a view to incorporating the BCP system into the darapladib template in order to improve the physicochemical profile of the series.

2.11 Synthesis of BCP

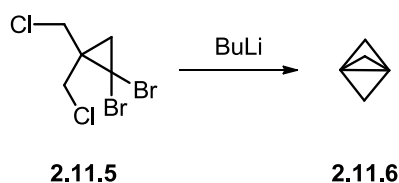
The BCP moiety has been known since the 1960s through the pioneering work of Wiberg *et al.* providing the first synthesis of the BCP using 3-bromomethylcyclobutyl bromide and lithium amalgam (Scheme 3).¹³⁷



Scheme 3 - First synthesis of BCP

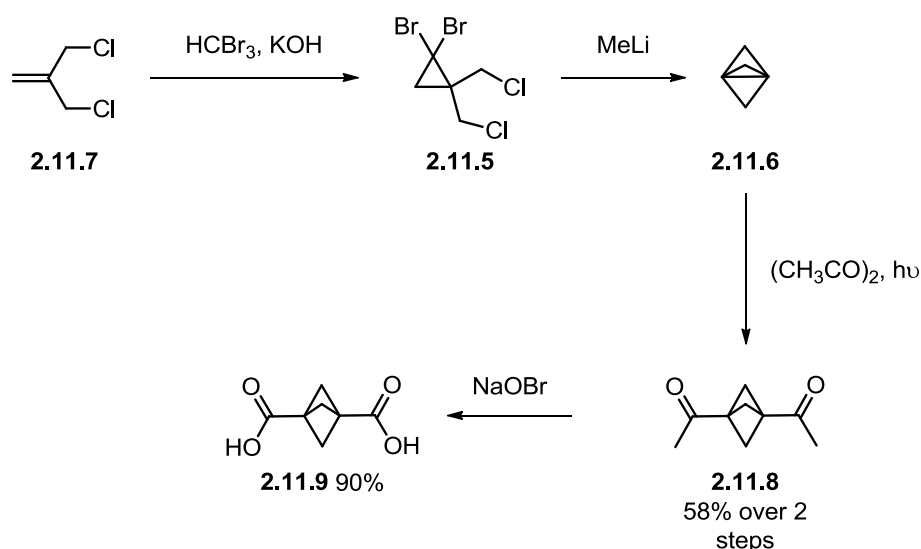
It was then possible to functionalise the BCP utilising radical chemistry to generate an acyl chloride, which could be further derivatised (Scheme 3).¹³⁸ This route to the BCP however is very low yielding and so alternative synthetic routes were desired.

Semmler *et al.* developed a route to the BCP in which they used a halogen-lithium exchange to drive a cyclisation reaction to generate a propellane (Scheme 4).^{139,140}

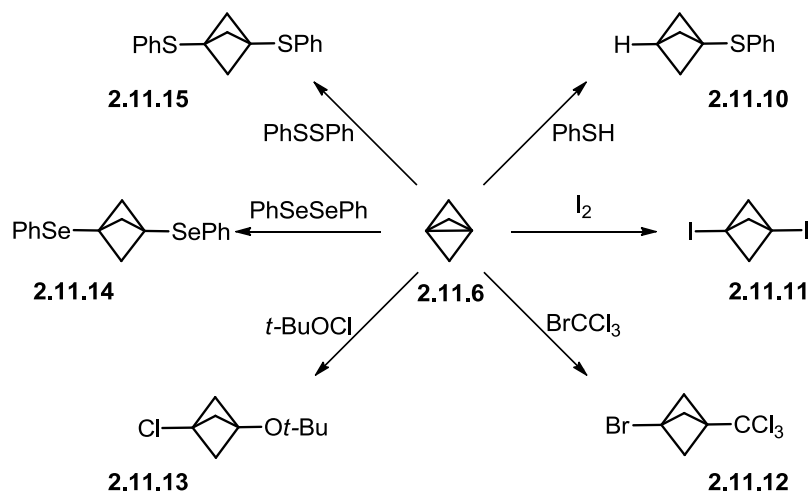


Scheme 4 - Semmler propellane generation

This propellane intermediate can be used as the basis for a variety of further functionalisation. Firstly, in 1988, Michl *et al.* reported a photochemical diacetylation of the propellane intermediate (Scheme 5).¹⁴¹

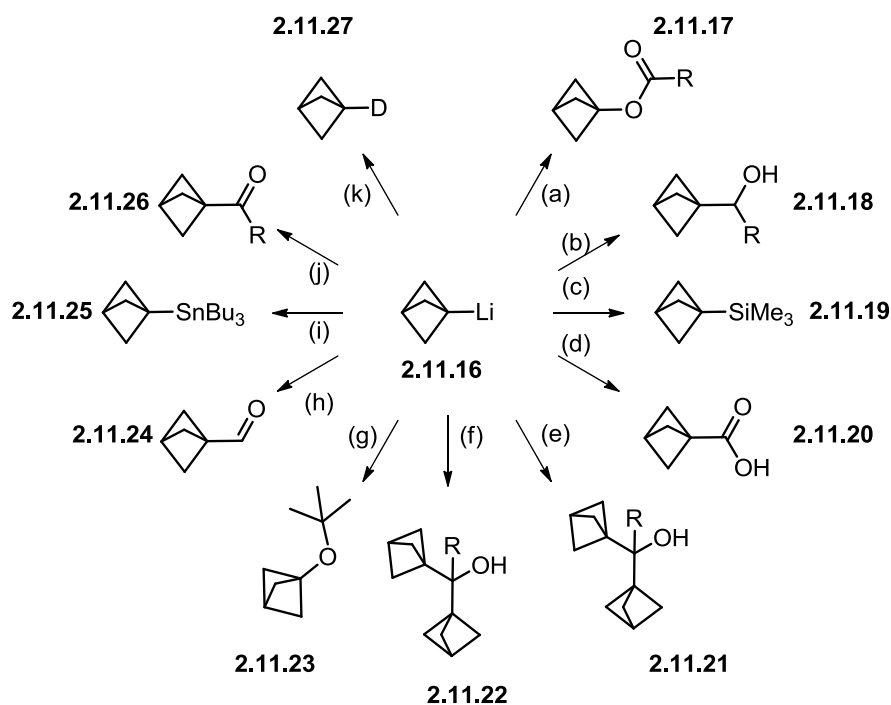
Scheme 5 - Photochemical diacetylation of propellane¹⁴¹

This radical addition to the propellane prompted further investigations into radical based reactions of propellanes. Wiberg *et al.* disclosed an extensive palette of such processes, which included iodination and addition of phenyl sulfide (Scheme 6).¹⁴²

Scheme 6 - Free radical additions to propellanes Adapted with permission from: *J. Am. Chem. Soc.*, 1990, 112, 2194-2216, Copyright 1990 American Chemical Society

This small subset was further explored by investigating radical additions of ketone and ester functionalities to the propellane intermediate with varying degrees of success.¹⁴² The variability observed was proposed to be due to the degradation of the ketone or ester functionality into further radical species. Additionally, polymerisation of the radical propellane was observed and difficult to control.¹⁴²

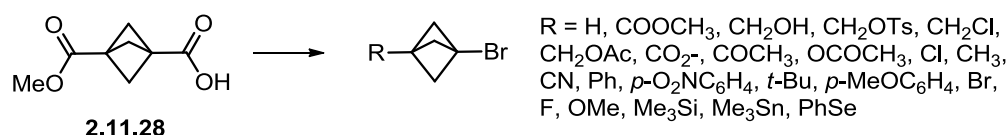
Building on the work of Screttas,¹⁴³ Wiberg and co-workers were also able to utilise the phenylthioether propellane (Scheme 6) to form the lithiated propellane, and functionalise this intermediate in a variety of ways (Scheme 7).¹⁴²



Scheme 7 - Functionalisation of lithiated propellane¹⁴² (a) = i) O_2 , ii) $RCOCl$, $R = t-Bu, Ph$ (b) = $RCHO$, $R = t-Bu, Ph$ (c) = $TMSCl$ (d) = i) CO_2 , ii) H^+ (e) = RCO_2Me , $R = t-Bu, Ph$ (f) = $RCOCl$, $R = t-Bu, Ph$ (g) = $t-BuOOt-Bu$ (h) = methyl formate (i) = Bu_3SnCl (j) = RCN , $R = t-Bu, Ph$ (k) = $MeOD$ Adapted with permission from: *J. Am. Chem. Soc.*, 1990, 112, 2194-2216, Copyright 1990 American Chemical Society

This work demonstrated how the utility of the organolithium intermediate could be used to enable the formation of a plethora of monosubstituted propellane moieties.

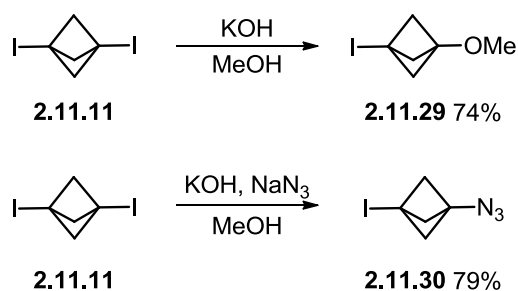
With the generation of the propellane intermediate now being readily reproducible, the synthesis of difunctionalised BCP systems utilising this intermediate was desired. Building upon the previously discussed synthesis of the symmetrical diester **2.11.8**¹⁴¹ and work by Eaton *et al.*,¹⁴⁴ the desymmetrisation of the diester and subsequent selective functionalisations of the half-ester **2.11.28** was investigated by Della *et al.*¹⁴⁵ This work gave access to a variety of difunctionalised systems utilising a range of different chemistry (Scheme 8).¹⁴⁵



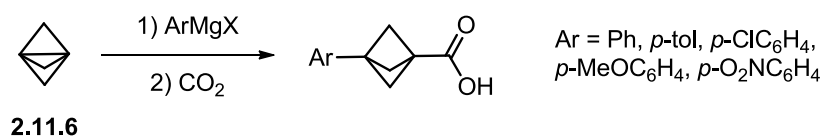
Scheme 8 - Generation of a multitude of bifunctionalised BCPs

It should be stated, however, the generation of these compounds occasionally required several steps with variable yields and/or the use of harmful reagents.

Utilising the di-iodinated BCP **2.11.11** Wiberg *et al.* extended their original work by investigating the generation of a BCP cation or anion species.¹⁴⁶ He observed that adding methoxide to **2.11.11** led to the generation of **2.11.29** in good yield (Scheme 9).¹⁴⁶ Investigation into the mechanism suggested the formation of the tertiary carbocation, which was then quenched with methoxide.¹⁴⁶ Additionally, he utilised this methodology to incorporate an azide to generate **2.11.30** (Scheme 9).¹⁴⁶

Scheme 9 - Synthesis of **2.11.29** and **2.11.30**

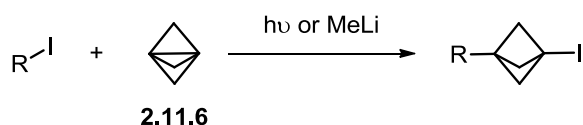
During this research Wiberg also investigated the addition of Grignard reagents across the propellane **2.11.6** and subsequent trapping of the resulting metalated species with carbon dioxide to generate the acid (Scheme 10).¹⁴⁶



Scheme 10 - Addition of Grignard reagents across propellane

This work has been enhanced by the use of cross-coupling methodology with the intermediate metalated species.¹⁴⁷ This investigation exemplified the effectiveness of nickel and palladium catalysis to couple a variety of aromatic and vinylic substituents to the BCP.¹⁴⁷ Furthermore, they studied the addition of alkyl and aryl

iodides to the propellane unit using either a photochemical radical addition or methyl lithium mediated additions (Scheme 11).¹⁴⁷

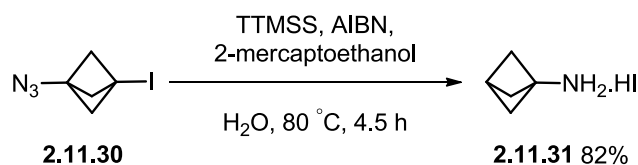


R = Me, ⁿPr, ⁿBu, ⁿC₇H₁₅, ⁿC₈H₁₇,
THPO(CH₂)_n, CH₃CH₂C≡CCH₂CH₂I, Cy,

Scheme 11 - Addition of alkyl or aryl iodides to propellane

Treatment of the iodide with *tert*-butyllithium or lithium 4,4'-di-*tert*-butylbiphenylide generates the lithiated species, which could in turn be converted into the zincate.¹⁴⁷ Subsequent palladium cross-coupling with these species was facile, producing a further enhancement of substrate scope.¹⁴⁷

It was not until nearly a decade later that the generation of the iodo-azide BCP **2.11.30**, mentioned previously (Scheme 9), was utilised as a basis for the synthesis of a terminal BCP amine (Scheme 12).¹⁴⁸ Adsool *et al.* investigated a variety of reducing agents, such as lithium aluminium hydride and tin hydride, before settling on the tin hydride replacement tris(trimethylsilyl)silane (TTMSS).¹⁴⁸ This was used to generate the desired terminal BCP **2.11.31** in good yield on a multigram scale.¹⁴⁸



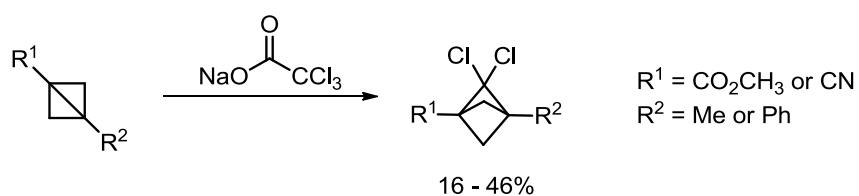
Scheme 12 - Terminal BCP amine synthesis¹⁴⁸

The most recent work on the BCP system has come from the Baran group, who have developed a so called strain release amination, which essentially builds on Wiberg's earlier work.^{146,149} This research focused on identifying a more scalable route to a variety of BCP amines. Using the propellane intermediate and a metalated nitrogen source, generation of over 25 amines with a terminal BCP was accomplished (Scheme 13) and the methodology was applied to six pharmaceuticals.¹⁴⁹



Scheme 13 - Strain release amination

It is worth noting that, at the outset of the current study, neither of the aforementioned scalable syntheses of BCP amine **2.11.31** had been published and there remained a need for methodology that provided robust access to BCP derivatives. Prior to the propellane derived route, Applequist *et al.* developed a synthesis of the disubstituted BCP which involved the addition of a dichlorocarbene across a bicyclo[1.1.0]butane (Scheme 14).¹⁵⁰

Scheme 14 - Applequist synthesis of BCP¹⁵⁰

This investigation examined a small range of substituents and their subsequent functionalisation. Wiberg *et al.* later exploited this methodology to generate a fully deuterated propellane.¹⁵¹

2.12 Aims and proposed work: application of the BCP bioisostere to Lp-PLA₂ inhibitors

Considering the evidence supporting the improvement in the physicochemical profile when utilising the BCP as a phenyl bioisostere, it was reasoned that this moiety could be applied to the darapladib scaffold, postulating that replacing one of the three aromatic rings would provide an improvement in the physicochemical profile of the compound.

As mentioned previously, disrupting any potential π -stacking or hydrophobic interactions can have a deleterious effect on the potency. This was important when considering the darapladib structure as there are three potential aromatic rings which could be replaced with the BCP system. The crystal structure of darapladib bound to Lp-PLA₂, solved in-house and comparable to the structure recently published,⁴³ could be used to make an informed choice as to which ring to replace. Therefore, all three possible permutations involving switching of each phenyl with a BCP were modelled in the binding site of Lp-PLA₂ at each different position (Figure 40). This was modelled using the Molecular Operating Environment (MOE) software using the crystal structure of darapladib generated in our laboratories.¹⁵² The structures were optimised using LigX and the Amber12/Extended Hückel theory (EHT) forcefield and generalised Born/volume integral implicit (GBVI) solvation model.¹⁵²⁻¹⁵⁴

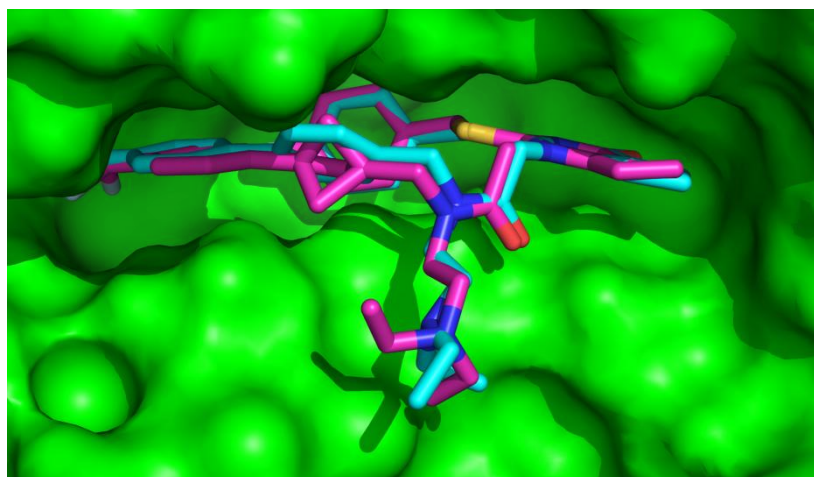
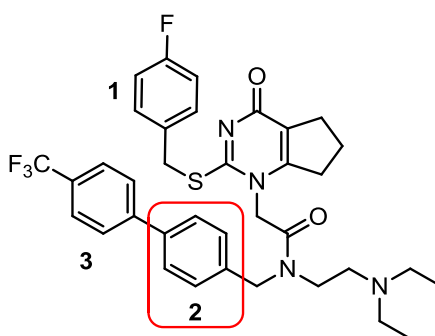


Figure 40 - Modelling of bioisosteric phenyl replacement overlaid with X-ray crystal structure of bound darapladib

Comparison of these models suggested phenyl system 2 was the ring of choice for replacement as it appeared to be acting primarily as a spacer unit rather than being essential to binding (Figure 41).

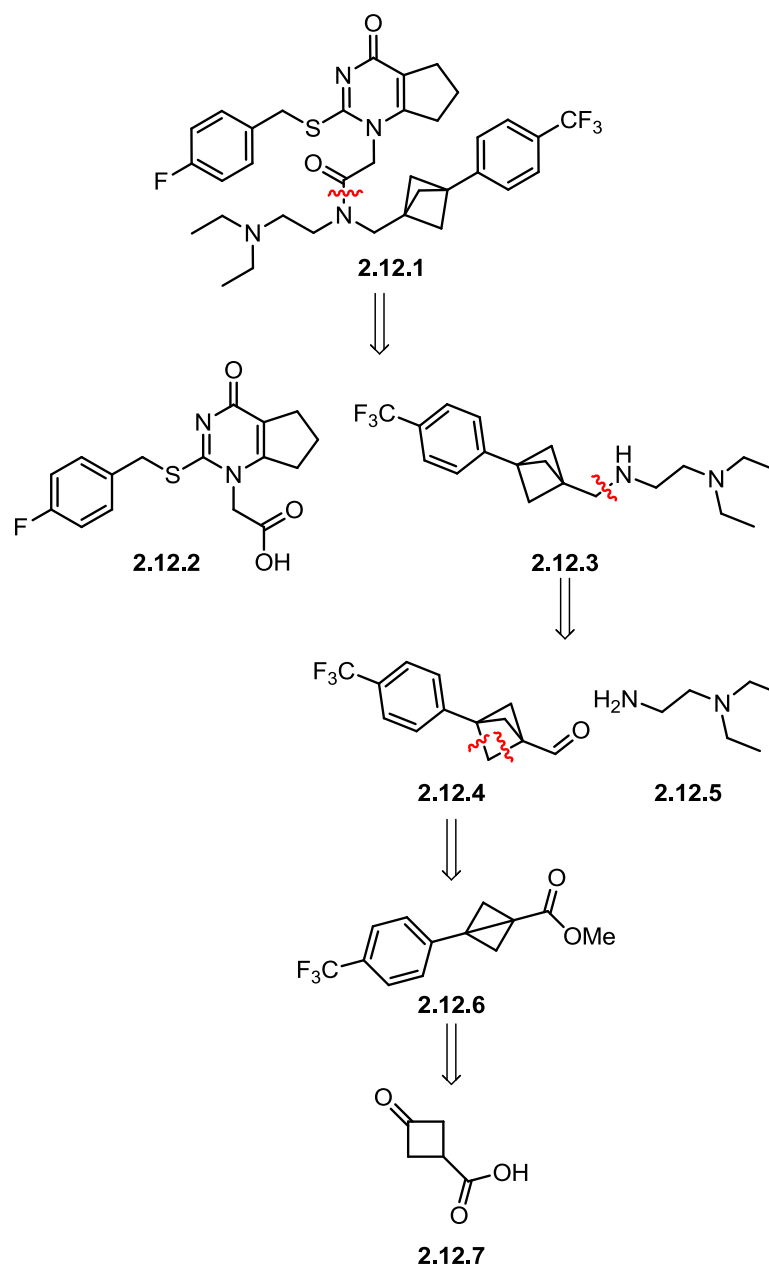


1.3.1

Figure 41 - Potential phenyl rings to be replaced

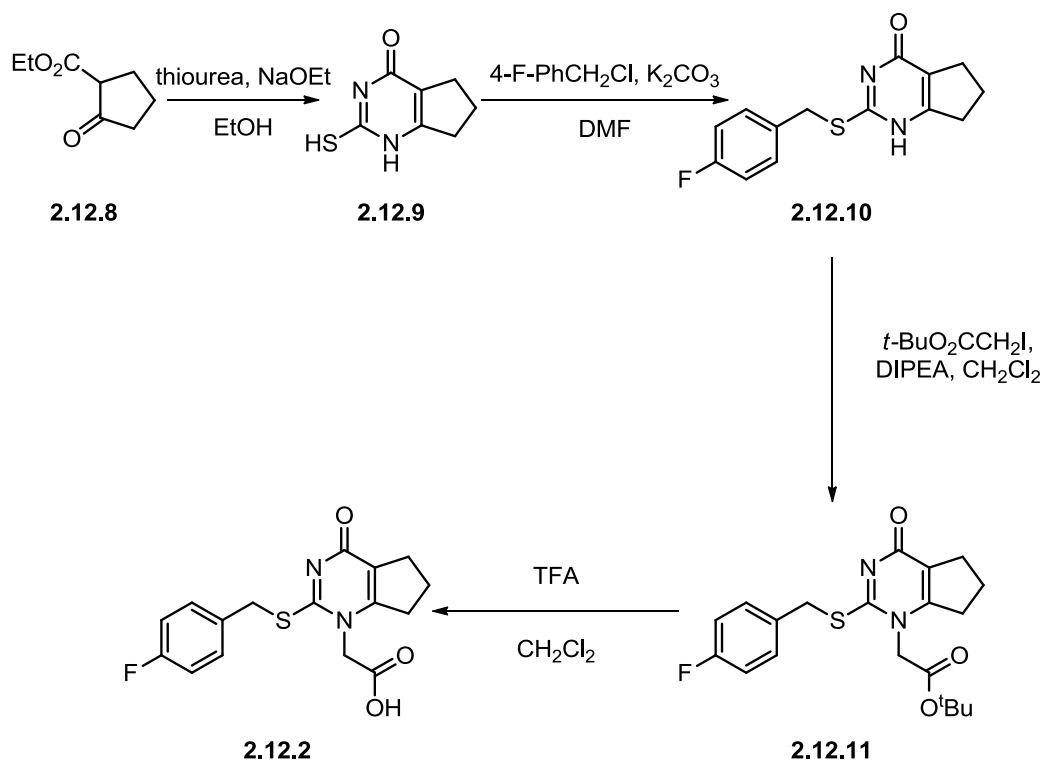
It was reasoned that incorporation of the BCP at this position would potentially enhance the physicochemical profile whilst potentially having limited impact on potency. It is also worth noting that modification of the biaryl unit would potentially lead to a yet greater improvement in physicochemical profile by disrupting the planarity of the extended π -system.

Based on the information available at the time, it was envisaged that access to the BCP target would require the application of the propellane or bicyclo[1.1.0]butane methodology described earlier. The propellane route has significant challenges associated with the incorporation of the required functionality as well as issues regarding handling and instability. As such, the dichlorocarbene method¹⁵⁰ (Scheme 14) was considered as the most tractable route to the desired BCP system with the investigation of alternative carbene sources leading to a potential improvement. Using this information, a retrosynthetic analysis was applied to the desired target compound **2.12.1** (Scheme 15). It was anticipated that **2.12.1** could be split into two fragments with an amide coupling being utilised in the final step to combine **2.12.2** and **2.12.3**.



Scheme 15 - Retrosynthetic analysis of darapladib analogue

The synthesis of fragment **2.12.2** has been previously reported by Blackie *et al.* in the process scale route towards darapladib (Scheme 16).³⁴

Scheme 16 - Blackie *et al.* synthesis of 2.12.2³⁴

The retrosynthetic analysis of **2.12.3** leads back to the commercially available ketoacid **2.12.7**. Initially, an organometallic addition to **2.12.7** and subsequent functional group interconversions could set up a cyclisation to the key intermediate **2.12.6**, which can in turn be used to generate the BCP structure using a carbene addition. Subsequent manipulation can lead to the amine coupling partner **2.12.3**. The synthesis of this fragment can also be modified to generate the amine coupling partner **2.12.12** for the incorporation into rilapladib (Figure 42).

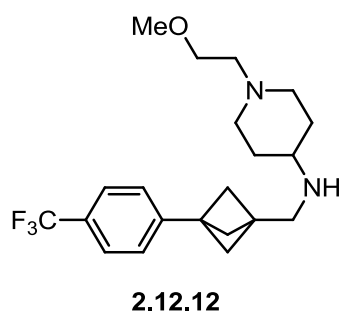


Figure 42 – Potential coupling partner for incorporation into rilapladib

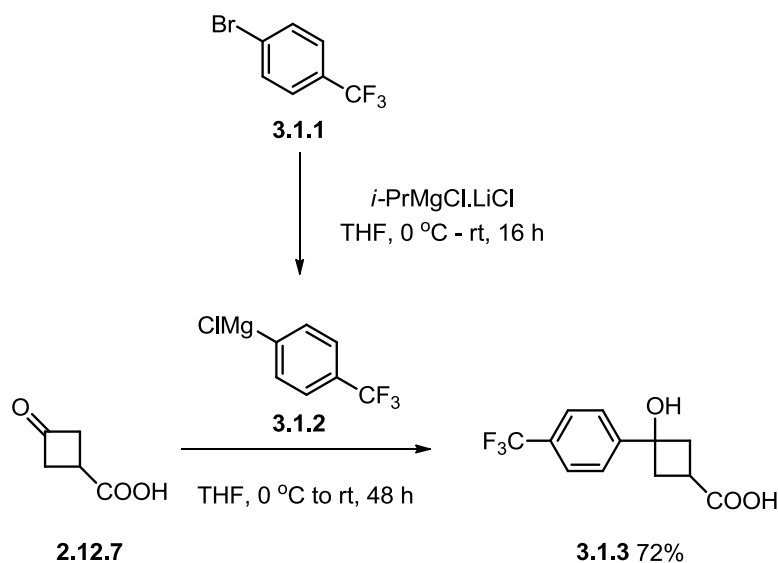
The aim of this project was therefore to incorporate the BCP moiety into the two Lp-PLA₂ inhibitors darapladib and rilapladib in order to enhance their physicochemical

profiles. Furthermore, improvement and development of the current BCP synthesis was desired.

3.0 BCP analogue as a phenyl bioisostere

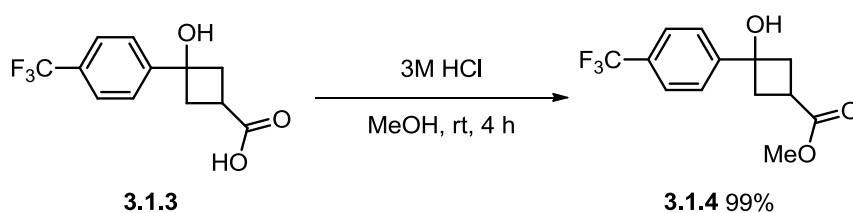
3.1 Synthesis of BCP analogues of Lp-PLA₂ inhibitors

It was anticipated that the first step in the synthesis of the proposed darapladib BCP analogue could be achieved by organometallic addition to a commercially available ketone. Indeed, addition of a readily accessible Grignard reagent **3.1.2** to ketone **2.12.7** furnished carboxylic acid **3.1.3**. The preparation of the organometallic was accomplished *in situ* by treating 1-bromo-4-(trifluoromethyl)benzene with isopropylmagnesium lithium chloride (turbo Grignard¹⁵⁵) (Scheme 17).



Scheme 17 – Initial Grignard addition to ketone **2.12.7**

The initial proposal was to convert acid **3.1.3** to the corresponding methyl ester **3.1.4**, then the alcohol into a suitable leaving group to facilitate the subsequent cyclisation step. Accordingly, transformation of carboxylic acid **3.1.3** to the methyl ester **3.1.4** proceeded in near quantitative yield (Scheme 18).



Scheme 18 – **3.1.4** ester formation

Following on from this, conversion of the benzylic OH group to a suitable leaving group such as a mesylate, tosylate or chloride was considered. Mesylate formation was investigated first due to its relative ease. Initial conditions involved using mesyl

chloride and triethylamine (Table 18, Entry 1). Unfortunately, the desired mesyl compound could not be isolated.

Table 18 – Conditions investigated for conversion of alcohol into a suitable leaving group

3.1.4

Entry	Conditions	LG	Observation
1	MsCl, Et ₃ N	OMs	Unable to isolate product
	CH ₂ Cl ₂ , rt, 4 h	3.1.5	
2	MsCl, py	OMs	Only SM observed
	THF, rt, 4 h	3.1.5	
3	TsCl, Et ₃ N	OTs	Only SM observed
	CH ₂ Cl ₂ , rt, 24 h	3.1.6	
4	HCl (4M in 1,4-dioxane)	Cl	Only SM and ester hydrolysis
	1,4-dioxane, 50 °C, 24 h	3.1.7	
5	HCl (4M in 1,4-dioxane)	Cl	Ester hydrolysis and starting material
	1,4-dioxane, MgSO ₄ , 50 °C, 48 h	3.1.7	
6	InCl ₃ , Me ₂ SiHCl, MeOH, PhC(O)C(O)Ph	Cl	Only SM observed
	CH ₂ Cl ₂ , rt, 16 h	3.1.7	
7	SOCl ₂ , Et ₃ N	Cl	Product formation, very unclean profile unable to isolate
	CH ₂ Cl ₂ , rt, 5 h	3.1.7	

A variety of alternative conditions were investigated (Table 18). Replacing the base and the solvent was not successful (Table 18, Entry 2). Using a tosylate as an alternative leaving group did not afford product either (Table 18, Entry 3). Another alternative leaving group that was considered was a chloride. Initially, stirring **3.1.4** in hydrochloric acid was considered, however only starting material and some hydrolysis of the ester was observed (Table 18, Entry 4). In order to mitigate against this and potentially drive the reaction forward, magnesium sulfate was added as a desiccant (Table 18, Entry 5). Unfortunately, this produced no change to the reaction profile. An alternative method developed by Yasuda *et al.* using indium chloride was

examined (Table 18, Entry 6).¹⁵⁶ Disappointingly, this resulted in an unsuccessful reaction with only starting material observed. Using thionyl chloride as an alternative chlorinating agent produced the first evidence of successful conversion, however this reaction produced a complex mixture of products and no desired product was isolated (Table 18, Entry 7). With the isolation of the product being an issue, the *in situ* generation of the mesylate and subsequent cyclisation to the desired bicyclobutane system **2.12.6** was explored (Table 19).

Table 19 – Mesylate formation and subsequent cyclisation conditions

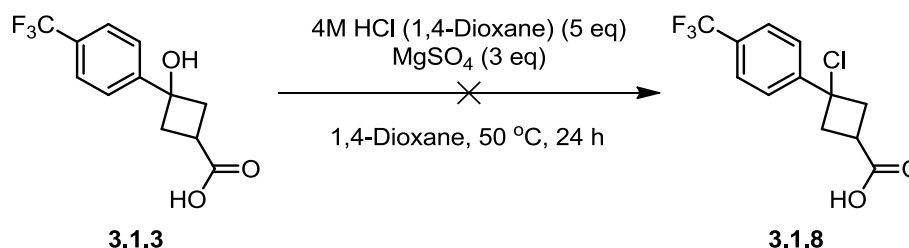
Entry	Conditions	Observation
1	NaH (2.4 eq), MsCl THF, 60 °C, 16 h	No desired product isolated
2	1) NaH, MsCl, THF, rt, 4 h 2) NaH, THF, 66 °C, 16 h	Only starting material recovered
3	1) Et ₃ N, MsCl, THF, 0 °C - rt, 4 h 2) NaH, THF, rt, 16 h	No desired product isolated

The three conditions investigated were; first using two equivalents of sodium hydride in the reaction mixture from the outset (Table 19, Entry 1); second with sequential addition of sodium hydride (Table 19, Entry 2); and third with initial use of triethylamine followed by the addition of sodium hydride (Table 19, Entry 3).^{151,157} Unfortunately, all of these experiments failed to generate desired product, presumably due to the instability of the material. It was hypothesised that the stability of the benzylic tertiary carbocation generated upon loss of the leaving group would facilitate regeneration of the starting material.

With the numerous issues encountered while attempting to convert the alcohol substituent of **3.1.4** into a suitable leaving group, the transformation using acid **3.1.3** was examined. Sieja *et al.* have previously reported the synthesis of the

bicyclobutane system as a means to generate polymers.¹⁵⁸ This method involves shaking the compound in a mixture of concentrated HCl and benzene. In order to avoid the use of carcinogenic benzene, modification of these conditions was explored.

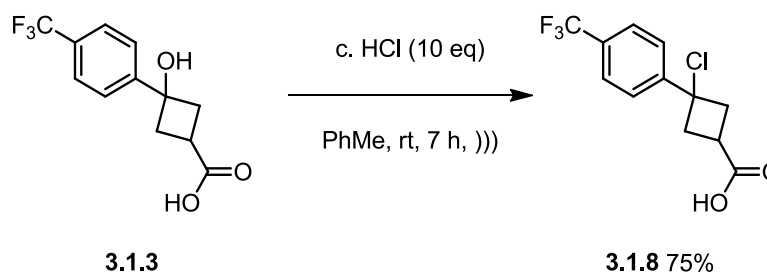
The S_N1 displacement of the alcohol was attempted on acid **3.1.3** under similar conditions to those used on ester **3.1.4**; however no conversion was observed (Scheme 19).



Scheme 19 – Initial chlorination condition of **3.1.3**

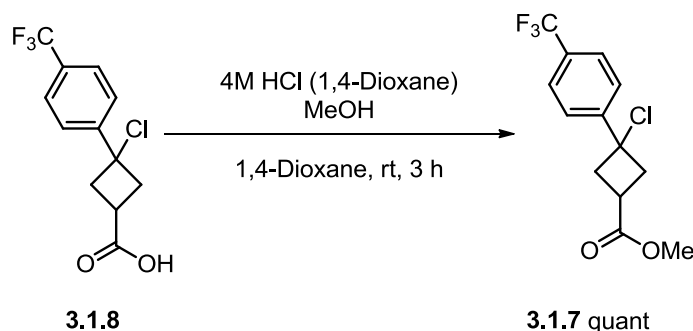
In order to more closely mimic the conditions used by Sieja *et al.*,¹⁵⁸ **3.1.3** was shaken with conc. HCl in toluene, as a safer alternative. Despite this not producing any product, it was noted that the solubility of the acid under these conditions was poor. In a slight modification to the published procedure sonication was employed. It was believed that this would aid solubilisation of acid **3.1.3** as well as provide a simpler method of agitating the reaction mixture for a prolonged period of time.

On small scale (100 mg), this reaction worked well with full conversion to desired chloride **3.1.8** after just 1 h. However, when this reaction was scaled up to ~16 g it took 7 h to achieve full conversion with an isolated yield of 75% (*mixture of diastereomers*), some product potentially being lost in the aqueous phase (Scheme 20). The time discrepancy was attributed to the smaller surface area to volume ratio between the organic and aqueous phases on a larger scale.



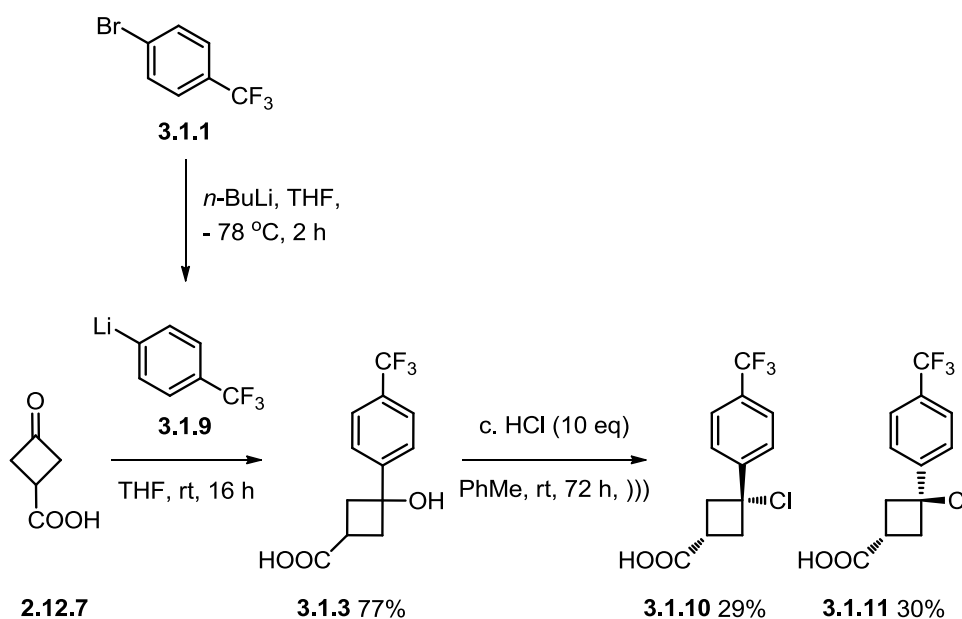
Scheme 20 – ultrasound assisted chlorination of **3.1.3**

With acid **3.1.8** in hand, conversion to the corresponding ester **3.1.7** was achieved in quantitative yield as a mixture of diastereomers (Scheme 21).



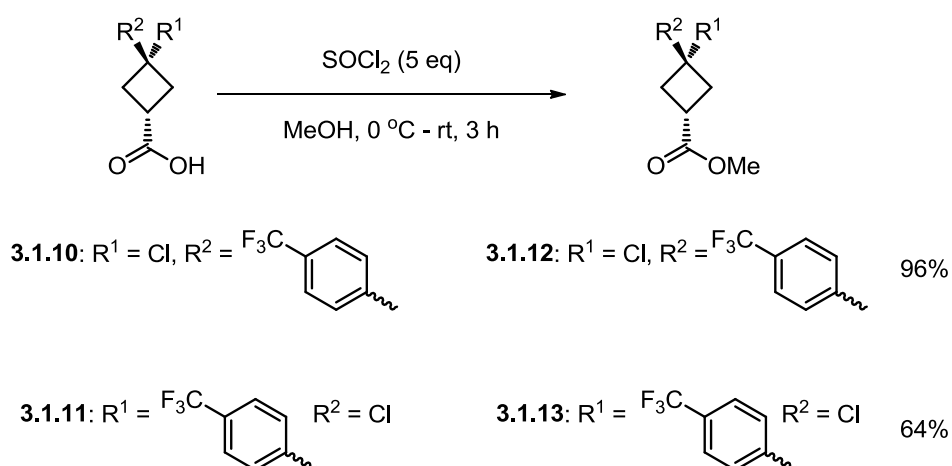
Scheme 21 – Ester **3.1.7** formation

After the route to **3.1.7** had been optimised, large scale synthesis was conducted *via* an external collaboration (Scheme 22).¹⁵⁹ **3.1.7** was accessed on a multigram scale with slight modifications to the planned procedure. Interestingly, the isomers of **3.1.8** could be separated *via* trituration with **3.1.10** remaining as solid and **3.1.11** dissolving in the solvent (hexane).



Scheme 22 – Outsourced synthesis of **3.1.8** and separation of the isomers **3.1.10** and **3.1.11**

Initial addition to ketone **2.12.7** was achieved in good yield using *n*-butyllithium as the metalating agent. Subsequent conversion of **3.1.3** to **3.1.8**, using the newly developed sonication methodology, proceeded in good yield with separation of the diastereomers (**3.1.10** and **3.1.11**) achieved at this stage, as noted above (Scheme 22).



Scheme 23 – Conversion of the isomers 3.1.10 and 3.1.11 into the corresponding methyl esters

Conversion of the individual isomers **3.1.10** and **3.1.11** to their corresponding ester derivatives **3.1.12** and **3.1.13** was achieved using thionyl chloride in good to excellent yields (Scheme 23).

With intermediates **3.1.12** and **3.1.13** in hand, the cyclisation to bicyclobutane **2.12.6** was now possible. The cyclisation step proved to be somewhat capricious with isolated yields particularly dependent on scale (Table 20).

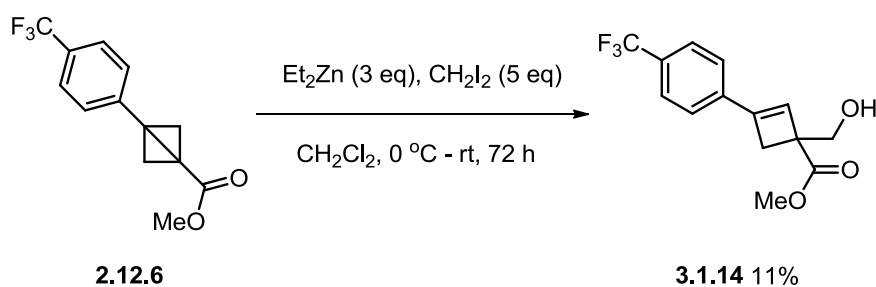
Table 20 – Cyclisation reaction with varying yields on different scales

Entry	Scale (g)	Yield Range
1	< 1	0 – 35%
2	1 – 5	59 – 72%
3	50	98%

This trend was rationalised by the presence of adventitious water reacting with the sodium hydride to produce hydroxide. This was supported by LCMS evidence in the small scale reaction where conversion of the ester to the acid was observed.

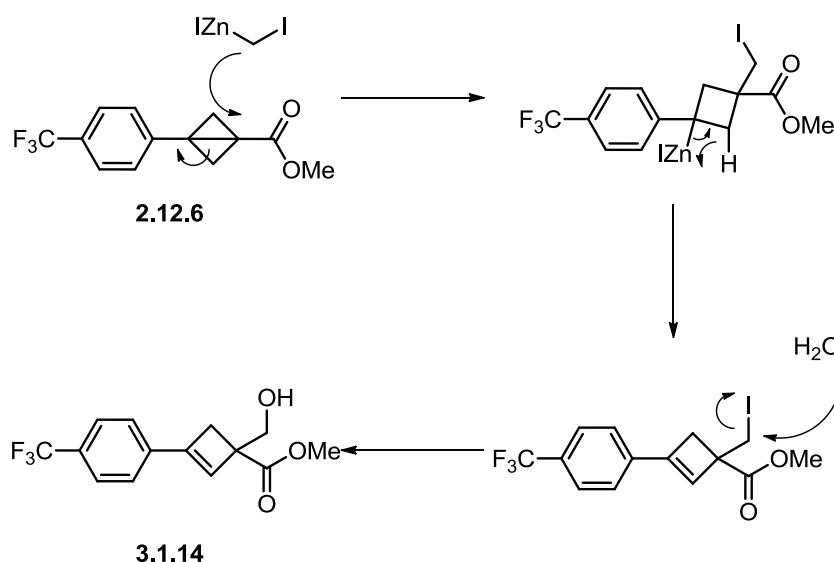
With access to **2.12.6** now achieved, the key step in the BCP synthesis was to perform a cyclopropanation on the central bond of bicyclobutane **2.12.6**. Previous

literature in this area only reported a handful of successful reactions, on a small number of substrates utilising a dichlorocarbene addition, followed by dechlorination using tributyltin hydride.^{150,151} It was proposed that the use of alternative cyclopropanation reagents might achieve this transformation without the need for a dechlorination step. To this end, initial reactions focused on using Simmons-Smith reagents.¹⁶⁰ The first attempt used diethylzinc and diiodomethane, however the desired product was not isolated. Instead cyclobutene **3.1.14** was isolated, albeit in low yield (Scheme 24).



Scheme 24 – Isolation of undesired by-product **3.1.14**

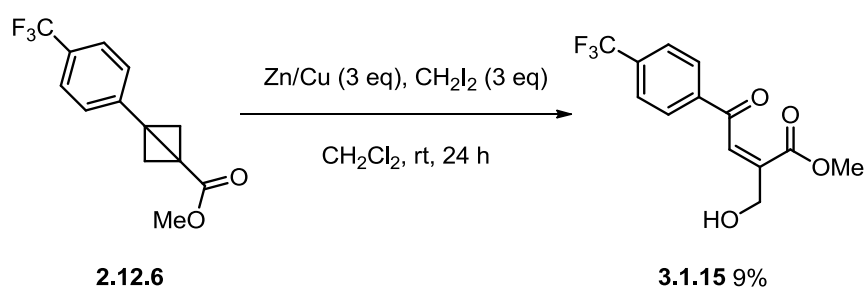
The proposed mechanistic rationale for the formation of this by-product suggested that addition of the carbene species was occurring without subsequent cyclisation. It was hypothesised that a β -hydride elimination was occurring, more readily than cyclisation, to generate the cyclobutene system. The iodide could then react with water upon work-up to generate the primary alcohol **3.1.14** (Scheme 25).



Scheme 25 – Potential mechanistic rationale for **3.1.14** formation

This reaction was repeated in order to isolate the undesired product **3.1.14** for full characterisation, however this was unsuccessful. Further attempts to repeat this reaction also proved unsuccessful, even on a larger scale (1 g), which casts doubt on the general utility of using this approach in the preparative sense. Based on this, no further work was undertaken to investigate this process.

Alternative Simmons-Smith conditions were investigated utilising zinc/copper powder and diiodomethane. Interestingly a different undesired product **3.1.15** was isolated in this case (Scheme 26).^{161,162}

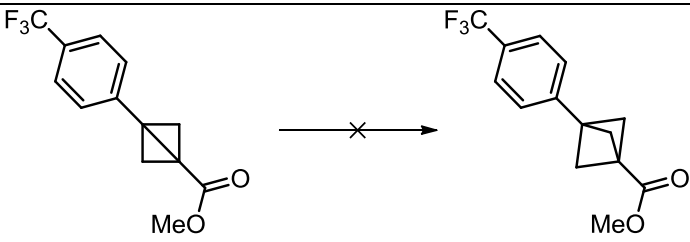


Scheme 26 – Isolation of undesired by-product **3.1.15** under Simmons-Smith conditions

This experiment was also repeated with a view to isolate further product, however again this was unsuccessful. It was proposed that this was a degradation product in which the zinc copper couple was acting as an oxidant as well as inducing ring-opening.

It has been suggested that the central bond of the bicyclobutane can be thought of as a pseudo-alkene due to its considerable p-character.^{163–167} Consequently, alternative cyclopropanation reactions known to work on olefins were considered. Due to the highly electron-deficient nature of bicyclobutane **2.12.6**, use of a Corey-Chaykovsky cyclopropanation was examined (Table 21).

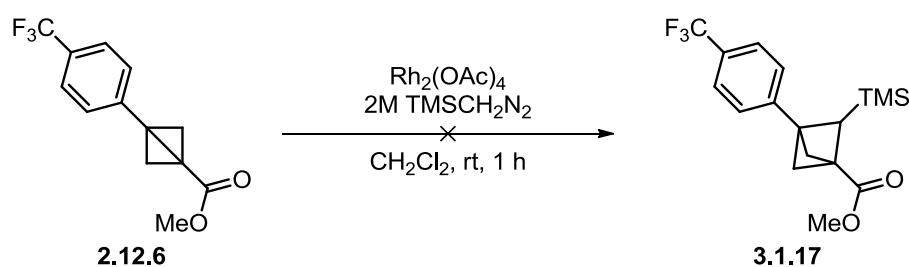
Table 21 – Corey-Chaykovsky cyclopropanation conditions investigated



2.12.6
3.1.16

Entry	Conditions	Scale (g)
1	(CH ₃) ₃ S(O)Cl, NaH (pre-stirred for 30 mins) DMSO, rt – 65 °C, 1.5 h	0.2
2	(CH ₃) ₃ S(O)Cl, NaH (pre-stirred for 30 mins) THF, rt – 70 °C, 1.5 h	0.2
3	(CH ₃) ₃ S(O)Cl (Dried), NaH (pre-stirred for 30 mins) THF, rt – 70 °C, 3.5 h	0.5
4	(CH ₃) ₃ S(O)Cl (Dried), NaH (pre-stirred for 30 mins) THF, rt – 70 °C, 3.5 h	2

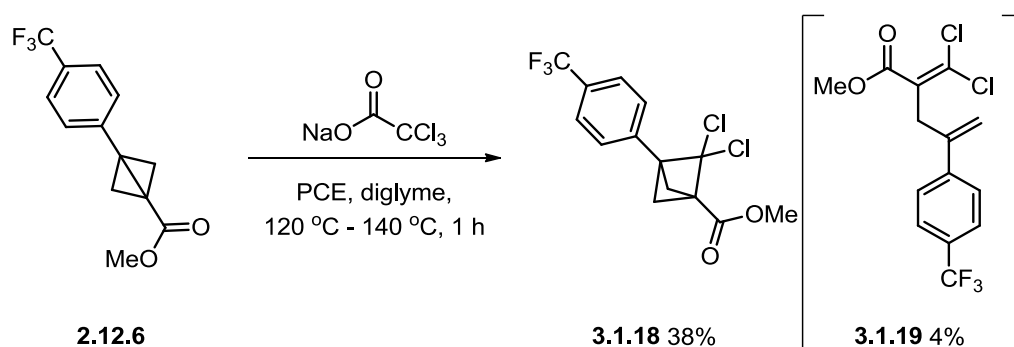
Varying the reaction conditions, such as solvent and drying the trimethylsulfoxonium chloride,¹⁶⁸ did not result in any product formation, with all reaction profiles being particularly unclean. As such, an alternative cyclopropanation utilising a rhodium carbene was considered.¹⁶⁹ However, again this reaction proved ineffective (Scheme 27).



Scheme 27 – Alternative rhodium diazocarbene investigation

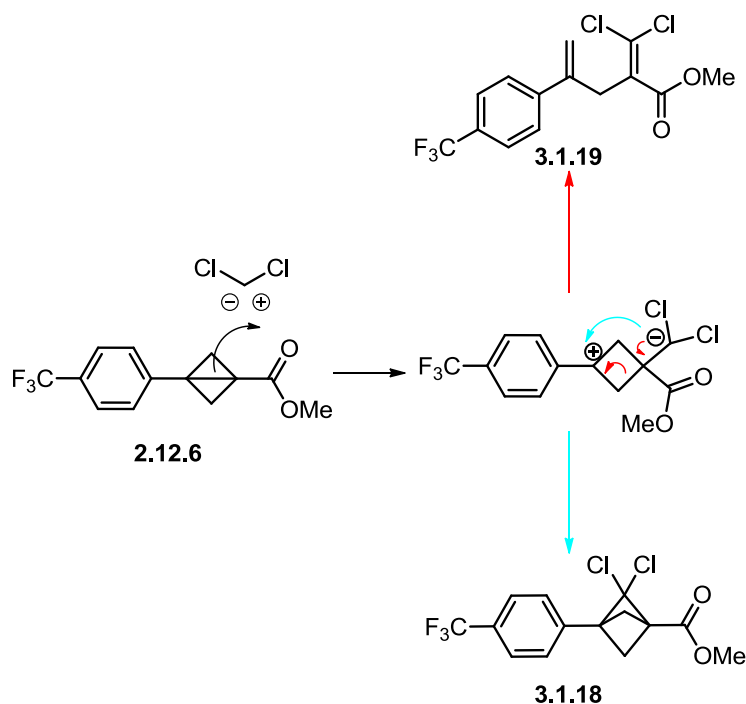
With the alternative carbene sources resulting in degradation of starting materials into unknown by-products, the literature preceded dichlorocarbene methodology was investigated.^{150,151} The initial attempt using the reported procedure was employed on a small scale. This unfortunately did not provide any improvement compared to the previously described carbene methods. The literature examples were

performed on larger scale, as such the reaction was repeated on a 5 g scale. Pleasingly, this produced the desired compound **3.1.18** in a reasonable yield when compared with the literature (Scheme 28).



Scheme 28 – Dichlorocarbene addition to **2.12.6**

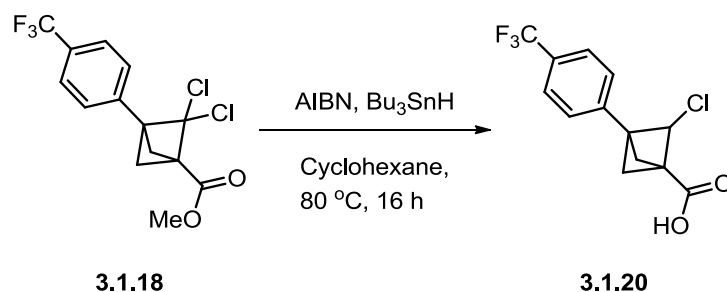
Additionally, by-product **3.1.19** was isolated. This could be rationalised by initial nucleophilic attack of the bicyclo[1.1.0]butane on the dichlorocarbene generated *in situ* (Scheme 29). This is followed by either cyclisation to the desired BCP ring system **3.1.18** or elimination to give the unstable by-product **3.1.19**.



Scheme 29 – Proposed mechanism for dichlorocarbene reaction

With a sufficient quantity of **3.1.18** in hand, the next step was removal of the chlorine from the BCP **3.1.18**. Literature procedures used tributyltin hydride in a

radical dechlorination, and this was attempted upon **3.1.18**.^{150,151} However, analysis of the reaction mixture using LCMS suggested the production of the mono-chlorinated analogue **3.1.20** but isolation of this material proved unsuccessful (Scheme 30).



Scheme 30 – Investigation into literature precedented dechlorination conditions

In parallel to applying the reported conditions, alternative methods were investigated. These included using hydrogenation methodology with either a nickel¹⁷⁰ or palladium catalyst, as well as the use of triethylsilane with aluminium chloride;¹⁷¹ however in each case only starting material was observed (Table 22).

Table 22 – Alternative dechlorination conditions

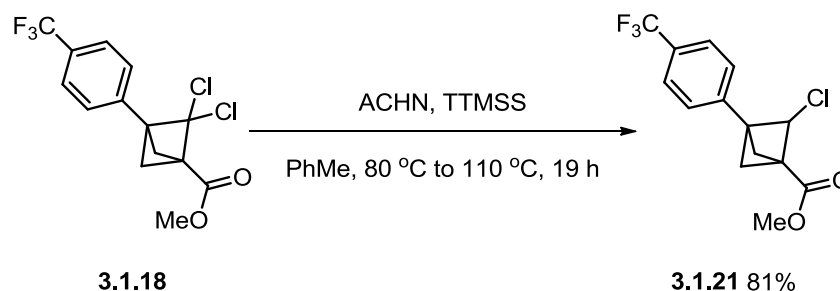
3.1.18
3.1.16

Entry	Conditions
1	Pd/C, H ₂ , EtOH, rt, 48 h
2	Ni, H ₂ , KOH, EtOH, rt, 60 h
3	AlCl ₃ , Et ₃ SiH, CH ₂ Cl ₂ , rt, 16 h

Alternative conditions utilising the less toxic TTMSS as the dechlorination agent were next investigated. This reagent has been shown to be an effective replacement for tin hydrides in other dechlorination reactions and has additionally been used successfully in the monodechlorination of a similar system.^{132,172,173}

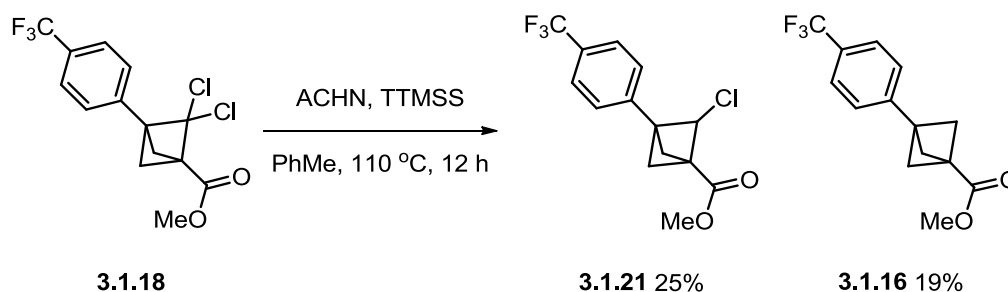
The initial attempts using the literature conditions using AIBN and TTMSS produced a disappointing yield of 27%.¹³² Repetition of this reaction using 1,1'-

azobis(cyclohexanecarbonitrile) (ACHN) as a more stable initiator was considered. Initially, heating the reaction for 16 h gave a 60% conversion of starting material **3.1.18** to product **3.1.21**. With the addition of extra initiator and increasing the temperature, the monochlorinated BCP **3.1.21** was produced in good yield (Scheme 31).



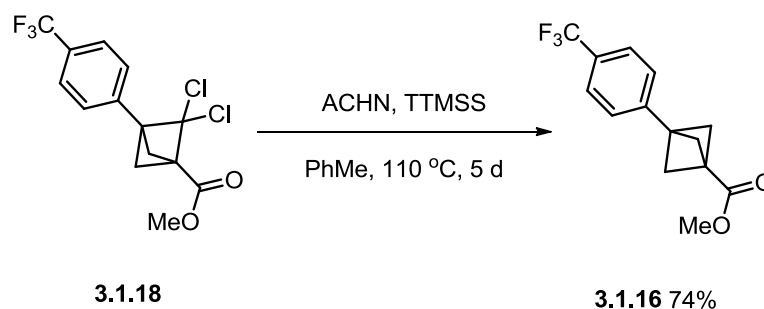
Scheme 31 – Successful mono-dechlorination of **3.1.18**

It was believed that more forcing conditions would allow access to the fully dechlorinated BCP **3.1.16**. Increasing the stoichiometry of silane and heating the reaction to reflux for 12 h produced a 2:1 ratio of **3.1.21** to **3.1.16** by NMR and were isolated in 25% and 19% yields, respectively (Scheme 32). The disappointing yields obtained can be attributed to the difficulty in separating the two products.



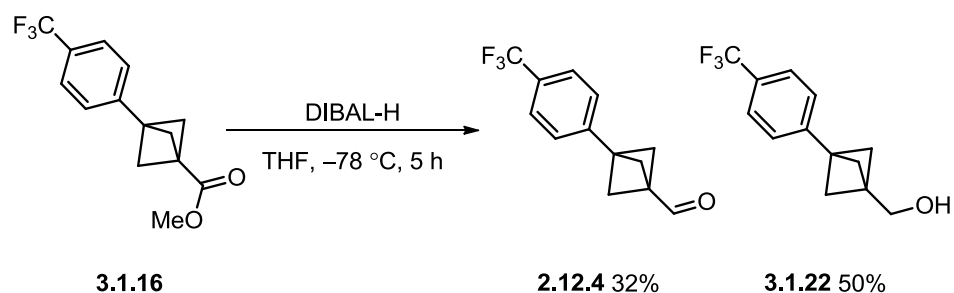
Scheme 32 – Separation of mono- and fully dichlorinated **3.1.18**

Despite the low yield, it was reasoned that this reaction could be forced to completion with additional silane and sequential addition of initiator. These optimised conditions ultimately afforded BCP **3.1.16** in good yield (Scheme 33).



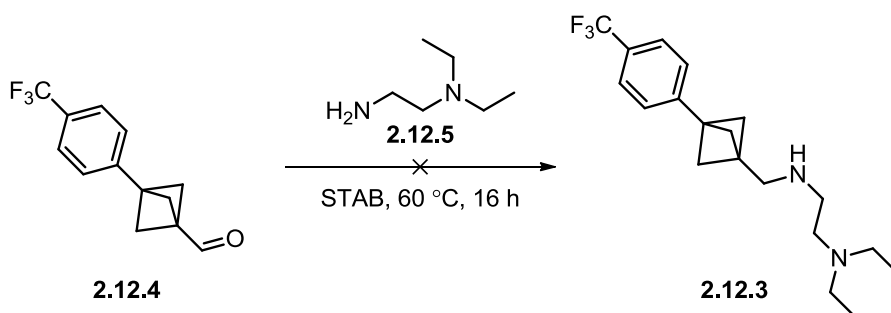
Scheme 33 – Optimised dechlorination conditions to generate 3.1.16

With intermediate **3.1.16** in hand, it was envisaged that reductive amination of aldehyde **2.12.4** with amine **2.12.5** would give rapid access to the desired target BCP building block. As such, an approach to aldehyde **2.12.4** was required. Initial reduction of the ester **3.1.16** to the target aldehyde **2.12.4** using diisobutylaluminium hydride (DIBAL-H) produced the desired product and the over reduced alcohol **3.1.22** in 32% and 50% yields, respectively (Scheme 34).



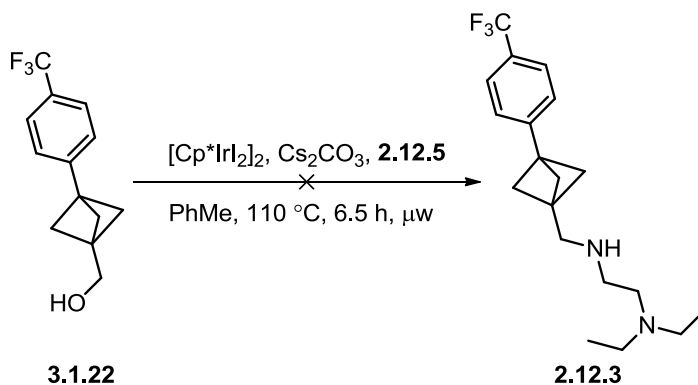
Scheme 34 – Reduction of 3.1.16 to 2.12.4 and the over reduced 3.1.22

Unfortunately, reductive amination using aldehyde **2.12.4** and the commercially available amine **2.12.5** in the presence of sodium triacetoxyborohydride (STAB) proved unsuccessful (Scheme 35). It was hypothesised that the steric hindrance of the BCP unit was disfavouring imine formation.



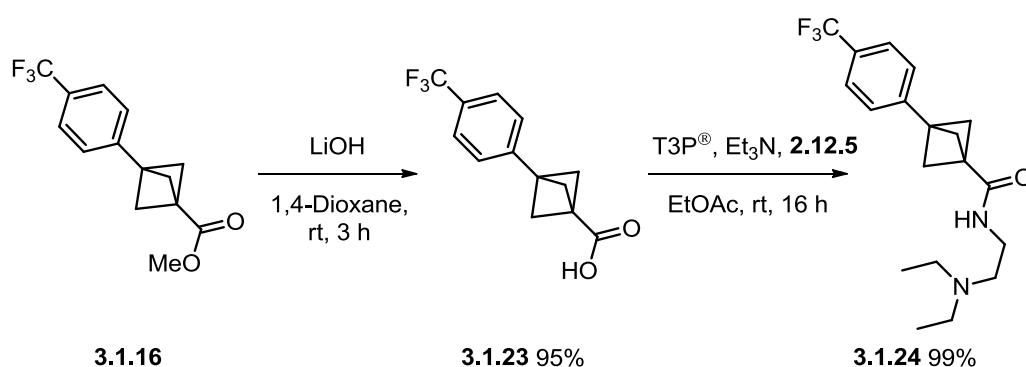
Scheme 35 – Reductive amination of 2.12.4 with 2.12.5

Based on this, as an alternative to reductive amination, hydrogen borrowing methodology using alcohol **3.1.22** was considered, however this also proved unsuccessful with only starting material observed by LCMS after extended heating in the microwave (Scheme 36).



Scheme 36 – Hydrogen borrowing methodology using iridium catalyst

With attempts at reductive amination proving unsuccessful, it was anticipated that saponification to the acid, followed by amide coupling, and then subsequent reduction could provide a more robust route. Accordingly, this was attempted starting from ester **3.1.16**.



Scheme 37 – Saponification and amide coupling to generate **3.1.24**

Initial saponification to **3.1.23** proceeded in excellent yield and subsequent amide coupling with amine **2.12.5** produced **3.1.24** in 99% yield (Scheme 37). A variety of conditions were then screened for the reduction of the amide **3.1.24** (Table 23).

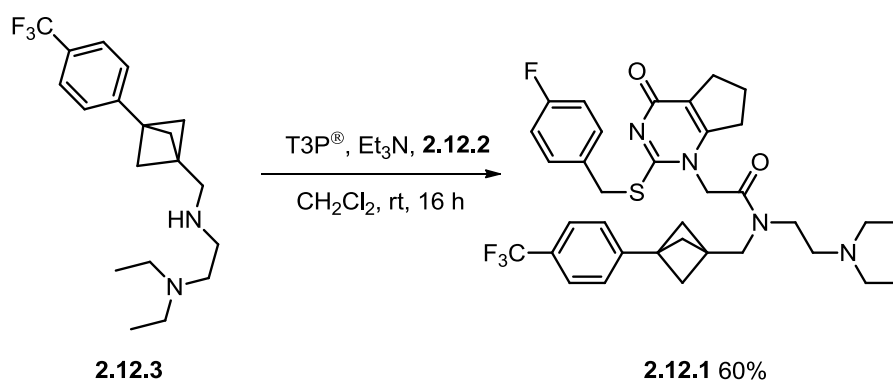
Table 23 – Amide reduction screen

Entry	Conditions	Conversion
1	BH ₃ .THF, THF, 66 °C, 26 h	90
2	BH ₃ .THF (sequential additions), THF, 66 °C, 19 h	94
3	RhH(CO)(PPh ₃) ₃ , Ph ₂ SiH ₂ , THF, rt, 6 h ¹⁷⁴	0
4	[Ir(COE) ₂ Cl] ₂ , Et ₂ SiH ₂ , CH ₂ Cl ₂ , rt, 16 h ¹⁷⁵	79
5	LiAlH ₄ , THF, rt, 16 h	100

A rhodium catalysed reduction produced no reaction (Table 23, Entry 3), however all the other reduction conditions resulted in conversion to the desired product. Despite this, isolation of the product proved very challenging. It appeared that purification by MDAP resulted in formylation of the desired amine. This was thought to be caused by formic acid contamination within the system. Concentration of the amine in the presence of this formic acid resulted in the formylated by-product.

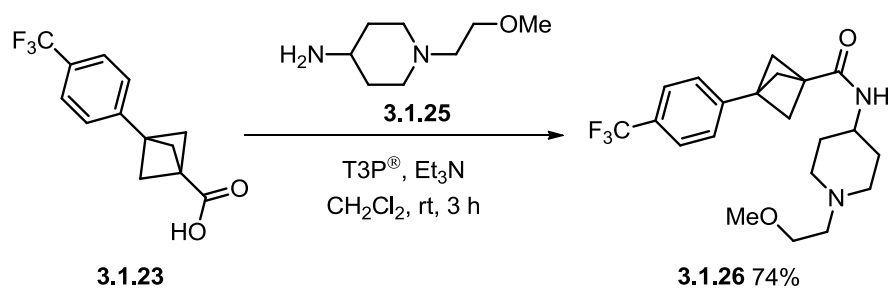
Based on this, it was considered that the reaction mixture could be taken on crude into the final amide coupling, thus avoiding the problematic purification. Using the lithium aluminium hydride conditions (Table 23, Entry 5), reduction of the amide **3.1.24** was successful with high conversion monitored by LCMS. The crude material was isolated in 56% yield (87% purity by LCMS) and used in the final amide coupling.

Amide coupling using the crude amine and acid fragment **2.12.2**, prepared elsewhere in our laboratories (Scheme 16),³⁴ generated the desired BCP analogue **2.12.1** in good yield (Scheme 38).



Scheme 38 – Final amide coupling to generate desired BCP analogue 2.12.1 of darapladib

Consequently, the synthesis of BCP analogue **2.12.1** was ultimately completed in 10 steps in 5% overall yield. With the challenging synthesis of the darapladib counterpart completed, focus shifted to the related rilapladib analogue. Again using acid **3.1.23** generated previously, amide coupling with the commercially available amine **3.1.25** furnished amide **3.1.26** in good yield (Scheme 39).



Scheme 39 – Amide coupling of 3.1.23 with 3.1.25

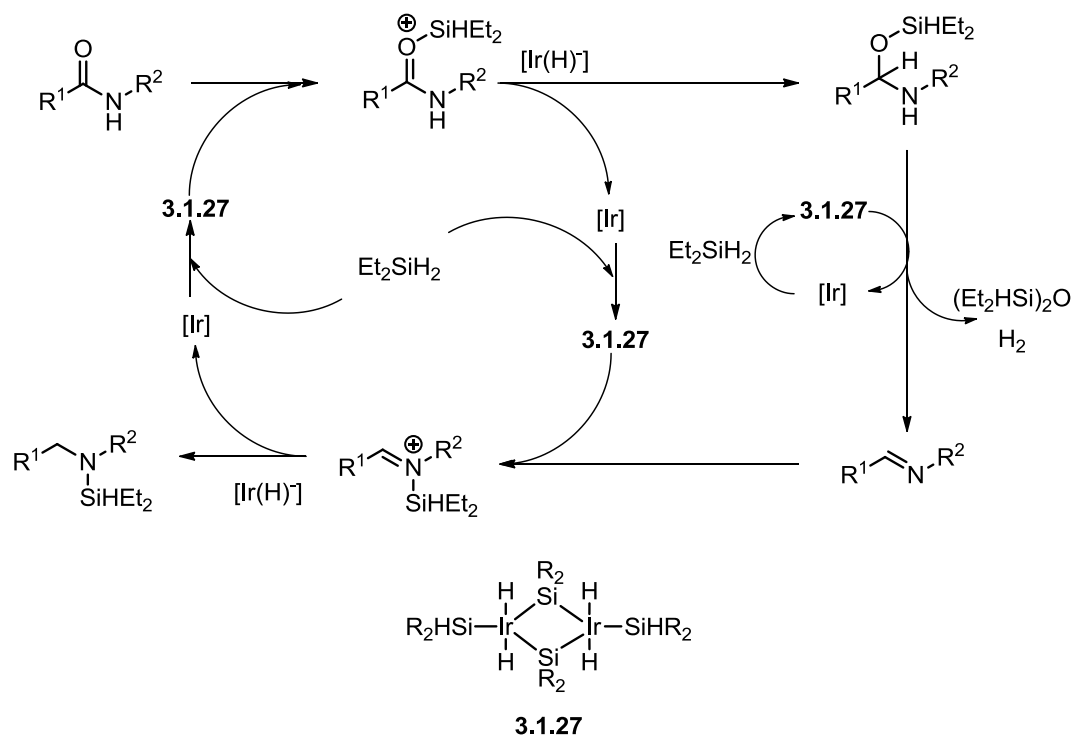
Initially, the reduction conditions used previously (Table 23, Entry 5) were investigated for this system. However, conversion to the desired reduced product was poor and no material was isolated; consequently, alternative conditions were sought. The previously investigated reduction conditions, utilised on the **3.1.24** template, were examined with the addition of an alternative Hantzsch ester (HE) mediate reduction developed by Charette *et al.* (Table 24, Entry 3).¹⁷⁶

Table 24 – Amide reduction screen

Entry	Conditions	Conversion (%) (Isolated (%))
1	LiAlH ₄ , 2-MeTHF, rt, 6 h	50 (19)
2	BH ₃ .THF, THF, rt, 16 h	0
3	HE, 2-Fpy, Et ₃ SiH, Tf ₂ O, CH ₂ Cl ₂ , -78 °C to rt, 21.5 h	0
4	[Ir(COE) ₂ Cl] ₂ , Et ₂ SiH ₂ , CH ₂ Cl ₂ , rt, 20 h	98 (59)

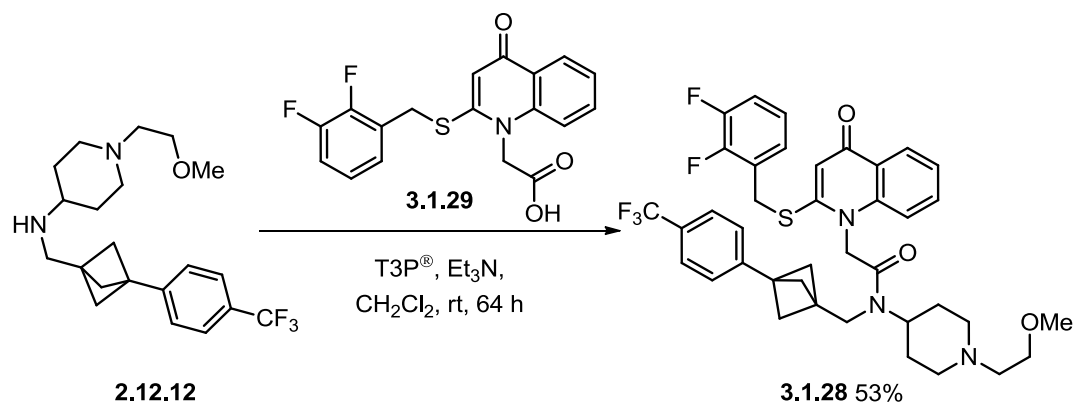
Switching the solvent to 2-MeTHF produced an increase in conversion, however the isolated yield was poor (Table 24, Entry 1). Disappointingly the alternative borane and HE conditions failed to demonstrate any conversion to the desired amine (Table 24, Entries 2 and 3). The poor conversions were attributed to the potential coordination of the hydride species between the nitrogen of the piperidine ring and the pendant methoxy group.

Pleasingly the iridium reduction conditions (Table 24, Entry 4) demonstrated excellent conversion of **3.1.26** to the desired amine **2.12.12** with an isolated yield of 59%; the diminished yield being ascribed to the purification technique employed. From a mechanistic perspective, it is believed that the amide initially attacks the catalytically active species **3.1.27** at the silicon to generate an activated amide and an iridium hydride, which subsequently reduces the activated amide to the hemiaminal. The hemiaminal then eliminates silanol to generate the imine. Iridium species **3.1.27** then catalyses a further hydrosilylation and hydride reduction to generate the silylated amine, which breaks down on work-up to the desired product (Scheme 40).



Scheme 40 - Mechanism of iridium reduction of amides¹⁷⁵ Adapted with permission from: *J. Am. Chem. Soc.*, 2012, 134, 11304-11307, Copyright 2012 American Chemical Society

Final amide coupling with acid fragment **3.1.29**¹⁷⁷ then furnished the target rilapladib analogue **3.1.28** in 53% yield (Scheme 41).



Scheme 41 – Final amide coupling to generate desired BCP analogue **3.1.28** of rilapladib

3.2 Comparison of BCP analogues to progenitor compounds

With both analogues **2.12.1** and **3.1.28** in hand, a comparison of the efficacy and the physicochemical profile to the progenitor compounds darapladib (**1.3.1**) and rilapladib (**1.3.2**) could be undertaken. Data collected included Lp-PLA₂ potency, solubility, ChromLog D_{7.4} (and subsequent PFI), as well as permeability determination using the AMP method.

Analogue **2.12.1** maintains high potency compared to that of its parent darapladib with a pIC₅₀ of 9.4 (darapladib: 10.2). This suggested that the bioisosteric moiety was well tolerated within the enzyme. In order to compare the binding mode of the bioisosteric analogue **2.12.1** with darapladib, an X-ray crystal structure of **2.12.1** in the Lp-PLA₂ protein was generated. The structure (solved at ~1.9 Å resolution) revealed a similar binding mode for both molecules (Figure 43), which is in agreement with the initial molecular modelling (Figure 40). The overlay of the two structures reveals that the BCP moiety precludes the adjacent trifluorophenyl moiety from extending quite as far towards Leu121 and Phe125. This is ascribed to the BCP system being approximately 1 Å shorter in length than the original phenyl, although the residues of the protein move slightly towards the inhibitor to fill the void. This sub-optimal occupancy of the pocket potentially explains the slight drop-off in potency as well as the potential impact that this might have on the π -stacking interaction between the trifluoromethyl aromatic and the enzyme binding site. Furthermore, the moiety has no impact on the key interactions within the oxyanion hole. The hydrogen bonding interactions between the cyclic carbonyl functionality and the backbone amide donors (Leu153 and Phe274) are conserved and subsequently the catalytic triad is blocked (Figure 43).

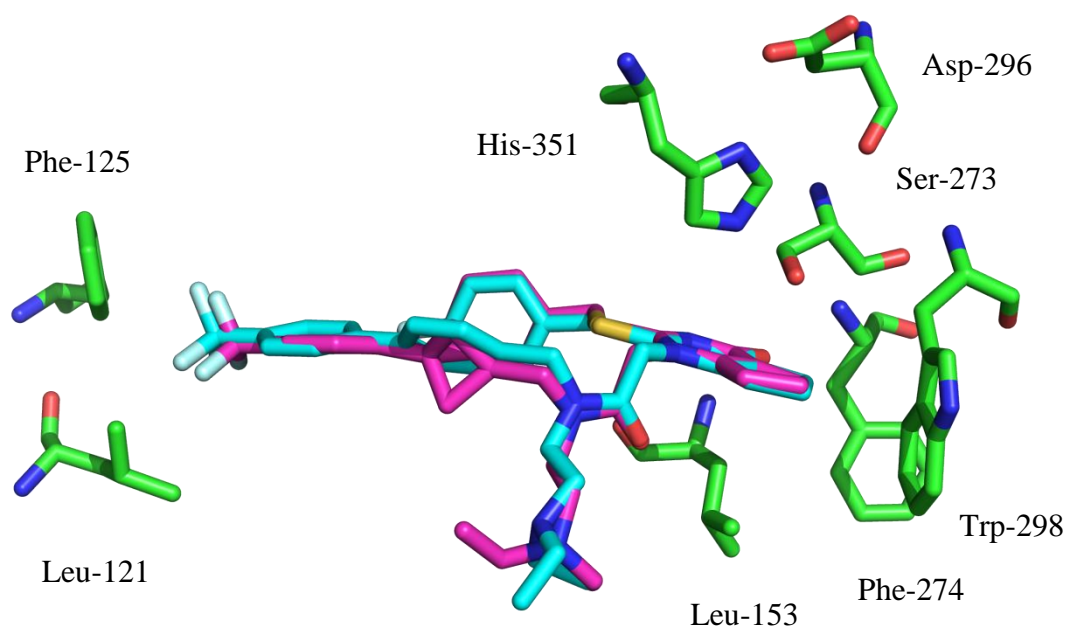


Figure 43 - Overlay of X-ray crystal structures of **2.12.1** and darapladib within Lp-PLA2 binding site

With the similar binding of darapladib and analogue **2.12.1** confirmed, a physicochemical comparison of the analogues **2.12.1** and **3.1.28** and their parent compounds darapladib and rilapladib was conducted (Table 25).

Table 25 – Summary of physicochemical data

	darapladib	2.12.1	rilapladib	3.1.28
pIC₅₀	10.2	9.4	9.6 ⁴⁴	NT*
CLND (μM)	5.5	74	<1	32
FaSSIF (μg/mL)	183, 399 [#]	>1000	203	635
AMP (nm/s)	255	705	160	220
ChromLogD	6.6	7.0	6.74	7.06
PFI	10.6	10.0	11.74	11.06

*NT = Not tested, [#]Two batches tested

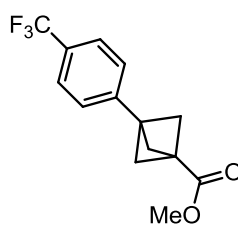
Analogue **2.12.1** showed an improved permeability of 705 nm/s related to 255 nm/s and a 13-fold increase in kinetic solubility over darapladib (74 vs. 5.5 μM, respectively). However, this was accompanied by an undesired increase in lipophilicity from 6.6 to 7.0 as determined by measured ChromLog D_{7.4}. Consequently, compounds **2.12.1** and darapladib have equivalent PFIs due to the removal of one aromatic ring, which compensates for the increase in lipophilicity.

Thermodynamic FaSSIF solubility was also obtained with analogue **2.12.1** exhibiting an approximately 3-fold improvement (>1000 µg/mL compared to 399 µg/mL). These data are echoed in the comparison of **3.1.28** and rilapladib, with **3.1.28** displaying improved solubility in both kinetic and thermodynamic measures as well as equivalent PFIs. Additionally, low clearance of 1.22 mL/min/g and 0.76 mL/min/g for both **2.12.1** and **3.1.28**, respectively in a human liver microsomal assay was observed. These data lend weight to the hypothesis that disrupting molecular planarity^{56,134,135} and reducing aromatic ring count⁴⁵ can be beneficial to solubility and the overall pharmacokinetic profile of the molecule.

In summary, the BCP bioisosteric moiety has been successfully incorporated into two Lp-PLA₂ inhibitor development compounds; darapladib and rilapladib. Unfortunately, efforts to identify an improved method for the incorporation of the BCP itself were unsuccessful. Nonetheless, a modification of literature conditions using a dichlorocarbene generated *in situ*, followed by dehalogenation with TTMS provided an effective route to this challenging motif. Overall, considerable route optimisation resulted in a 10 step sequence and an overall isolated yield of 5% for darapladib BCP analogue **2.12.1** and a 3.5% yield over 10 steps for rilapladib analogue **3.1.28**. BCP analogue **2.12.1** was tested in a biochemical assay measuring Lp-PLA₂ enzyme inhibition and exhibited similar potency to its parent molecule. Furthermore, comparison of the physicochemical profiles of both inhibitors **2.12.1** and **3.1.28** showed an improvement upon switching from phenyl to BCP, particularly in terms of solubility and permeability.

3.3 Substrate scope

With the utility of the BCP phenyl replacement confirmed, attention turned to enhancing the scope of the chemistry used to access the darapladib and rilapladib analogues **2.12.1** and **3.1.28**. It was considered that the ester **3.1.16** could be used to attach a range of functionality (Figure 44). If the substituents on the aromatic ring could be varied this would provide a greater diversity of biaryl isosteres.



3.1.16

Figure 44 – Structure of intermediate **3.1.16**

For this reason, the aim of this section was to increase the variation of the more challenging aromatic portion of the compound. Using the already established route as a starting point, the scope of the initial aromatic addition was investigated using a range of different substrates.

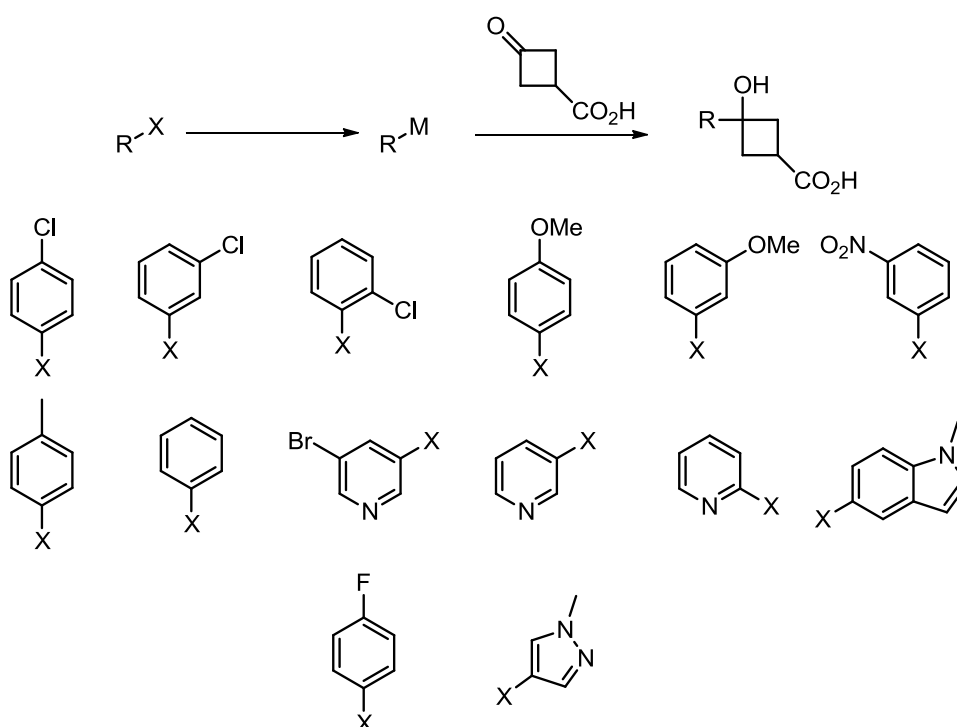
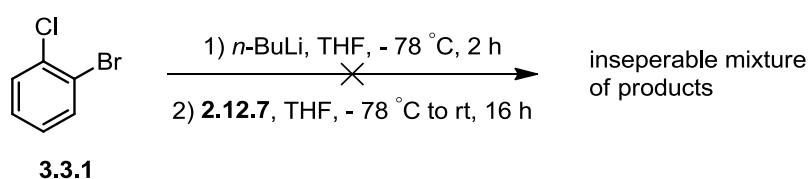


Figure 45 – Proposed aromatic and heterocyclic groups

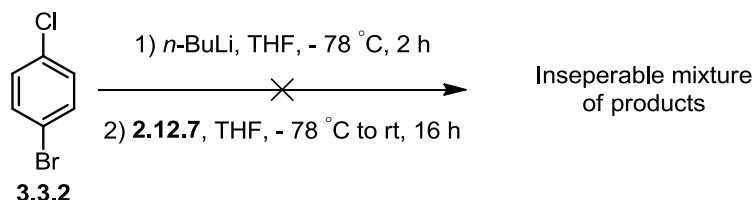
A range of variously substituted phenyls and heterocycles were investigated using a bromide or iodide as a functional handle for metal-halogen exchange. The organometallic reagent generated could then be used for the addition into the ketone **2.12.7** (Figure 45).

Initially, dihalogenated aromatics such as 1-bromo-2-chlorobenzene were examined. However, application of the conditions used in the synthesis of analogue **3.1.3** produced a mixture of inseparable products (Scheme 42). This was postulated to result from halogen-lithium exchange with either the bromide or the chloride which would generate similar products.



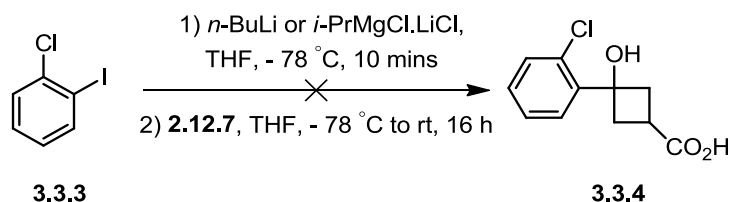
Scheme 42 – Unsuccessful metalation and addition of **3.3.1** to **2.12.7**

Moving the bromide to the *para*-position and subjecting 1-bromo-4-chlorobenzene **3.3.2** to the same conditions led to a similar mixture of inseparable products (Scheme 43).



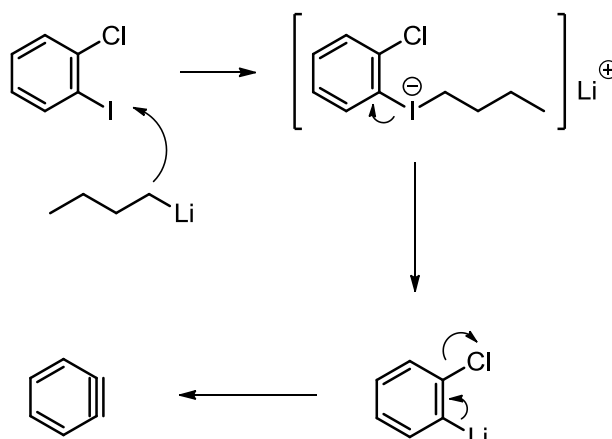
Scheme 43 – Unsuccessful metalation and addition of **3.3.2** to **2.12.7**

Following on from this, it was envisaged that utilising an iodide rather than a bromide might lead to a more selective reaction profile.¹⁷⁸ Disappointingly, using both *n*-butyllithium and turbo-Grignard with 1-chloro-2-iodobenzene **3.3.3** did not generate any of the desired product (Scheme 44).



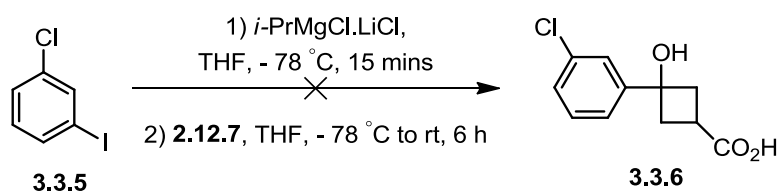
Scheme 44 – Switching from bromine to iodine to enhance selectivity

It was suggested that in this case halogen-lithium exchange was occurring but the resulting intermediate underwent elimination to generate a reactive benzyne (Scheme 45), which could generate a variety of products.¹⁷⁹

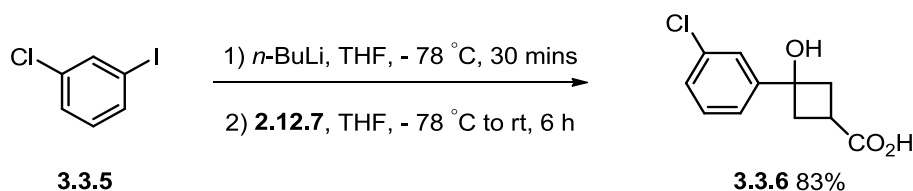


Scheme 45 – Potential benzyne formation

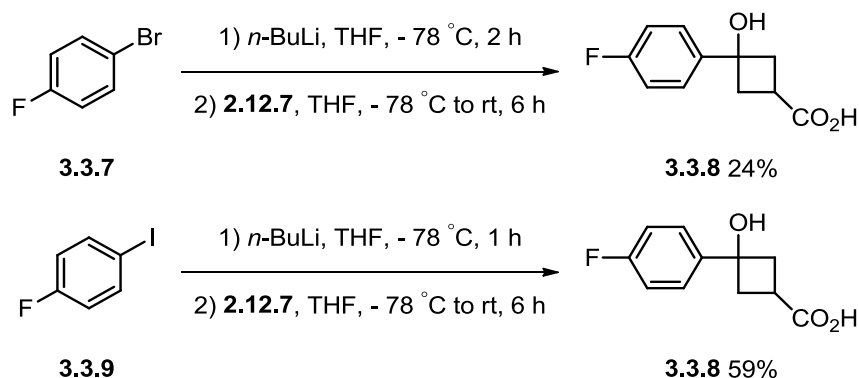
It was envisaged that moving the iodide to the *meta*-position would disfavour this reactivity and this was tested initially using turbo-Grignard as the metalating agent (Scheme 46).

Scheme 46 – Switching chloride to *meta*-position to avoid benzyne formation

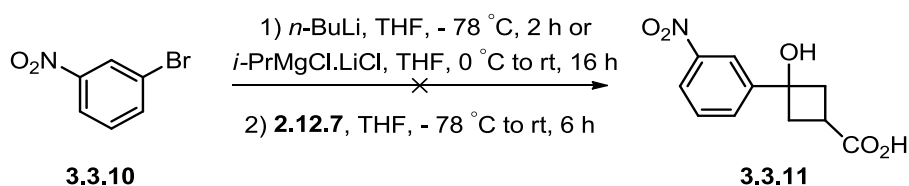
In this case, isolation of the product from a white solid (suspected to be lithium and magnesium salts of the carboxylic acid) proved challenging, however switching to *n*-butyllithium resulted in simpler isolation of product in 83% yield (Scheme 47).

Scheme 47 – Successful generation of 3.3.6 using *n*-BuLi

An alternative dihalogenated substrate investigated was the *para*-fluorobromobenzene **3.3.7**. Using *n*-butyllithium produced the desired compound **3.3.8** in a disappointing 24% yield (Scheme 48). Pleasingly, switching to the iodo fluoro **3.3.9** improved this yield to 59%

Scheme 48 – Generation of *para*-fluorinated aromatic substrate 3.3.8

Attention now turned to an alternative electron-withdrawing substituent which might allow for alternative subsequent functionalisation. In this instance a *meta*-nitro group was considered (Scheme 49).

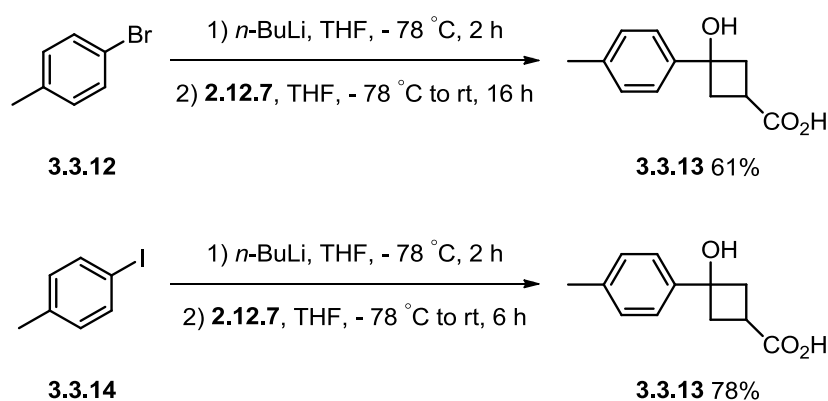


Scheme 49 – Unsuccessful nitro substrate

However, even at low temperatures the nitro group proved problematic with the organometallic generation using *n*-butyllithium at -78°C causing the solution to turn black. Additionally, with turbo Grignard at 0°C no product was isolated from the reaction. This is not unsurprising considering the reactivity of nitro groups towards organometallics.¹⁸⁰ This is most predominantly exemplified by the Bartoli indole

synthesis, which involves initial attack of the organometallic onto the nitro group.^{181,182}

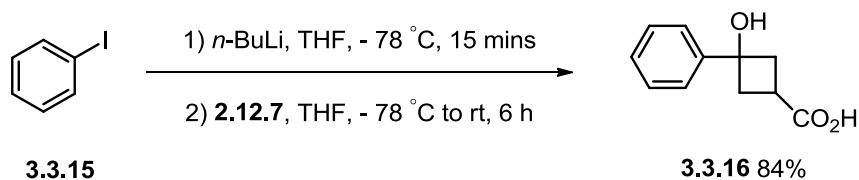
With several electron-withdrawing substituents already investigated, electron-neutral and electron-rich aromatics were next considered. Initially the *para*-tolyl substituent was investigated using the bromotoluene **3.3.12**. Turbo Grignard and *n*-butyllithium were examined in parallel with *n*-butyllithium providing the desired product **3.3.13** in good to moderate yield (Scheme 50).



Scheme 50 – Successful generation of tolyl substrate **3.3.13**

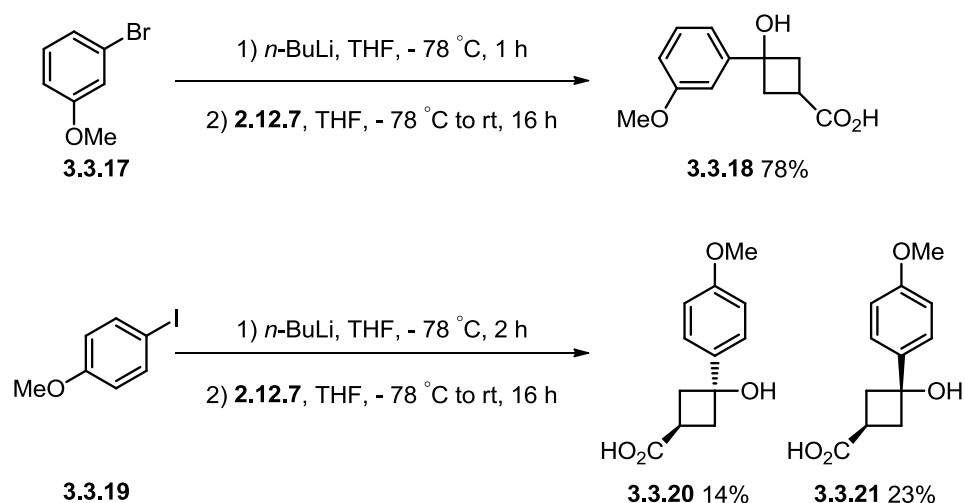
Switching to the iodide **3.3.14** on a small scale produced the desired product in a similar yield, but upon reaction scale-up (5 g) the yield was improved to 78% (Scheme 50).

An unsubstituted phenyl group was also investigated using iodobenzene **3.3.15** with the yield on small scale being excellent (Scheme 51), however when attempted on a larger scale this yield dropped to 41%. The difference in yield observed was attributed to the short time frame for the halogen-lithium exchange, resulting in a diminished quantity of the metalated species available for the addition.



Scheme 51 – Synthesis of barer phenyl substrate **3.3.16**

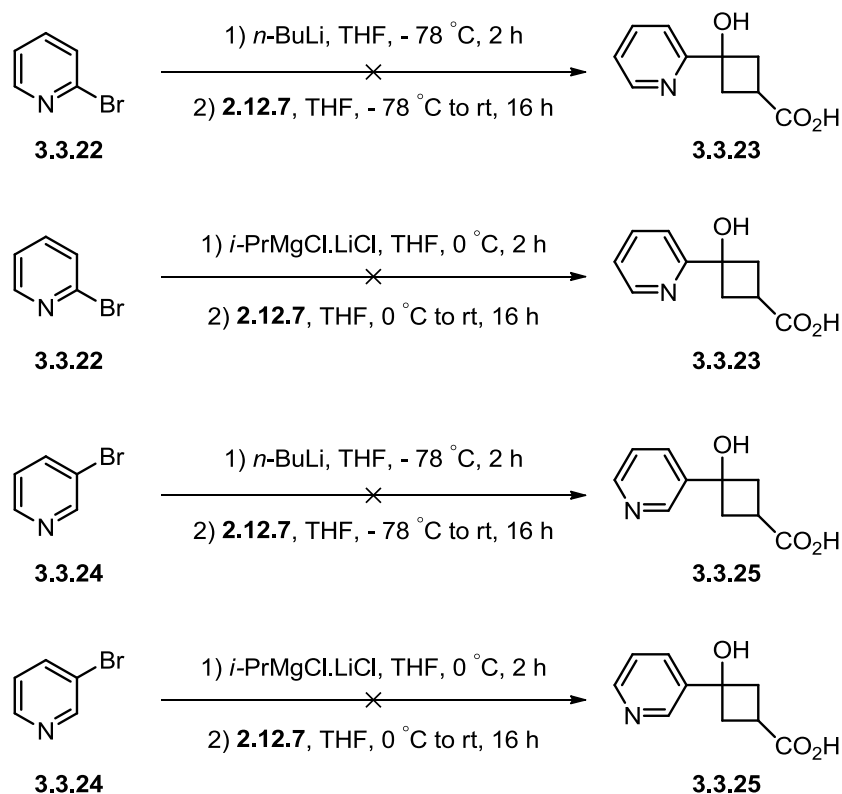
In order to test electron-rich aromatic systems, methoxy substituents at the *para*- and *meta*- positions were investigated, with *n*-butyllithium providing the best results compared to the turbo Grignard reagent.



Scheme 52 – Methoxy-substituted aromatics

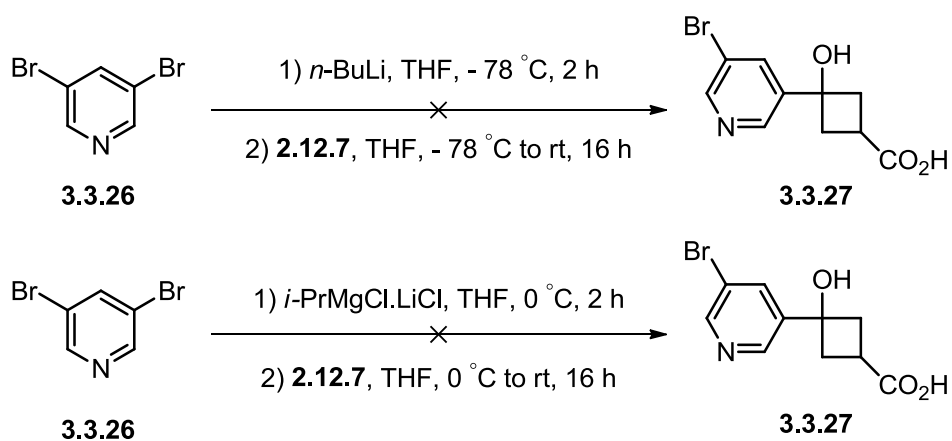
The *meta*-methoxybromobenzene **3.3.17** provided the desired product in good yield as a mixture of diastereomers. Meanwhile, the *para*-methoxyiodobenzene **3.3.19** provided a lower yield, however in this case the isomers **3.3.20** and **3.3.21** were separable by MDAP (Scheme 52).

Aromatic heterocycles are ubiquitous in drug molecules and therefore it was important to investigate whether this route would be able to tolerate their functionality. Pyridines are commonly utilised within medicinal chemistry programmes, and so this important moiety was investigated initially. 2-Bromopyridine **3.3.22** and 3-bromopyridine **3.3.24** were examined with a view to incorporating a pyridine, and 3,5-bromopyridine **3.3.26** was also used to determine if a further functional handle on the pyridine would be tolerated.



Scheme 53 – Pyridine substrates

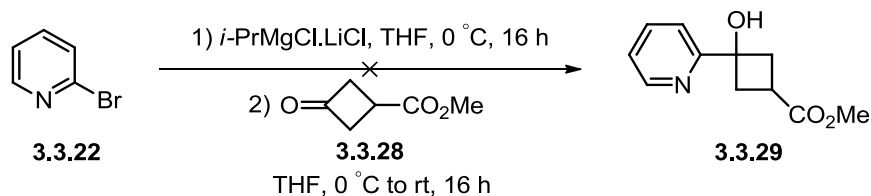
Initially, the conditions attempted previously using *n*-butyllithium and turbo Grignard were applied to both **3.3.22** and **3.3.24** (Scheme 53). However, no product was isolated from these reactions. These conditions were also applied to the dibromo system **3.3.26** but again proved unsuccessful (Scheme 54).



Scheme 54 – Disubstituted pyridine substrates

To establish whether the acid itself might be responsible for the poor outcome, the reaction was repeated with the commercially available ester **3.3.28**. It was believed

that there would be sufficient selectivity for reaction of the organometallic at the ketone since the inherently higher reactivity of the ketone would be further enhanced by its strained nature. However, a subsequent attempt using turbo Grignard at 0 °C did not provide the desired product (Scheme 55).



Scheme 55 – Attempted addition to ester 3.3.28

In an attempt to investigate whether the desired organometallic species was being generated a time study was performed using the 2- and 3-bromopyridine. Using turbo Grignard as the metalating agent, the reaction was monitored by TLC quenching with methanol. Unfortunately, at each time point (1 – 15 mins (every minute), 30 mins, 1 h, 2 h, 4 h) only a weak spot for pyridine was observed. This indicated that the metalation process was problematic with this species.

Having failed to generate the organometallic on the pyridine substrates, attention turned to indole **3.3.30**. The original conditions were employed, however, these were unsuccessful. In all cases, whether using *n*-butyllithium or turbo Grignard, some starting bromoindole was recovered suggesting that the halogen-lithium exchange for this substrate was slow (Table 26).

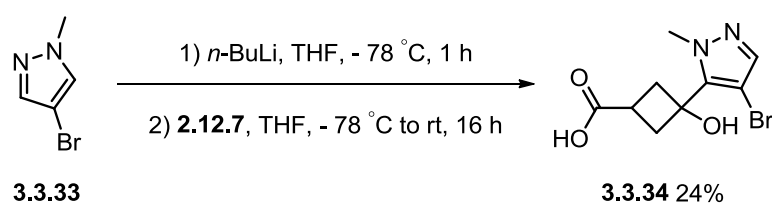
Table 26 – Indole 3.3.30 substrate investigation

3.3.30

Entry	Conditions
1 (R = H 3.3.31)	1) <i>i</i> -PrMgCl.LiCl, THF, 0 °C to rt, 16 h 2) 2.12.7 , THF, rt, 6 h
2 (R = H 3.3.31)	1) <i>n</i> -BuLi, THF, - 78 °C, 2 h 2) 2.12.7 , THF, - 78 °C to rt, 6 h
3 (R = Me 3.3.32)	1) <i>n</i> -BuLi, THF, - 78 °C, 2 h 2) 3.3.28 , THF, - 78 °C to rt, 16 h
4 (R = Me 3.3.32)	1) <i>i</i> -PrMgCl.LiCl, THF, 0 °C to rt, 16 h 2) 3.3.28 , THF, rt, 6 h
5 (R = Me 3.3.32)	1) <i>i</i> -PrMgCl.LiCl, THF, - 78 °C, 6 h 2) 3.3.28 , THF, - 78 °C to rt, 16 h

Both sets of conditions were again investigated using the methyl ester **3.3.28**. Using *n*-butyllithium the major component that could be isolated was recovered starting material but some debrominated starting material was isolated suggesting halogen lithium exchange had occurred (Table 26 Entry 3). Despite this, none of the addition product was observed.

Lastly, methyl pyrazole **3.3.33** was investigated using turbo Grignard, however again no desired product was observed. Pleasingly, switching to *n*-butyllithium did generate a new product. However, this was not a result of halogen-lithium exchange but rather from a deprotonation of the pyrazole and subsequent addition into the ketone. The product was isolated in a relatively low yield and repetition of the reaction failed to give an improvement (Scheme 56).



Scheme 56 – Synthesis of unexpected by-product 3.3.34

The next step in assessing the scope of this sequence was to form the bicyclic ring system followed by carbene reaction to generate the BCP system. With the exception of pyrazole **3.3.34**, the acids produced in the initial screen were progressed to the chlorination step (Figure 46). The methyl pyrazole **3.3.34** was omitted as it could not be produced in sufficient quantities to support the subsequent synthetic sequence.

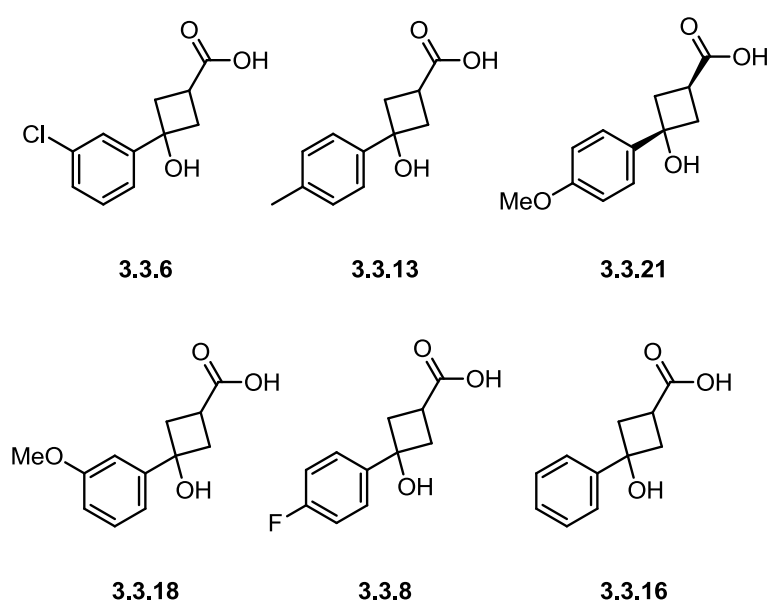
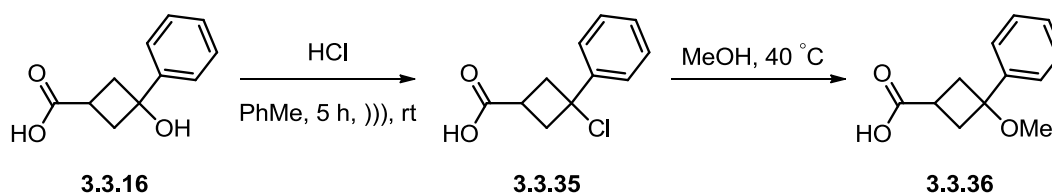


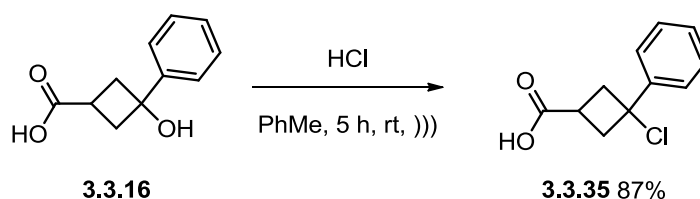
Figure 46 - Substrates advanced to full BCP synthesis

The chlorination of the previously reported substrate **3.3.16** was undertaken and proceeded with good conversion.¹⁵⁸ Subsequent transfer of the compound using MeOH and heating to 40 °C caused the displacement of the chloride with MeOH to generate compound **3.3.36**, observed by NMR (Scheme 57). This is proposed to be due to the lability of the chloride in an S_N1 fashion generating a comparatively stable benzylic tertiary carbocation.



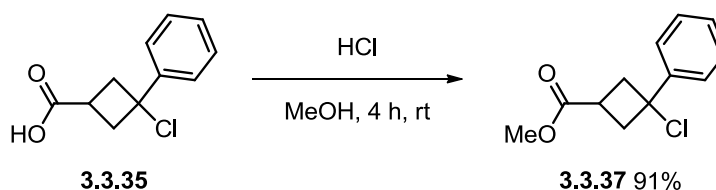
Scheme 57 – Unexpected production of 3.3.36 after successful conversion of 3.3.16 to 3.3.35

This reaction was subsequently repeated on a larger scale, with an alternative isolation procedure avoiding the use of methanol, generating the desired chlorinated intermediate **3.3.35** in 87% yield (Scheme 58).



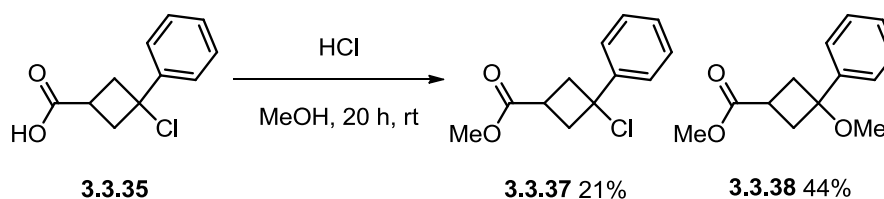
Scheme 58 – Successful conversion of 3.3.16 to 3.3.35 under ultrasound conditions

The methyl ester formation was tested on small scale using HCl in MeOH and proceeded in excellent yield (Scheme 59).



Scheme 59 – Small scale ester 3.3.37 formation

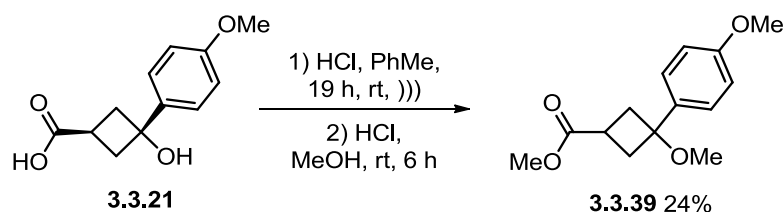
When performing this reaction on an increased scale, displacement of the chloride with MeOH was observed after stirring for 4 h. The mixture was stirred for a further 16 h before the desired product **3.3.37** and undesired by-product **3.3.38** were isolated in poor yield (Scheme 60).



Scheme 60 – Isolation of desired ester 3.3.37 and the undesired displaced product 3.3.38

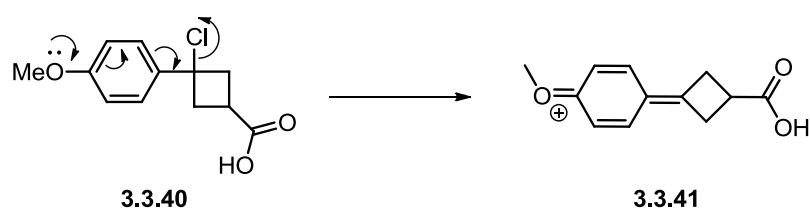
Consequently, this substrate was not progressed further and attention turned to the alternative substrates, which had not been previously reported in the literature.

As the electron deficient trifluoromethyl phenyl derivative **3.1.1** had already been used in the synthesis of **3.1.16** attention turned to electron-rich systems. To this end the methoxy substituted aromatics **3.3.21** and **3.3.18** were investigated. The chlorination of a **3.3.21** proved challenging showing only modest conversion by TLC after sonication for 19 h. It was anticipated that separation of starting material and product would be difficult at this stage and therefore the crude product was stirred for 6 h in methanolic HCl. However, the undesired **3.3.39** was isolated from this reaction suggesting MeOH was displacing the chloride produced in the initial step (Scheme 61).



Scheme 61 – Isolation of undesired by-product **3.3.39**

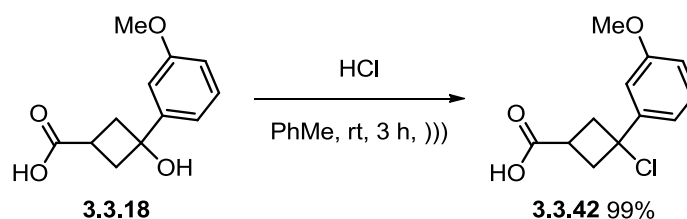
A repeat of the reaction with monitoring by NMR showed a complex profile. This suggested product instability which could be rationalised by the ability of the oxygen lone pair to stabilise the carbocation formed by loss of chloride ion. This carbocation could subsequently be trapped with water to reform starting material or form an adduct with MeOH. The intermediate could also potentially degrade into other by-products *via* the reactive quinone methide intermediate **3.3.41** generated (Scheme 62).



Scheme 62 – Potential generation of reactive quinone species **3.3.41**

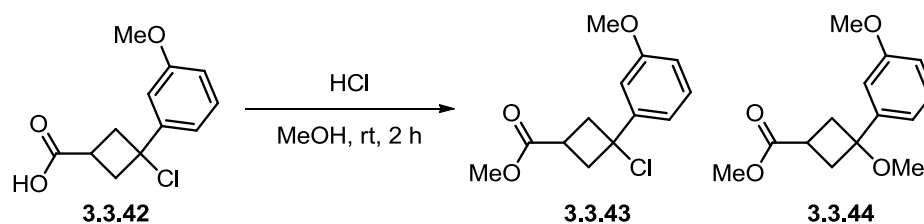
It was reasoned that using the 3-methoxyphenyl system would potentially curtail this reactivity. However, initial attempts at this reaction proved unsuccessful with a complex reaction profile observed by LCMS. This was attributed to the LCMS sample being dissolved in MeOH which could potentially displace the chloride. Additionally, the water in the mobile phase of the LCMS could react with **3.3.42** to

generate further by-products. Repeating this reaction with monitoring using NMR provided a clearer picture, with full conversion to the chloride **3.3.42** after 3 h of sonication and an excellent isolated yield (Scheme 63).



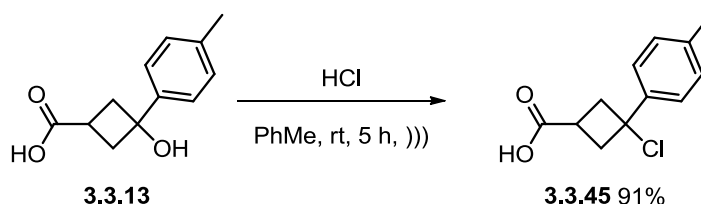
Scheme 63 – Successful conversion of **3.3.18** to **3.3.42** under ultrasound conditions

The methanol with HCl conditions used previously was attempted in the synthesis of methyl ester **3.3.43**. After 2 hours the conversion to the desired product was observed, however, in attempting to isolate the product the double substitution product **3.3.44** was observed by NMR after removing the solvent under reduced pressure at 40 °C (not isolated, Scheme 64). With this disappointing observation, the focus shifted to an alternative substrate.



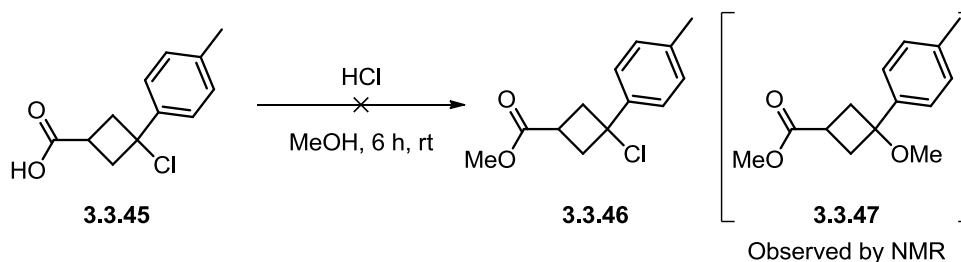
Scheme 64 – Observed conversion of **3.3.42** to desired product with undesired further reaction to **3.3.44**

The tolyl substituted system **3.3.13** was the next for consideration with the expectation that the weakly donating methyl group would not facilitate the displacement of the chloride leaving group. With **3.3.13** in hand, the chlorination step was investigated however, issues with MeOH were again observed. Monitoring the reaction by LCMS proved difficult with a complex reaction profile. Moving to reaction monitoring by NMR again proved a superior analytical technique and subsequently the desired product **3.3.45** was produced in excellent yield on a range of scales (Scheme 65).



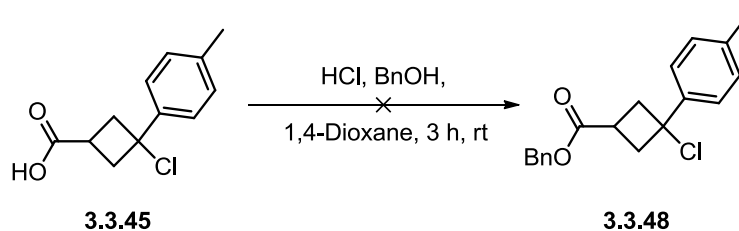
Scheme 65 – Successful conversion of 3.3.13 to 3.3.45 under ultrasound conditions

The next step was to form the methyl ester **3.3.46**. Initial conditions investigated were stirring in MeOH and HCl, however this produced mainly the double substituted product **3.3.47** through displacement of the chloride, as observed by NMR (Scheme 66).



Scheme 66 – Conversion of 3.3.45 to undesired 3.3.47

It was envisaged that the use of a more bulky alcohol might prevent displacement of the chloride and produce only the desired ester. To this end, both benzyl alcohol and *tert*-butyl alcohol were explored. Benzyl alcohol was stirred with HCl and **3.3.45** in 1,4-dioxane for 3 h (Scheme 67).



Scheme 67 – Unsuccessful benzyl ester formation

The LCMS profile indicated the presence of a variety of different components with displacement of the chloride with benzyl alcohol as well as the bis-benzyl compound **3.3.49** (Figure 47), although these were not isolated.

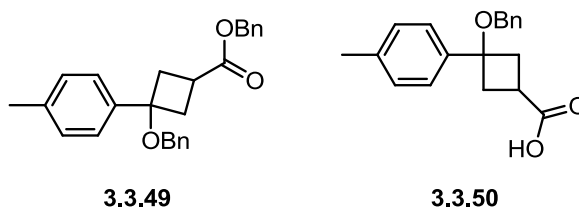
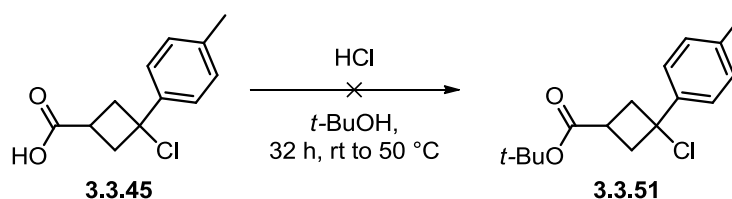
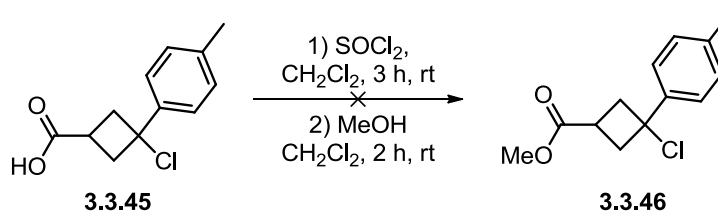


Figure 47 – Observed by-products in benzyl ester formation

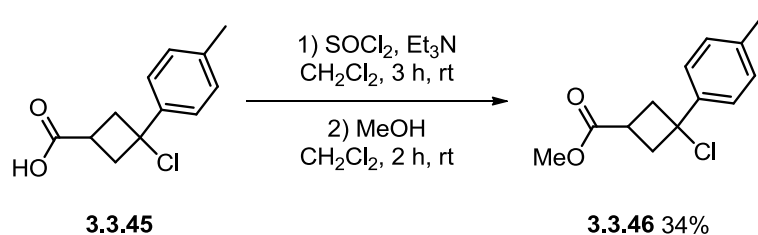
These results suggested that, when using benzyl alcohol, displacement of the chloride was faster than the ester formation. Therefore attention turned to the much bulkier *tert*-butyl alcohol. Initial attempts using similar conditions to those applied with benzyl alcohol were explored. However, under these conditions predominantly unreacted starting material was observed by NMR of the reaction after 4 h. This reaction was repeated and allowed to stir overnight but little conversion of the starting material was observed *via* NMR. The reaction was then heated to 50 °C for a further 16 h but without success (Scheme 68).

Scheme 68 –*tert*-Butyl ester synthesis

With little success in switching alcohol, an alternative strategy was considered. It was envisaged that the reactivity of the acid could be increased by conversion to the acid chloride. As such, this was generated *in situ* before quenching with MeOH. This was attempted using thionyl chloride and stirring for 3 h (Scheme 69). Upon addition of the MeOH, the undesired displacement of the chloride was again observed.

Scheme 69 – Methyl ester synthesis *via* acid chloride

This reaction was repeated with the addition of base to speed up the generation of the acid chloride intermediate. Encouragingly, in this case the desired product **3.3.46** was isolated albeit in poor yield (Scheme 70).



Scheme 70 - Methyl ester synthesis *via* acid chloride

This reaction was repeated on larger scale under the same conditions, however the isolated yield was reduced to 15% with a considerable amount of acid still present in the reaction mixture. Following this disappointing result attention turned to examination of more electron deficient substrates.

It was reasoned that a *para*-fluoro substituent, as with the trifluoromethyl group, would sufficiently destabilise the cationic S_N1 intermediate, therefore preventing displacement at that position (Figure 48).

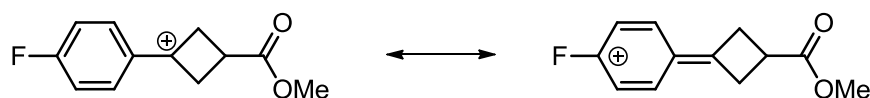
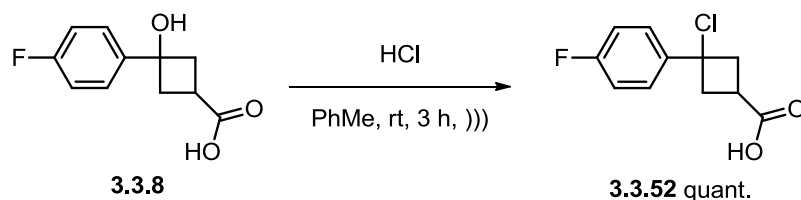


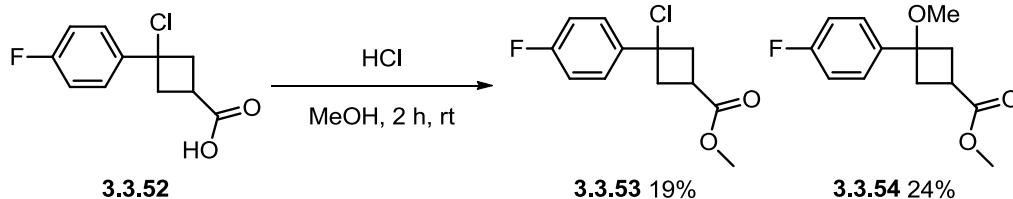
Figure 48 - Resonance destabilised S_N1 transition state

As described previously, **3.3.8** was generated in good yield and was subjected to the chlorination procedure. An initial small scale attempt showed good conversion by NMR, however unfortunately purification by MDAP degraded the product. A repeat of this reaction using alternative isolation conditions generated the desired compound **3.3.52** in quantitative yield on a variety of scales (Scheme 71).



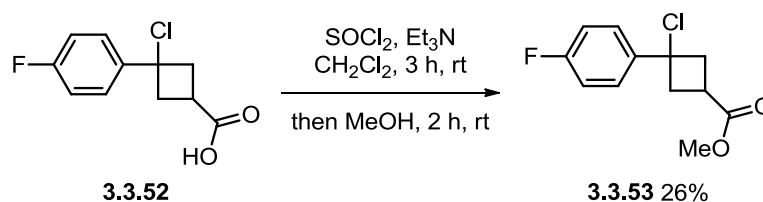
Scheme 71 – Chlorination of **3.3.8**

Subsequent ester formation proved challenging with MeOH again displacing the chloride when **3.3.52** was stirred in HCl and MeOH overnight. Reducing the reaction time to just 2 h gave an improved result with 19% isolated **3.3.53** and 24% undesired by-product **3.3.54** (Scheme 72).



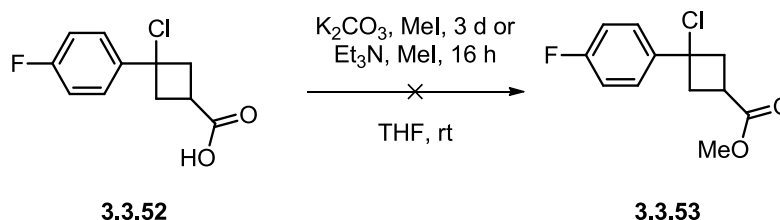
Scheme 72 – Isolation of desired ester **3.3.53** and by-product **3.3.54**

It was hoped in this case that enhancing the reactivity of the acid with thionyl chloride would provide facile access to the desired methyl ester **3.3.53**. Initially treatment with thionyl chloride, DIPEA and one equivalent of MeOH generated the desired product in 12% yield. However, switching to Et₃N produced **3.3.53** in an improved, yet still disappointing, 26% yield (Scheme 73).



Scheme 73 – Alternative synthesis of **3.3.53** via acid chloride

Following on from this, it was considered that alkylation of the acid might prevent displacement of the chloride due to the lack of external nucleophile present in the reaction mixture. Subsequent attempts using potassium carbonate or Et₃N with methyl iodide were however unsuccessful (Scheme 74).

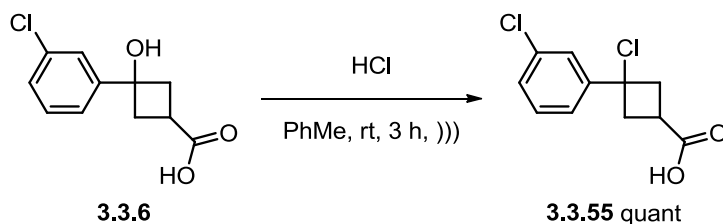


Scheme 74 – Alkylation of acid **3.3.52**

Due to the limited success in generating the esters **3.3.37**, **3.3.46**, and **3.3.53** in sufficient yield, these examples were not progressed any further. Additionally,

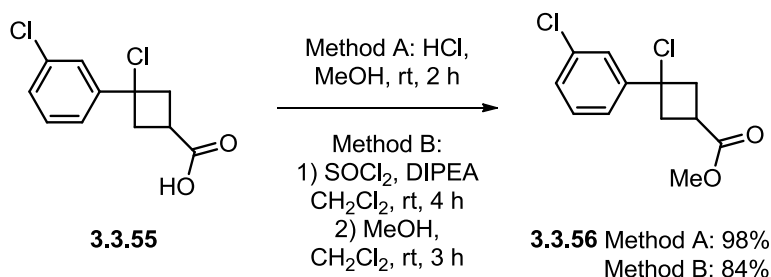
changing the order of steps into the methyl esters **3.3.37**, **3.3.46** and **3.3.53** was considered, however with the limited success using the trifluoromethyl substrate **3.1.4** this was not investigated.

The final substrate examined was the *meta*-chloro substituted aromatic **3.3.6**. Chlorination of this substrate proceeded with excellent yields, ranging from 93% to quantitative on a variety of scales (Scheme 75).



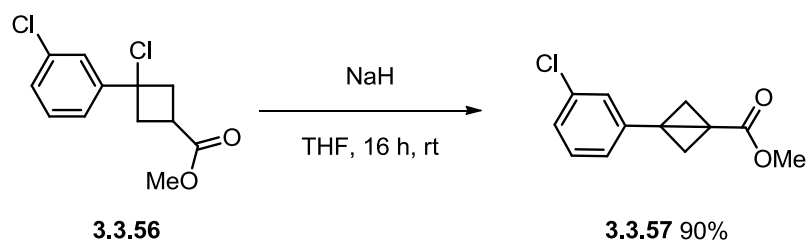
Scheme 75 – Chlorination of **3.3.6**

Subsequent ester formation was carried out using both pre-activation with thionyl chloride and stirring with MeOH in HCl. Both proceeded in excellent yield with the HCl/MeOH conditions proving superior when repeated on a larger scale, giving near quantitative yields of **3.3.56** (Scheme 76).



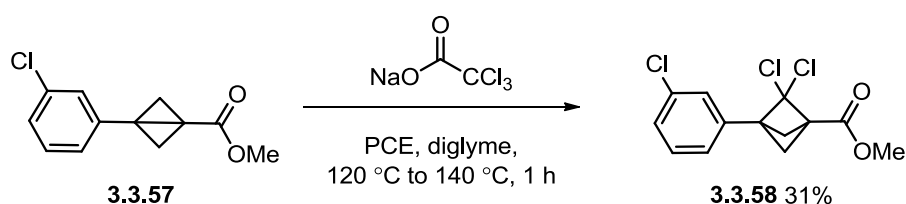
Scheme 76 – Successful synthesis of ester **3.3.56**

With the desired compound **3.3.56** in hand, the cyclisation to the strained ring intermediate **3.3.57** was investigated. An initial test reaction on 100 mg scale was undertaken. From this reaction, an isolated fraction after column chromatography displayed peaks in the NMR characteristic of desired product and starting material. It had been noted previously with **2.12.6** that the yield increased when performing this reaction on larger scale. Consequently, upon scaling this reaction, the desired product **3.3.57** was generated in 90% isolated yield (Scheme 77).



Scheme 77 – Cyclisation to 3.3.57

The last step was the addition of the dichlorocarbene unit into the central bond of the [1.1.0] ring system of **3.3.57**. Employing the literature conditions utilised previously, the reaction generated the desired compound **3.3.58** in a reasonable yield (Scheme 78).



Scheme 78 – Dichlorocarbene addition to 3.3.57

Significant effort has been made to demonstrate the scope of the methodology developed to access a Phenyl-BCP moiety. Two substrates bearing differing phenyl substitution were successfully converted to the desired Phenyl-BCP cores in reasonable yield. Unfortunately a general synthetic approach to a wide range of such cores was not identified, with significant challenges associated with the stability of the carbocation generated on route to the BCP encountered. Nonetheless, electron-deficient systems were viable and it is reasonable to assume that this methodology could generally be applied to such systems, allowing access to the desired BCP analogues. In order to synthesise more electron-rich examples, considerable further investigation would be required and may need a new synthetic strategy. Although disappointing, these studies have tested the limits of this methodology and give a clear indication on where any future studies should be focussed.

3.4 Cross coupling as an approach to derivatising the BCP system

During the synthetic approaches towards the BCP intermediates, one structure was particularly intriguing. The generation of the monochlorinated system **3.1.21** via the radical dechlorination reaction (Scheme 31) in good yield prompted the idea that the chloride could be used as a further functional handle for derivatisation. Introducing functionality at this position would potentially allow the investigation of novel chemical space. Comparing to a phenyl group, this position would allow access to a previously unexplored vector at 90° to the plane of the molecule, as opposed to the conventional 60° and 120° from a phenyl group (Figure 49).

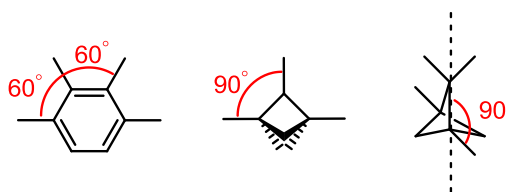


Figure 49 – Geometries associated with phenyl and BCP systems

This could be particularly useful within a medicinal chemistry setting as this new directionality could provide a unique means of exploring binding with a target protein and could potentially provide a platform to improve the overall profile of a drug molecule.

In addition to this, investigation of transition metal based sp^3 - sp^2 coupling is of growing interest in the chemical literature.¹⁸³ Cross-coupling methodology has been extensively used by both industry and academia to form C-C bonds for a variety of processes. The vast array of coupling partners and transition metals utilised in these reactions has saturated the area, however, there are some templates which still provide significant challenges.

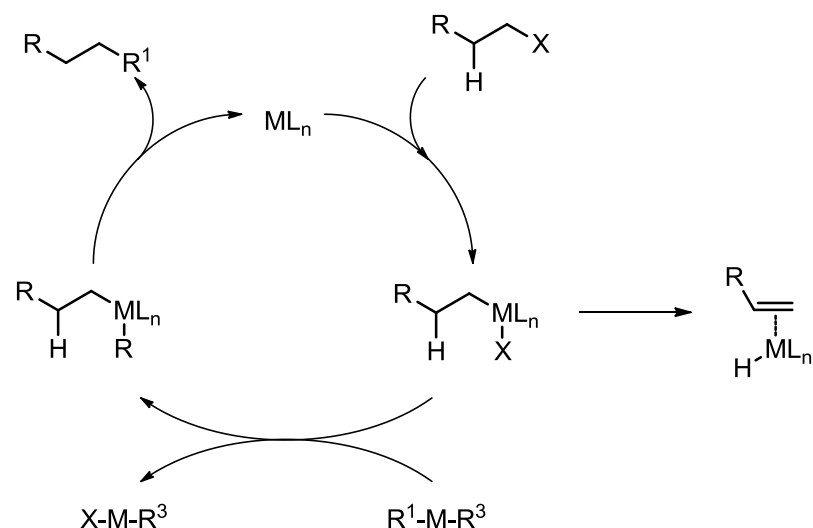


Figure 50 – Generic alkyl cross-coupling mechanism

One particular area which has received attention is the cross-coupling of alkyl halides. These substrates present significant challenges pertaining to two factors: slow oxidative addition and fast β -hydride elimination.^{183,184} Recent advances reported in the literature have tried to address these particular challenges. The Fu group investigated the application of bulky alkyl phosphines in the coupling of alkyl bromides, chlorides and tosylates to alkyl boron reagents in a Suzuki-Miyaura cross-coupling.^{185–187} The successful results were attributed to the high electron-donating ability of the phosphines facilitating oxidative addition and the large steric effect of the ligands suppressing β -hydride elimination.¹⁸³

With suppression of β -hydride elimination being a particular challenge in alkyl halide cross-couplings, it is fortuitous that on this particular template there are no β -hydrogens available for this undesired pathway. Additionally, considering the vast amount of literature based around the Suzuki-Miyaura cross-coupling, a boronic acid was envisaged as a sensible coupling partner for this transformation. Accordingly, phenyl boronic acid was chosen as a model coupling partner in these investigations. The screening parameters examined included the palladium source, ligand, solvent and temperature.

Table 27 – Initial screening conditions for cross-coupling of 3.1.21

Entry	Pd	Ligand	Solvent (10:1)	T (°C)	Outcome
1	Pd(OAc) ₂	DavePhos	THF:H ₂ O	90	Minor by-product, not isolated
2		RuPhos	THF:H ₂ O	90	Only SM
3		JohnPhos	THF:H ₂ O	90	Only SM
4		XantPhos	THF:H ₂ O	90	Only SM
5		XPhos	THF:H ₂ O	90	Only SM
6		PPh ₃	THF:H ₂ O	90	Minor by-product, not isolated

Firstly, the palladium source and ligands were examined using 1.1 eq of phenyl boronic acid, 2 eq of base in THF:H₂O at 90 °C for 16 h (Table 27). Palladium acetate was the first source of palladium to be studied with six different phosphine based ligands: DavePhos, RuPhos, JohnPhos, XantPhos, XPhos and triphenylphosphine.

In this initial screen no reaction was observed for 4 out of the 6 ligands. Some reaction was observed by TLC using DavePhos and triphenylphosphine, however in these cases only starting material was isolated upon purification. Based on this, replacing the source of palladium was thought to offer improved reactivity. Tris(dibenzylideneacetone)dipalladium was deemed a suitable alternative and accordingly was screened with the same ligand set under matching conditions (Table 28).

Table 28 – Alternative palladium source for cross-coupling of 3.1.21

Entry	Pd	Ligand	Solvent (10:1)	T (°C)	Outcome
1	Pd ₂ (dba) ₃	DavePhos	THF:H ₂ O	90	Minor by-product, not isolated
2		RuPhos	THF:H ₂ O	90	Only SM
3		JohnPhos	THF:H ₂ O	90	Only SM
4		XantPhos	THF:H ₂ O	90	Only SM
5		XPhos	THF:H ₂ O	90	Only SM
6		PPh ₃	THF:H ₂ O	90	Minor by-product, not isolated

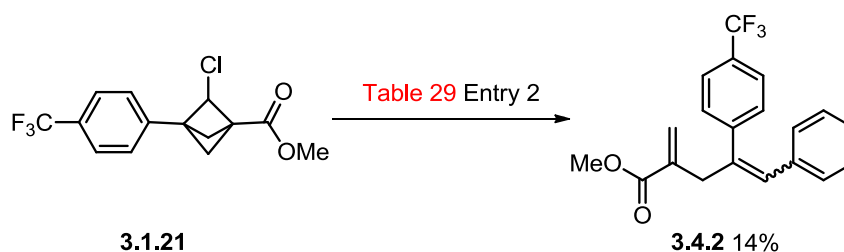
However, the results of this screen were equally disappointing. It was thought that combining the reaction mixtures for Table 28 entries 1 and 6 would allow the isolation of the newly observed product, however this proved unsuccessful.

Table 29 – Further conditions screened

Entry	Pd	Solvent (10:1)	T (°C)	Outcome
1	PdCl ₂ (dppf)	THF:H ₂ O	90	Only SM
2	RuPhos Precat	THF:H ₂ O	90	By-product

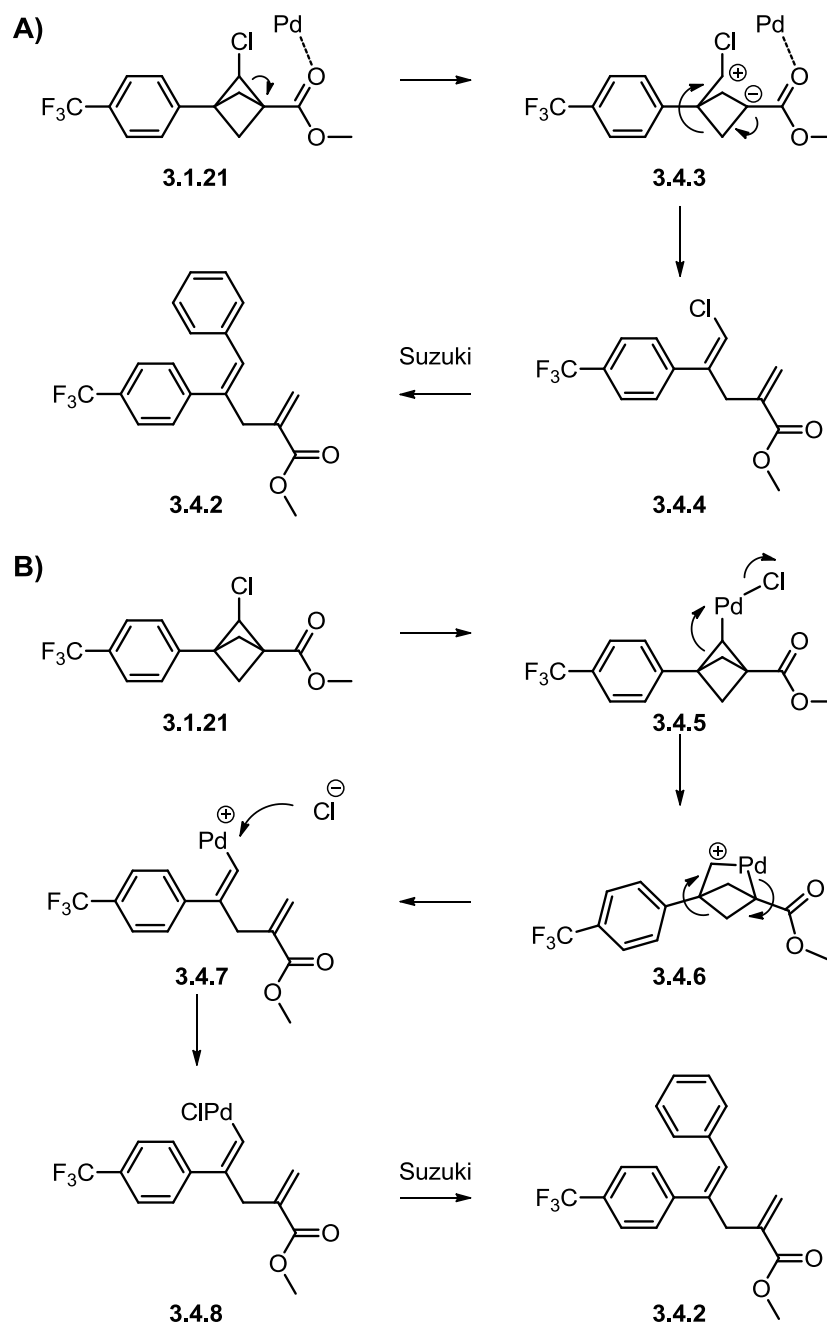
Using similar conditions to those in the first two screens, two alternative catalysts were considered: PdCl₂(dppf) and RuPhos precatalyst. Furthermore, it was thought that increasing the amount of boronic acid coupling partner in the reaction mixture

could promote desired reaction. With PdCl₂(dppf) (Table 29, Entry 1) no reaction was observed and only starting material was isolated from this reaction. However, pleasingly the use of the RuPhos precatalyst saw conversion of starting material. Upon isolation of the major product it was determined that this was not the desired coupled product **3.4.1** but a dialkene species **3.4.2** (Scheme 79).



Scheme 79 – Isolation of by-product **3.4.2**

Considering the stability of the ring system under the high temperature dechlorination conditions two mechanisms for this degradation were postulated. Firstly, the palladium species in the reaction mixture could be acting as a Lewis acid to activate the ring system towards a degradation pathway in which a rearrangement occurs. This could be either through a concerted pathway or a step-wise bond breakage to form a stable enolate which then eliminates to generate the chlorinated alkene species. Such an intermediate could then undergo a Suzuki cross-coupling to give the product observed (Scheme 80). Alternatively, it was postulated that the palladium species could oxidatively insert into the carbon-chlorine bond and then subsequent ring opening of the BCP system could occur to relieve the ring strain and generate a palladacycle. The palladacycle intermediate could then degrade to the dialkene species with the palladium complexed to the alkene. This could then perform a Suzuki coupling with the phenyl boronic acid to generate the product **3.4.2** (Scheme 80).



Scheme 80 – A) Lewis acid assisted thermal degradation with Suzuki coupling, B) Palladacycle mediated degradation

The original screening conditions were repeated using the extra equivalents of base and boronic acid, this time using toluene as solvent to allow heating to a higher temperature (Table 30).

Table 30 – More forcing conditions used for cross-coupling of 3.1.21

Entry	Pd	Ligand	Solvent (10:1)	T (°C)	Outcome
1	Pd(OAc) ₂	DavePhos	PhMe:H ₂ O	110	By-product
2		RuPhos	PhMe:H ₂ O	110	By-product
3		JohnPhos	PhMe:H ₂ O	110	By-product
4		XantPhos	PhMe:H ₂ O	110	Only SM
5		XPhos	PhMe:H ₂ O	110	By-product
6		PPh ₃	PhMe:H ₂ O	110	Only SM
7	Pd ₂ (dba) ₃	DavePhos	PhMe:H ₂ O	110	By-product
8		RuPhos	PhMe:H ₂ O	110	By-product
9		JohnPhos	PhMe:H ₂ O	110	By-product
10		XantPhos	PhMe:H ₂ O	110	Only SM
11		XPhos	PhMe:H ₂ O	110	By-product
12		PPh ₃	PhMe:H ₂ O	110	Only SM

This survey of reaction conditions showed conversion to the undesired dialkene **3.4.2** using four of the six ligands with palladium diacetate. Switching to Pd₂(dba)₃ gave similar results with the same four ligands generating the undesired by-product **3.4.2**. In both cases the reactions producing the undesired by-product needed to be combined in order to isolate sufficient quantities for characterisation.

In order to obtain an isolated yield for a specific reaction, RuPhos was considered the logical choice considering the successful conversion using the precatalyst (Table 29 Entry 2) and the production of the by-product as observed by TLC in Table 30 Entries 2 and 8. The RuPhos conditions were therefore attempted on a 50 mg scale using stoichiometric amounts of the metal and phosphine ligand, and the by-product **3.4.2** was isolated in 35% yield (Scheme 81).

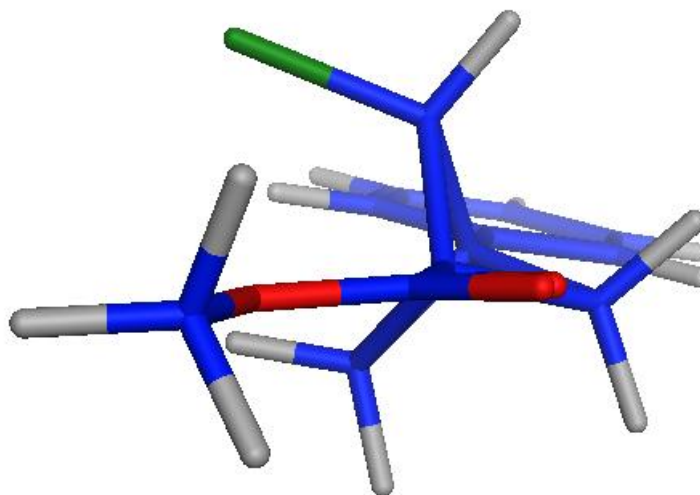
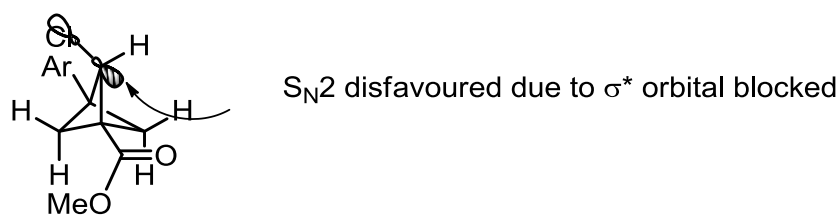
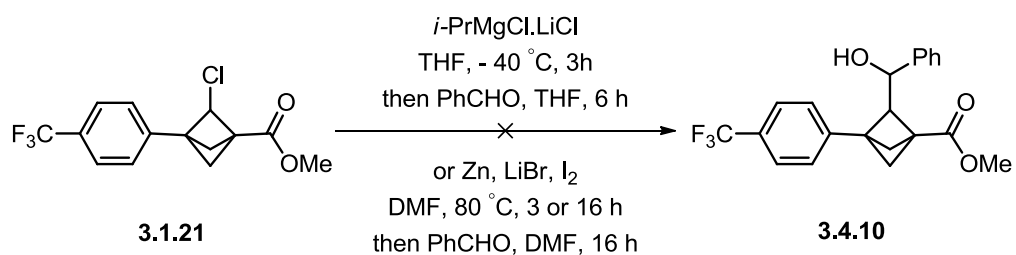


Figure 51 – Energy minimised structure demonstrating hypothesis for lack of reactivity of 3.1.21

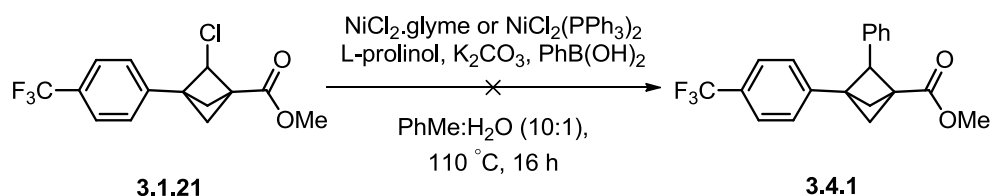
This consideration directed the investigation into trying to reverse the reactivity of the chloride. It was envisaged that an organometallic exchange could provide a useful intermediate for a subsequent cross-coupling or addition reaction. Formation of the zincate or magnesium species followed by addition of benzaldehyde to trap the metalated species was examined (Scheme 84).



Scheme 84 – Metalation of 3.1.21

In all cases, however, no desired product was obtained and only starting material was observed. This suggested that metalation of this intermediate was not occurring which may again be attributed to the low reactivity of the chloride.

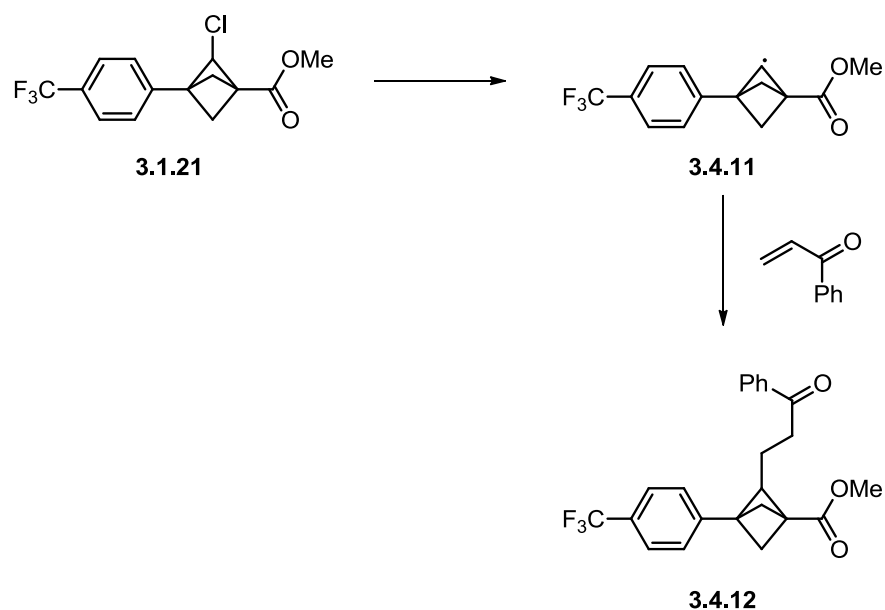
Finally, nickel was considered as an alternative to palladium for the direct cross-coupling. Nickel has a smaller atomic radius than palladium; allowing for facile oxidative addition and can allow access to radical pathways. With this in mind, it was considered that nickel might not facilitate ring opening of the strained ring system.¹⁸⁸ Additionally, considering that the dechlorination step is radical in nature proving generation of a radical intermediate is possible without ring opening, the ability to access radical pathways might allow coupling to occur. However, initial attempts using nickel catalysis did not generate any desired product with only starting material recovered (Scheme 85).¹⁸⁹



Scheme 85 – Alternative nickel cross-coupling

In summary, despite the comprehensive investigation of the monochlorinated BCP **3.1.21** as a potential cross-coupling partner, no desired cross-coupling product was observed. With the limited reactivity of **3.1.21** and its degradation under palladium catalysed conditions, this investigation was not progressed any further.

Additional investigation into this type of functionalisation of the BCP structure is certainly viable. With the ability to dechlorinate the ring system using a radical process having been established, it can be envisaged that that merging these dechlorination conditions with addition of a Michael acceptor could allow functionalisation at the desired position (Scheme 86).



Scheme 86 – Potential radical pathway to functionalise 3.1.21

The dichlorinated precursor BCP **3.1.18** could also be considered as a starting point for these kind of reactions. The generation of a radical on this species is more facile, therefore coupling of this might have a greater probability of success. Furthermore, with the use of a nickel catalyst having the potential to access radical pathways for cross-coupling, it was considered that the enhanced ability to generate a radical species using the dichlorinated BCP **3.1.18** could improve the potential coupling process.

3.5 Conclusions and Future work

Ultimately, the main aim of this work has been achieved with the successful incorporation of the BCP unit into the darapladib and rilapladib scaffolds. It has also been clearly shown that the increased sp³ character of this moiety has a beneficial effect to the physicochemical profile of the two inhibitors. Improvements were observed in both the solubility and permeability of the two isosteric inhibitors with the binding mode of **2.12.1** confirmed to be the same as its parent darapladib. Moreover with many of the steps being performed on multi-gram scale, it can be extrapolated that this synthetic route could be utilised in a process chemistry setting. Further investigation into methods of improving the synthetic route is, however, still desirable.

With this route being inherently scalable, the ability to modify the templates was desired. Utilising the synthetic route already established, the applicability of the methodology was investigated in a variety of templates. Unfortunately, with each template providing significant challenges, a general synthetic route was not established. Electron deficient aromatics proved the most effective substrates in the general scheme with two examples carried through to the BCP structure.

It is believed that modifications of the route would allow access to the alternative substrates. With iodinated starting materials proving more effective for aromatic substituents, it could be possible to utilise iodinated heterocycles analogously. Additionally, with the carbocation stability in the ester formation step providing a significant challenge, it could be possible to mitigate this by activating the acid with thionyl chloride in combination with a bulkier alcohol to prevent S_N1 displacement. Alternatively, a more comprehensive investigation into alkylating on the acid could be performed with a stronger base potentially being employed. Despite the unsuccessful conversion of the alcohol to a leaving group using substrate **3.1.4**, the challenges associated with the subsequent templates investigated could provide cause to revisit the order of steps.

Finally, the potential cross-coupling of **3.1.21** has been thoroughly investigated. Despite the breakdown of the compounds using palladium catalysis, it is believed that a radical process for functionalisation at this position is plausible. It is also of

interest to utilise the dichlorinated **3.1.18** system as an alternative coupling partner with the intermediate radical species being inherently more stable and therefore potentially more accessible. This prospective functionalisation could be accomplished using either a Michael acceptor or an alternative metal species for the coupling reaction.

4.0 Bioisosteres in modulating metabolic stability

4.1 Soft-drugs

As discussed previously, carbonyl bioisosteres are inherently interchangeable. As such, esters could be used as isosteres of amides; however, esters are intrinsically unstable both from a chemical and metabolic perspective which generally negates their use in an oral drug molecule. Having stated this, the use of ester functionality can incorporate a predictable metabolic soft-spot into a drug-like compound. Classically this can be used in two ways: a pro-drug or a soft-drug. There is extensive literature on the use of pro-drugs in which the parent compound is converted by metabolism in a predictable way to the active species (Figure 52).¹⁹⁰ These are generally used to improve the physicochemical properties of the lead compound, for example to increase absorption or tune any potential side effect profiles.¹⁹⁰ A soft-drug is the opposite, in that it is dosed as the active species and is metabolised to an inactive compound in a predictable fashion (Figure 52).¹⁹⁰

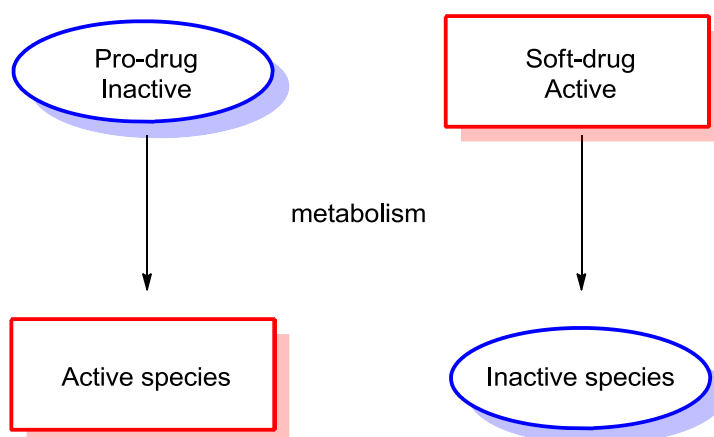


Figure 52 - Pro- and Soft-drugs

The soft-drug concept was proposed by Bodor *et al.* in the 1980s while investigating the application of a metabolically labile centre within antimicrobials, antitumor agents, and anti-cholinergics.^{191–193} Since then the development of soft-drugs has relied on 4 main approaches:¹⁹⁰

- 1) Soft analogues – a close structural relative to a known active drug which has a specific metabolic liability built in.
- 2) Inactive metabolite approach – an active compound designed from a known or hypothetical metabolite of an existing drug.

- 3) Active metabolite based soft-drug – metabolic products of a drug that retain significant activity can be developed with further metabolic liabilities.
- 4) Pro-soft-drugs – Inactive pro-drugs of a soft-drug from any of the above designs.

All of the above approaches are exemplified in the literature with the most common being the use of soft analogues or the inactive metabolite approach.¹⁹⁰ The basic principles of soft analogues are:¹⁹⁰

- 1) Close structural analogues of a selected lead compound
- 2) A metabolically labile position is built into the molecular structure of the lead preferably a hydrolytic centre
- 3) The metabolic liability is located so that the overall profile is very close to that of the lead; usually isosteric to the lead
- 4) The built in metabolism is the major, or preferably the only, route for deactivation
- 5) The rate of deactivation is controllable by structural modifications
- 6) The metabolites are non-toxic and have no significant biological activity including at off-targets
- 7) The metabolism does not require enzymatic processes which lead to highly reactive intermediates

As stated above, the soft-drug approach is prevalent in the medicinal chemistry literature. One simple example comes from antimicrobials developed around pyridinium salts (Figure 53).¹⁹¹ The incorporation of the ester group does not significantly alter the physicochemical properties when comparing **4.1.1** and **4.1.2**, however the lethal dose when compared between **4.1.1** and **4.1.3** is significantly improved, with **4.1.3** being approximately 40 times less toxic.¹⁹¹

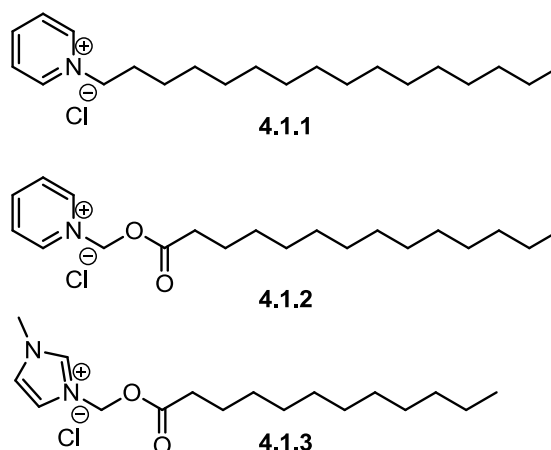


Figure 53 - Development of antimicrobial soft drugs¹⁹¹

Using the inactive metabolite approach, a variety of soft β -blockers were developed. The β -blocker metoprolol has a well established metabolic fate. Carboxylic acid derivative 4.1.5 is one such metabolite which was investigated as a starting point for the inactive metabolite approach to soft-drug design (Figure 54).

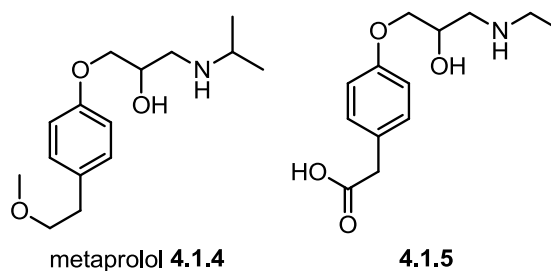


Figure 54 - Metoprolol and its inactive metabolite 4.1.5

Converting the acid metabolite to the ester functionality and homologating the carbon chain produced esmolol (Figure 55). In 1986, Esmolol was approved for intravenous clinical use by the food and drug administration (FDA) for temporary ventricular control in supraventricular arrhythmias.¹⁹⁴

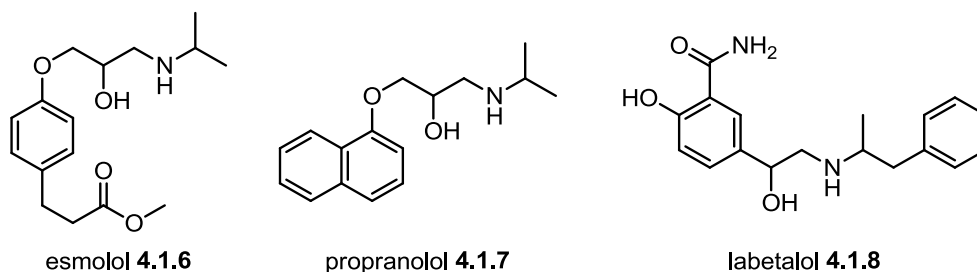


Figure 55 - β -blockers

Esmolol demonstrates a markedly reduced half life (5 – 15 mins) when compared to other β -blockers propranolol (2 – 4 h),¹⁹⁰ metoprolol (3 – 7 h)¹⁹⁵ and labetalol (6 – 8 h) (Figure 55)¹⁹⁶ with dissipation of its pharmacological effect within 15-20 minutes.^{190,197} It is also noteworthy that the acid metabolite **4.1.5** has a long half life of 3.7 h, however it is inactive at the β -receptor and has no clinical effect.^{190,197}

Further examples of the soft-analogue approach can be seen in an anti-arrhythmic agent developed by Du Pont which utilised an ester instead of an amide.¹⁹⁸ The amide ACC-9358 exhibited suppression of spontaneous ventricular arrhythmias for up to 6 h after oral or intravenous dosing (Figure 56).¹⁹⁹

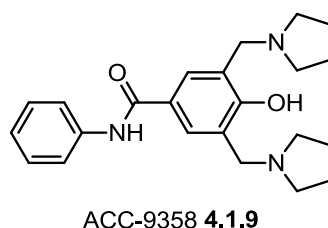
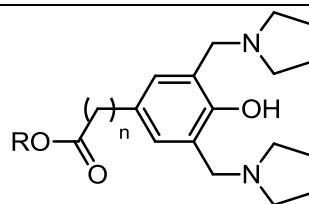


Figure 56 - Anti-arrhythmic agent ACC-9358

Incorporation of a variety of alkyl ester functionalities produced compounds with similar activity (Table 31).¹⁹⁸

Table 31 - Anti-arrhythmic activity and metabolism of soft analogues of ACC-9358¹⁹⁸ Reprinted with permission from: *J. Med. Chem.*, 1989, 32, 1910-1913, Copyright 1989 American Chemical Society



Compound	R	n	Guinea pig right atria, ED ₅₀ (µg/mL)	Human blood metabolism, t _{1/2} , min
ACC-9358 4.1.9	N/A	N/A	11	Not metabolised
4.1.10	(CH ₃) ₂ CH	0	11.4 ± 6.9	Not metabolised
4.1.11	CH ₃ CH ₂ CH(CH ₃)	0	6.7 ± 1.7	Not metabolised
4.1.12	(CH ₃) ₂ CHCH ₂	0	2.3 ± 1.1	Not metabolised
4.1.13	(CH ₃) ₂ CHCH ₂	1	5.0 ± 0.0	8.7 ± 2.1
4.1.14	(CH ₃) ₂ CHCH ₂	2	14.0 ± 4.1	25.9 ± 3.0
4.1.15	(CH ₃) ₂ CHCH ₂	3	6.0 ± 4.0	1.96 ± 0.57

A shorter acting anti-arrhythmic agent was desired due to potential toxicity problems especially in prophylactic administration for acute MI. Homologation of the chain between the aromatic ring and the ester was investigated in order to promote

metabolism through increasing lipophilicity and minimising steric bulk at the ester carbonyl centre.^{190,198} **4.1.13** displayed the optimum chain length with good potency and the desired short half life of around 10 mins (Table 31).^{190,198} This provided the basis for the development of compounds **4.1.16** and **4.1.17**, which display short half lives (3.5 and 7.1 mins, respectively) and good potency ($ED_{50} = 5.5$ and $7.3 \mu\text{g/mL}$, respectively) (Figure 57).^{190,200}

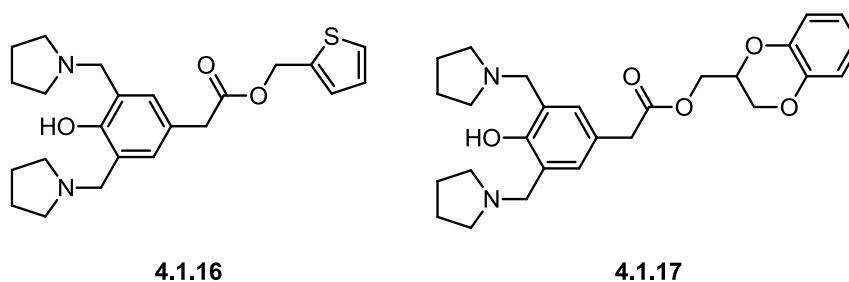


Figure 57 - Short acting anti-arrhythmic agents

4.1.16 and **4.1.17** were evaluated in *in vivo* models and **4.1.17** was taken forward as a development candidate because it possessed the most desirable profile.^{190,200}

Considering the effectiveness of this approach in improving the toxicological profile of drug molecules, it was proposed that a soft-drug approach could be applied to an inhaled bromodomain (Brd) and extra-terminal (BET) domain family inhibitor, a class of compound which is of interest to our own laboratories as a treatment for inflammatory diseases. The background to this target and the proposed study is outlined in the subsequent sections.

4.2 Bromodomain (Brd) and extra-terminal domain (BET) proteins

Deoxyribonucleic acid (DNA) carries the genetic code of every individual within a eukaryotic cell. To facilitate storage within the cell, the DNA is wrapped around positively charged proteins called histones to form nucleosomes.²⁰¹ These undergo further bundling to form densely packed DNA structures called chromatin (Figure 58).²⁰¹ These chromatin structures further bundle into the chromosome structure with each chromosome packing approximately 2×10^8 nucleotide pairs (Figure 59). When packed in this way, genes are unable to undergo transcription and are effectively silenced.

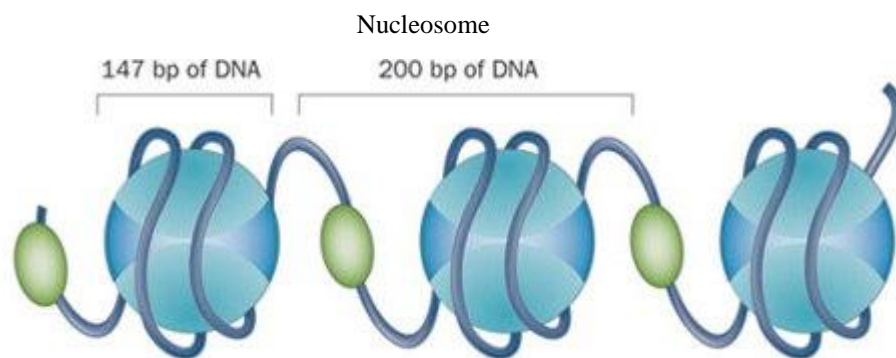


Figure 58 - Structure of chromatin²⁰¹ *Reprinted by permission from Macmillan Publishers Ltd: Nat. Rev. Urol., 2012, 9, 147-155, Copyright 2012*

Accordingly, control of transcription can be achieved through post-translational modifications (PTMs) of histones. The packing of these structures is dynamic with protrusions from the chromatin structure known as histone tails being susceptible to a variety of PTMs.

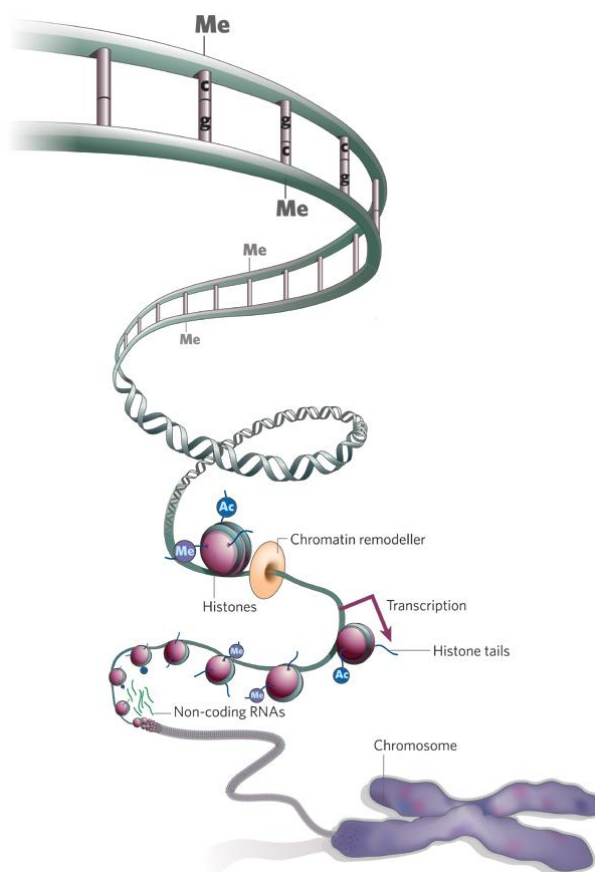


Figure 59 - Structure of a chromosome²⁰² *Reprinted by permission from Macmillan Publishers Ltd: Nature, 2008, 454, 711-715, Copyright 2008*

Direct methylation of DNA and these PTMs of the histone proteins, including methylation, acetylation, phosphorylation and ubiquitination, are created by a series of enzymes, known as “writers”.²⁰³ PTMs can also be removed by another subset of enzymes termed “eraser” enzymes. PTMs protrude from the nucleosome structure and make up the epigenetic code.²⁰⁴ “Reader” enzymes or transcription regulators bind to these features and recruit further proteins such as transcription factors to allow for ribonucleic acid (RNA) transcription.²⁰³ Clearly, modulation of the activity of enzymes which either add or remove a PTM could be of interest in treating disease as this ultimately controls protein expression.

Acetylation of lysine residues weakens the DNA-histone interaction and exposes DNA for transcription.²⁰⁵ Bromodomains (Brds) are “reader” proteins which are able to recognise and bind these sites and, through protein-protein interactions, recruit protein complexes that enable transcription of the DNA code.^{206–208} To date, 61 Brds

have been identified across 46 different proteins, which are made up of approximately 110 amino acids.^{206–209} These can be displayed on what is termed a phylogenetic tree, which groups the Brd proteins into 8 sub-families based on protein sequence homology (Figure 60).²⁰⁸

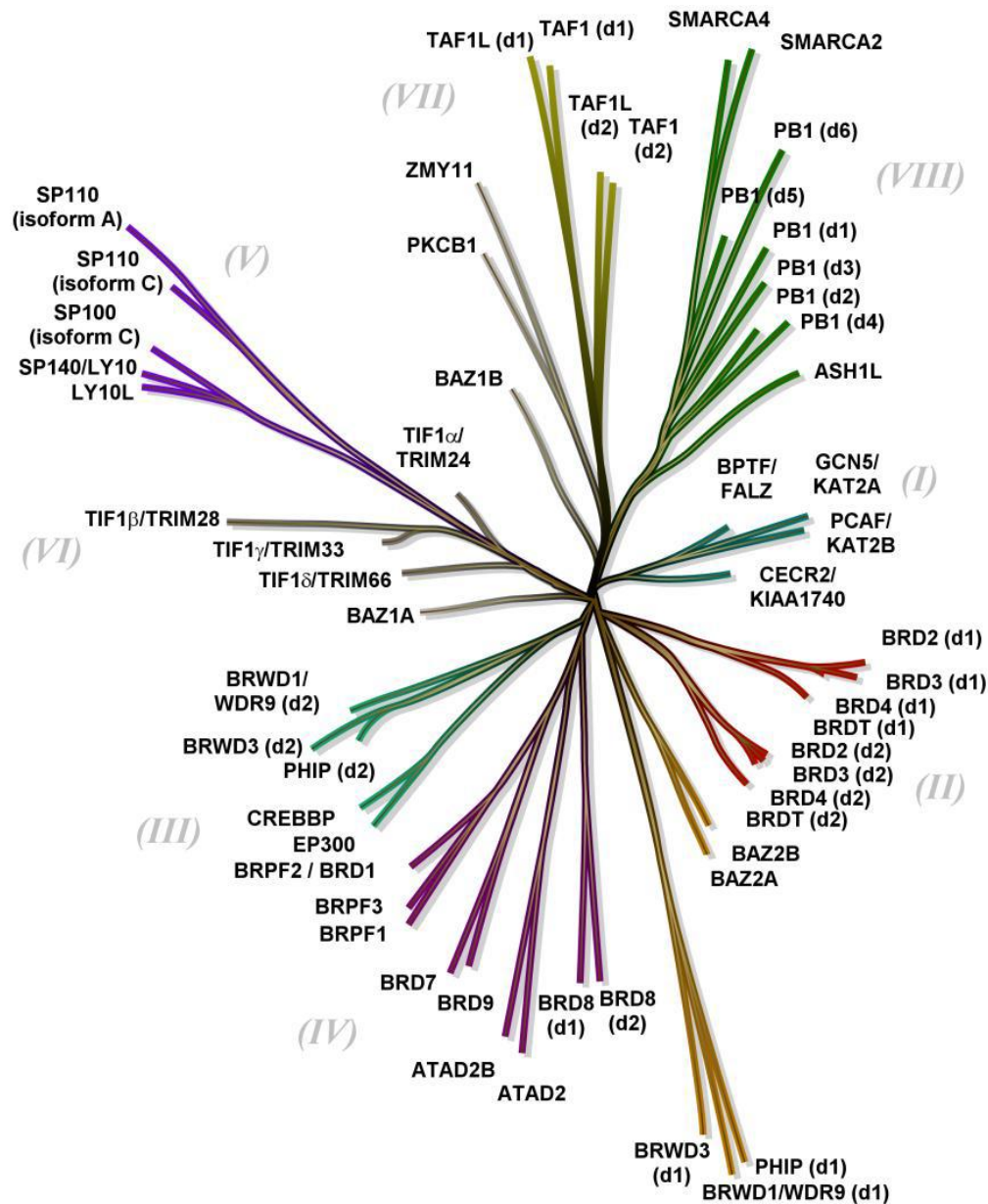


Figure 60 - Phylogenetic tree of the Brd family²¹⁰

Sub-group II (Figure 60) is termed the BET family of Brds and consists of Brd2, Brd3, Brd4 and BrdT.^{208,211} Brds 2-4 are ubiquitously expressed throughout the body, whereas BrdT is a testes specific Brd containing protein (BCP).²⁰⁵ Each of these BCPs contain two Brds classed as BD1 and BD2 as well as an extra terminal domain

(Figure 61).²⁰⁵ Each Brd within the protein shares significant structural similarities but there is a greater similarity between BD1 or BD2 domains across the proteins compared to the domains within the same protein.^{205,212}



Figure 61 – BET protein sequence structure²¹²

Many individual Brd crystal structures have been solved.²¹³ These structures confirmed an earlier prediction made by Dhalluin *et al.* that all Brds adopt a conserved structural bundle of four helices (α_Z , α_A , α_B , α_C) with inter-helical ZA and BC loops (Figure 62A).^{203,214–216} The loops are variable in length and sequence and fold to form a hydrophobic pocket in which the acetyl lysine residues of the histone systems can bind.^{205,216}

Despite the variability in ZA and BC loops leading to Brd differentiation, the amino acid residues which engage the acetylated lysines are highly conserved across the Brds.^{205,216} These include two tyrosine residues and an asparagine.²¹⁶ Water molecules at the base of the ZA channel also contribute to the acetylated lysine binding with interactions through hydrogen bonds to the amide carbonyl groups of the protein backbone.²¹⁶ The specificity of each Brd is achieved by recognition of residues which flank the acetylated lysine itself.²¹⁶

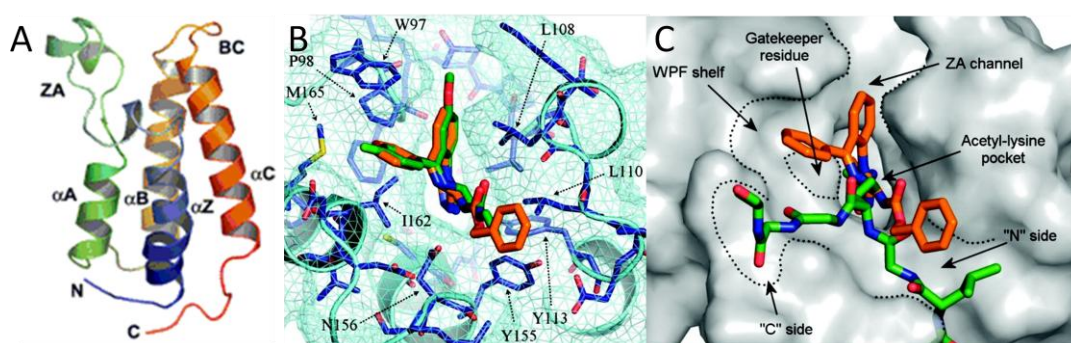


Figure 62 – A) X-ray crystal structure of Brd2 BD1,²¹³ B) Brd2 BD1 complexed with I-BET762 (green) and GW841819X (orange),²⁰³ C) Surface representation of Brd2 BD1 with GW841819X overlaid with acetylated histone 4 peptide.²⁰³ B and C Adapted with permission from: *J. Med. Chem.*, 2011, 54, 3827-3838, Copyright 2011 American Chemical Society

The structural similarities between the 8 BET Brds has made it particularly challenging to access molecules which are selective for any one BET Brd. As a result, efforts in the first instance has primarily focused on developing pan-BET inhibitors. The first disclosure of pan-BET inhibitors was in 2010 upon publication of (+)-JQ1 and I-BET762 (Figure 63).^{207,217}

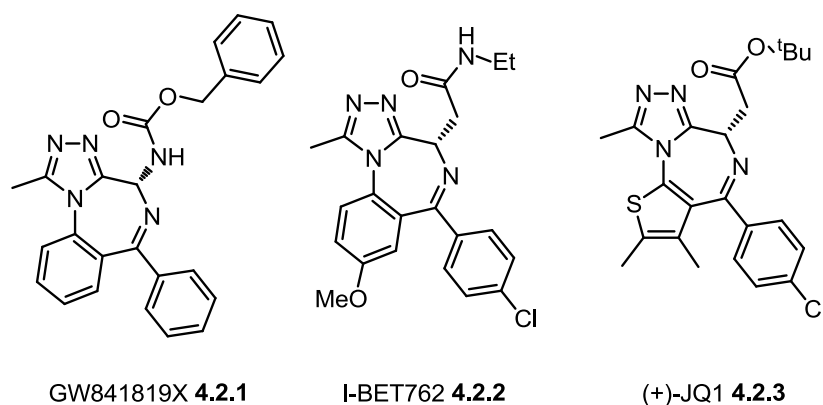


Figure 63 – GW841819X, I-BET762 and (+)-JQ1

I-BET762 was initially developed to promote up-regulation of apolipoprotein A1, which is involved in atherosclerosis progression and inflammation.^{203,218} A chemoproteomic study concluded that I-BET762 was an inhibitor of Brd2, Brd3 and Brd4.²⁰³ (+)-JQ1, which has the same benzodiazepine scaffold, was developed by Filippakopoulos *et al.* and displays an *in vitro* IC₅₀ of 77 nM at Brd4 BD1 and an IC₅₀ of 33 nM at Brd4 BD2, with good selectivity over other non-BET Brds.²⁰⁷ This is comparable to I-BET762, which has an IC₅₀ of 36 nM, again with selectivity over non-BET Brds.^{217,218} X-ray crystal structures of I-BET762 and the related compound GW841819X have been solved and elucidated the binding pocket of the BET family (Figure 62B).²⁰³ This consists of the key acetylated lysine pocket, and recognition regions denoted the “WPF shelf” and the “ZA channel” (Figure 62C).²⁰³

Further investigation of the BET family of Brds has led to the development of inhibitors which have potential utility for a variety of diseases including asthma, chronic obstructive pulmonary disease and a selection of cancers. A study carried out by other members of our laboratories investigated I-BET762 in an inflammatory model, demonstrating that it was able to suppress the production of a variety of cytokines and chemokines stimulated by lipopolysaccharide (LPS).²¹⁷ This study also

demonstrated the selective effects of BET inhibition with non-LPS stimulated macrophages displaying minimal changes in expression of other genes.²¹⁷

(+)-JQ1 has been investigated by Filippakopoulos *et al.* as a treatment for NUT midline carcinoma, a rare and aggressive cancer.^{207,211} It was demonstrated that (+)-JQ1 caused tumour regression and reduction in tumour growth in xenograft models.^{207,211} The BET proteins have also been implicated in a number of other cancer types including: acute myeloid leukaemia,²¹⁹ Burkitt's lymphoma,²¹⁹ multiple myeloma,²²⁰ and lung adenocarcinoma.²²¹ Since the initial development of I-BET762 and (+)-JQ1, a diverse range of BET inhibitors have been developed for the treatment of a raft of diseases (Figure 64).²⁰⁴

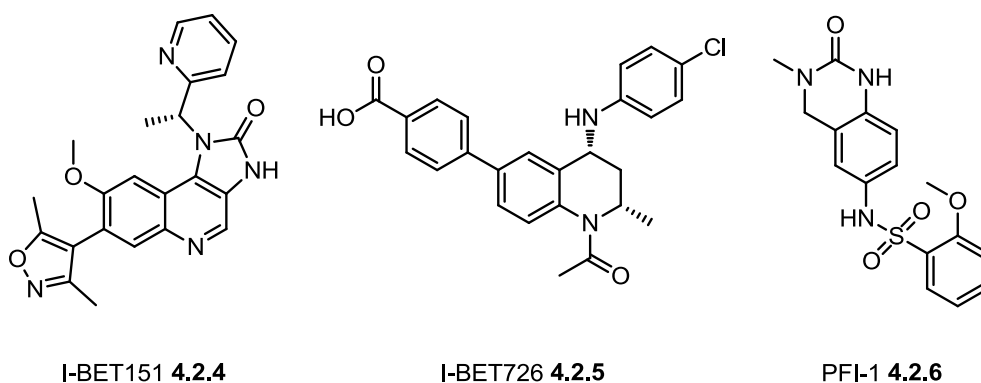
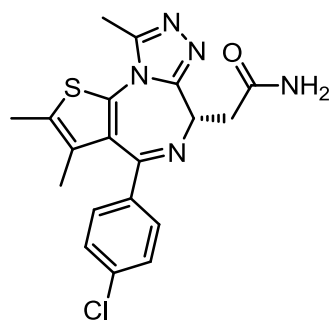


Figure 64 - Selection of pan-BET inhibitors²⁰⁴

Inflammation is a common issue caused by many disease states and, as discussed previously, BET Brds are involved in the production of inflammatory cytokines and chemokines.²¹⁷ The inflammatory response mediated by the BET family has been investigated in a pulmonary arterial hypertension (PAH) model using (+)-JQ1.²²² PAH is a fatal disease which is caused by nuclear factor kappa B (NF- κ B) mediated inflammatory gene expression, as well as endothelial cell proliferation.²²² BET inhibition with (+)-JQ1 demonstrated a decrease in inflammation and cell remodelling indicating its potential therapeutic use.²²² (+)-JQ1 has also been used to reduce inflammation within epithelial cells obtained from cystic fibrosis sufferers by reducing the over-expression of the inflammatory chemokine interleukin 8 (IL-8).²²³



CPI-203 4.2.7

Figure 65 - Pan-BET inhibitor CPI-203

A further study of BET inhibitor CPI-203 (Figure 65), investigating effects on cystic fibrosis was carried out by Chen *et al.*²²⁴ This investigation demonstrated that BET inhibition can regulate T-cell responses of T-helper cell 17 (Th17) mediated inflammation.²²⁴ It was shown that the production of the pro-inflammatory chemokine IL-17 in human bronchial epithelial cells was reduced.²²⁴ This was extended to a murine model demonstrating decreased inflammation without exacerbating infection.²²⁴

The alternative inhibitor I-BET762 has been investigated as a treatment for asthma.²²⁵ As the previous reports have shown, I-BET762 inhibits the production of inflammatory chemokines and cytokines.²¹⁷ In this investigation Yang *et al.* demonstrated the effectiveness of the compound on steroid resistant airway hyper-responsiveness in two murine models.²²⁵ Administration of I-BET762 resulted in a decrease in macrophage and neutrophil infiltration into the airways and suppressed key pro-inflammatory cytokines such as MCP-1, INF- γ and IL-27.²²⁵ Based on all of the above, research into BET inhibition provides conclusive evidence for its implication in a variety of diseases and its potential therapeutic utility.

4.3 Aims

The fundamental role of BET proteins in gene transcription means inhibition can have potential toxic implications. It has been reported that strong suppression of BET Brd 4 proteins has toxic effects in a variety of tissues resulting in epidermal stem cell depletion within the small intestine, alopecia, decreased cellular diversity, and hyperplasia.²²⁶ Furthermore, it can lead to sensitivity to organ stress and impaired regeneration. With these potential toxic implications, a tissue selective inhibitor could be desirable. Accordingly, a soft-drug might provide such selectivity by utilising the body's internal mechanisms. With BET proteins being potential anti-inflammatory targets within the lungs, selective inhibition at this site of action *via* inhaled delivery is viable. Upon inhalation the potential drug would be deposited in the lungs and be absorbed into the relevant cells to impart its therapeutic activity. After entering the blood stream the soft-drug's incorporated liability would result in metabolism to generate an inactive (or peripherally restricted) compound, thus achieving site (lung) selectivity.

Considering that approximately 80% of an inhaled dose enters the body *via* the oesophagus (i.e. is swallowed), downstream toxicological implications from this route of administration could be foreseen. However, a further benefit of a soft-drug approach could be degradation of the drug within the gastrointestinal tract, preventing systemic exposure and therefore minimising the risk of toxicology. The potential toxicity risks associated with BET inhibition meant that a soft-drug approach could improve the therapeutic window for an inhaled BET inhibitor. This hypothesis was subsequently investigated on a range of molecules identified as BET inhibitors in our laboratories.

5.0 Bioisosteric acetyl-lysine mimetics

5.1 Application to BET inhibitors

As discussed in the previous chapter, Brds recognise and bind acetylated lysine residues on histone tails. Many Brd inhibitors block the key acetyl amide to Brd interaction and incorporate an acetylated lysine bioisostere. Application of a metabolically labile isostere could provide a BET inhibitor, which upon metabolism would be rendered inactive. Such a “soft-drug” could offer the opportunity of site selective inhaled therapy. Inhalation of the drug in question would direct the compound to the site of action within the lung, however upon entering the blood stream the labile functionality would be hydrolysed to the inactive acid. This would ensure biological activity only within the lungs and avoid potential toxicological liabilities brought about as a result of systemic exposure. In its simplest form, the acetyl-lysine isostere is a methyl amide moiety. Three compounds utilising a methyl amide/reverse amide were identified from screening of the library of BET inhibitors available in our laboratories (Figure 66).

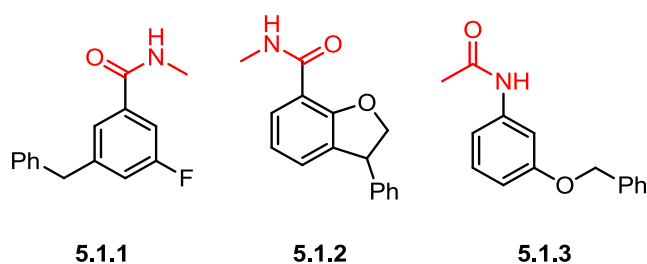


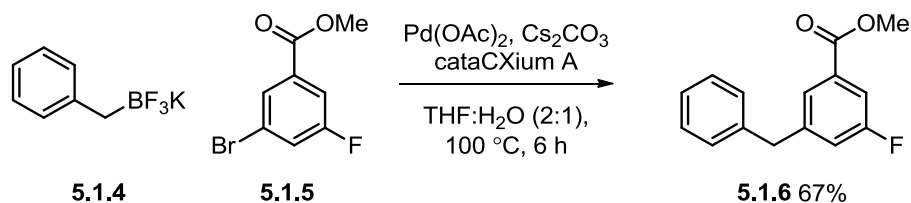
Figure 66 - Selected compounds 5.1.1,²²⁷ 5.1.2²²⁸ and 5.1.3²²⁹

The compounds each demonstrated measureable potency against Brd 4 BD1 and/or BD2 (used as a surrogate for other BET Brds) and had high ligand efficiencies (LEs) (a measure of affinity per heavy atom),⁵¹ thereby making them a good starting point for optimisation (Table 32).

Table 32 – Potency and ligand efficiency data of 5.1.1, 5.1.2, and 5.1.3

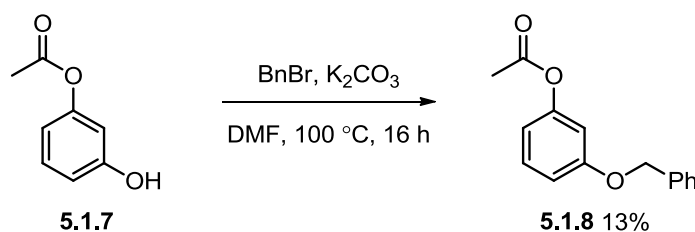
Compound	5.1.1	5.1.2	5.1.3
BD1 pIC₅₀	5.1	4.4	4.4, <4.3
BD2 pIC₅₀	5.4	5.7	4.5
BD1 LE	0.39	0.32	0.33
BD2 LE	0.41	0.41	0.34

The initial focus of the study was to determine whether replacing the methyl amide with a methyl ester would have a detrimental effect on potency. As such, compound **5.1.6** was targeted as a direct comparator to **5.1.1** and was readily synthesised in one step using a Suzuki-Miyaura cross-coupling between the commercially available coupling partners **5.1.4** and **5.1.5** (Scheme 87).



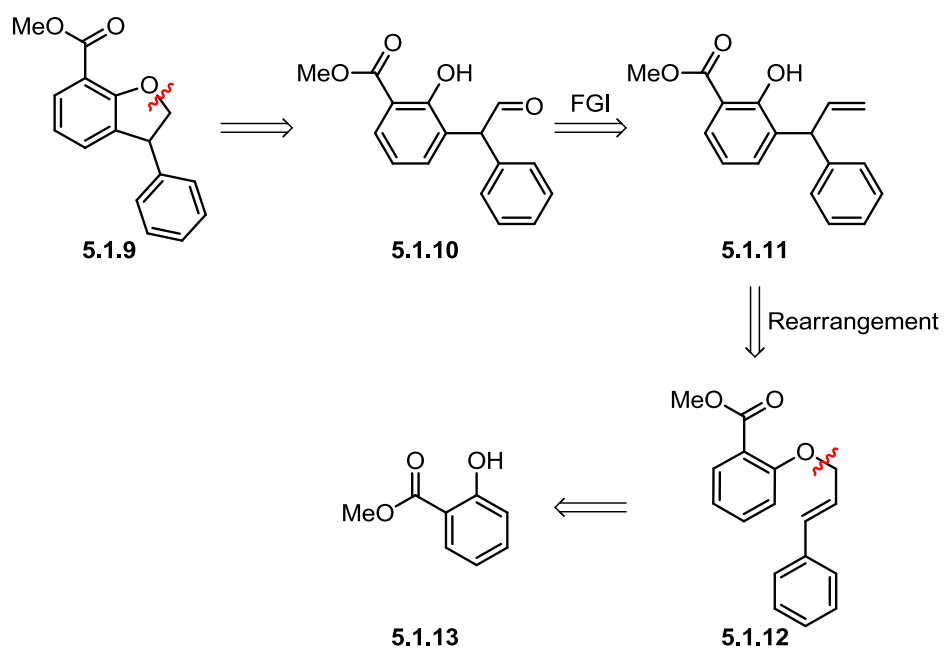
Scheme 87 – Suzuki coupling of **5.1.4** and **5.1.5**

Similarly, compound **5.1.8** was targeted and synthesised *via* a straightforward benzylation of the commercially available phenol **5.1.7** (Scheme 88).

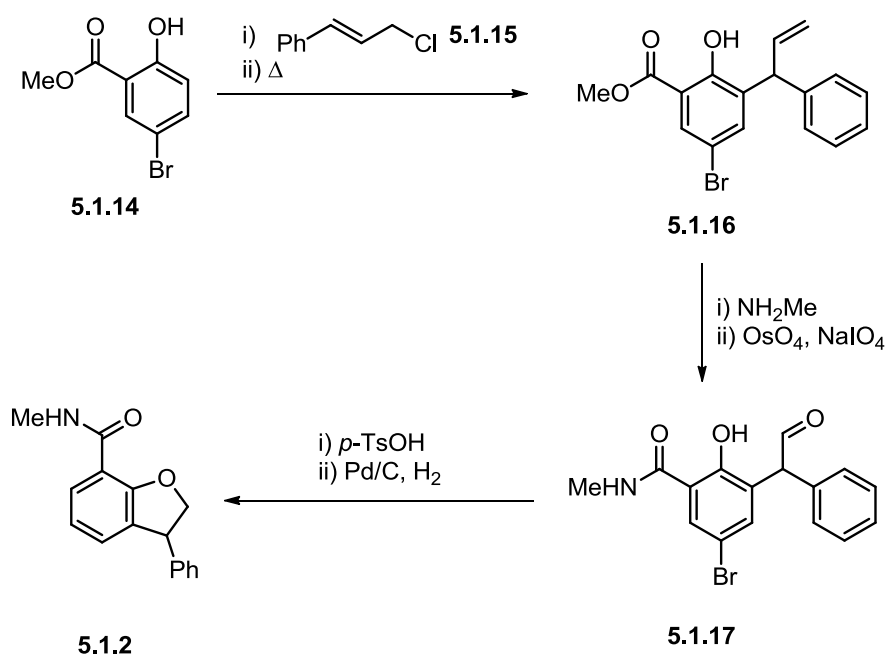


Scheme 88 – Benzylation of **5.1.7**

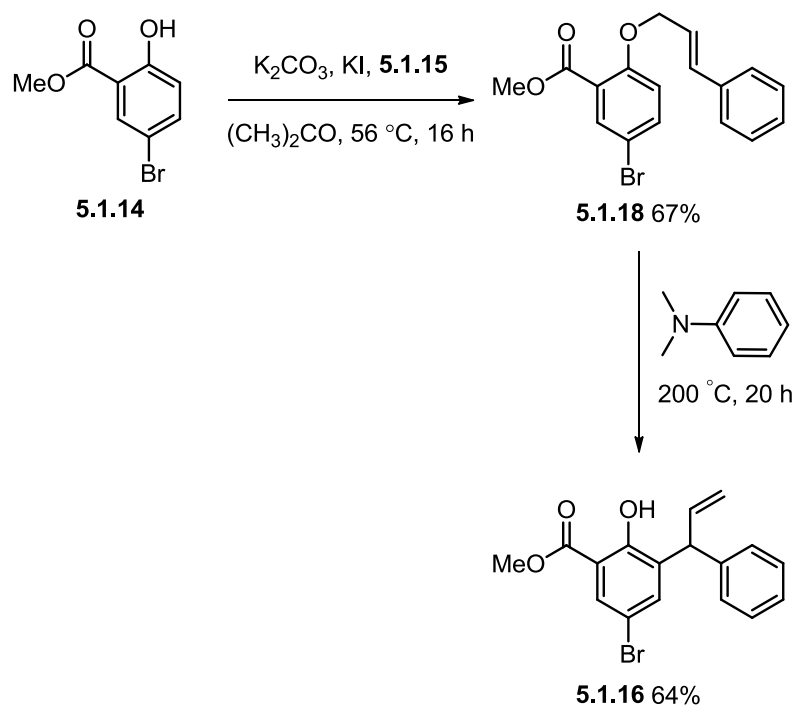
The methyl ester analogue of dihydrobenzofuran **5.1.2** posed a more significant synthetic challenge and therefore a retrosynthetic analysis was applied to this particular template (Scheme 89) in order to identify a suitable forward synthesis.

Scheme 89 - Retrosynthetic analysis of **5.1.9**

Utilising previous experience within the group,²³⁰ it was envisaged that the core could be synthesised using a ring closure onto an aldehyde with a subsequent hydrogenation to generate the desired dihydrobenzofuran **5.1.9**. Aldehyde **5.1.10** could be produced from the oxidation of alkene **5.1.11**. This alkene could ultimately originate from phenol **5.1.13** by alkylation and Claisen rearrangement methodology. In a forward sense, this methodology has been previously utilised in the synthesis of **5.1.2** (Scheme 90).

Scheme 90 - Synthesis of 5.1.2²³⁰

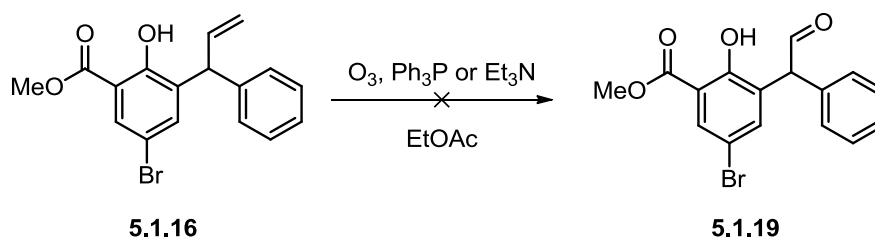
Consequently, the synthesis of **5.1.9** began with alkylation using cinnamyl chloride, producing **5.1.18** in good yield. Subsequent Claisen rearrangement produced the desired terminal olefin **5.1.16** in 64% yield (Scheme 91). The bromine moiety, although not desired within the final ester **5.1.9**, was incorporated as it could enable functionalisation and develop structure activity relationships around the template (**5.1.64**) discussed later.



Scheme 91 – Synthesis of intermediate 5.1.16

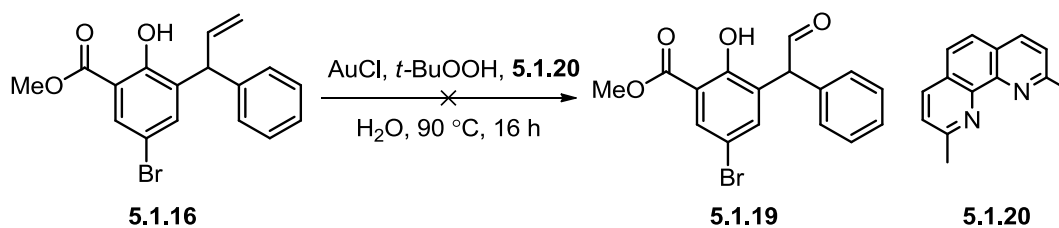
The next step was to convert the alkene into an aldehyde in preparation for subsequent cyclisation to the benzofuran. Conditions previously applied to related analogues involved the use of the highly toxic osmium tetroxide as a catalyst to generate the diol.²³¹ This diol could then be oxidatively cleaved *in situ* with sodium periodate to generate the desired aldehyde. Not only was the sodium periodate required to achieve oxidative cleavage, an excess was used to affect reoxidation of the catalytic osmium.

However, due to the highly toxic nature of the osmium tetroxide alternative conditions were sought. Initially, ozonolysis was considered for the direct cleavage of the alkene to the aldehyde. Unfortunately, both attempts proved unsuccessful with only starting material recovered (Scheme 92).



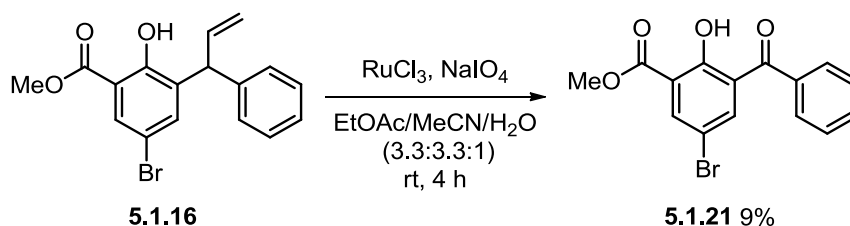
Scheme 92 – Ozonolysis of 5.1.16

An alternative gold catalysed cleavage, which has been reported by Shi *et al.*, was also investigated (Scheme 93).²³² However, after 16 h only starting material and the ligand were observed in the LCMS profile.



Scheme 93 – Gold catalysed oxidation of 5.1.16

Another group 8 metal, ruthenium was considered as an alternative for osmium. This had previously been reported by Niggemann *et al.* for the dihydroxylation of alkenes with the addition of sulfuric acid to prevent diol cleavage to the aldehyde.²³³ Since cleavage to the aldehyde was desirable in our case, it was anticipated that these conditions could be adapted, with the removal of the acid and addition of excess sodium periodate, to facilitate direct production of the aldehyde in one pot.

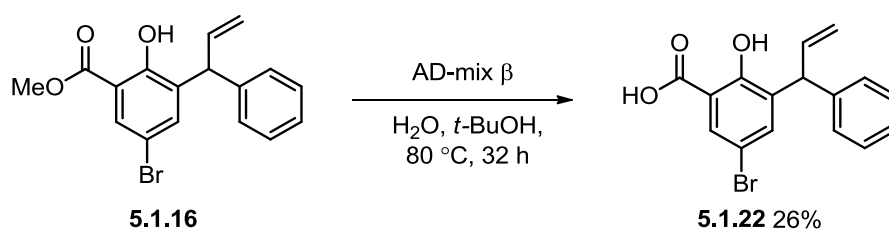


Scheme 94 – Ruthenium catalysed generation of undesired 5.1.21

The LCMS profile of the reaction mixture after 4 h indicated the presence of product, as well as the by-product 5.1.21. However, only 5.1.21 could be isolated in low yield upon work-up and purification (Scheme 94). Extending the reaction time and carrying out the procedure on a slightly larger scale (300 mg) resulted in reduced amount of desired product observed. As a result, the literature conditions using the addition of 20 mol% sulfuric acid with excess sodium periodate were examined. However, only the undesired ketone 5.1.21 was isolated in a similarly poor yield (8%). It was proposed that the production of the undesired ketone could be due to migration of the terminal olefin into conjugation with the aromatic rings by the strong acid. Subsequent diol formation and oxidative cleavage would then lead to the observed by-product 5.1.21. Additionally, the reaction profiles of both these

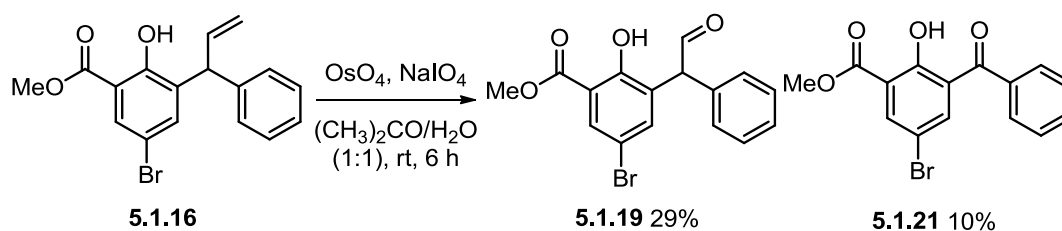
experiments displayed peaks of higher polarity compared to the desired and isolated products. Although these were not isolated, such compounds could have potentially been generated by further oxidation of the substrate.

A further alternative examined was AD-mix, which is a commercially available blend of reagents that acts as an asymmetric catalyst for a range of oxidative processes.²³⁴ AD-mix also offers a safer alternative to osmium tetroxide. Firstly, AD-mix β was stirred with **5.1.16** for 16 h, however conversion was observed to be slow. Addition of sodium periodate at this point did not generate any desired aldehyde as determined by LCMS analysis of the reaction mixture. The reaction was repeated in order to isolate the suspected diol product from the initial AD-mix addition, however acid **5.1.22** was in fact recovered (Scheme 95).



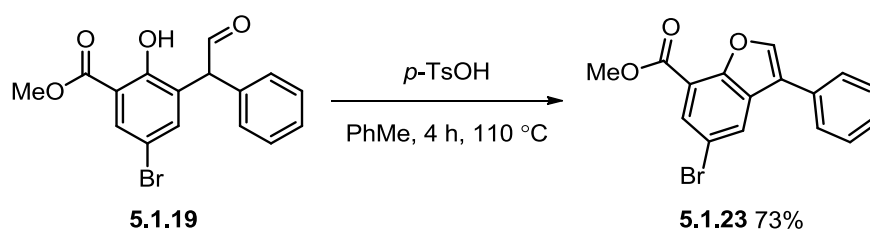
Scheme 95 – Isolation of by-product **5.1.22** from attempted AD-mix oxidation

The unsuccessful attempts to replace osmium tetroxide led to the decision to return to the known osmium conditions to facilitate rapid access to the desired aldehyde. Treatment of **5.1.16** with catalytic osmium tetroxide in the presence of sodium periodate generated **5.1.19**, which could be isolated in 29% yield. This was accompanied by 10% of the undesired ketone **5.1.21**, which has been observed in previous reactions (Scheme 96).



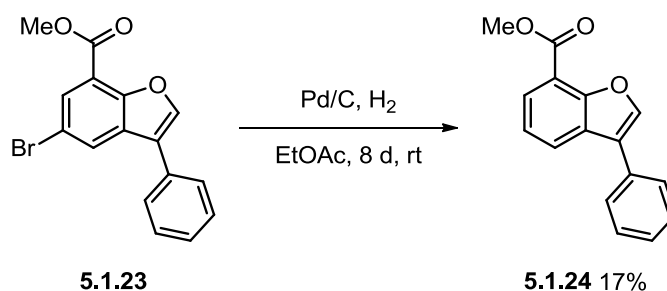
Scheme 96 – Successful osmium catalysed oxidation of **5.1.16** to aldehyde **5.1.19** and ketone **5.1.21**

With a sufficient quantity of material in hand, aldehyde **5.1.19** was heated in the presence of *p*-toluenesulfonic acid to facilitate cyclisation to the benzofuran **5.1.23** in good yield (Scheme 97).²³¹



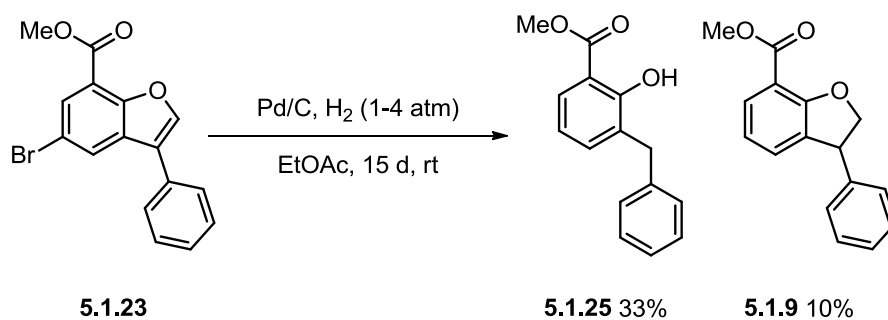
Scheme 97 – Cyclisation to benzofuran **5.1.23**

Subsequent hydrogenation to generate the desired dihydrobenzofuran proved challenging. Initial conditions, using palladium on carbon in ethyl acetate, generated a mixture of starting material, debrominated by-product and desired product, however only **5.1.24** was isolated from the reaction mixture (Scheme 98).



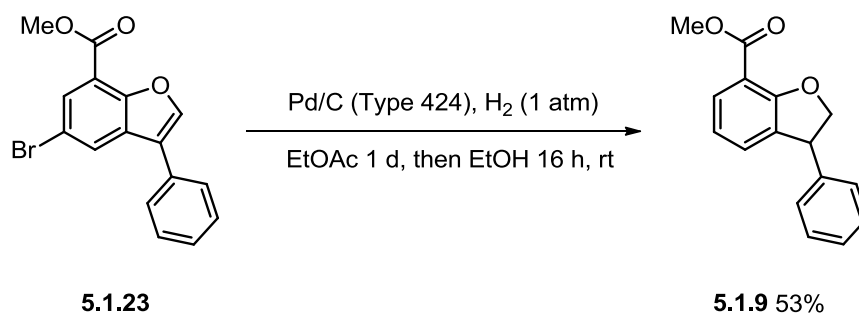
Scheme 98 – Debromination of **5.1.23**

In order to force the reaction to completion, the same conditions were utilised in COware apparatus²³⁵ with the pressure of hydrogen increased to approximately 4 atmospheres. After 5 days under these conditions only starting material and debrominated compound **5.1.24** were observed. The crude material was then further hydrogenated using a new batch of catalyst under one atmosphere of hydrogen for 7 days. This converted ~90% starting material into either **5.1.24** or the desired product **5.1.9**. The reaction mixture was then transferred to the COware apparatus to increase the pressure of hydrogen with this more effective batch of catalyst. After a further 3 days under these conditions ~20% desired product **5.1.9** and ~60% undesired by-product **5.1.25** was observed by LCMS and both were isolated in poor yield (Scheme 99).



Scheme 99 – Hydrogenation of 5.1.23

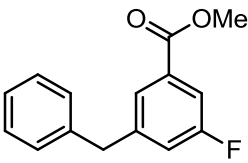
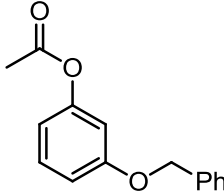
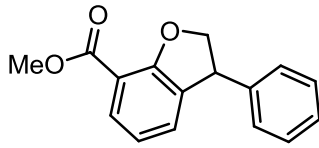
Previous work within our laboratories identified a more activated palladium on carbon (type 424) as the optimum catalyst on a closely related 3-phenylbenzofuran.²³⁶ Benzofuran **5.1.23** was insoluble in the preferred solvent ethanol, therefore the new catalyst was utilised with ethyl acetate as solvent and clean conversion to the debrominated product was achieved after 24 h. Exchanging solvent to ethanol at this stage led to the full hydrogenation to the desired dihydrobenzofuran **5.1.9** in good yield (Scheme 100).



Scheme 100 – Hydrogenation of 5.1.23 using alternative catalyst

Although not necessarily in optimal yield, the three methyl ester analogues of initial hits **5.1.1**, **5.1.2** and **5.1.3** had been prepared. Initially, this was all that was required to ascertain if the methyl ester moiety was indeed a viable replacement for the methyl amide and would maintain potency. All three methyl ester analogues were tested in Brd4 BD1 and BD2 biochemical assays and compared to the parent methyl amide (data in brackets, Table 33).

Table 33 – Comparison of bioisosteric methyl ester derivatives to their parent amides

Compound	5.1.6 (5.1.1)	5.1.8 (5.1.3)	5.1.9 (5.1.2)
Structure			
pIC ₅₀ BD1	<4.3 (5.1)	<4.3 (4.4)	<4.3, 4.3 (4.4)
pIC ₅₀ BD2	4.6 (5.4)	<4.3 (4.5)	6.0 (5.7)

It was expected that some potency would be lost upon switching from a methyl amide to a methyl ester, which is indeed the case for compounds **5.1.6** and **5.1.8**. Since compound **5.1.3** only exhibited low potency at Brd4 BD1 and BD2, it was perhaps unsurprising that compound **5.1.8** lost all potency and dropped below the lower limit of the assay (pIC₅₀ <4.3); consequently this scaffold was not progressed further. Disappointingly, compound **5.1.6** lost almost 10-fold of potency in switching from amide to ester. The potency at BD1 dropped below the limit of the assay, however **5.1.6** retains some potency at BD2 giving confidence that optimisation of this small fragment could provide a suitably potent lead. Pleasingly, compound **5.1.9** retained potency at both BD1 and BD2, providing the first indication that the hypothesis of replacing a methyl amide with a methyl ester might be viable within this template. Based on this positive result, attention was focussed on this dihydrobenzofuran template and further optimisation of **5.1.6** and **5.1.8** was halted.

With confirmation of the potency of compound **5.1.9**, a variety of other ester groups were targeted including ethyl **5.1.26**, isopropyl **5.1.27**, cyclobutyl **5.1.28**, methylcyclopropyl **5.1.29**, hexafluoroisopropyl **5.1.30**, and trifluoroethyl **5.1.31** (Figure 67). This was of interest to investigate the steric and electronic impact of small ester functionality on both potency and metabolic stability. It was hypothesised that the rate of metabolism could be controlled by the type of ester utilised, however there was a requirement that these be kept small to more closely mimic the acetyl-lysine of the endogenous substrate.

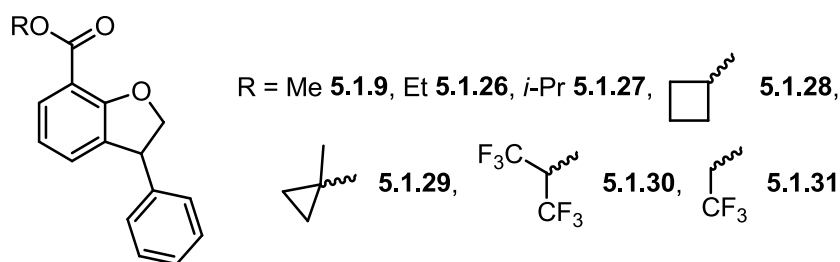


Figure 67 –Alternative ester groups to be examined

Examination of data generated elsewhere in our laboratories on more elaborated dihydrobenzofuran molecules identified compound **5.1.32**²³¹ as an equipotent ($pIC_{50} = 5.8$) exemplar of **5.1.2** (Figure 68). It was anticipated that the incorporation of the hydroxymethyl could remove the issues associated with the oxidation and subsequent cyclisation involved in the synthesis of the dihydrobenzofuran **5.1.9** by utilising epoxidation methodology, previously used in our laboratories,²³⁰ on intermediate **5.1.16**. Additionally, this hydroxymethyl unit could enhance the physicochemical properties of the compound, with an approximately 14-fold reduction in lipophilicity noted between the amide counterparts **5.1.32** and **5.1.2** (ChromLogD_{7.4}: 3.42 vs. 4.88, respectively).

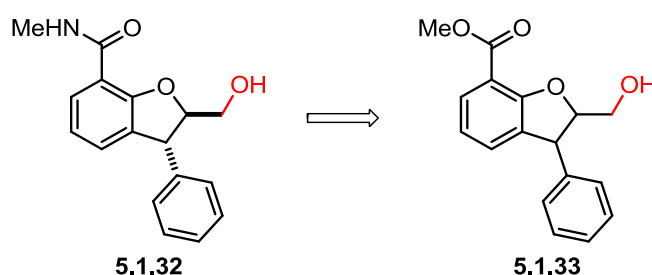
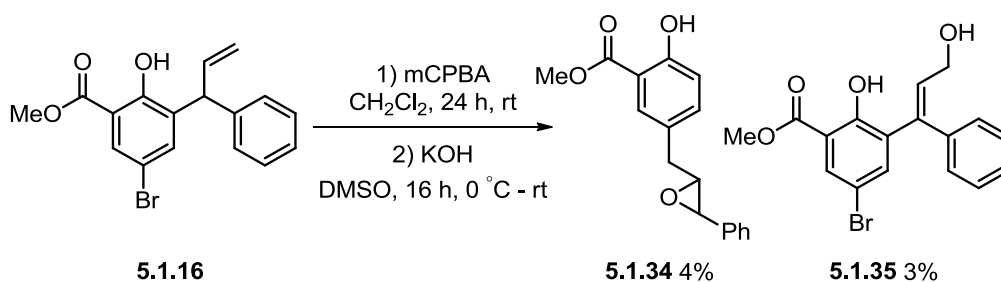


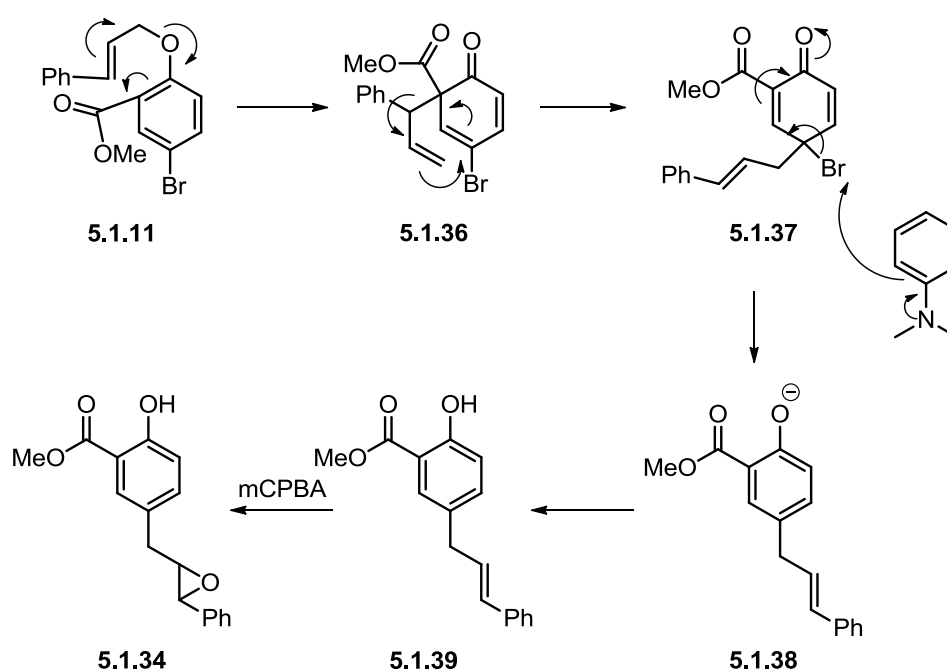
Figure 68 - Modified template

The subsequent investigation focused on the synthesis of the methyl ester analogue of **5.1.32** to determine if the potency could be retained in the **5.1.33** template. The first attempt, using a method previously established by another member of our laboratories,²³¹ produced two undesired by-products **5.1.34** and **5.1.35** in low yield (Scheme 101).

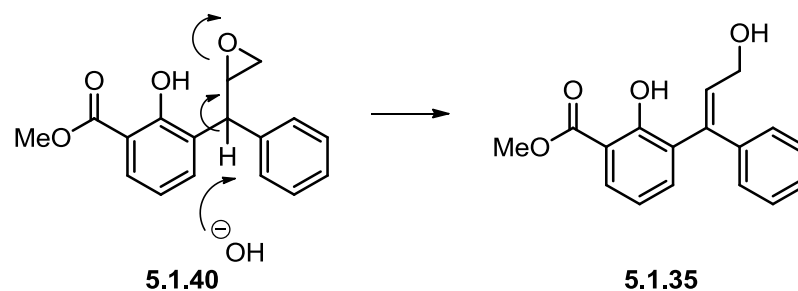


Scheme 101 – Epoxidation by-products

From a mechanistic perspective, it can be inferred that epoxide **5.1.34** could be generated by epoxidation of a minor by-product **5.1.39**, which was an inseparable impurity generated in the previous step. Olefin **5.1.39** itself could have been generated by a *para*-Claisen rearrangement which proceeds through a classical Claisen rearrangement to the already occupied *ortho*-position (Scheme 102). A subsequent Cope rearrangement leads to intermediate **5.1.37**, which upon loss of bromine to the solvent under the forcing reaction conditions (200 °C) regenerates aromaticity and upon work-up the by-product **5.1.39**.

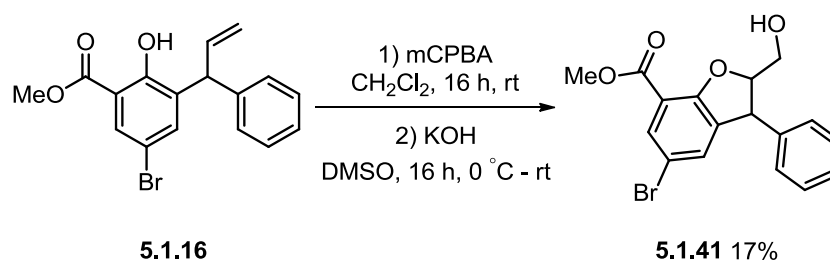
Scheme 102 – By-product **5.1.38** formation via *para*-Claisen rearrangement

Additionally, isolation of by-product **5.1.35** (Scheme 101) suggests that the epoxidation of **5.1.16** was occurring, however an elimination ring-opening pathway was competing against the desired cyclisation (Scheme 103).



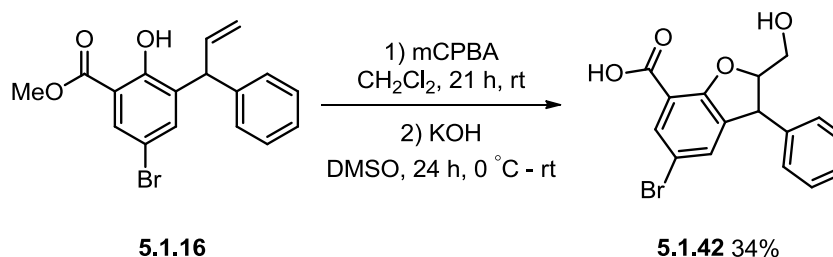
Scheme 103 – Formation of by-product 5.1.35

In order to avoid the generation of by-product **5.1.34**, the reaction was repeated using starting material of a higher degree of purity. Subjecting the purified material to the same epoxidation conditions produced the desired compound **5.1.41**, albeit in low isolated yield (Scheme 104).



Scheme 104 – Successful epoxidation of 5.1.16

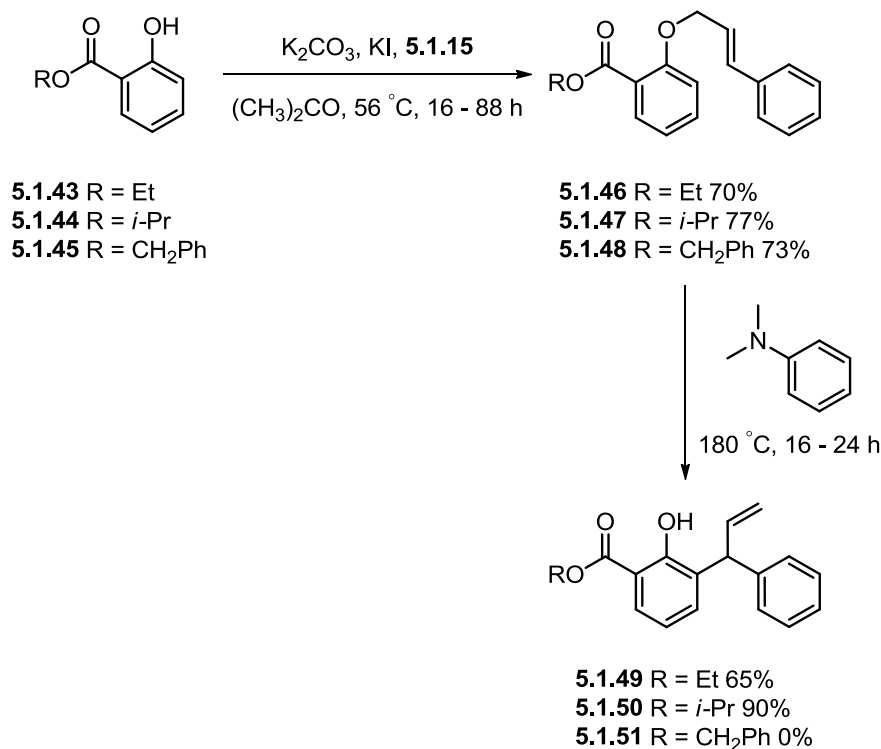
In all cases, treatment of **5.1.16** with *meta*-chloroperbenzoic acid (mCPBA) led to a low mass balance, whether it be desired product or unwanted by-products. In order to account for the mass balance of the reaction, the experiment was repeated with comprehensive extractions of the aqueous layer during work-up. This led to the isolation of acid **5.1.42**, however this was still in low yield (Scheme 105).



Scheme 105 – Acid 5.1.42 by-product synthesis

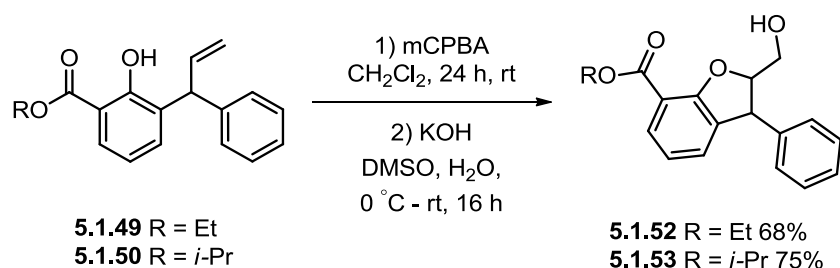
The fact that hydrolysis of the methyl ester was observed during the epoxidation suggested that replacing this with an alternative, more stable ester could facilitate more effective synthesis of the target dihydrobenzofuran systems. Three alternative

esters were examined (isopropyl, ethyl and benzyl) with the bromine omitted due to commercial availability of the requisite starting materials. Initial alkylation of ethyl ester **5.1.43**, isopropyl ester **5.1.44**, and benzyl ester **5.1.45** proceeded in good yield (Scheme 106). Subsequent Claisen rearrangements produced variable results with good to excellent yields for the ethyl and isopropyl derivatives **5.1.46** and **5.1.47** (Scheme 106), however the benzyl ester analogue **5.1.51** could not be isolated due to poor conversion.

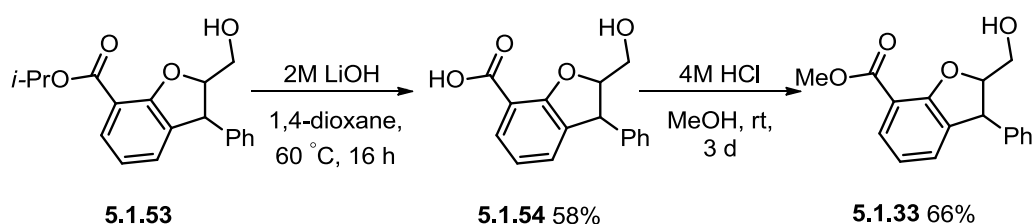


Scheme 106 – Alkylation and Claisen rearrangements using ethyl, isopropyl and benzyl esters **5.1.43**, **5.1.44** and **5.1.45**

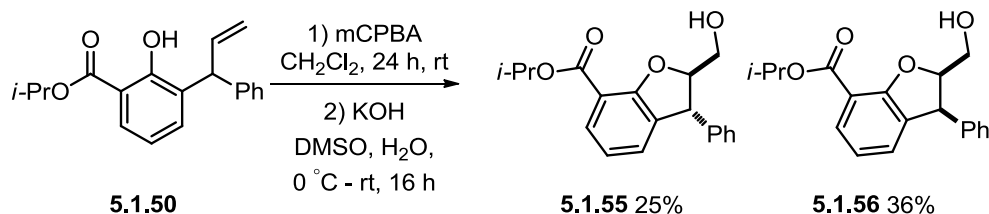
With **5.1.49** and **5.1.50** in hand, epoxidation and subsequent cyclisation to generate the dihydrobenzofuran core were investigated. In both cases, the reactions proceeded well with **5.1.52** and **5.1.53** being isolated in good yield as an approximately 1:1 mixture of diastereomers (Scheme 107), supporting the hypothesis that modification of the ester could lead to improved isolation of the requisite dihydrobenzofurans.

Scheme 107 – Epoxidation of ethyl and isopropyl esters **5.1.49** and **5.1.50**

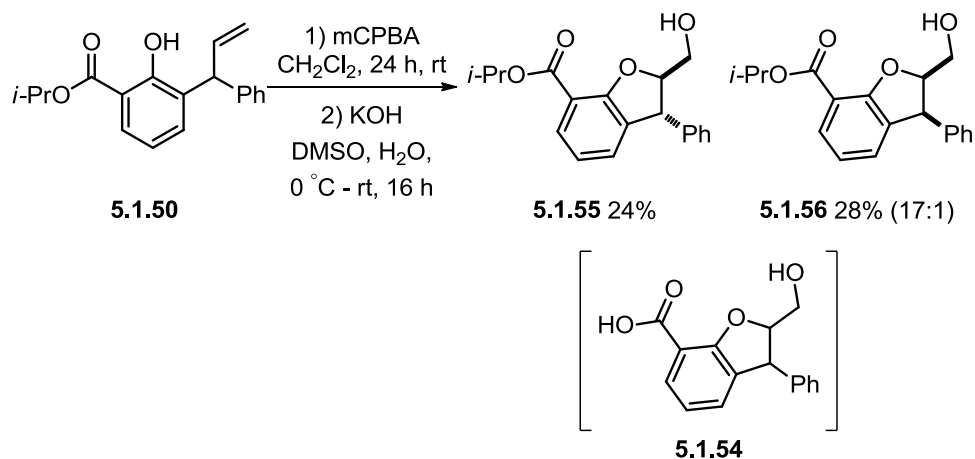
Following on from this, ester hydrolysis of isopropyl ester **5.1.53** using lithium hydroxide produced acid **5.1.54** in reasonable yield and subsequent methyl ester formation gave the desired compound **5.1.33** in adequate yield (Scheme 108).

Scheme 108 – Synthesis of desired methyl ester **5.1.33**

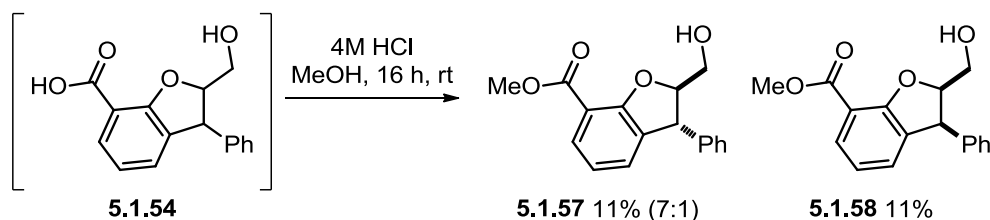
Generally superior yields were obtained in the synthesis of isopropyl ester **5.1.53**. As a result, this route was repeated to provide material for chromatographic separation of the diastereomers **5.1.55** and **5.1.56** at the final stage (Scheme 109).

Scheme 109 – Separation of diastereomers **5.1.55** and **5.1.56**

On one occasion when this reaction was repeated, it was noted that some acid **5.1.54** was produced. The isopropyl ester derivatives **5.1.55** and **5.1.56** were still isolated in reasonable yield (Scheme 110) with the acid by-product **5.1.54** recovered from the aqueous layer after rigorous extraction.

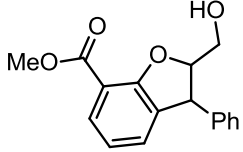
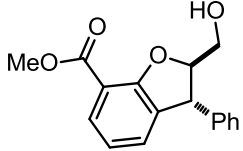
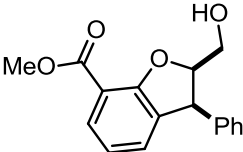
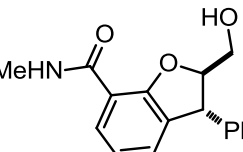
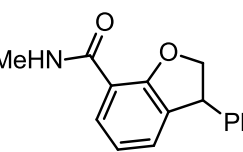
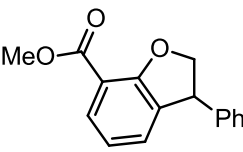
Scheme 110 – Separation of diastereomers **5.1.55** and **5.1.56** and crude acid **5.1.54**

This crude sample of **5.1.54** was reacted further using methanolic HCl to give the methyl ester and the resulting diastereomers were then separated (Scheme 111).

Scheme 111 – Conversion of crude acid **5.1.54** to methyl esters **5.1.57** and **5.1.58**

With both the separated racemic diastereomers **5.1.57** and **5.1.58** and the stereomeric mixture **5.1.33** analogues in hand, these were tested for their potency against Brd4 BD1 and BD2 (Table 34).

Table 34 – Comparison of esters 5.1.33, 5.1.57 and 5.1.58 to the methyl amide 5.1.32

Compound	Structure	pIC ₅₀ Brd4 BD1	pIC ₅₀ Brd4 BD2	ChromLogD _{7.4}
5.1.33		<4.3	4.9	4.62
5.1.57		<4.3	5.0	n.d.
5.1.58		<4.3, 4.6	4.5	n.d.
5.1.32		4.5	5.8	3.42
5.1.2		4.4	5.7	4.88
5.1.9		4.3	6.0	5.96

n.d. = Not determined

Methyl amide analogue **5.1.32** was known to exhibit similar potency to the parent **5.1.2** (BD2 pIC₅₀ = 5.8 and 5.7, respectively). However, it was evident that the same modification was having a detrimental effect on the potency of the methyl ester analogue. Examination of an X-ray crystal structure of Brd2 BD1 protein gave no indication as to the cause of this decrease. It had been a concern that the lack of a HBD in the methyl ester isostere may impact the Brd binding affinity. However, the data generated for **5.1.32** indicated that the HBD was not essential. To gain some insight as to why the hydroxymethyl unit was having a detrimental effect, molecular

modelling experiments, using MOE, were undertaken to compare energy minimised conformations of the ester **5.1.57** vs. amide **5.1.32**.

It was reasoned that the methyl amide analogue **5.1.32** was forming an internal hydrogen bond with the oxygen of the benzofuran thus holding the carbonyl functionality in the correct geometry for binding. By comparison, the methyl ester analogue **5.1.57** does not have this HBD. The carbonyl oxygen may therefore point towards the benzofuran and potentially create a through water hydrogen bonding interaction with the pendant alcohol group (Figure 69). This conformational bias could explain the reduction in potency when compared to the parent methyl amide **5.1.32**.

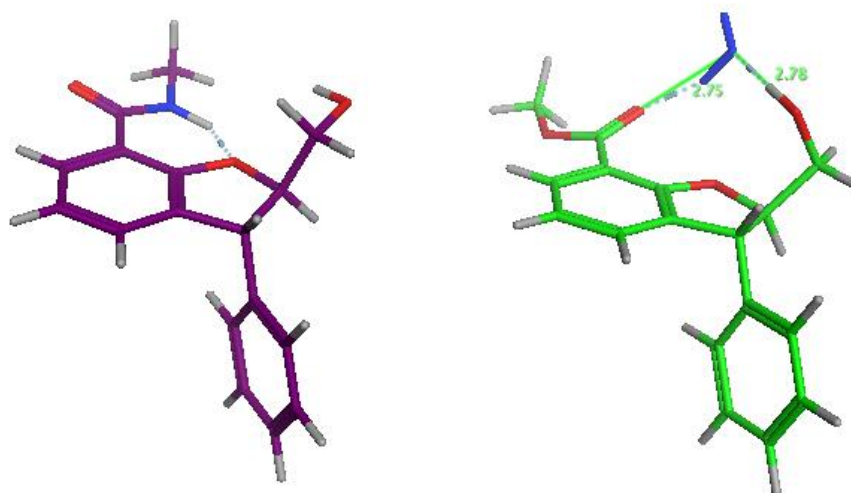
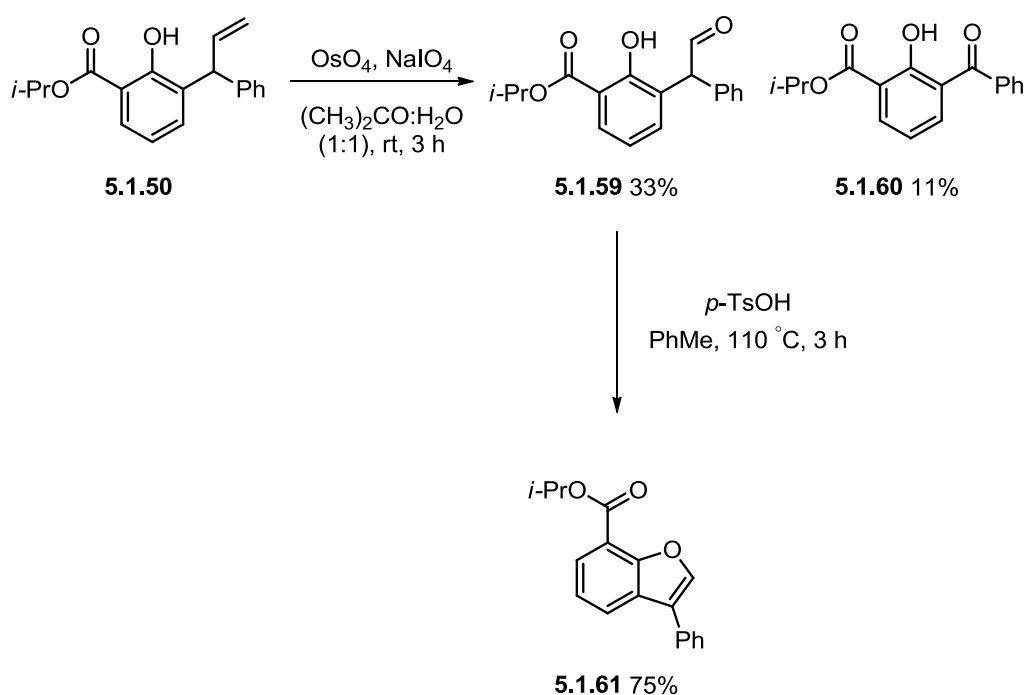


Figure 69 – Comparison of potential conformations of **5.1.32** (purple) and **5.1.57** (green) as modelled using MOE™ software

This result was disappointing since the incorporation of the hydroxy methylene provided the opportunity for an improved compound synthesis and physicochemical profile, with the methyl alcohol unit displaying a 13-fold reduction in lipophilicity. Nonetheless, the main aim of this effort was to examine a variety of esters and the ability to tune metabolic properties. Therefore, attention returned to the previous template which lacked the methylene alcohol moiety. Accordingly, it was proposed that the desired esters (ethyl **5.1.26**, isopropyl **5.1.27**, cyclobutyl **5.1.28**,

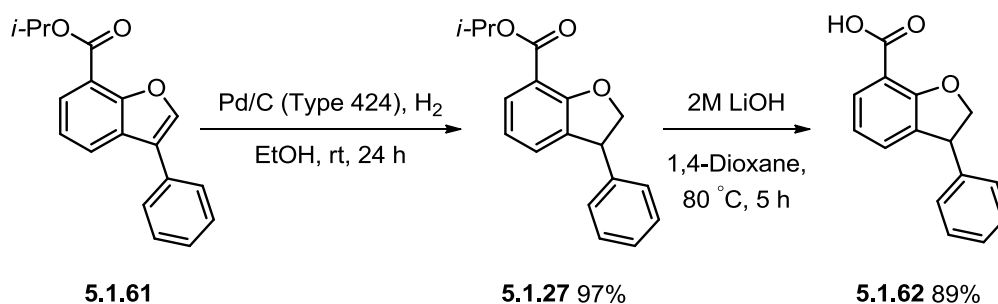
methylcyclopropyl **5.1.29**, hexafluoroisopropyl **5.1.30**, trifluoroethyl **5.1.31** and methyl **5.1.9** (Figure 67)) could all be accessed from alkene intermediate **5.1.50**.

Accordingly, conversion of **5.1.50** into the aldehyde **5.1.59** was accomplished using osmium tetroxide and sodium periodate (Scheme 112). Despite the disappointing yield of this particular step, use of the isopropyl rather than the methyl ester provided a more robust route displaying consistently higher yields despite the isolation of the undesired ketone **5.1.60**.



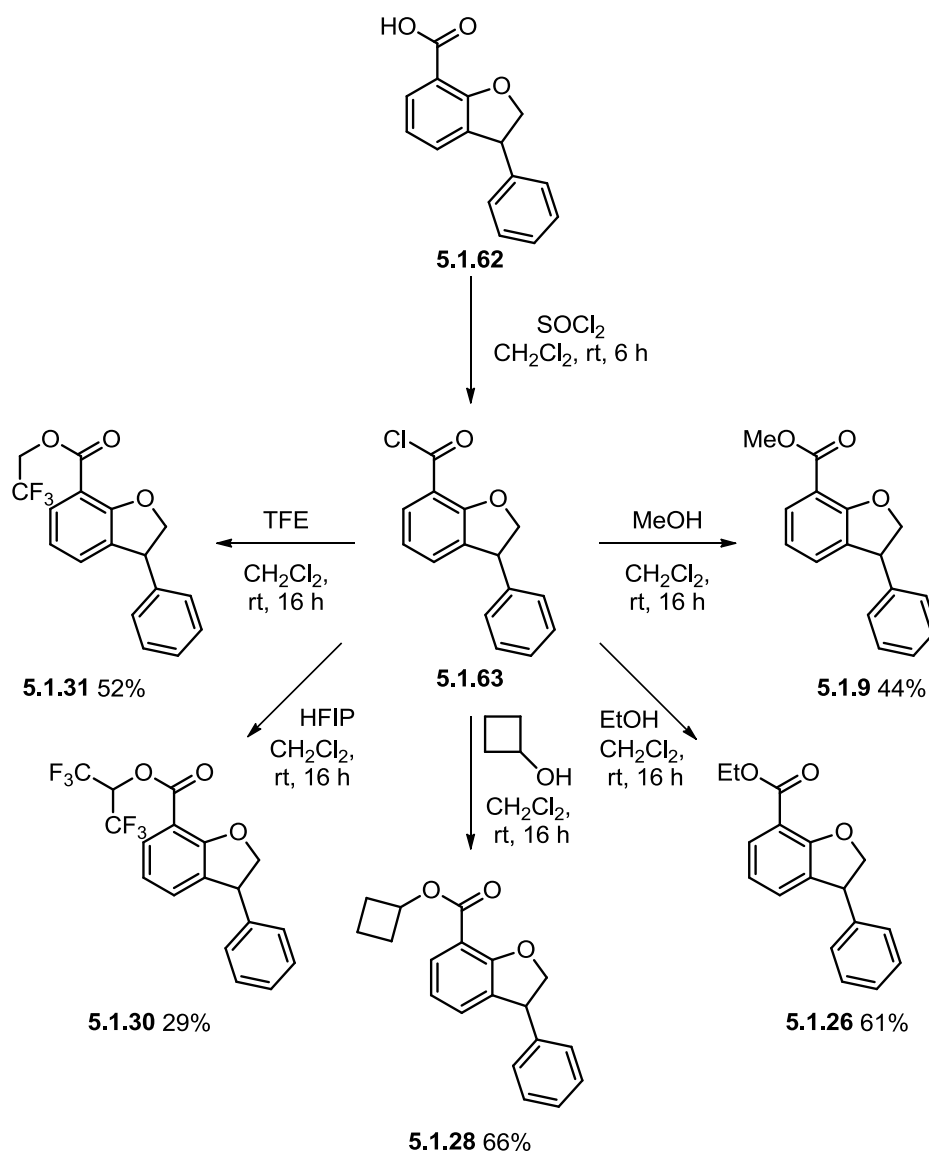
Scheme 112 – Synthesis of benzofuran **5.1.61**

Subsequently, intermediate **5.1.59** was cyclised to give benzofuran **5.1.61** in good yield (Scheme 112). Utilising the previously established hydrogenation conditions,²³⁶ **5.1.61** was converted into the desired isopropyl ester **5.1.27** and subsequent saponification provided acid intermediate **5.1.62** in excellent yield (Scheme 113).



Scheme 113 – Synthesis of acid 5.1.62

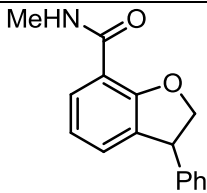
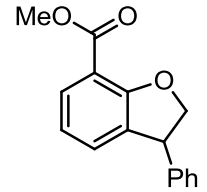
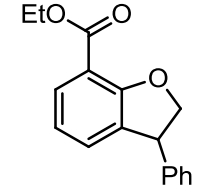
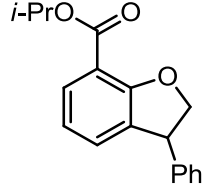
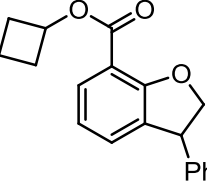
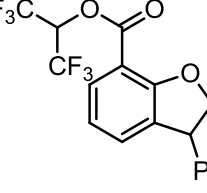
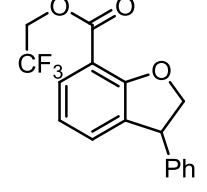
With a sufficient quantity of the acid intermediate **5.1.62** in hand, the range of ester derivatives alluded to previously could be synthesised. Treatment of acid **5.1.62** with thionyl chloride generated acid chloride **5.1.63**. The reaction mixture was then aliquoted into six equal portions, each of which was treated with a different alcohol to generate a range of esters (Scheme 114). The use of 1-methylcyclopropanol, however, produced no desired product, with increased steric hindrance around the alcohol being a potential reason for this. With the exception of 1-methylcyclopropanol, all esterifications were successful and generated the target molecules in reasonable yield.

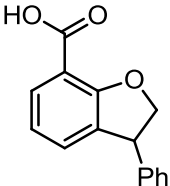


Scheme 114 – Synthesis of ester derivatives 5.1.9, 5.1.26, 5.1.28, 5.1.30, and 5.1.31 via acid chloride 5.1.63

Potency data was generated for all six ester derivatives (5.1.9, 5.1.26 – 5.1.28, 5.1.30 and 5.1.31) with the second batch of methyl ester 5.1.9 being tested again to confirm the veracity of the original hit (Table 35). Additionally, the acid 5.1.62 was tested in the Brd4 biochemical potency assay. It was anticipated that this would be inactive; a key requirement for a soft-drug degradation product (Table 35). Additionally, carboxylic acids tend to have limited permeability thus limiting systemic exposure and enhancing the loss of biological efficacy to such soft-drug metabolites.

Table 35 – Comparison of potency and human blood stability of desired ester derivatives

Compound	Structure	pIC ₅₀ Brd4 BD1	pIC ₅₀ Brd4 BD2	t _{1/2} (min)
5.1.2		4.4	5.7	Stable
5.1.9		4.4 (4.3)	5.9 (6.0)	42.8
5.1.26		<4.3	5.2	47.2
5.1.27		<4.3	4.6	115
5.1.28		<4.3, 4.8	4.6	83.5
5.1.30		<4.3	<4.3, 4.6	NT
5.1.31		<4.3	4.5	54.2

5.1.62		<4.3	<4.3	NT
--------	---	------	------	----

Importantly, the second batch of **5.1.9** confirmed the validity of the original hit with a very similar potency value of 5.9 at Brd 4 BD2, which is within the experimental error of the assay. The data for the alternative ester derivatives displays a general trend of decreased potency at BD2 as steric bulk increases. The addition of an extra methyl giving the ethyl ester derivative **5.1.26** displays an approximately 7-fold reduction in potency. Addition of further steric bulk as with the isopropyl derivative **5.1.27** leads to a similar reduction from the ethyl ester **5.1.26**. This trend is also observed in the cyclobutyl ester **5.1.28**. Comparing **5.1.27** to its fluorinated counterpart **5.1.30** reveals no difference in potency, however when comparing **5.1.26** to its fluorinated equivalent **5.1.31** a further 7-fold drop in potency is observed. With **5.1.27**, **5.1.30**, and **5.1.31** displaying similar potencies, this suggests that there is a limit on the impact of sterics against the potency of this particular template.

Another key factor in this investigation was to confirm that hydrolytic metabolism of these esters would produce an inactive compound. Acid **5.1.62** was therefore tested and exhibited no activity at either BD1 or BD2. This provided further evidence to the viability of the soft-drug approach in this template.

A further aspect in this investigation was to consider the human blood stability of the ester moieties. In order to facilitate the soft-drug approach, the compounds are required to be metabolised to the inactive acid **5.1.62** upon systemic exposure, thereby imparting site selectivity in the lungs. This investigation was achieved by incubation of the ester in human whole blood at 37 °C for four hours, with analysis using LCMS at multiple time points, with a target concentration of 1000 mg/mL.²³⁷ The methyl ester **5.1.9** displays a half-life of only 42.8 mins suggesting that the compound is unstable in human blood (Figure 70A). Additionally, the production of acid **5.1.62** was monitored in parallel with the concentration increasing proportionally with the decrease in parent ester concentration (Figure 70B). A phosphate-buffered saline (PBS) solution was used as a control to confirm that

degradation was indeed occurring within the blood rather than under mildly acidic conditions. It is important to note that the methyl ester was stable in the PBS buffer over the same period (Figure 70C). Therefore these data, in combination with amide **5.1.2** being stable under the same human whole blood conditions, supports the viability of the soft-drug approach.

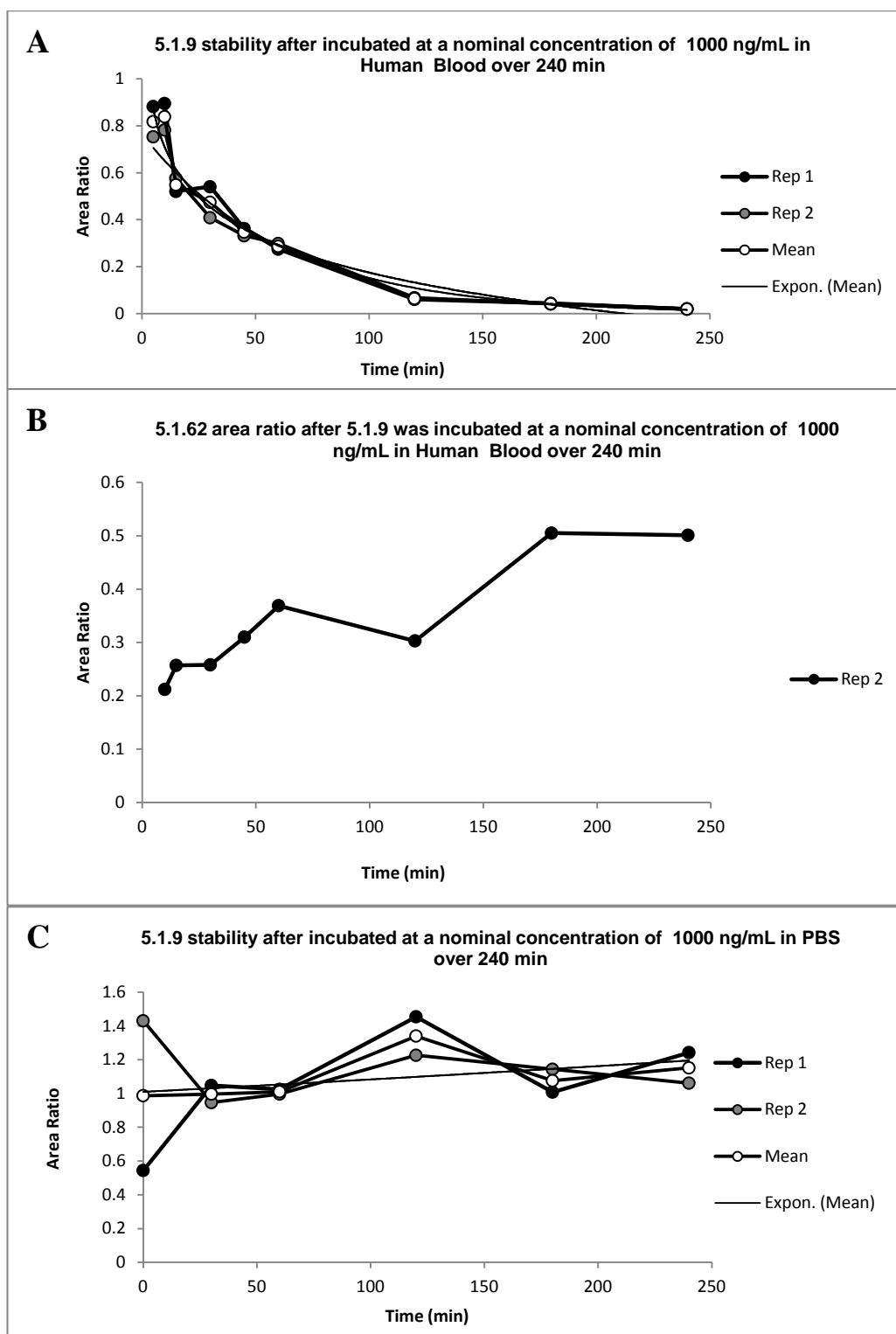
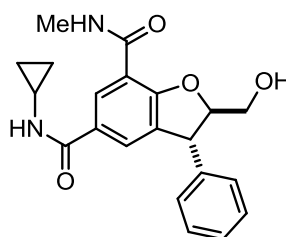


Figure 70 – A) Methyl ester 5.1.9 concentration over time in human whole blood, B) Acid concentration over time in human whole blood when dosed with 5.1.9, C) 5.1.9 concentration over time in PBS control²³⁷

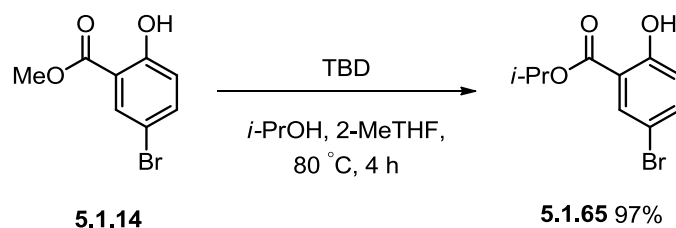
Perhaps unsurprisingly, the more sterically bulky the ester the more stable they were in blood (as demonstrated by the longer half-lives in human whole blood, Table 35)

Presumably, this is due to the steric hindrance at the reacting carbonyl centre, inhibiting access by the metabolising enzymes. This pattern is exemplified by cyclobutyl ester **5.1.28** and isopropyl ester **5.1.27** with half-lives of 83.5 and 115 mins, respectively. Interestingly, the fluorinated equivalent **5.1.31** of the ethyl ester **5.1.26**, which was expected to have a shorter half-life due to the electron-withdrawing effect of the fluorine atoms, displayed a similar half-life of 54.2 mins compared to 47.2 mins. This suggests that the electron-withdrawing effect had less influence than the steric bulk the fluorines provide. The methyl ester blood stability plots are mirrored by the plots of the other esters tested albeit with ranging half-life. With all esters demonstrating short half-lives, it was important to note whether the metabolism was as a result of the labile ester functionality as opposed to an alternative unknown route. In all cases, as with the methyl ester, the production of acid **5.1.62** was observed supporting the hypothesised route of metabolism.

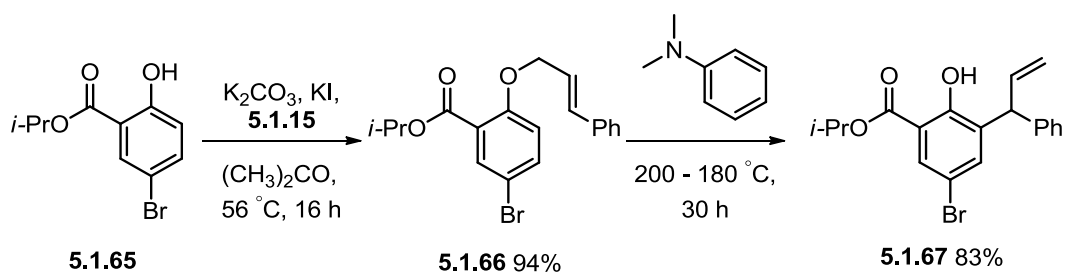
The body of evidence supports the use of a soft-drug within the dihydrobenzofuran template and its potential application to BET inhibitors. In parallel to these investigations, a synthesis of a more elaborated scaffold was devised. Compound **5.1.64**²³⁸ (Figure 71) demonstrated high potency in the BD2 assay (BD1 pIC₅₀ = 4.5, BD2 pIC₅₀ = 7.0) and it was reasoned, with the previous results in mind, that a soft-drug approach could be utilised on this more potent compound.

**5.1.64****Figure 71 –Elaborated methyl amide 5.1.64**

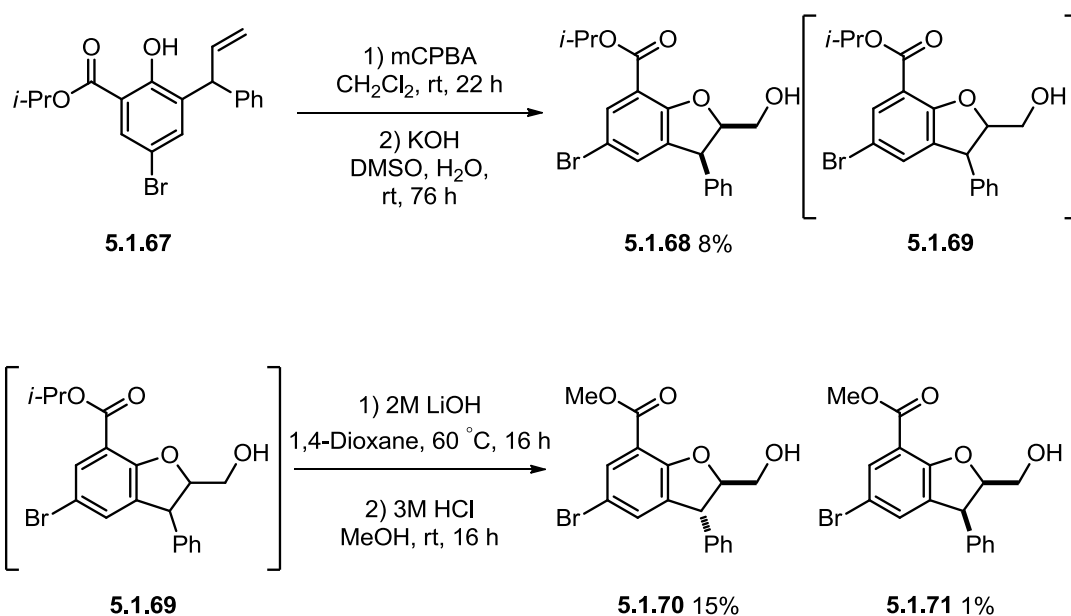
In order to incorporate the cyclopropylamide functionality at the 5-position of the dihydrobenzofuran ring, it was logical that the previous route could be applied.²³⁰ With ester **5.1.65** not commercially available, it was synthesised from the previous starting material **5.1.14**. Using chemistry first reported by Hedrick *et al.*,^{239–241} conversion of **5.1.14** using 1,5,7-triazabicyclo[4.4.0]dec-5-ene (TBD) in a mixture of isopropanol and 2-MeTHF proceeded in excellent yield (Scheme 115).

Scheme 115 – Switching from methyl ester **5.1.14** to isopropyl ester **5.1.64**

With a sufficient quantity of **5.1.65** in hand, alkylation and Claisen rearrangement both proceeded in excellent yield using the previously optimised conditions (Scheme 116).

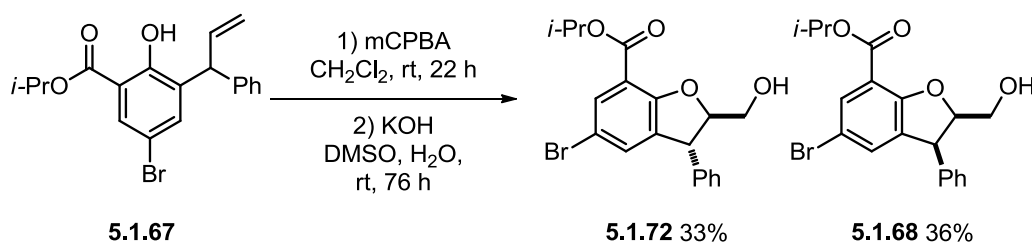
Scheme 116 – Alkylation and Claisen rearrangement to give **5.1.67**

5.1.67 was subsequently cyclised using the established epoxidation conditions, however isolation of the desired product proved challenging (Scheme 117). Although isolation of diastereomer **5.1.68** was achieved, the majority of the mass balance remained as a crude stereomeric mixture of isomers **5.1.69**. It was considered that transformation to the methyl ester might allow simpler purification. The crude mixture **5.1.69** was therefore hydrolysed to the acid and next converted to the methyl ester. The methyl ester diastereoisomers **5.1.70** and **5.1.71** were isolated in poor yield with this being attributed to the unoptimised isolation procedure (Scheme 117).



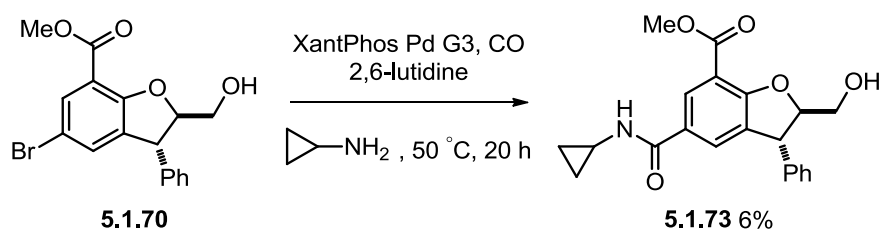
Scheme 117 – Isolation of methyl ester diastereomers 5.1.70 and 5.1.71 and isopropyl ester diastereomer 5.1.68

A subsequent repeat of this reaction produced the diastereomeric isopropyl ester derivatives 5.1.72 and 5.1.68 in good yield after optimisation of the purification (Scheme 118).



Scheme 118 – Successful separation of isopropyl ester diastereomers 5.1.72 and 5.1.68

Despite the poor yielding synthesis of methyl esters 5.1.70 and 5.1.71, the *trans*-diastereomer 5.1.70 was utilised in a final amidocarbonylation reaction, using a modified set of conditions developed by Buchwald *et al.*,²⁴² to generate the desired compound 5.1.73, albeit in an unoptimised low yield (Scheme 119).



Scheme 119 – Amidocarbonylation to desired elaborated analogue 5.1.73

With the successful generation of the more elaborated methyl ester scaffold, this was tested for its potency and compared with the parent amide (Table 36).

Table 36 – Comparison of methyl ester 5.1.73 and its parent 5.1.64

Compound	Structure	pIC ₅₀ Brd4 BD1	pIC ₅₀ Brd4 BD2
5.1.64		<4.3, 4.5	7.0
5.1.73		<4.3	6.1

These data clearly indicate a similar trend to the methyl ester analogue **5.1.57** (Table 34) investigated previously, with an approximately 10-fold drop in potency. This reduction in potency could again be attributed to the conformational difference between the two analogues as discussed in the previous template (Figure 69).

5.2 Conclusions and Future work

The overall aim of the studies described herein has been to demonstrate the utility of bioisosteres in different, state-of-the-art drug discovery settings. While the initial efforts focused very much on overcoming the considerable synthetic challenges associated with accessing the BCP moiety with a view to improving physicochemical properties, the second area of research concentrated on the incorporation of a bioisosteric soft centre to mitigate potential toxicological side-effects. In terms of the latter, the initial hypothesis was that the bioisosteric replacement of the key methyl amide acetyl lysine binding mimetic (present in a series of BET inhibitors) with a methyl ester, could provide an opportunity to achieve this.

To test this proposal compound **5.1.9** was targeted and assessed in comparison to the parent amide **5.1.2**. This compound exhibited similar potency to the amide and, upon exposure to human blood rapidly hydrolysed to the corresponding acid thus destroying the acetyl lysine binding mimetic and consequently, BET activity. This provided strong evidence that a soft-drug approach was indeed viable and that **5.1.9**, or analogues thereof, could deliver:

- Equivalent potency to known BET inhibitors
- Rapid metabolism of the soft centre upon exposure to blood resulting in inactivity

A notable drawback of the ester is the corresponding increase in lipophilicity it engenders. In an attempt to overcome this, the more elaborated scaffolds **5.1.33** and **5.1.73** were synthesised to investigate whether the potency and physicochemical properties could be improved. Despite the enhanced physicochemical profile, inhibitor **5.1.33** displayed a loss of potency compared to its progenitor amide **5.1.32**. The fully elaborated **5.1.73** also exhibited a similar reduction in biological activity when compared to original amide **5.1.64**. Molecular modelling studies were undertaken to gain further insight into these somewhat surprising and disappointing results. These studies indicated that the parent amide, the amide NH could engage in an internal hydrogen bond to the furan oxygen, thus holding the carbonyl in the required orientation for binding. However, the methyl ester does not possess a proton

suitable for such hydrogen bonding. In this case it was postulated that ester carbonyl could engage in a through-water hydrogen bond to the hydroxyl group holding the ester in an undesired conformation for binding. Clearly further investigation is required to provide definitive evidence for the loss of potency observed for **5.1.33** and **5.1.73**. Crystallographic analysis could be used to gain a deeper understanding of the binding and ground-state conformation of the molecules in question. Alternatively, the next step in this investigation could be to explore more elaborated analogues in which the hydroxyl is replaced by functionality that does not possess a hydrogen bond donor (e.g. isosteric fluorine). Subsequent analysis of the BET potency of such analogues could then elucidate the importance of the hydrogen bond donor.

Encouraged by the result obtained using the methyl ester ‘soft’ bioisostere, further investigations into a variety of different ester motifs was undertaken. Since the ester is acting as an acetyl mimetic, it is perhaps unsurprising that small esters exhibited greater BET activity and larger exemplars were inactive. Investigation around structure activity relationship could provide a more activated soft-drug. With a more elaborated template, further human blood stability investigations would provide additional evidence to the applicability of the soft-drug approach and a suitable tool molecule could be tested *in vivo*. In adapting the compounds to maximise the potency the esters investigated here could be utilised to modulate metabolism to provide a compound with the desired overall profile.

In a more general sense, should this approach be applied to other biological targets the carbonyl functionality may not always be essential for activity. Although in such circumstances hydrolysis would not be expected to lead to reduced activity the resulting carboxylic acid products themselves generally suffer from poor permeability and consequently, lower systemic exposure would be expected relative to the parent ester. Consequently these scoping studies were of interest since they provided insight into the effect of differing ester properties on rate of hydrolysis in blood. As a result the set investigated are the first step in generating a suite of different esters, which offer the opportunity to pick and choose depending on the rate of degradation required. Moving forward, a more comprehensive array of esters

could be synthesised and tested to enhance the set. Another consideration would be the stability of the esters in cells themselves. Once a suitable library of soft-esters had been assembled, a further step would be to determine the half-lives within the target cells.

6.0 General experimental

Solvents and reagents. Unless otherwise stated, all reactions were carried out under an atmosphere of nitrogen in heat- or oven-dried glassware and using anhydrous solvent. Solvents and reagents were purchased from commercial suppliers and used as received. Reactions were monitored by thin layer chromatography (TLC) or liquid chromatography-mass spectroscopy (LCMS). Heating was conducted using hotplates with DrySyn adaptors.

Chromatography. Thin layer chromatography (TLC) was carried out using plastic-backed 50 precoated silica plates (particle size 0.2 mm). Spots were visualised by ultraviolet (UV) light ($\lambda_{\text{max}} = 254 \text{ nm}$ or 365 nm) and then stained with potassium permanganate solution followed by gentle heating. Flash column chromatography was carried out using the Teledyne ISCO CombiFlash® Rf+ apparatus with RediSep® or GraceResolv™ silica cartridges.

Liquid chromatography mass spectrometry. LCMS analysis carried out using system 1 described below unless otherwise stated as using system 2.

System 1

LCMS analysis was carried out on an H₂O_s Acquity UPLC instrument equipped with a BEH column (50 mm x 2.1 mm, 1.7 μm packing diameter) and H₂O_s micromass ZQ MS using alternate-scan positive and negative electrospray. Analytes were detected as a summed UV wavelength of 210 – 350 nm. Three liquid phase methods were used:

Method A - Formic – 40 °C, 1 mL/min flow rate. Gradient elution with the mobile phases as (A) H₂O containing 0.1% volume/volume (v/v) formic acid and (B) acetonitrile containing 0.1% (v/v) formic acid. Gradient conditions were initially 1% B, increasing linearly to 97% B over 1.5 min, remaining at 97% B for 0.4 min then increasing to 100% B over 0.1 min.

Method B - High pH – 40 °C, 1 mL/min flow rate. Gradient elution with the mobile phases as (A) 10 mM aqueous ammonium bicarbonate solution, adjusted

to pH 10 with 0.88 M aqueous ammonia and (B) acetonitrile. Gradient conditions were initially 1% B, increasing linearly to 97% B over 1.5 min, remaining at 97% B for 0.4 min then increasing to 100% B over 0.1 min.

Method C - TFA – 40 °C, 1 mL/min flow rate. Gradient elution with the mobile phases as (A) H₂O containing 0.1% volume/volume (v/v) TFA and (B) acetonitrile containing 0.1% (v/v) TFA. Gradient conditions were initially 1% B, increasing linearly to 97% B over 1.5 min, remaining at 97% B for 0.4 min then increasing to 100% B over 0.1 min.

System 2

LCMS analysis was carried out on an Agilent 1290 Infinity equipped with an acquity BEH column (50 mm x 2.1 mm, 1.7 µm packing diameter). Analytes were detected as a summed UV wavelength of 190 – 400 nm. Liquid phase method used:

Formic – 35 °C, 0.6 mL/min flow rate. Gradient elution with the mobile phases as (A) H₂O containing 0.1% volume/volume (v/v) formic acid and (B) acetonitrile containing 0.1% (v/v) formic acid. Gradient conditions were initially 3% B for 0.4 min, increasing linearly to 98% B over 2.8 min, remaining at 98% B for 0.6 min then decreasing to 3% B over 0.4 min then remaining at 3% B for 0.3 min.

Nuclear magnetic resonance (NMR) spectroscopy. Proton (¹H), carbon (¹³C), and fluorine (¹⁹F) spectra were recorded in deuterated solvents at ambient temperature (unless otherwise stated) using standard pulse methods on any of the following spectrometers and signal frequencies: Bruker AV-400 (¹H = 400 MHz, ¹³C = 101 MHz, ¹⁹F = 376 MHz) and Bruker AV-600 (¹H = 600 MHz, ¹³C = 150 MHz). Chemical shifts are reported in ppm and are referenced to tetramethylsilane (TMS) or the following solvent peaks: CDCl₃ (¹H = 7.27 ppm, ¹³C = 77.0 ppm), DMSO-*d*₆ (¹H = 2.50 ppm, ¹³C = 39.5 ppm), and MeOH-*d*₄ (¹H = 3.31 ppm, ¹³C = 49.15 ppm). Peak assignments were made on the basis of chemical shifts, integrations, and coupling constants, using COSY, DEPT, and HSQC where appropriate. Coupling constants are quoted to the nearest 0.1 Hz and multiplicities are described as singlet (s),

doublet (d), triplet (t), quartet (q), quintet (quin), sextet (sxt), septet (sept), br. (broad) and multiplet (m).

Infrared (IR) spectroscopy. Infrared spectra were recorded using a Perkin Elmer Spectrum 1 machine. Absorption maxima (ν_{\max}) are reported in wavenumbers (cm^{-1}) and are described as strong (s), medium (m), weak (w) and broad (br).

High-resolution mass spectrometry (HRMS). High-resolution mass spectra were recorded on a Micromass Q-ToF Ultima hybrid quadrupole time-of-flight mass spectrometer, with analytes separated on an Agilent 1100 Liquid Chromatography equipped with a Phenomenex Luna C18 (2) reversed phase column (100 mm x 2.1 mm, 3 μm packing diameter). LC conditions were 0.5 mL/min flow rate, 35 $^{\circ}\text{C}$, injection volume 2–5 μL . Gradient elution with (A) H_2O containing 0.1% (v/v) formic acid and (B) acetonitrile containing 0.1% (v/v) formic acid. Gradient conditions were initially 5% B, increasing linearly to 100% B over 6 min, remaining at 100% B for 2.5 min then decreasing linearly to 5% B over 1 min followed by an equilibration period of 2.5 min prior to the next injection. Mass to charge ratios (m/z) are reported in Daltons.

Melting points. Melting points were recorded on a Stuart SMP40 melting point apparatus.

Mass directed auto preparation (MDAP). Mass-directed automated purification was carried out using an H_2O s ZQ MS using alternate-scan positive and negative electrospray and a summed UV wavelength of 210–350 nm. Two liquid phase methods were used:

Formic – Sunfire C18 column (100 mm x 19 mm, 5 μm packing diameter, 20 mL/min flow rate) or Sunfire C18 column (150 mm x 30 mm, 5 μm packing diameter, 40 mL/min flow rate). Gradient elution at ambient temperature with the mobile phases as (A) H_2O containing 0.1% volume/volume (v/v) formic acid and (B) acetonitrile containing 0.1% (v/v) formic acid.

High pH – Xbridge C18 column (100 mm x 19 mm, 5 μm packing diameter, 20 mL/min flow rate) or Xbridge C18 column (150 mm x 30 mm, 5 μm packing

diameter, 40 mL/min flow rate). Gradient elution at ambient temperature with the mobile phases as (A) 10 mM aqueous ammonium bicarbonate solution, adjusted to pH 10 with 0.88 M aqueous ammonia and (B) acetonitrile.

TFA – Sunfire C18 column (100 mm x 19 mm, 5 µm packing diameter, 20 mL/min flow rate) or Sunfire C18 column (150 mm x 30 mm, 5 µm packing diameter, 40 mL/min flow rate). Gradient elution at ambient temperature with the mobile phases as (A) H₂O containing 0.1% volume/volume (v/v) TFA and (B) acetonitrile containing 0.1% (v/v) TFA.

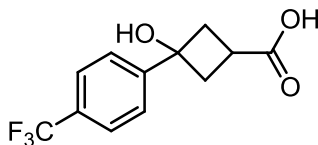
The elution gradients used were at a flow rate of 40 mL/min over 10 or 20 min:

Gradient A	5-30% B
Gradient B	15-55% B
Gradient C	30-85% B
Gradient D	50-99% B
Gradient E	80-99% B

7.0 Experimental

7.1 Lp-PLA₂ experimental

3-Hydroxy-3-(4-(trifluoromethyl)phenyl)cyclobutanecarboxylic acid 3.1.3¹⁵⁹



Method A:

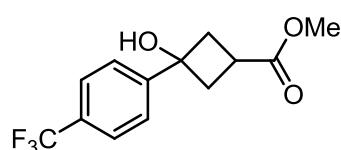
To 1-bromo-4-(trifluoromethyl)benzene (28.0 mL, 219 mmol) in THF (150 mL) was added isopropylmagnesium lithium chloride (1.3 M in THF) (170 mL, 221 mmol) at 0 °C. This was stirred for 16 h before 3-oxocyclobutanecarboxylic acid (10 g, 88 mmol) in THF (150 mL) was added at 0 °C. This was warmed to ambient temperature and was stirred for 48 h. Water (200 mL), EtOAc (300 mL) and 2M NaOH_(aq) (45 mL) was added to the reaction mixture and the layers were separated. The organic layer was extracted with water and 2M NaOH_(aq) (100 + 10 mL × 10). The aqueous layer was acidified with conc. HCl_(aq) and EtOAc (200 mL) was added. The layers were separated and the aqueous layer was extracted with EtOAc (100 mL × 10). The organics were combined and evaporated under reduced pressure to give 3-hydroxy-3-(4-(trifluoromethyl)phenyl)cyclobutanecarboxylic acid (16.39 g, 63 mmol, 72%) as a white solid.

Method B:

To 1-bromo-4-(trifluoromethyl)benzene (197 g, 876 mmol) in THF (1000 mL) was added *n*-BuLi (2.5M in hexanes) (500 mL, 1250 mmol) at -78 °C. The reaction was stirred for 2 h before 3-oxocyclobutanecarboxylic acid (50 g, 438 mmol) in THF (250 mL) was added dropwise at -78 °C. The reaction was allowed to warm to ambient temperature and was stirred for 16 h. The reaction mixture was quenched with sat. NH₄Cl_(aq) solution (200 mL) and basified with 2M NaOH_(aq) (500 mL) and washed with EtOAc (700 mL). The layers were separated and the aqueous layer was acidified with 2M HCl_(aq) (1000 mL). The aqueous was extracted with EtOAc (1000 mL) which was then dried over Na₂SO₄ and evaporated under reduced pressure to afford 3-hydroxy-3-(4-(trifluoromethyl)phenyl)cyclobutanecarboxylic acid (100 g, 339 mmol, 77%) as a pale brown solid.

M.p. 113 – 115 °C; LCMS (System 2, ESI) $R_t = 2.21$ $[M-H]^- = 259.1$, 88%; 1H NMR (400 MHz, DMSO- d_6) $\delta = 12.45 - 11.90$ (br. s., 1H), 7.77 – 7.68 (m, 4H), 2.85 – 2.74 (m, 1H), 2.67 – 2.53 (m, 4H) 1.92 (s, 1H); ^{13}C NMR (101 MHz, DMSO- d_6) $\delta = 175.7$, 151.6, 127.3 (q, $^2J_{C-F} = 31.5$ Hz), 125.7, 124.9 (q, $^3J_{C-F} = 3.6$ Hz), 124.3 (q, $^1J_{C-F} = 271.4$ Hz), 70.8, 40.9, 28.5; ^{19}F NMR (376 MHz, DMSO- d_6) $\delta = -61.3$ (s, 3F); ν_{max}/cm^{-1} (thin film) 3208 (br), 2957, 1701, 1683. Failed to ionise under high resolution mass spectrometry conditions.

Methyl 3-hydroxy-3-(4-(trifluoromethyl)phenyl)cyclobutanecarboxylate 3.1.4



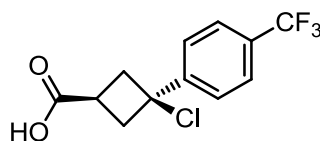
To 3-hydroxy-3-(4-(trifluoromethyl)phenyl)cyclobutanecarboxylic acid (1.6 g, 6.15 mmol) in MeOH (20 mL) was added HCl (3M in MeOH) (4.20 mL, 12.60 mmol) and the reaction mixture was stirred for 6 h. Water (30 mL) and CH_2Cl_2 (50 mL) were added and the layers were separated. The aqueous layer was extracted with CH_2Cl_2 (3 \times 10 mL). The organics were combined, filtered through a hydrophobic frit and evaporated under reduced pressure to give methyl 3-hydroxy-3-(4-(trifluoromethyl)phenyl)cyclobutanecarboxylate (1.674 g, 6.10 mmol, 99%) as a yellow oil.

LCMS (Method B, UV, ESI) $R_t = 1.07$ $[M-H]^- = 273.2$, 80%; 1H NMR (400 MHz, DMSO- d_6) $\delta = 7.77 - 7.68$ (m, 4H), 5.96 (s, 1H), 3.65 (s, 3H), 2.97 – 2.86 (m, 1H), 2.71 – 2.63 (m, 2H), 2.61 – 2.53 (m, 2H); ^{13}C NMR (101 MHz, $CDCl_3$) $\delta = 176.8$, 148.8, 129.7 (q, $^2J_{C-F} = 32.2$ Hz), 125.4 (q, $^3J_{C-F} = 3.7$ Hz), 125.3, 124.1 (q, $^1J_{C-F} = 272.2$ Hz), 73.4, 52.3, 41.0, 29.7; ^{19}F NMR (376 MHz, $CDCl_3$) $\delta = -62.6$ (s, 3F); ν_{max}/cm^{-1} (thin film) 3438 (br), 2954, 1730, 1715.

3-Chloro-3-(4-(trifluoromethyl)phenyl)cyclobutanecarboxylic acid 3.1.8

To 3-hydroxy-3-(4-(trifluoromethyl)phenyl)cyclobutanecarboxylic acid (16.18 g, 62.2 mmol) in PhMe (300 mL) was added conc. HCl_(aq) (50 mL, 617 mmol) at ambient temperature and the reaction was sonicated for 7 h. The layers were separated and the aqueous layer was extracted with PhMe (2 × 50 mL). The organics were combined and washed with water (2 × 50 mL) and brine (2 × 50 mL). The organics were filtered through a hydrophobic frit and evaporated under reduced pressure to give 3-chloro-3-(4-(trifluoromethyl)phenyl)cyclobutanecarboxylic acid (13.1 g, 46.9 mmol, 75%) as a white solid.

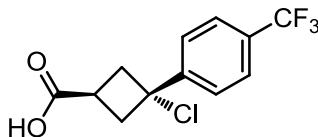
Alternatively, to a solution of 3-hydroxy-3-(4-(trifluoromethyl)phenyl)cyclobutanecarboxylic acid (78 g, 300 mmol) in PhMe (1500 mL) was added HCl_(aq) (250 mL, 3000 mmol) at ambient temperature and the reaction was sonicated under ultrasound for 72 h. The reaction mixture was diluted with EtOAc (1000 mL) and the layers were separated. The organic layer was dried over Na₂SO₄ and evaporated under reduced pressure to afford a crude product (70 g). This was triturated with hexane (500 mL) and this was filtered to collect the solid and washed with hexane (100 mL). The solid was dried to afford *cis*-3-chloro-3-(4-(trifluoromethyl)phenyl)cyclobutanecarboxylic acid (25 g, 88 mmol, 29%) as an off white solid. The filtrate was evaporated under reduced pressure to afford *trans*-3-chloro-3-(4-(trifluoromethyl)phenyl)cyclobutanecarboxylic acid (30 g, 88 mmol, 30%).

***cis*-3-Chloro-3-(4-(trifluoromethyl)phenyl)cyclobutanecarboxylic acid 3.1.10¹⁵⁹**

M.p. 172 – 174 °C; LCMS (Method B, UV, ESI) R_t = 0.72 [M-H]⁻ = No mass ion peak, 100%; ¹H NMR (400 MHz, DMSO-*d*₆) δ = 12.50 (br. s., 1H), 7.88 – 7.74 (m, 4H), 3.34 – 3.21 (m, 2H), 3.08 – 2.97 (m, 2H), 2.92 – 2.80 (m, 1H); ¹³C NMR (101 MHz, DMSO-*d*₆) δ = 174.5, 147.8, 128.5 (q, ²J_{C-F} = 31.5 Hz), 127.0, 125.2 (q, ³J_{C-F} = 3.6 Hz), 124.0 (q, ¹J_{C-F} = 272.2 Hz), 65.0, 41.9, 31.1; ¹⁹F NMR (376 MHz,

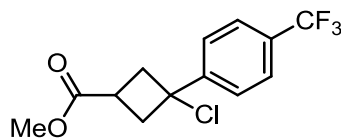
CDCl_3) $\delta = -62.8$ (s, 3F); $\nu_{\text{max}}/\text{cm}^{-1}$ (thin film) 2989, 1687; HRMS: Calculated for $\text{C}_{12}\text{H}_9\text{ClF}_3\text{O}_2$ 277.0249 Found $[\text{M}-\text{H}]^-$: 277.0251 (0.8 ppm).

***trans*-3-Chloro-3-(4-(trifluoromethyl)phenyl)cyclobutanecarboxylic acid**
3.1.11¹⁵⁹



M.p. 114 – 116 °C; LCMS (Method B, UV, ESI) $R_t = 0.71$ $[\text{M}-\text{H}]^- = 277.4$, 81%; ^1H NMR (400 MHz, CDCl_3) $\delta = 7.66$ (d, $J = 8.3$ Hz, 2H), 7.49 (d, $J = 8.1$ Hz, 2H), 3.78 (quin, $J = 8.8$ Hz, 1H), 3.15 – 3.02 (m, 4H) (1H not observed, exchangeable); ^{13}C NMR (101 MHz, CDCl_3) $\delta = 179.6$, 148.3 130.3 (q, $^2J_{\text{C-F}} = 32.8$ Hz), 125.7 (q, $^3J_{\text{C-F}} = 4.0$ Hz), 125.5, 123.8 (q, $^1J_{\text{C-F}} = 272.3$ Hz), 66.8, 41.5, 32.5; ^{19}F NMR (376 MHz, CDCl_3) $\delta = -63.2$ (s, 3F); $\nu_{\text{max}}/\text{cm}^{-1}$ (thin film) 2947, 1705; HRMS: Calculated for $\text{C}_{12}\text{H}_{11}\text{ClF}_3\text{O}_2$ 279.0394 Found $[\text{M}+\text{H}]^+$: 279.0401 (2.3 ppm).

Methyl 3-chloro-3-(4-(trifluoromethyl)phenyl)cyclobutanecarboxylate 3.1.7



Method A:

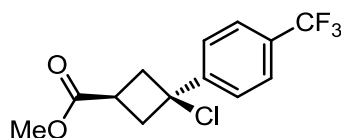
To a solution of 3-chloro-3-(4-(trifluoromethyl)phenyl)cyclobutanecarboxylic acid (10 g, 35.9 mmol) and HCl (4M in 1,4-dioxane) (45 mL, 180 mmol) in 1,4-dioxane (100 mL) stirred under nitrogen at ambient temperature was added MeOH (100 mL, 2472 mmol). The reaction mixture was stirred at ambient temperature for 3 h. Sat. $\text{NaHCO}_3(\text{aq})$ (20 mL) and EtOAc (20 mL) were added and the layers were separated. The aqueous layer was extracted with EtOAc (3 × 20 mL) and the combined organics were evaporated under reduced pressure to give methyl 3-chloro-3-(4-(trifluoromethyl)phenyl)cyclobutanecarboxylate (10.5 g, 35.9 mmol, quant.) as a pale yellow liquid.

Method B (using pure 3.1.10):¹⁵⁹

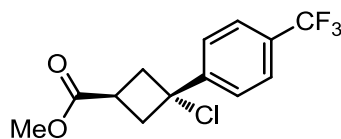
To a solution of *cis*-3-chloro-3-(4-(trifluoromethyl)phenyl)cyclobutanecarboxylic acid (77 g, 276 mmol) in MeOH (800 mL) was added SOCl₂ (80 mL, 1096 mmol) at 0 °C and stirred at ambient temperature for 3 h. The reaction mixture was evaporated under reduced pressure to afford crude product as a dark brown oil and this was purified by using column chromatography eluting with petroleum ether: EtOAc 95:5. Fractions containing product were evaporated under reduced pressure to afford *cis*-methyl 3-chloro-3-(4-(trifluoromethyl)phenyl)cyclobutanecarboxylate (80 g, 265 mmol, 96%) as an off white solid.

Method C (using pure 3.1.11):¹⁵⁹

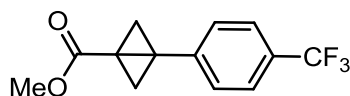
To a solution of *trans*-3-chloro-3-(4-(trifluoromethyl)phenyl)cyclobutanecarboxylic acid (65 g, 233 mmol) in MeOH (650 mL) was added SOCl₂ (70 mL, 959 mmol) at 0 °C and stirred at ambient temperature for 3 h. The reaction mixture was evaporated under reduced pressure to afford crude product as a dark brown oil and this was purified by using column chromatography eluting with petroleum ether: EtOAc 95:5. Fractions containing product were evaporated under reduced pressure to afford *trans*-methyl 3-chloro-3-(4-(trifluoromethyl)phenyl)cyclobutanecarboxylate (45 g, 148 mmol, 64%) as pale yellow liquid.

***cis*-Methyl 3-chloro-3-(4-(trifluoromethyl)phenyl)cyclobutanecarboxylate**
3.1.12¹⁵⁹

M.p. 52 – 54 °C; LCMS (Method B, UV, ESI) R_t = 1.29 [M-H]⁻ = No mass ion peak, 100%; ¹H NMR (400 MHz, CDCl₃) δ = 7.71 – 7.63 (m, 4H), 3.77 (s, 3H), 3.28 – 3.16 (m, 4H), 2.95 – 2.84 (m, 1H); ¹³C NMR (101 MHz, CDCl₃) δ = 173.6, 147.3, 130.3 (q, ²J_{C-F} = 33.1 Hz), 126.3, 125.7 (q, ³J_{C-F} = 3.6 Hz), 123.8 (q, ¹J_{C-F} = 272.2 Hz), 63.4, 52.2, 42.4, 31.8; ¹⁹F NMR (376 MHz, CDCl₃) δ = -62.7 (s, 3F); ν_{max}/cm⁻¹ (thin film) 2957, 1739. Failed to ionise under high resolution mass spectrometry conditions.

trans*-Methyl 3-chloro-3-(4-(trifluoromethyl)phenyl)cyclobutanecarboxylate*3.1.13**¹⁵⁹

LCMS (Method B, UV, ESI) $R_t = 1.31$ $[M+H]^+ =$ No mass ion peak, 80%; 1H NMR (400 MHz, $CDCl_3$) $\delta = 7.66$ (d, $J = 8.3$ Hz, 2H), 7.50 (d, $J = 8.3$ Hz, 2H), 3.80 – 3.67 (m, 4H), 3.14 – 2.98 (m, 4H); ^{13}C NMR (101 MHz, $CDCl_3$) $\delta = 174.1$, 148.5, 130.2 (q, $^2J_{C-F} = 32.8$ Hz), 125.7 (q, $^3J_{C-F} = 4.0$ Hz), 125.5, 123.8 (q, $^1J_{C-F} = 272.3$ Hz), 67.1, 52.0, 41.6, 32.6; ^{19}F NMR (376 MHz, $CDCl_3$) $\delta = -63.2$ (s, 3F); ν_{max}/cm^{-1} (thin film) 2955, 1733; HRMS: Calculated for $C_{13}H_{13}ClF_3O_2$ 293.0551 Found $[M+H]^+$: 293.0551 (0.1 ppm).

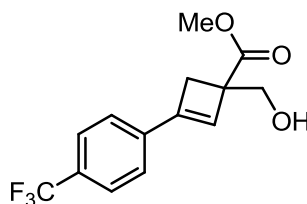
Methyl 3-(4-(trifluoromethyl)phenyl)bicyclo[1.1.0]butane-1-carboxylate 2.12.6

To solid sodium hydride (60% dispersion in oil) (8.2 g, 205 mmol) in THF (250 mL) stirred under nitrogen at ambient temperature was added a solution of *cis*-methyl 3-chloro-3-(4-(trifluoromethyl)phenyl)cyclobutanecarboxylate (50 g, 171 mmol) in THF (250 mL) portionwise. The reaction mixture was stirred at ambient temperature for 3 h. To the reaction mixture was added $NH_4Cl_{(aq)}$ (100 mL) and EtOAc (350 mL) then water (100 mL). The layers were separated and the aqueous layer was extracted with EtOAc (3 \times 50 mL). The organics were combined and dried through a hydrophobic frit. The solvent was evaporated under reduced pressure to give methyl 3-(4-(trifluoromethyl)phenyl)bicyclo[1.1.0]butane-1-carboxylate (43.1 g, 168 mmol, 98%) as a yellow solid.

M.p. 102 – 104, LCMS (Method B, UV, ESI) $R_t = 1.21$ $[M+H]^+ =$ No mass ion peak, 100%; 1H NMR (400 MHz, $CDCl_3$) $\delta = 7.56$ (d, $J = 8.3$ Hz, 2H), 7.39 (d, $J = 8.1$ Hz, 2H), 3.51 (s, 3H), 2.96 (t, $J = 1.1$ Hz, 2H), 1.67 (t, $J = 1.1$ Hz, 2H); ^{13}C NMR

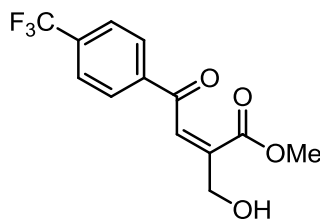
(101 MHz, CDCl₃) δ = 169.4, 138.3, 129.0 (q, ²J_{C-F} = 33.1 Hz), 126.1, 125.4 (q, ³J_{C-F} = 43.3 Hz), 124.1 (q, ¹J_{C-F} = 272.1 Hz), 52.0, 36.0, 31.6, 24.4; ¹⁹F NMR (376 MHz, CDCl₃) δ = -62.5 (s, 3F); $\nu_{\max}/\text{cm}^{-1}$ (thin film) 2956, 1708; HRMS: Calculated for C₁₃H₁₂F₃O₂ 257.0784 Found [M+H]⁺: 257.0785 (0.5 ppm).

Methyl 1-(hydroxymethyl)-3-(4-(trifluoromethyl)phenyl)cyclobut-2-enecarboxylate 3.1.14



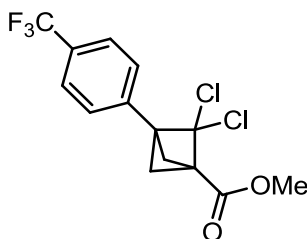
To a solution of methyl 3-(4-(trifluoromethyl)phenyl)bicyclo[1.1.0]butane-1-carboxylate (132 mg, 0.515 mmol) and diethylzinc (15% w/w in hexanes) (1.77 mL, 1.548 mmol) in CH₂Cl₂ (3 mL) stirred under nitrogen at 0 °C was added neat diiodomethane (0.21 mL, 2.60 mmol) dropwise. The reaction mixture was allowed to warm up to ambient temperature and was then stirred for 72 h. To the reaction mixture was added water (2 mL) and CH₂Cl₂ (2 mL). The layers were separated and the aqueous was extracted with CH₂Cl₂ (3 × 2 mL). The organics were combined and evaporated under reduced pressure to give a crude product. This was purified using column chromatography eluting with 0-50 cyclohexane: EtOAc. Fractions containing product were evaporated under reduced pressure to give methyl 1-(hydroxymethyl)-3-(4-(trifluoromethyl)phenyl)cyclobut-2-enecarboxylate (16 mg, 0.056 mmol, 11%).

LCMS (Method B, UV, ESI) R_t = 1.10 [M+H]⁺ = No mass ion peak, 98%; ¹H NMR (600 MHz, CDCl₃) δ = 7.62 (d, *J* = 8.1 Hz, 2H), 7.47 (d, *J* = 8.1 Hz, 2H), 6.54 (s, 1H), 3.97 (s, 2H), 3.76 (s, 3H), 3.17 (d, *J* = 13.0 Hz, 1H), 2.80 (d, *J* = 13.0 Hz, 1H) 2.32 (br s, 1H); ¹³C NMR (151 MHz, CDCl₃) δ = 174.6, 147.3, 136.6 (q, ⁴J_{C-F} = 1.7 Hz), 130.4 (q, ²J_{C-F} = 32.6 Hz), 129.5, 125.5 (q, ³J_{C-F} = 3.9 Hz), 125.1, 124.0 (q, ¹J_{C-F} = 272.0 Hz), 67.0, 52.3, 52.0, 35.8.

(Z)-Methyl 2-(hydroxymethyl)-4-oxo-4-(4-(trifluoromethyl)phenyl)but-2-enoate
3.1.15

To a solution of methyl 3-(4-(trifluoromethyl)phenyl)bicyclo[1.1.0]butane-1-carboxylate (152 mg, 0.593 mmol) and zinc copper couple powder (240 mg, 1.862 mmol) in CH_2Cl_2 (2 mL) stirred under nitrogen at ambient temperature was added diiodomethane (0.12 mL, 1.859 mmol) dropwise. The reaction mixture was stirred for 24 h. To the reaction mixture was added water (2 mL) and CH_2Cl_2 (2 mL). The layers were separated and the aqueous layer was extracted with CH_2Cl_2 (3×2 mL). The organics were combined and evaporated under reduced pressure to give a crude product. This was purified using column chromatography eluting with 0-50 cyclohexane:EtOAc. Fractions containing product were evaporated under reduced pressure to give (Z)-methyl 2-(hydroxymethyl)-4-oxo-4-(4-(trifluoromethyl)phenyl)but-2-enoate (16 mg, 0.056 mmol, 9%) as a colourless oil.

LCMS (Method B, UV, ESI) $R_t = 0.98$ $[\text{M}-\text{H}]^- = 289.0$, 86%; ^1H NMR (600 MHz, CDCl_3) $\delta = 8.05$ (d, $J = 8.1$ Hz, 2H), 7.75 (d, $J = 8.3$ Hz, 2H), 7.04 (t, $J = 1.7$ Hz, 1H), 4.53 (d, $J = 1.7$ Hz, 2H), 3.63 (s, 3H), 2.20 (br s, 1H); ^{13}C NMR (151 MHz, CDCl_3) $\delta = 192.2$, 165.9, 141.5, 139.0, 134.7 (q, $^2J_{\text{C-F}} = 32.6$ Hz), 131.8, 128.9, 125.8 (q, $^3J_{\text{C-F}} = 3.9$ Hz), 123.5 (q, $^1J_{\text{C-F}} = 272.8$ Hz), 62.1, 52.3

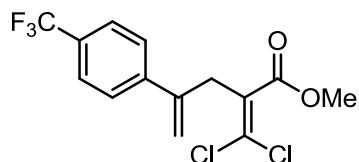
Methyl 2,2-dichloro-3-(4-(trifluoromethyl)phenyl)bicyclo[1.1.1]pentane-1-carboxylate 3.1.18

Methyl 3-(4-(trifluoromethyl)phenyl)bicyclo[1.1.0]butane-1-carboxylate (5 g, 19.51 mmol) was dissolved in diethylene glycol dimethyl ether (10 mL) and tetrachloroethylene (PCE) (30 mL) and the reaction mixture was heated to 120 °C. Solid sodium 2,2,2-trichloroacetate (18.09 g, 98 mmol) was added portionwise over 30 min and the reaction was stirred at 140 °C for an additional 30 min. Water (100 mL) and CH₂Cl₂ (100 mL) were added and the layers were separated. The organic layer was washed with brine (10 × 50 mL) and was then filtered through a hydrophobic frit. CH₂Cl₂ (100 mL) was added and this was washed with brine (5 × 50 mL) and then 5% LiCl_(aq) (5 × 50 mL). The organic layer was filtered through a hydrophobic frit and the solvent was removed under reduced pressure to give the crude product. This was purified using column chromatography eluting with 0-20 cyclohexane:TBME. Collected fractions containing product were evaporated under reduced pressure to give methyl 2,2-dichloro-3-(4-(trifluoromethyl)phenyl)bicyclo[1.1.1]pentane-1-carboxylate (2.5 g, 7.37 mmol, 38%) as a yellow oil.

LCMS (Method B, UV, ESI) R_t = 1.38 [M-H]⁻ = No mass ion peak, 81%; ¹H NMR (600 MHz, CDCl₃) δ = 7.66 (d, J = 8.1 Hz, 2H), 7.51 (d, J = 7.9 Hz, 2H), 3.85 (s, 3H), 3.14 (d, J = 1.3 Hz, 2H), 2.47 (d, J = 1.3 Hz, 2H); ¹³C NMR (150 MHz, CDCl₃) δ = 165.4, 135.9 (q, ⁴J_{C-F} = 1.4 Hz), 130.9 (q, ²J_{C-F} = 32.6 Hz), 127.6, 125.5 (q, ³J_{C-F} = 3.8 Hz), 123.9 (q, ¹J_{C-F} = 272.3 Hz), 94.0, 57.0, 52.5, 52.4, 49.4; ¹⁹F NMR (376 MHz, CDCl₃) δ = -63.2 (s, 3F); ν_{max}/cm⁻¹ (thin film) 2957, 1737; HRMS: Calculated for C₁₄H₁₂Cl₂F₃O₂ 339.0161 Found [M+H]⁺: 339.0169 (2.5 ppm).

methyl 2-(dichloromethylene)-4-(4-(trifluoromethyl)phenyl)pent-4-enoate has also been isolated from a similar reaction in a 4% yield.

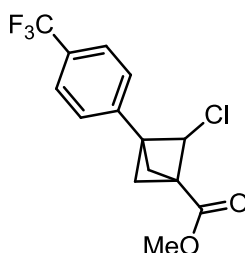
Methyl 2-(dichloromethylene)-4-(4-(trifluoromethyl)phenyl)pent-4-enoate 3.1.19



LCMS (Method A, UV, ESI) $R_t = 1.46$ $[M+H]^+ = 339.2$, 92%; $^1\text{H NMR}$ (600 MHz, CDCl_3) $\delta = 7.63 - 7.59$ (m, 2H), 7.50 (d, $J = 8.1$ Hz, 2H), 5.44 (s, 1H), 5.21 (s, 1H), 3.73 (s, 3H), 3.71 (s, 2H); $^{13}\text{C NMR}$ (151 MHz, CDCl_3) $\delta = 165.4$, 143.9 (q, $^4J_{C-F} = 1.1$ Hz), 142.1, 130.6, 129.9 (q, $^2J_{C-F} = 32.4$ Hz), 128.8, 126.5, 125.3 (q, $^3J_{C-F} = 3.8$ Hz), 124.1 (q, $^1J_{C-F} = 272.0$ Hz), 116.1, 52.4, 37.9.

Sample degraded

Methyl 2-chloro-3-(4-(trifluoromethyl)phenyl)bicyclo[1.1.1]pentane-1-carboxylate 3.1.21



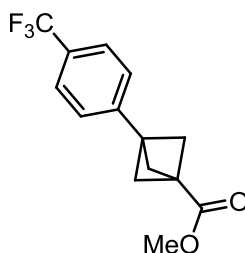
To ACHN (0.110 g, 0.450 mmol) and methyl 2,2-dichloro-3-(4-(trifluoromethyl)phenyl)bicyclo[1.1.1]pentane-1-carboxylate (2.58 g, 7.61 mmol) in PhMe (40 mL) was added 1,1,1,3,3,3-hexamethyl-2-(trimethylsilyl)trisilane (7 mL, 22.69 mmol). This was heated at 80 °C for 16 h. Further ACHN (43 mg) was added and the reaction was stirred at 110 °C for 3 h. The solvent was evaporated under reduced pressure to give a crude product. This was purified using column chromatography eluting with 9:1 petroleum ether:EtOAc. Fractions containing product were evaporated under reduced pressure to give methyl 2-chloro-3-(4-

(trifluoromethyl)phenyl)bicyclo[1.1.1]pentane-1-carboxylate (1.876 g, 6.16 mmol, 81%) as a yellow oil.

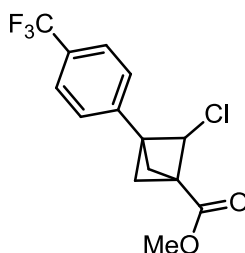
^1H NMR (400 MHz, CDCl_3) δ = 7.61 (d, J = 8.1 Hz, 2H), 7.38 (d, J = 8.1 Hz, 2H), 4.58 (d, J = 7.1 Hz, 1H), 3.78 (s, 3H), 3.22 (dd, J = 2.9, 9.9 Hz, 1H), 2.63 (d, J = 2.8 Hz, 1H), 2.41 (dd, J = 3.0, 7.1 Hz, 1H), 2.25 (dd, J = 3.0, 10.1 Hz, 1H) ^{13}C NMR (101 MHz, CDCl_3) δ = 167.4, 139.2, 130.1 (q, $^2J_{\text{C-F}}$ = 32.8 Hz), 127.0, 125.4 (q, $^3J_{\text{C-F}}$ = 4.0 Hz), 124.0 (q, $^1J_{\text{C-F}}$ = 272.3 Hz), 72.1, 52.1, 48.7, 48.5, 47.7, 43.6; ^{19}F NMR (376 MHz, CDCl_3) δ = -62.7 (s, 3F) $\nu_{\text{max}}/\text{cm}^{-1}$ (thin film) 2957, 1735. Failed to ionise under high resolution mass spectrometry conditions.

Methyl 2-chloro-3-(4-(trifluoromethyl)phenyl)bicyclo[1.1.1]pentane-1-carboxylate 3.1.21 and methyl 3-(4-(trifluoromethyl)phenyl)bicyclo[1.1.1]pentane-1-carboxylate 3.1.16

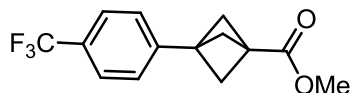
To ACHN (0.096 g, 0.393 mmol) and methyl 2,2-dichloro-3-(4-(trifluoromethyl)phenyl)bicyclo[1.1.1]pentane-1-carboxylate (2.665 g, 7.86 mmol) in PhMe (60 mL) was added TTMSS (9.70 mL, 31.4 mmol). This was heated under reflux for 12 h. The solvent was removed under reduced pressure and the crude material was purified using column chromatography eluting with a gradient of 0-20 cyclohexane:EtOAc. The collected fractions were impure so these were re-purified using column chromatography eluting with a gradient of 0-10 cyclohexane:EtOAc. First eluting fraction was evaporated under reduced pressure to give methyl 3-(4-(trifluoromethyl)phenyl)bicyclo[1.1.1]pentane-1-carboxylate (400 mg, 1.480 mmol, 19%) as a colourless oil. Second eluting fraction was evaporated under reduced pressure to give methyl 2-chloro-3-(4-(trifluoromethyl)phenyl)bicyclo[1.1.1]pentane-1-carboxylate (600 mg, 1.969 mmol, 25%) as a colourless oil.

Methyl 3-(4-(trifluoromethyl)phenyl)bicyclo[1.1.1]pentane-1-carboxylate 3.1.16

M.p. 54 – 56 °C; LCMS (Method B, UV, ESI) $R_t = 1.30$ $[M+H]^+ =$ No mass ion, 91%; ^1H NMR (400 MHz, CDCl_3) $\delta = 7.59$ (d, $J = 8.1$ Hz, 2H), 7.34 (d, $J = 7.8$ Hz, 2H), 3.75 (s, 3H), 2.38 (s, 6H); ^{13}C NMR (101 MHz, CDCl_3) $\delta = 170.3$, 143.5 (q, $^4J_{C-F} = 1.5$ Hz), 129.2 (q, $^2J_{C-F} = 32.3$ Hz), 126.5, 125.2 (q, $^3J_{C-F} = 3.7$ Hz), 124.2 (q, $^1J_{C-F} = 272.2$ Hz), 53.4, 51.7, 41.5, 37.1; ^{19}F NMR (376 MHz, CDCl_3) $\delta = -62.5$ (s, 3F); $\nu_{\text{max}}/\text{cm}^{-1}$ (thin film) 2982, 1737; HRMS: Calculated for $\text{C}_{14}\text{H}_{14}\text{F}_3\text{O}_2$ 271.0940 Found $[M+H]^+$: 271.0944 (1.4 ppm).

Methyl 2-chloro-3-(4-(trifluoromethyl)phenyl)bicyclo[1.1.1]pentane-1-carboxylate 3.1.21

LCMS (Method B, UV, ESI) $R_t = 1.30$ $[M+H]^+ =$ No mass ion, 86%; data consistent with previous isolation.

Methyl 3-(4-(trifluoromethyl)phenyl)bicyclo[1.1.1]pentane-1-carboxylate 3.1.16

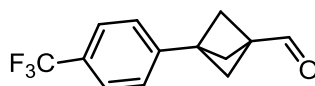
To ACHN (94 mg, 0.39 mmol) was added methyl 2,2-dichloro-3-(4-(trifluoromethyl)phenyl)bicyclo[1.1.1]pentane-1-carboxylate (2.3 g, 6.78 mmol) in PhMe (50 mL). Then TTMSS (11 mL, 38.9 mmol) was added. The reaction was heated under reflux for 3 h. ACHN (1.9 g, 7.77 mmol) was added portionwise over

4 d with continued heating under reflux. The solvent was removed under reduced pressure and the crude product was purified using column chromatography eluting with 0-20 cyclohexane:TBME. Fractions containing product were impure and these were purified using column chromatography eluting with 0-10 cyclohexane:TBME. Fractions containing product were evaporated under reduced pressure to give methyl 3-(4-(trifluoromethyl)phenyl)bicyclo[1.1.1]pentane-1-carboxylate (1.36 g, 5.03 mmol, 74%) as a white solid.

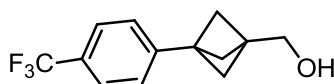
LCMS (Method B, UV, ESI) $R_t = 1.31$ $[M+H]^+ =$ No mass ion peak, 100%; data consistent with previous isolation.

3-(4-(Trifluoromethyl)phenyl)bicyclo[1.1.1]pentane-1-carbaldehyde 2.12.4 and (3-(4-(trifluoromethyl)phenyl)bicyclo[1.1.1]pentan-1-yl)methanol 3.1.22

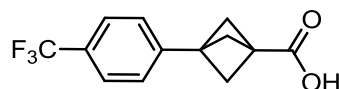
To methyl 3-(4-(trifluoromethyl)phenyl)bicyclo[1.1.1]pentane-1-carboxylate (550 mg, 2.035 mmol) in THF (6 mL) was added DIBAL-H (1M in THF) (2.5 mL, 2.500 mmol) at -78 °C. This was stirred under nitrogen for 3 h. Further DIBAL-H (1M in THF) (2.5 mL, 2.5 mmol) was added and this was stirred for a further 2 h at -78 °C. Sat. $NH_4Cl_{(aq)}$ (10 mL), EtOAc (40 mL), 2M $NaOH_{(aq)}$ (40 mL) were added. The layers were separated and the aqueous layer was extracted with EtOAc (50 mL). The organic layers were combined, filtered through hydrophobic frit and the solvent was removed under reduced pressure to give a crude product. This was purified using column chromatography eluting with a gradient of 0-20 cyclohexane:TBME. Collected fraction 1 was evaporated under reduced pressure to give 3-(4-(trifluoromethyl)phenyl)bicyclo[1.1.1]pentane-1-carbaldehyde (158 mg, 0.658 mmol, 32%). Collected fraction 2 was evaporated under reduced pressure to give (3-(4-(trifluoromethyl)phenyl)bicyclo[1.1.1]pentan-1-yl)methanol (248 mg, 1.024 mmol, 50%).

3-(4-(Trifluoromethyl)phenyl)bicyclo[1.1.1]pentane-1-carbaldehyde 2.12.4

LCMS (Method C, UV, ESI) $R_t = 1.10$ $[M+H]^+ =$ No mass ion, 86%; 1H NMR (400 MHz, $CDCl_3$) $\delta = 9.70$ (s, 1H), 7.59 (d, $J = 8.1$ Hz, 2H), 7.35 (d, $J = 8.1$ Hz, 2H), 2.36 (s, 6H).

(3-(4-(Trifluoromethyl)phenyl)bicyclo[1.1.1]pentan-1-yl)methanol 3.1.22

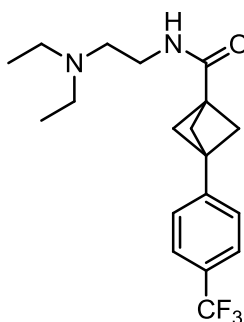
LCMS (Method C, UV, ESI) $R_t = 1.12$ $[M+H]^+ =$ No mass ion, 94%; 1H NMR (400 MHz, $CDCl_3$) $\delta = 7.57$ (d, $J = 8.1$ Hz, 2H), 7.34 (d, $J = 8.1$ Hz, 2H), 3.73 (s, 2H), 2.04 (s, 6H) (1H not observed, exchangeable); ^{13}C NMR (101 MHz, $CDCl_3$) $\delta = 144.8$, 128.8 (q, $^2J_{C-F} = 32.6$ Hz), 126.4, 125.1 (q, $^3J_{C-F} = 3.8$ Hz), 124.3 (q, $^1J_{C-F} = 271.4$ Hz), 63.1, 50.7, 41.8, 39.2; ^{19}F NMR (376 MHz, $CDCl_3$) $\delta = -62.4$ (s, 3F); ν_{max}/cm^{-1} (thin film) 3349 (br), 2972, 2913, 2873, 1619.

3-(4-(Trifluoromethyl)phenyl)bicyclo[1.1.1]pentane-1-carboxylic acid 3.1.23

To methyl 3-(4-(trifluoromethyl)phenyl)bicyclo[1.1.1]pentane-1-carboxylate (1.3 g, 4.81 mmol) in 1,4-dioxane (10 mL) was added 1M LiOH (9.62 mL, 9.62 mmol). This was stirred at ambient temperature for 3 h. To the reaction was added 2M $HCl_{(aq)}$ (5 mL) and EtOAc (30 mL). The layers were separated and the aqueous layer was extracted with EtOAc (3 \times 10 mL). The organic layers were combined, filtered through a hydrophobic frit and evaporated under reduced pressure to give 3-(4-(trifluoromethyl)phenyl)bicyclo[1.1.1]pentane-1-carboxylic acid (1.17 g, 4.57 mmol, 95%) as a white solid.

M.p. 233 – 235 °C; LCMS (Method B, UV, ESI) $R_t = 0.73$ $[M-H]^- = 255.6$, 98%; 1H NMR (400 MHz, DMSO- d_6) $\delta = 12.60 - 12.27$ (m, 1H), 7.68 (d, $J = 8.1$ Hz, 2H), 7.47 (d, $J = 7.8$ Hz, 2H), 2.28 (s, 6H); ^{13}C NMR (101 MHz, DMSO- d_6) $\delta = 170.9$, 144.2, 127.5 (q, $^2J_{C-F} = 32.8$ Hz), 126.9, 125.1 (q, $^3J_{C-F} = 3.7$ Hz), 124.3 (q, $^1J_{C-F} = 272.2$ Hz), 52.6, 40.6, 36.8; ^{19}F NMR (376 MHz, DMSO- d_6) $\delta = -60.9$ (s, 3F); ν_{max}/cm^{-1} (thin film) 2939, 1698; HRMS: Calculated for $C_{13}H_{12}F_3O_2$ 257.0784 Found $[M+H]^+$: 257.0789 (2.0 ppm).

***N*-(2-(Diethylamino)ethyl)-3-(4-(trifluoromethyl)phenyl)bicyclo[1.1.1]pentane-1-carboxamide 3.1.24**



T3P[®] (50% in EtOAc) (2.8 mL, 4.70 mmol), 3-(4-(trifluoromethyl)phenyl)bicyclo[1.1.1]pentane-1-carboxylic acid (800 mg, 3.12 mmol) and Et₃N (0.9 mL, 6.46 mmol) was stirred in EtOAc (10 mL) for 30 min. Then *N*1,*N*1-diethylethane-1,2-diamine (0.66 mL, 4.70 mmol) was added and the reaction mixture was stirred for 16 h. Water (15 mL) and CH₂Cl₂ (20 mL) were added and the layers separated. The aqueous was extracted with CH₂Cl₂ (3 × 5 mL) and the organics were combined and evaporated under reduced pressure to give *N*-(2-(diethylamino)ethyl)-3-(4-(trifluoromethyl)phenyl)bicyclo[1.1.1]pentane-1-carboxamide (1.10 g, 3.10 mmol, 99%) as a orange solid.

M.p. 81 – 83 °C; LCMS (Method B, UV, ESI) $R_t = 1.17$ $[M+H]^+ = 355.5$, 94%; 1H NMR (400 MHz, CDCl₃) $\delta = 7.58$ (d, $J = 7.8$ Hz, 2H), 7.34 (d, $J = 8.1$ Hz, 2H), 6.48 – 6.36 (m, 1H), 3.39 – 3.27 (m, 2H), 2.61 – 2.52 (m, 6H), 2.32 (s, 6H), 1.05 (t, $J = 7.1$ Hz, 6H); ^{13}C NMR (101 MHz, CDCl₃) $\delta = 169.7$, 143.7, 129.2 (q, $^2J_{C-F} =$

33.0 Hz), 126.5, 125.2 (q, $^3J_{C-F} = 3.7$ Hz), 124.1 (q, $^1J_{C-F} = 272.2$ Hz), 52.8, 51.3, 47.0, 40.5, 38.8, 36.7, 12.1; ^{19}F NMR (376 MHz, CDCl_3) $\delta = -62.5$ (s, 3F); $\nu_{\text{max}}/\text{cm}^{-1}$ (thin film) 3320 (br) 2975, 1642; HRMS: Calculated for $\text{C}_{19}\text{H}_{26}\text{F}_3\text{N}_2\text{O}$ 355.1992 Found $[\text{M}+\text{H}]^+$: 355.2000 (2.2 ppm).

***N*,*N*-Diethyl-*N*2-((3-(4-(trifluoromethyl)phenyl)bicyclo[1.1.1]pentan-1-yl)methyl)ethane-1,2-diamine 2.12.3**

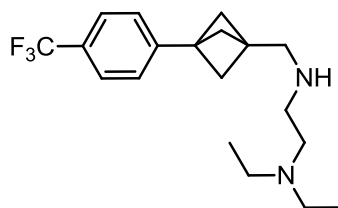


Table 23 Entry 1:

To *N*-(2-(diethylamino)ethyl)-3-(4-(trifluoromethyl)phenyl)bicyclo[1.1.1]pentane-1-carboxamide (50 mg, 0.141 mmol) in THF (2 mL) was added $\text{BH}_3\cdot\text{THF}$ (1M, 0.56 mL, 0.560 mmol) and the reaction mixture was heated under reflux for 6 h. Further $\text{BH}_3\cdot\text{THF}$ (1M, 0.28 mL, 0.28 mmol) was added and the reaction mixture was heated under reflux for a further 20 h. Conversion 90% by LCMS. Due to the strongly co-ordinating nature of the diamine, the product could not be isolated.

Table 23 Entry 2:

To *N*-(2-(diethylamino)ethyl)-3-(4-(trifluoromethyl)phenyl)bicyclo[1.1.1]pentane-1-carboxamide (500 mg, 1.411 mmol) in THF (20 mL) was added $\text{BH}_3\cdot\text{THF}$ (1M, 0.7 mL, 0.700 mmol) and the reaction mixture was heated under reflux for 1 h. Further $\text{BH}_3\cdot\text{THF}$ (1M, 0.7 mL, 0.700 mmol) was added and the reaction mixture was heated under reflux for a further 1 h. Additions of $\text{BH}_3\cdot\text{THF}$ were repeated a further 2 times and then the reaction was heated under reflux for 16 h. Conversion 94% by LCMS. Due to the strongly co-ordinating nature of the diamine, the product could not be isolated.

Table 23 Entry 3:

To *N*-(2-(diethylamino)ethyl)-3-(4-(trifluoromethyl)phenyl)bicyclo[1.1.1]pentane-1-carboxamide (50 mg, 0.141 mmol) and tris(triphenylphosphine)rhodium(I)carbonyl hydride (1.3 mg, 1.411 μ mol) in THF (2 mL) was added diphenylsilane (0.06 mL, 0.324 mmol) at ambient temperature. The reaction was stirred for 6 h at ambient temperature. No conversion observed.

Table 23 Entry 4:

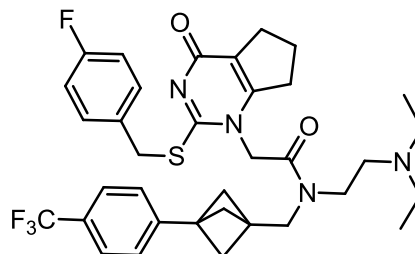
To $[\text{Ir}(\text{COE})_2\text{Cl}]_2$ (48 mg, 0.054 mmol) was added diethylsilane (0.22 mL, 1.698 mmol) and CH_2Cl_2 (1 mL). To the reaction mixture was added *N*-(2-(diethylamino)ethyl)-3-(4-(trifluoromethyl)phenyl)bicyclo[1.1.1]pentane-1-carboxamide (120 mg, 0.339 mmol) in CH_2Cl_2 (2 mL). The reaction was stirred at ambient temperature for 16 h. Conversion 79% by LCMS. Due to the strongly coordinating nature of the diamine, the product could not be isolated.

Table 23 Entry 5:

To *N*-(2-(diethylamino)ethyl)-3-(4-(trifluoromethyl)phenyl)bicyclo[1.1.1]pentane-1-carboxamide (978 mg, 2.76 mmol) in THF (30 mL) was added LiAlH_4 (2.3 M in 2-MeTHF) (2.4 mL, 5.52 mmol) at ambient temperature and the reaction mixture was stirred for 16 h. The reaction was quenched by the addition of wet THF (20 mL) initially dropwise then portionwise. Water (20 mL) was then added portionwise, followed by 2M $\text{HCl}_{(\text{aq})}$ (50 mL) and EtOAc (50 mL). The layers were separated and the organic layer was extracted with 2M $\text{HCl}_{(\text{aq})}$ (3×10 mL). The aqueous layers were combined and basified with 2M $\text{NaOH}_{(\text{aq})}$ (100 mL) then extracted with CH_2Cl_2 (10×50 mL). The organics were combined and filtered through a hydrophobic frit and evaporated under reduced pressure to give the crude *N*1,*N*1-diethyl-*N*2-((3-(4-(trifluoromethyl)phenyl)bicyclo[1.1.1]pentan-1-yl)methyl)ethane-1,2-diamine (527 mg, 1.55 mmol, 56%). LCMS showed 87% product and this was taken on as is to the next step without further purification.

LCMS (Method B, UV, ESI) $R_t = 1.29$ $[\text{M}+\text{H}]^+ = 340.6$, 87%.

***N*-2-(2-(4-fluorobenzyl)thio)-4-oxo-4,5,6,7-tetrahydro-1*H*-cyclopenta[*d*]pyrimidin-1-yl)-*N*-((3-(4-(trifluoromethyl)phenyl)bicyclo[1.1.1]pentan-1-yl)methyl)acetamide, Formic acid salt 2.12.1**



2-(2-(4-Fluorobenzyl)thio)-4-oxo-4,5,6,7-tetrahydro-1*H*-cyclopenta[*d*]pyrimidin-1-yl)acetic acid (634 mg, 1.90 mmol), triethylamine (0.350 mL, 2.509 mmol) and T3P[®] (50% in EtOAc) (1.1 mL, 1.85 mmol) were stirred in CH₂Cl₂ (5 mL) for 30 min. Then *N*,*N*-diethyl-*N*2-((3-(4-(trifluoromethyl)phenyl)bicyclo[1.1.1]pentan-1-yl)methyl)ethane-1,2-diamine (427 mg, 1.25 mmol) in CH₂Cl₂ (5 mL) was added and this was stirred for 16 h. To the reaction mixture was added 2M NaOH_(aq) (20 mL), water (20 mL) and CH₂Cl₂ (40 mL). The layers were separated and the aqueous layer was extracted with CH₂Cl₂ (10 × 15 mL). The organics were combined and evaporated under reduced pressure. The crude product was purified by HpH MDAP (Method D) to give product contaminated with formic acid and HpH modifier. The product was purified using HpH MDAP (Method D) and the solvent was removed under reduced pressure to give *N*-2-(2-(diethylamino)ethyl)-2-(2-(4-fluorobenzyl)thio)-4-oxo-4,5,6,7-tetrahydro-1*H*-cyclopenta[*d*]pyrimidin-1-yl)-*N*-((3-(4-(trifluoromethyl)phenyl)bicyclo[1.1.1]pentan-1-yl)methyl)acetamide, Formic acid salt (526 mg, 0.75 mmol, 60%) as a yellow solid.

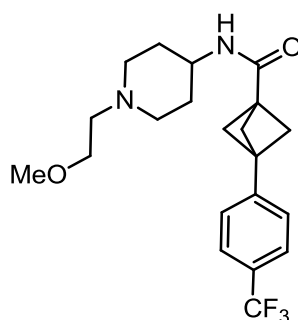
M.p. 88 – 90 °C; LCMS (Method B, UV, ESI) R_t = 1.44 [M+H]⁺ = 657.7, 100%; ¹H NMR (400 MHz, DMSO-*d*₆, 393 K) δ = 8.14 (s, 1H), 7.64 (d, *J* = 8.1 Hz, 2H), 7.47 – 7.41 (m, 2H), 7.41 – 7.36 (m, 2H), 7.03 (br. s., 2H), 5.00 – 4.80 (m, 2H), 4.46 (s, 2H), 3.57 (br. s., 2H), 3.40 (t, *J* = 6.5 Hz, 2H), 2.79 (t, *J* = 7.6 Hz, 2H), 2.67 – 2.52 (m, 8H), 2.14 – 1.95 (m, 8H), 0.98 (t, *J* = 7.1 Hz, 6H); ¹³C NMR (101 MHz, CDCl₃) δ = 167.6, 167.1, 164.9, 163.5, 160.7, 156.0, 155.6, 144.2, 143.2, 131.6, 131.1, 130.1,

126.3, 125.3, 125.2, 121.4, 121.2, 115.7, 115.4, 115.4, 52.4, 52.2, 51.4, 49.7, 49.6, 48.8, 47.8, 47.4, 47.1, 46.4, 43.8, 42.3, 41.8, 37.2, 37.0, 36.3, 36.3, 32.0, 31.9, 28.3, 20.8, 20.7, 11.6, 9.8; ^{19}F NMR (376 MHz, CDCl_3) $\delta = -62.5$ (s, 3F), -114.2 (s, 1F); $\nu_{\text{max}}/\text{cm}^{-1}$ (thin film) 2969, 1618; HRMS: Calculated for $\text{C}_{35}\text{H}_{41}\text{F}_4\text{N}_4\text{O}_2\text{S}$ 657.2881 Found $[\text{M}+\text{H}]^+$: 657.2883 (0.4 ppm).

N-(2-(diethylamino)ethyl)-2-(2-((4-fluorobenzyl)thio)-4-oxo-4,5,6,7-tetrahydro-1*H*-cyclopenta[d]pyrimidin-1-yl)-*N*-((3-(4-(trifluoromethyl)phenyl)bicyclo[1.1.1]pentane-1-yl)methyl)acetamide, Formic acid salt (100 mg, 0.152 mmol) was dissolved in MeOH (2 mL) then passed through an SAX cartridge eluting with MeOH (3 CVs). This collected fractions were evaporated under reduced pressure to give *N*-(2-(diethylamino)ethyl)-2-(2-((4-fluorobenzyl)thio)-4-oxo-4,5,6,7-tetrahydro-1*H*-cyclopenta[d]pyrimidin-1-yl)-*N*-((3-(4-(trifluoromethyl)phenyl)bicyclo[1.1.1]pentane-1-yl)methyl)acetamide (87 mg, 0.132 mmol) as a yellow solid.

LCMS (Method B, UV, ESI) $R_t = 1.45$ $[\text{M}+\text{H}]^+ = 657.3$, 100%; ^1H NMR (400 MHz, CDCl_3) $\delta = 7.58$ (dd, $J = 3.5, 7.9$ Hz, 2H), 7.40 – 7.29 (m, 2H), 7.25 (t, $J = 8.1$ Hz, 2H), 7.02 – 6.94 (m, 1H), 6.89 – 6.81 (m, 1H), 4.92 – 4.64 (m, 2H), 4.53 (d, $J = 4.2$ Hz, 2H), 3.63 – 3.52 (m, 3H), 3.40 – 3.31 (m, 1H), 2.92 – 2.75 (m, 6H), 2.62 – 2.52 (m, 3H), 2.17 – 1.94 (m, 9H), 1.19 – 1.06 (m, 3H), 1.02 (t, $J = 7.2$ Hz, 3H).

***N*-(1-(2-Methoxyethyl)piperidin-4-yl)-3-(4-trifluoromethyl)phenyl)bicyclo[1.1.1]pentane-1-carboxamide 3.1.26**



T3P[®] (50% in DMF) (0.68 mL, 1.17 mmol), 3-(4-(trifluoromethyl)phenyl)bicyclo[1.1.1]pentane-1-carboxylic acid (200 mg,

0.781 mmol) and Et₃N (0.22 mL, 1.58 mmol) were stirred in CH₂Cl₂ (1 mL) for 20 min. Then 1-(2-methoxyethyl)piperidin-4-amine (0.194 mL, 1.17 mmol) was added and the reaction mixture was stirred for 3 h. Water (2 mL) and CH₂Cl₂ (5 mL) were added and the layers separated. The organic layer was washed with 5% LiCl_(aq) (2 × 2 mL). The combined aqueous layers were extracted with CH₂Cl₂ (2 × 3 mL). The organics were combined and filtered through a hydrophobic frit. The solvent was removed under reduced pressure to give *N*-(1-(2-methoxyethyl)piperidin-4-yl)-3-(4-(trifluoromethyl)phenyl)bicyclo[1.1.1]pentane-1-carboxamide (228 mg, 0.58 mmol, 74% yield) as an off white solid.

M.p. 185 – 187 °C; LCMS (Method B, UV, ESI) R_t = 1.07 [M+H]⁺ = 397.2, 100%; ¹H NMR (400 MHz, DMSO-*d*₆) δ = 7.68 (d, *J* = 8.1 Hz, 2H), 7.62 (d, *J* = 7.8 Hz, 1H), 7.45 (d, *J* = 8.1 Hz, 2H), 3.58 - 3.47 (m, 1H), 3.41 (t, *J* = 6.0 Hz, 2H), 3.23 (s, 3H), 2.84 (m, 2H), 2.45 (t, *J* = 6.0 Hz, 2H), 2.22 (s, 6H), 2.04 – 1.94 (m, 2H), 1.70 – 1.61 (m, 2H), 1.53 – 1.40 (m, 2H); ¹³C NMR (101 MHz, DMSO-*d*₆) δ = 168.2, 144.7, 127.3 (q, ²*J*_{C-F} = 31.5 Hz), 126.8, 125.1 (q, ³*J*_{C-F} = 3.8 Hz), 124.3 (q, ¹*J*_{C-F} = 271.4 Hz), 70.1, 57.9, 57.0, 52.8, 52.3, 46.2, 38.3, 31.5 (1C not observed); ¹⁹F NMR (376 MHz, CDCl₃) δ = -62.5 (s, 3F); ν_{max}/cm⁻¹ (thin film) 3345, 2942, 1637; HRMS: Calculated for C₂₁H₂₈F₃N₂O₂ 397.2097 Found [M+H]⁺: 397.2096 (-0.4 ppm).

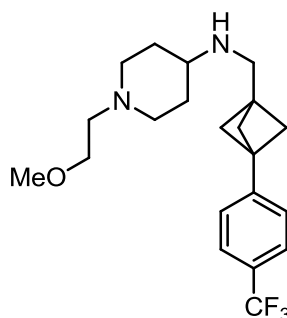
1-(2-Methoxyethyl)-N-((3-(4-(trifluoromethyl)phenyl)bicyclo[1.1.1]pentan-1-yl)methyl)piperidin-4-amine, formic acid salt 2.12.12

Table 24 Entry 1:

To N -(1-(2-methoxyethyl)piperidin-4-yl)-3-(4-(trifluoromethyl)phenyl)bicyclo[1.1.1]pentane-1-carboxamide (50 mg, 0.126 mmol) in 2-MeTHF (0.5 mL) was added LiAlH_4 (2.3M, 0.110 mL, 0.252 mmol). The reaction mixture as stirred at ambient temperature for 6 h. Wet THF (3 mL) was added dropwise and then water (1 mL), 2M NaOH (4 mL) and THF (12 mL) were added. The reaction mixture was stirred at ambient temperature for 15 mins. One spatula of magnesium sulfate was added and this was stirred for a further 15 mins. The reaction mixture was then filtered under reduced pressure. The filtrate was concentrated *in vacuo* to give a crude product. This was purified using a high pH MDAP (Method C) to give 1-(2-methoxyethyl)- N -((3-(4-(trifluoromethyl)phenyl)bicyclo[1.1.1]pentan-1-yl)methyl)piperidin-4-amine (9 mg, 0.024 mmol, 19%) as a yellow solid.

Table 24 Entry 2:

To N -(1-(2-methoxyethyl)piperidin-4-yl)-3-(4-(trifluoromethyl)phenyl)bicyclo[1.1.1]pentane-1-carboxamide (18 mg, 0.045 mmol) in THF (1 mL) was added $\text{BH}_3\cdot\text{THF}$ (1M, 0.1 mL, 0.100 mmol) at ambient temperature. This was then heated under reflux for 16 h. No conversion to desired product was observed.

Table 24 Entry 3:

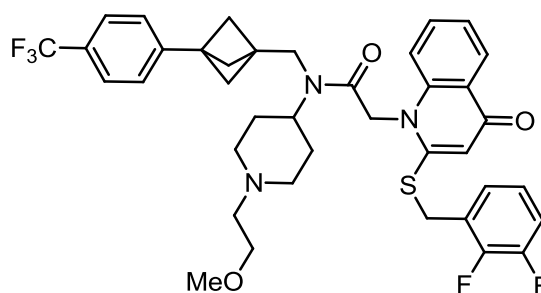
N-(1-(2-methoxyethyl)piperidin-4-yl)-3-(4-(trifluoromethyl)phenyl)bicyclo[1.1.1]pentane-1-carboxamide (20 mg, 0.050 mmol) and 2-Fpy (5 μ L, 0.058 mmol) were dissolved in CH₂Cl₂ (0.5 mL). This was cooled to – 78 °C and stirred for 10 mins. Tf₂O (9 μ L, 0.053 mmol) was added dropwise and the reaction mixture was stirred for a further 10 mins. The solution was allowed to warm to 0 °C and stirred for a further 10 mins. Triethylsilane (9 μ L, 0.056 mmol) was added dropwise at 0 °C and stirred for a further 10 mins. The reaction mixture was allowed to warm to ambient temperature and stirred for 5 h. HE (18 mg, 0.071 mmol) in CH₂Cl₂ (0.5 mL) was added and the reaction was stirred for 16 h. No conversion to desired product was observed.

Table 24 Entry 4:

To [Ir(COE)₂Cl]₂ (48.4 mg, 0.054 mmol) was added diethylsilane (0.210 mL, 1.62 mmol) and CH₂Cl₂ (0.5 mL). To this was added *N*-(1-(2-methoxyethyl)piperidin-4-yl)-3-(4-(trifluoromethyl)phenyl)bicyclo[1.1.1]pentane-1-carboxamide (107 mg, 0.27 mmol) in CH₂Cl₂ (1.5 mL). The reaction mixture was stirred for 20 h at ambient temperature. To the reaction mixture was added 4M HCl in 1,4-dioxane (3 mL), however no solid precipitation. 2M NaOH_(aq) was added until alkaline pH achieved. CH₂Cl₂ (20 mL) was added and the layers were separated. The aqueous layer was extracted with CH₂Cl₂ (3 \times 10 mL). The organic layers were combined and evaporated under reduced pressure to give a crude product. To the crude product was added CH₂Cl₂ (10 mL) and 2M HCl_(aq) (10 mL) and the layers were separated. The organic layer was extracted with 2M HCl_(aq) (3 \times 5 mL). The aqueous layers were combined and 2M NaOH_(aq) was added until alkaline pH. CH₂Cl₂ (30 mL) was added and the layers were separated. The aqueous layer was extracted with CH₂Cl₂ (6 \times 20 mL) and the organics were combined and evaporated under reduced pressure to give a residue which was purified using HpH MDAP (Method C) to give 1-(2-methoxyethyl)-*N*-((3-(4-(trifluoromethyl)phenyl)bicyclo[1.1.1]pentan-1-yl)methyl)piperidin-4-amine, formic acid salt (61 mg, 0.16 mmol, 59%) as a yellow solid.

M.p. 118 – 120 °C; LCMS (Method B, UV, ESI) $R_t = 1.33$ $[M+H]^+ = 383.2$, 100%; 1H NMR (400 MHz, $CDCl_3$) $\delta = 8.46$ (s, 1H), 7.54 (d, $J = 8.1$ Hz, 2H), 7.31 – 7.27 (m, 2H), 5.23 (br. s., 2H), 3.61 (t, $J = 5.1$ Hz, 2H), 3.35 (s, 3H), 3.26 – 3.19 (m, 2H), 3.05 – 2.96 (m, 3H), 2.80 (t, $J = 5.3$ Hz, 2H), 2.47 – 2.37 (m, 2H), 2.17 – 2.10 (m, 8H), 1.95 – 1.82 (m, 2H); ^{13}C NMR (101 MHz, $CDCl_3$) $\delta = 167.5$, 144.0, 128.9 (q, $^2J_{C-F} = 32.3$ Hz), 126.4, 125.1 (q, $^3J_{C-F} = 3.6$ Hz), 69.2, 58.8, 56.8, 53.6, 52.2, 51.6, 45.6, 42.0, 36.4, 28.3 (1C not observed); ^{19}F NMR (376 MHz, $CDCl_3$) $\delta = -62.4$ (s, 3F); ν_{max}/cm^{-1} (thin film) 2782 (br), 1619, 1560; HRMS: Calculated for $C_{21}H_{30}F_3N_2O$ 383.2305 Found $[M+H]^+$: 383.2307 (0.5 ppm).

2-(2-((2,3-Difluorobenzyl)thio)-4-oxoquinolin-1(4H)-yl)-N-(1-(2-methoxyethyl)piperidin-4-yl)-N-((3-(4-(trifluoromethyl)phenyl)bicyclo[1.1.1]pentan-1-yl)methyl)acetamide 3.1.28

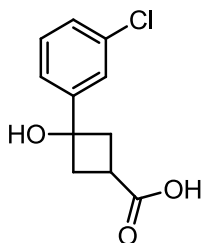


2-(2-((2,3-Difluorobenzyl)thio)-4-oxoquinolin-1(4H)-yl)acetic acid (28.3 mg, 0.078 mmol), Et_3N (0.015 mL, 0.11 mmol) and T3P[®] (50% in DMF) (0.046 mL, 0.078 mmol) in CH_2Cl_2 (0.5 mL) was stirred for 15 min at ambient temperature. To the reaction mixture was added 1-(2-methoxyethyl)-N-((3-(4-(trifluoromethyl)phenyl)bicyclo[1.1.1]pentan-1-yl)methyl)piperidin-4-amine (20 mg, 0.052 mmol) in CH_2Cl_2 (0.5 mL) at ambient temperature stirred for 64 h. Water (1 mL) was added and the layers were separated. The aqueous layer was extracted with CH_2Cl_2 (3×1 mL). The organic layers were combined and evaporated under reduced pressure give a crude product. This was purified by HpH MDAP (Method D) to give 2-(2-((2,3-difluorobenzyl)thio)-4-oxoquinolin-1(4H)-yl)-N-(1-(2-

methoxyethyl)piperidin-4-yl)-*N*-((3-(4-(trifluoromethyl)phenyl)bicyclo[1.1.1]pentan-1-yl)methyl)acetamide (20 mg, 0.028 mmol, 53%) as a yellow solid.

M.p. 57 – 59 °C; LCMS (Method B, UV, ESI) $R_t = 1.36$ $[M+H]^+ = 726.2$, 100%; 1H NMR (400 MHz, DMSO- d_6 , 393 K) $\delta = 8.18$ (dd, $J = 1.5, 8.1$ Hz, 1H), 7.71 – 7.59 (m, 3H), 7.47 – 7.32 (m, 4H), 7.32 – 7.21 (m, 2H), 7.17 – 7.07 (m, 1H), 6.35 (s, 1H), 5.41 (br. s., 2H), 4.43 (s, 2H), 3.83 – 3.72 (m, 1H), 3.57 (br. s., 2H), 3.48 (t, $J = 5.7$ Hz, 2H), 3.28 (s, 3H), 3.00 (m, 2H), 2.56 (t, $J = 5.6$ Hz, 2H), 2.27 – 1.68 (m, 12H); ^{13}C NMR (101 MHz, CDCl₃) $\delta = 176.5, 176.4, 166.5, 165.2, 152.1, 152.0, 142.3, 132.6, 132.4, 127.0, 126.9, 126.4, 126.3, 125.9, 125.3, 125.1, 124.5, 123.9, 117.5, 117.4, 115.3, 115.1, 113.3, 113.1, 77.2, 69.9, 69.1, 58.9, 58.9, 57.5, 56.9, 54.8, 53.2, 53.0, 52.9, 52.8, 52.2, 50.1, 49.9, 44.7, 43.4, 41.7, 41.0, 38.1, 37.8, 33.1, 33.0, 30.8, 28.3$; ^{19}F NMR (376 MHz, DMSO- d_6) $\delta = -60.79$ (s, 3F), -138.67 (m, 1F), -142.15 (m, 1F); ν_{max}/cm^{-1} (thin film) 3402 (br), 2964, 1652, 1617, 1593; HRMS: Calculated for C₃₉H₄₁F₅N₃O₃S 726.2783 Found $[M+H]^+$: 726.2796 (1.8 ppm).

3-(3-Chlorophenyl)-3-hydroxycyclobutanecarboxylic acid 3.3.6

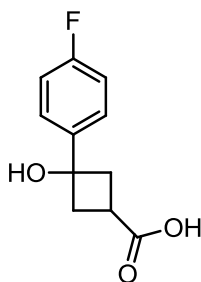


To 1-chloro-3-iodobenzene (0.543 mL, 4.38 mmol) in THF (2 mL) was added *n*-BuLi (1.753 mL, 4.38 mmol) dropwise at -78 °C. This was stirred for 30 min then 3-oxocyclobutanecarboxylic acid (200 mg, 1.753 mmol) in THF (2 mL) was added and this was stirred for a further 6 h warming to ambient temperature. Water (5 mL) and EtOAc (10 mL) were then added to the reaction mixture. The layers were separated and the organic layer was extracted with 2M NaOH_(aq) (3×5 mL). The combined aqueous layers were acidified using conc. HCl_(aq) and then CH₂Cl₂ (5 mL) was added. The layers were separated and the aqueous layer was extracted with CH₂Cl₂ (5×5 mL). The combined organic layers were filtered through a hydrophobic frit

and evaporated under reduced pressure to give 3-(3-chlorophenyl)-3-hydroxycyclobutanecarboxylic acid (329 mg, 1.452 mmol, 83%) as an off white solid.

M.p. 136 – 138 °C; LCMS (Method B, UV, ESI) $R_t = 0.52$ $[M-H]^- = 225.1$, 90%; 1H NMR (400 MHz, $CDCl_3$) $\delta = 7.50$ (t, $J = 1.8$ Hz, 1H), 7.41 – 7.36 (m, 1H), 7.33 – 7.28 (m, 1H), 7.27 – 7.23 (m, 1H), 2.95 – 2.80 (m, 3H), 2.67 – 2.60 (m, 2H) (2H not observed, exchangeable); ^{13}C NMR (101 MHz, $CDCl_3$) 178.9, 147.4, 134.4, 129.7, 127.4, 125.5, 123.2, 73.4, 40.8, 30.1; ν_{max}/cm^{-1} (thin film) 3354 br, 2994, 1714. Failed to ionise under high resolution mass spectrometry conditions.

3-(4-Fluorophenyl)-3-hydroxycyclobutanecarboxylic acid 3.3.8



Method A:

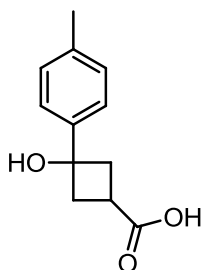
To 1-bromo-4-fluorobenzene (2.4 mL, 21.85 mmol) in THF (10 mL) was added *n*-BuLi (2.5 M in hexanes) (8.5 mL, 21.25 mmol) dropwise at -78 °C. This was stirred for 2 h then 3-oxocyclobutanecarboxylic acid (1 g, 8.76 mmol) in THF (10 mL) was added and this was stirred for a further 6 h warming to ambient temperature. Water (20 mL), EtOAc (50 mL) and 2M $NaOH_{(aq)}$ (20 mL) were then added to the reaction mixture. The layers were separated and the organic layer was extracted with 2M $NaOH_{(aq)}$ (3×10 mL). The combined aqueous layers were acidified using conc. $HCl_{(aq)}$ and then CH_2Cl_2 (90 mL) was added. The layers were separated and the aqueous layer was extracted with CH_2Cl_2 (3×50 mL). The combined organic layers were filtered through a hydrophobic frit and evaporated under reduced pressure to give a crude product. CH_2Cl_2 (100 mL) was added and white solid precipitated. The

white solid was filtered off to give 3-(4-fluorophenyl)-3-hydroxycyclobutanecarboxylic acid (437 mg, 2.079 mmol, 24%) as a white solid.

Method B:

To 1-fluoro-4-iodobenzene (12.5 mL, 108 mmol) in THF (50 mL) was added *n*-BuLi (43 mL, 108 mmol) dropwise at $-78\text{ }^{\circ}\text{C}$ and was stirred for 1 h. 3-oxocyclobutanecarboxylic acid (5 g, 43.8 mmol) in THF (50 mL) was added and this was stirred for a further 6 h allowing to warm to ambient temperature. Water (50 mL) and EtOAc (10 mL) were then added to the reaction mixture. The layers were separated and the organic layer was extracted with 2M NaOH_(aq) (3×50 mL). The combined aqueous layers were acidified using conc. HCl_(aq) and then CH₂Cl₂ (100 mL) was added. The layers were separated and the aqueous layer was extracted with CH₂Cl₂ (3×50 mL). The combined organic layers were filtered through a hydrophobic frit and evaporated under reduced pressure to give crude product (7.3 g). The crude product was triturated with CH₂Cl₂ to give 3-(4-fluorophenyl)-3-hydroxycyclobutanecarboxylic acid (5.47 g, 26.0 mmol, 59%) as a white solid.

M.p. $157 - 159\text{ }^{\circ}\text{C}$; LCMS (Method B, UV, ESI) $R_t = 0.45$ $[\text{M}-\text{H}]^- = 209.21$, 92%; ¹H NMR (400 MHz, CDCl₃) $\delta = 7.51 - 7.43$ (m, 2H), $7.08 - 6.98$ (m, 2H), $4.62 - 3.50$ (br s., 1H), $2.88 - 2.77$ (m, 3H), $2.67 - 2.57$ (m, 2H) (1H not observed, exchangeable); ¹³C NMR (101 MHz, DMSO-*d*₆) 175.8, 161.0 (d, ¹*J*_{C-F} = 242.1 Hz), 142.9 (d, ⁴*J*_{C-F} = 2.9 Hz), 127.1, (d, ³*J*_{C-F} = 8.1 Hz), 114.6 (q, ²*J*_{C-F} = 20.5 Hz), 70.6, 40.9, 28.5; ¹⁹F NMR (376 MHz, DMSO-*d*₆) $\delta = -116.6$ (s, 1F); $\nu_{\text{max}}/\text{cm}^{-1}$ (thin film) 3281 br, 3005, 1695. Failed to ionise under high resolution mass spectrometry conditions.

3-Hydroxy-3-(*p*-tolyl)cyclobutanecarboxylic acid 3.3.13**Method A:**

To 1-bromo-4-methylbenzene (7.5 g, 43.9 mmol) in THF (20 mL) was added *n*-BuLi (2.5 M in hexanes) (17.53 mL, 43.8 mmol) at $-78\text{ }^{\circ}\text{C}$. The reaction was then stirred for 2 h before 3-oxocyclobutanecarboxylic acid (2 g, 17.53 mmol) in THF (20 mL) was added portionwise at $-78\text{ }^{\circ}\text{C}$. The reaction mixture was allowed to warm to ambient temperature and was stirred for a further 16 h. Water (40 mL) and EtOAc (40 mL) were added and a white solid precipitated. The solid was filtered off and washed with EtOAc (20 mL) and water (20 mL). The filtrate layers were separated and the organic layer was washed with brine (20 mL). The aqueous layers were combined and brine (30 mL) and ethyl acetate (50 mL) were added. The layers were separated and the aqueous layer was washed with ethyl acetate (2 x 30 mL). The aqueous layer was then acidified using conc HCl and the organic layer was extracted with CH_2Cl_2 (100 mL then 3 x 50 mL). The organic layers were combined, filtered through a hydrophobic frit and the solvent removed under reduced pressure to give 3-hydroxy-3-(*p*-tolyl)cyclobutanecarboxylic acid (2.2 g, 10.67 mmol, 61% yield) as a brown semi-solid.

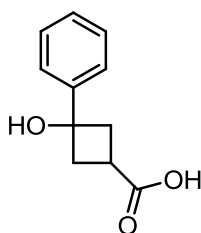
Method B:

To 1-iodo-4-methylbenzene (23 g, 105 mmol) in THF (50 mL) was added *n*-BuLi (2.5 M in hexanes) (42.1 mL, 105 mmol) dropwise at $-78\text{ }^{\circ}\text{C}$. This was stirred for 2 h then 3-oxocyclobutanecarboxylic acid (5 g, 43.8 mmol) in THF (50 mL) was added and this was stirred for a further 6 h. The reaction mixture was left to stand for 5 d. Water (50 mL) and EtOAc (100 mL) were added to the reaction mixture and the layers were separated. The organic layer was extracted with 2M $\text{NaOH}_{(\text{aq})}$ (3 x

50 mL). The aqueous layers were combined and acidified with conc $\text{HCl}_{(\text{aq})}$. CH_2Cl_2 (50 mL) was added and the layers were separated. The aqueous layer was extracted with CH_2Cl_2 (4×50 mL) and the organics were then combined, filtered through a hydrophobic frit and evaporated under reduced pressure to give 3-hydroxy-3-(p-tolyl)cyclobutanecarboxylic acid (7.067 g, 34.3 mmol, 78%) as an off white solid.

M.p. 143 – 145 °C; LCMS (Method B, UV, ESI) $R_t = 0.49$ $[\text{M}-\text{H}]^- = 205.2$, 99%; ^1H NMR (400 MHz, CDCl_3) $\delta = 7.46 - 7.34$ (m, 2H), 7.18 (d, $J = 8.1$ Hz, 2H), 2.92 – 2.77 (m, 3H), 2.73 – 2.57 (m, 2H), 2.41 – 2.30 (s, 3H) (2H not observed, exchangeable); ^{13}C NMR (101 MHz, CDCl_3) 179.0, 142.0, 137.0, 129.0, 124.9, 73.3, 40.6, 29.8, 20.9; $\nu_{\text{max}}/\text{cm}^{-1}$ (thin film) 3366 br, 2941, 1713. Failed to ionise under high resolution mass spectrometry conditions.

3-Hydroxy-3-phenylcyclobutanecarboxylic acid 3.3.16¹⁵⁸



Small Scale:

To iodobenzene (0.490 mL, 4.38 mmol) in THF (2 mL) was added *n*-BuLi (1.753 mL, 4.38 mmol) dropwise at -78 °C. This was stirred for 15 min then 3-oxocyclobutanecarboxylic acid (200 mg, 1.753 mmol) in THF (2 mL) was added and this was stirred for a further 6 h warming to ambient temperature. Water (5 mL) and EtOAc (10 mL) were added to the reaction mixture and the layers were separated. The organic layer was extracted with 2M $\text{NaOH}_{(\text{aq})}$ (3×5 mL) and the combined aqueous layers were acidified with c. $\text{HCl}_{(\text{aq})}$. CH_2Cl_2 (20 mL) was added and the layers were separated. The aqueous layer was extracted with CH_2Cl_2 (3×10 mL). The organic layers were combined and evaporated under reduced pressure to give 3-

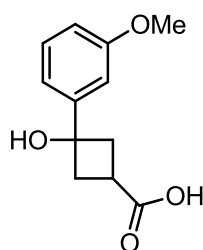
hydroxy-3-phenylcyclobutanecarboxylic acid (282 mg, 1.467 mmol, 84%) as an off white solid.

Large scale:

To iodobenzene (12.26 mL, 110 mmol) in THF (50 mL) was added *n*-BuLi (43.8 mL, 110 mmol) dropwise at -78 °C. This was stirred for 15 min then 3-oxocyclobutanecarboxylic acid (5 g, 43.8 mmol) in THF (50 mL) was added and this was stirred for a further 6 h warming to ambient temperature. Water (50 mL) and EtOAc (100 mL) were added to the reaction mixture and the layers were separated. The organic layer was extracted with 2M NaOH_(aq) (3×50 mL) and the combined aqueous layers were acidified with conc. HCl_(aq). CH₂Cl₂ (50 mL) was added and the layers were separated. The aqueous layer was extracted with CH₂Cl₂ (5×50 mL). The organic layers were combined and evaporated under reduced pressure to give 3-hydroxy-3-phenylcyclobutanecarboxylic acid (3.42 g, 17.79 mmol, 41%) as an off white solid. (90% purity by LCMS)

A 100 mg sample of this was taken and purified using HpH MDAP (Method A) to give 66 mg of 3-hydroxy-3-phenylcyclobutanecarboxylic acid as a white solid.

M.p. 134 – 136 °C; LCMS (Method B, UV, ESI) $R_t = 0.40$ $[M-H]^- = 191.2$, 100%; ¹H NMR (400 MHz, DMSO-*d*₆) $\delta = 7.68 - 7.45$ (m, 3H), 7.37 – 7.31 (m, 2H), 7.26 – 7.20 (m, 1H), 2.71 – 2.54 (m, 3H), 2.48 – 2.40 (m, 2H) (1H not observed, exchangeable); ¹³C NMR (101 MHz, DMSO-*d*₆) 177.2, 147.0, 127.9, 126.4, 124.9, 71.5, 41.1, 30.1; $\nu_{\max}/\text{cm}^{-1}$ (thin film) 3353 br, 2944, 1713. Failed to ionise under high resolution mass spectrometry conditions.

3-Hydroxy-3-(3-methoxyphenyl)cyclobutanecarboxylic acid 3.3.18

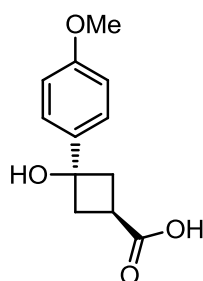
To 1-bromo-3-methoxybenzene (13.9 mL, 110 mmol) in THF (50 mL) was added *n*-BuLi (2.5M in hexanes) (43.8 mL, 110 mmol) dropwise at $-78\text{ }^{\circ}\text{C}$. This was stirred for 1 h then 3-oxocyclobutanecarboxylic acid (5 g, 43.8 mmol) in THF (50 mL) was added and this was stirred for a further 6 h warming to ambient temperature. Water (50 mL) and EtOAc (100 mL) were added to the reaction mixture and the layers were separated. The organic layer was extracted with 2M NaOH_(aq) ($3 \times 50\text{ mL}$) and the combined aqueous layers were acidified with conc. HCl_(aq). CH₂Cl₂ (50 mL) was added and the layers were separated. The aqueous layer was extracted with CH₂Cl₂ ($5 \times 50\text{ mL}$). The organic layers were combined, filtered through a hydrophobic frit and evaporated under reduced pressure to give 3-hydroxy-3-(3-methoxyphenyl)cyclobutanecarboxylic acid (7.571 g, 34.1 mmol, 78%) as an off white solid.

100 mg sample purified using HpH MDAP (Method A) to give 79 mg 3-hydroxy-3-(3-methoxyphenyl)cyclobutanecarboxylic acid.

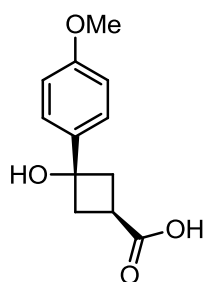
M.p. $125 - 127\text{ }^{\circ}\text{C}$; LCMS (Method B, UV, ESI) $R_t = 0.44$ $[\text{M}-\text{H}]^- = 205.2$, 100%; ¹H NMR (400 MHz, CDCl₃) $\delta = 7.34 - 7.27$ (m, 1H), $7.11 - 7.05$ (m, 2H), $6.86 - 6.81$ (m, 1H), 3.83 (s, 3H), $2.93 - 2.79$ (m, 3H), $2.71 - 2.58$ (m, 2H) (2H not observed, exchangeable); ¹³C NMR (101 MHz, CDCl₃) 179.2, 159.7, 146.7, 129.4, 117.2, 112.8, 110.9, 73.5, 55.2, 40.7, 29.9; $\nu_{\text{max}}/\text{cm}^{-1}$ (thin film) 3382 br, 2938, 1704. Failed to ionise under high resolution mass spectrometry conditions.

***cis*-3-Hydroxy-3-(4-methoxyphenyl)cyclobutanecarboxylic acid 3.3.20 and *trans*-3-hydroxy-3-(4-methoxyphenyl)cyclobutane-1-carboxylic acid 3.3.21**

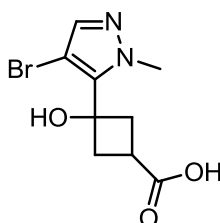
To 1-iodo-4-methoxybenzene (2.56 g, 10.96 mmol) in THF (10 mL) was added *n*-BuLi (1.6 M, 6.85 mL, 10.96 mmol) at -78 °C dropwise. This was stirred for 2 h before 3-oxocyclobutanecarboxylic acid (0.5 g, 4.38 mmol) in THF (10 mL) was added. This was then warmed to ambient temperature and stirred for 16 h. Water (10 mL), 2M NaOH_(aq) (25 mL), and EtOAc (40 mL) were added and the layers were separated. The organic layer was extracted with 2M NaOH_(aq) (3 × 25 mL). The aqueous layers were combined and acidified with conc HCl_(aq). CH₂Cl₂ (50 mL) was then added and the layers were separated. The aqueous layer was extracted with CH₂Cl₂ (3 × 50 mL) and the organic layers were combined, filtered through a hydrophobic frit and evaporated under reduced pressure to give a brown oil. This was purified using a high pH MDAP (Method A) to give *cis*-3-hydroxy-3-(4-methoxyphenyl)cyclobutane-1-carboxylic acid (141 mg, 0.634 mmol, 14%) and *trans*-3-hydroxy-3-(4-methoxyphenyl)cyclobutane-1-carboxylic acid (220 mg, 0.990 mmol, 23%) both as white solids.

***cis*-3-Hydroxy-3-(4-methoxyphenyl)cyclobutane-1-carboxylic acid 3.3.20**

M.p. 128 – 130 °C; LCMS (Method B, UV, ESI) $R_t = 0.42$ $[M-H]^- = 221.2$, 94%; ¹H NMR (600 MHz, DMF-*d*₇) $\delta = 7.53$ (d, $J = 8.7$ Hz, 2H), 6.97 (d, $J = 8.9$ Hz, 2H), 3.83 (s, 3H), 2.78 – 2.72 (m, 1H), 2.75 – 2.68 (m, 2H), 2.65 – 2.59 (m, 2H) (2H not observed, exchangeable); ¹³C NMR (151 MHz, DMF-*d*₇) $\delta = 176.2$, 158.7, 139.0, 126.5, 113.4, 71.2, 54.9, 41.3, 29.1; ν_{max}/cm^{-1} (thin film) 3397, 2987, 2938, 1704. Failed to ionise under high resolution mass spectrometry conditions.

trans-3-Hydroxy-3-(4-methoxyphenyl)cyclobutane-1-carboxylic acid 3.3.21

M.p. 81 – 83 °C; LCMS (Method B, UV, ESI) $R_t = 0.36$ $[M-H]^- = 221.2$, 70% (20% **3.3.20** present); 1H NMR (600 MHz, DMF- d_7) $\delta = 7.44$ (d, $J = 8.7$ Hz, 2H), 7.05 – 6.84 (m, 2H), 3.82 (s, 3H), 3.41 (quin, $J = 8.8$ Hz, 1H), 2.71 – 2.66 (m, 2H), 2.54 – 2.49 (m, 2H) (2H not observed, exchangeable); ^{13}C NMR (151 MHz, DMF- d_7) $\delta = 176.7$, 158.5, 140.4, 126.2, 113.3, 73.2, 54.9, 40.6, 31.6; ν_{max}/cm^{-1} (thin film) 3387, 2995, 2946, 1702, 1672. Failed to ionise under high resolution mass spectrometry conditions.

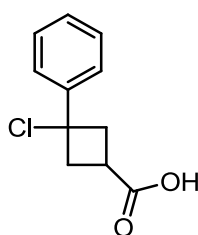
3-(4-Bromo-1-methyl-1H-pyrazol-5-yl)-3-hydroxycyclobutanecarboxylic acid 3.3.34

To 4-bromo-1-methyl-1H-pyrazole (0.453 mL, 4.38 mmol) in THF (2 mL) was added *n*-BuLi (1.753 mL, 4.38 mmol) dropwise at -78 °C. This was stirred for 1 h then 3-oxocyclobutanecarboxylic acid (200 mg, 1.753 mmol) in THF (2 mL) was added in one charge and stirred for 16 h warming to ambient temperature. Water (5 mL) and EtOAc (10 mL) were then added to the reaction mixture and the layers were separated. The organic layer was extracted with 2M NaOH_(aq) (3 × 5 mL). The aqueous layers were combined and acidified with conc. HCl_(aq). CH₂Cl₂ (10 mL) was added and the layers were separated. The aqueous layer was extracted with CH₂Cl₂

(3 × 10 mL). The organic layers were combined, filtered through a hydrophobic frit and evaporated under reduced pressure to give a crude product. This was purified using HpH MDAP (Method A) to give 3-(4-bromo-1-methyl-1*H*-pyrazol-5-yl)-3-hydroxycyclobutanecarboxylic acid (114 mg, 0.414 mmol, 24%) as an off white solid.

M.p. 139 – 141 °C; LCMS (Method B, UV, ESI) $R_t = 0.38$ $[M-H]^- = 273.0, 275.0, 100\%$; 1H NMR (400 MHz, DMSO- d_6) $\delta = 7.38$ (s, 1H), 3.79 (s, 3H), 3.08 – 3.00 (m, 2H), 2.73 – 2.64 (m, 1H), 2.45 – 2.39 (m, 2H) (2H not observed, exchangeable); ^{13}C NMR (101 MHz, DMSO- d_6) 177.3, 141.3, 138.5, 89.7, 68.8, 39.2, 39.0, 33.3; ν_{max}/cm^{-1} (thin film) 3354 (br), 2918, 2850, 1718, 1682; HRMS: Calculated for $C_9H_{12}BrN_2O_3$ 275.0031 Found $[M+H]^+$: 275.0040 (3.3 ppm).

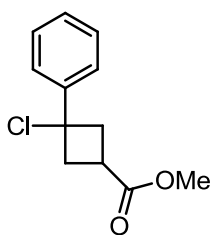
3-Chloro-3-phenylcyclobutanecarboxylic acid 3.3.35¹⁵⁸



To 3-hydroxy-3-phenylcyclobutanecarboxylic acid (500 mg, 2.60 mmol) in PhMe (15 mL) was added conc. $HCl_{(aq)}$ (37.5%, 5 mL, 61.7 mmol). This was sonicated for 5 h. The layers were separated and the aqueous layer was extracted with PhMe (3 × 5 mL). The organics were combined, filtered through a hydrophobic frit and evaporated under reduced pressure to give 3-chloro-3-phenylcyclobutanecarboxylic acid (477 mg, 2.264 mmol, 87%) as a white solid. (~3:1 mixture of diastereomers)

1H NMR (400 MHz, $CDCl_3$) $\delta = 7.53 - 7.49$ (m, 1H), 7.43 – 7.26 (m, 4H), 3.80 – 3.69 (m, 0.75H, Isomer 1), 3.29 – 3.14 (m, 1H, Isomer 2), 3.13 – 2.99 (m, 3H, Isomer 1), 2.96 – 2.85 (m, 0.25H, Isomer 2) (1H not observed, exchangeable).

Sample degraded

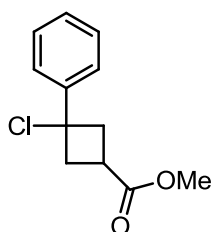
Methyl 3-chloro-3-phenylcyclobutanecarboxylate 3.3.37¹⁵⁸

To 3-chloro-3-phenylcyclobutanecarboxylic acid (80 mg, 0.380 mmol) in MeOH (0.5 mL) was added HCl (3M in MeOH) (0.25 mL, 0.750 mmol). This was stirred at ambient temperature for 4 h. The solvent was then evaporated under reduced pressure to give methyl 3-chloro-3-phenylcyclobutanecarboxylate (78 mg, 0.347 mmol, 91%) as a yellow oil. (~2:1 mixture of diastereomers)

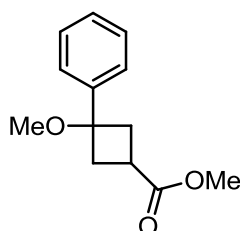
¹H NMR (400 MHz, CDCl₃) δ = 7.55 – 7.53 (m, 0.5H), 7.44 – 7.28 (m, 4.5H), 3.77 – 3.67 (m, 3.7H), 3.27 – 3.15 (m, 1.3H), 3.13 – 2.97 (m, 2.7H), 2.93 – 2.83 (m, 0.3H); ¹³C NMR (101 MHz, CDCl₃) 176.6, 144.7, 128.5, 127.5, 125.0, 73.5, 52.1, 40.7, 29.6; $\nu_{\max}/\text{cm}^{-1}$ (thin film) 2951, 1729, 1705.

Methyl 3-chloro-3-phenylcyclobutanecarboxylate 3.3.37 and methyl 3-methoxy-3-phenylcyclobutanecarboxylate 3.3.38

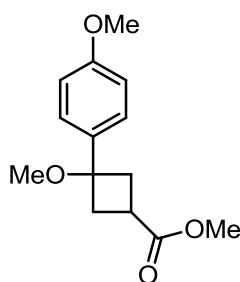
To 3-chloro-3-phenylcyclobutanecarboxylic acid (2.377 g, 11.28 mmol) in MeOH (25 mL) was added HCl (3M in MeOH) (8 mL, 24 mmol). This was stirred at ambient temperature for 20 h. The solvent was then evaporated under reduced pressure to give a crude product. This was purified using column chromatography eluting with a gradient of 0-20 cyclohexane:TBME. Fractions collected were evaporated under reduced pressure to give methyl 3-chloro-3-phenylcyclobutanecarboxylate (528 mg, 2.350 mmol, 21%) as a yellow semi solid (~2:1 mixture of diastereomers) and methyl 3-methoxy-3-phenylcyclobutanecarboxylate (1.088 g, 4.94 mmol, 44%) as a colourless oil. (~ 2:1 mixture of diastereomers)

Methyl 3-chloro-3-phenylcyclobutanecarboxylate 3.3.37¹⁵⁸

Data consistent with previous isolation

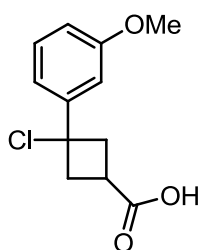
Methyl 3-methoxy-3-phenylcyclobutanecarboxylate 3.3.38

LCMS (Method B, UV, ESI) $R_t = 1.08$ $[M-H]^- =$ No mass ion, 100%; 1H NMR (400 MHz, $CDCl_3$) $\delta = 7.48 - 7.27$ (m, 5H), 3.71 (s, 2H, Isomer 1), 3.66 (s, 1H, Isomer 2), 3.42 – 3.31 (m, 0.4H), 2.98 (s, 1H, Isomer 2), 2.93 (s, 2H, Isomer 1), 2.83 – 2.59 (m, 4.6H); ^{13}C NMR (101 MHz, $CDCl_3$) 175.6, 175.0, 142.4, 141.7, 128.4, 128.2, 127.6, 127.5, 126.3, 126.0, 79.8, 77.3, 51.8, 51.7, 50.9, 50.4, 36.8, 35.0, 32.1, 29.1; ν_{max}/cm^{-1} (thin film) 2949, 1732. Failed to ionise under high resolution mass spectrometry conditions.

Methyl 3-methoxy-3-(4-methoxyphenyl)cyclobutanecarboxylate 3.3.39

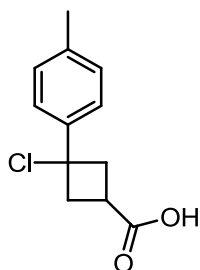
To 3-hydroxy-3-(4-methoxyphenyl)cyclobutanecarboxylic acid (**3.3.21**) (750 mg, 3.37 mmol) in PhMe (7 mL) was added conc. HCl_(aq) (4 mL, 48.7 mmol) which was then sonicated for 16 h. The reaction was then sonicated for a further 3 h. The layers were separated and the aqueous layer was extracted with PhMe (2 × 5 mL). The organics were combined and evaporated under reduced pressure to give a brown oil. MeOH (4 mL) and HCl (3M in MeOH) (4 mL, 12.00 mmol) were added and this was stirred for 6 h. CH₂Cl₂ (10 mL) and water (10 mL) were added and the layers were separated. The aqueous layer was extracted with CH₂Cl₂ (2 × 10 mL). The organic layers were combined, filtered through a hydrophobic frit and evaporated under reduced pressure to give a crude product. This was purified using column chromatography eluting with 8:2 petroleum ether: EtOAc. Fractions collected were evaporated under reduced pressure to give methyl 3-methoxy-3-(4-methoxyphenyl)cyclobutanecarboxylate (200 mg, 0.799 mmol, 24%). (~1.5:1 mixture of diastereomers)

¹H NMR (400 MHz, CDCl₃) δ = 7.41 – 7.36 (m, 1.2H), 7.26 – 7.22 (m, 0.8H), 6.96 – 6.88 (m, 2H), 3.85 (s, 1.8H, Isomer 1), 3.83 (s, 1.2H, Isomer 2), 3.73 (s, 1.8H, Isomer 1), 3.68 (s, 1.2H, Isomer 2), 3.41 – 3.31 (m, 0.4H), 2.98 (s, 1.2H, Isomer 2), 2.93 (s, 1.8H, Isomer 1), 2.80 – 2.60 (m, 4.6H).

3-Chloro-3-(3-methoxyphenyl)cyclobutanecarboxylic acid 3.3.42

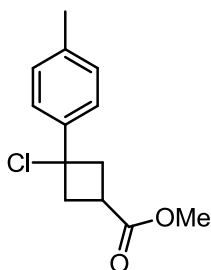
3-Hydroxy-3-(3-methoxyphenyl)cyclobutanecarboxylic acid (5.73 g, 25.8 mmol) was dissolved in PhMe (100 mL) and conc HCl_(aq) (37.5%, 40 mL, 494 mmol) was added. This was sonicated for 3 h. The layers were separated and the aqueous layer was extracted with PhMe (3 × 30 mL). The combined organics were filtered through a hydrophobic frit and the solvent evaporated under reduced pressure. Acetonitrile (50 mL) and cyclohexane (50 mL) were then added and the layers separated. The acetonitrile layer was evaporated under reduced pressure to give 3-chloro-3-(3-methoxyphenyl)cyclobutanecarboxylic acid (6.132 g, 25.5 mmol, 99%) as a dark orange oil. (~ 2:1 mixture of diastereomers)

¹H NMR (400 MHz, CDCl₃) δ = 7.33 – 7.24 (m, 1H), 7.06 (ddd, J = 0.7, 1.8, 7.8 Hz, 0.3H), 7.03 (t, J = 2.2 Hz, 0.3H), 6.97 – 6.90 (m, 0.7H), 6.89 – 6.80 (m, 1.7H), 3.82 (s, 1H, Isomer 1), 3.81 (s, 2H, Isomer 2), 3.75 – 3.68 (m, 0.7H), 3.25 – 3.12 (m, 1.2H), 3.11 – 2.95 (m, 2.8H), 2.94 – 2.85 (m, 0.3H) (1H not observed, exchangeable); ¹³C NMR (101 MHz, CDCl₃) 180.0, 179.7, 159.8, 159.7, 146.2, 144.8, 129.70, 129.66, 118.0, 117.2, 113.44, 113.37, 112.1, 110.9, 68.1, 64.3, 55.32, 55.29, 42.4, 41.6, 32.6, 31.9; $\nu_{\max}/\text{cm}^{-1}$ (thin film) 3003 br, 2944 1702. Failed to ionise under high resolution mass spectrometry conditions.

3-Chloro-3-(*p*-tolyl)cyclobutanecarboxylic acid 3.3.45

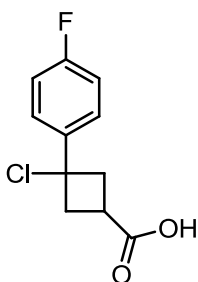
To 3-hydroxy-3-(*p*-tolyl)cyclobutanecarboxylic acid (5.443 g, 26.4 mmol) in PhMe (150 mL) was added conc HCl_(aq) (37.5%, 50 mL, 617 mmol). This was sonicated for 5 h. The layers were separated and the aqueous layer was extracted with PhMe (3 × 50 mL). The organic layers were combined, filtered through a hydrophobic frit and evaporated under reduced pressure to give 3-chloro-3-(*p*-tolyl)cyclobutanecarboxylic acid (5.38 g, 23.94 mmol, 91%) as an off white solid. (~ 2:1 mixture of diastereomers)

M.p. 134 – 136 °C; ¹H NMR (400 MHz, CDCl₃) δ = 7.42 – 7.38 (m, 0.5H), 7.28 – 7.13 (m, 3.5H), 3.78 – 3.67 (m, 0.7H, Isomer 1), 3.26 – 3.14 (m, 1.2H), 3.10 – 2.97 (m, 2.8H), 2.94 – 2.84 (m, 0.3H, Isomer 2), 2.36 (s, 1H, Isomer 2), 2.35 (s, 2H, Isomer 1) (1H not observed, exchangeable); ¹³C NMR (101 MHz, CDCl₃) 179.9, 179.5, 142.0, 140.3, 138.1, 137.9, 129.34, 129.26, 125.8, 124.9, 68.4, 64.3, 42.5, 41.7, 32.7, 31.8, 21.14, 21.09; ν_{max}/cm⁻¹ (thin film) 2999 br, 2914, 1705. Failed to ionise under high resolution mass spectrometry conditions.

Methyl 3-chloro-3-(*p*-tolyl)cyclobutanecarboxylate 3.3.46

To 3-chloro-3-(*p*-tolyl)cyclobutanecarboxylic acid (502 mg, 2.234 mmol) and Et₃N (0.374 mL, 2.68 mmol) in CH₂Cl₂ (5 mL) was added SOCl₂ (0.196 mL, 2.68 mmol). This was stirred at ambient temperature for 3 h then MeOH (0.090 mL, 2.234 mmol) was added. This was stirred for a further 2 h then left overnight. The solvent was evaporated under reduced pressure. CH₂Cl₂ (5 mL) was then added and this was again evaporated under reduced pressure. This was repeated a further 4 times to give a crude product. To this was added CH₂Cl₂ (10 mL) and water (5 mL). The layers were separated and the aqueous layer was extracted with CH₂Cl₂ (5 mL). The organic layers were combined and evaporated under reduced pressure. This crude product was then purified using column chromatography eluting with a gradient of 0-20 cyclohexane: EtOAc. Collected fractions were evaporated under reduced pressure to give methyl 3-chloro-3-(*p*-tolyl)cyclobutanecarboxylate (182 mg, 0.766 mmol, 34%) as an orange semi solid. (~ 1.5:1 mixture of diastereomers)

¹H NMR (400 MHz, CDCl₃) δ = 7.41 – 7.37 (m, 1H), 7.32 – 7.29 (m, 1H), 7.22 – 7.14 (m, 2H), 3.72 (s, 1.8H, Isomer 1), 3.67 (s, 1.2H, Isomer 2), 3.55 – 3.41 (m, 0.5H), 2.92 – 2.73 (m, 2.5H), 2.67 – 2.49 (m, 2H), 2.35 (s, 1.8H, Isomer 1), 2.34 (s, 1.2H, Isomer 2); ¹³C NMR (101 MHz, CDCl₃) 176.5, 175.7, 143.0, 141.8, 137.3, 137.2, 129.2, 129.1, 125.0, 124.6, 77.2, 75.0, 73.3, 52.1, 51.8, 40.7, 39.5, 31.7, 29.6, 21.0; $\nu_{\max}/\text{cm}^{-1}$ (thin film) 2949 br, 2995, 1702, 1607.

3-Chloro-3-(4-fluorophenyl)cyclobutanecarboxylic acid 3.3.52

To 3-(4-fluorophenyl)-3-hydroxycyclobutanecarboxylic acid (3 g, 14.27 mmol) in PhMe (60 mL) was added HCl_(aq) (37.5%, 25 mL, 309 mmol). This was sonicated for 3 h. PhMe (50 mL) was added and the layers were separated. The aqueous layer was extracted with PhMe (3 × 20 mL). The organics were then combined, filtered through a hydrophobic frit and then evaporated under reduced pressure to give 3-chloro-3-(4-fluorophenyl)cyclobutanecarboxylic acid (3.25 g, 14.21 mmol, 100%) as an off white solid. (~ 1:1 mixture of diastereomers)

M.p. 87 – 89 °C; ¹H NMR (400 MHz, CDCl₃) δ = 7.52 – 7.44 (m, 1H), 7.36 – 7.29 (m, 1H), 7.12 – 7.00 (m, 2H), 3.73 (quin, *J* = 8.8 Hz, 0.5H), 3.22 – 3.17 (m, 2H), 3.11 – 2.97 (m, 2H), 2.97 – 2.85 (m, 0.5H) (1H not observed, exchangeable); ¹³C NMR (101 MHz, CDCl₃) 179.8, 179.4, 162.3 (d, ¹*J*_{C-F} = 248.7 Hz), 162.2 (d, ¹*J*_{C-F} = 248.0 Hz), 140.7 (d, ⁴*J*_{C-F} = 3.7 Hz), 139.2 (d, ⁴*J*_{C-F} = 2.9 Hz), 127.8 (d, ³*J*_{C-F} = 8.8 Hz), 127.0 (d, ³*J*_{C-F} = 8.8 Hz), 115.59 (d, ²*J*_{C-F} = 22.0 Hz), 115.55 (d, ²*J*_{C-F} = 22.0 Hz), 67.6, 63.8, 42.5, 41.8, 32.6, 31.7; ν_{max}/cm⁻¹ (thin film) 2995 br, 2937, 1698. Failed to ionise under high resolution mass spectrometry conditions.

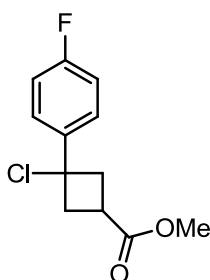
Methyl 3-chloro-3-(4-fluorophenyl)cyclobutanecarboxylate 3.3.53 and methyl 3-(4-fluorophenyl)-3-methoxycyclobutanecarboxylate 3.3.54

To 3-chloro-3-(4-fluorophenyl)cyclobutanecarboxylic acid (100 mg, 0.437 mmol) in MeOH (1 mL) was added HCl (0.1 mL, 0.300 mmol). This was stirred for 2 h. The solvent was then evaporated under reduced pressure to give a crude product. This was purified using column chromatography eluting with 0-20 gradient of

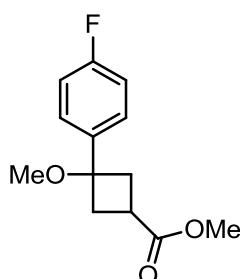
cyclohexane:Et₂O. Fraction 1 collected was evaporated under reduced pressure to give methyl 3-chloro-3-(4-fluorophenyl)cyclobutanecarboxylate (20 mg, 0.083 mmol, 19%) as a colourless oil. (~2:1 mixture of diastereomers)

Fraction 2 collected was evaporated under reduced pressure to give methyl 3-(4-fluorophenyl)-3-methoxycyclobutanecarboxylate (25 mg, 0.105 mmol, 24%) as an orange semi solid. (~ 1:1 mixture of diastereomers)

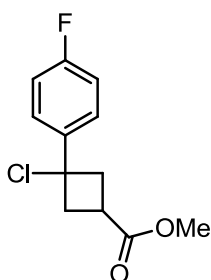
Methyl 3-chloro-3-(4-fluorophenyl)cyclobutanecarboxylate 3.3.53



¹H NMR (400 MHz, CDCl₃) δ = 7.53 – 7.47 (m, 0.6H), 7.37 – 7.30 (m, 1.4H), 7.12 – 7.01 (m, 2H), 3.72 – 3.65 (m, 3.7H), 3.21 – 3.16 (m, 1H), 3.10 – 2.96 (m, 3H), 2.92 – 2.81 (m, 0.3H, Isomer 2); ¹³C NMR (101 MHz, CDCl₃) 174.3, 173.8, 162.24 (d, ¹J_{C-F} = 248.0 Hz), 162.17 (d, ¹J_{C-F} = 247.2 Hz), 140.9 (d, ⁴J_{C-F} = 3.7 Hz), 139.4 (d, ⁴J_{C-F} = 2.9 Hz), 127.9 (d, ³J_{C-F} = 8.8 Hz), 127.0 (d, ³J_{C-F} = 8.8 Hz), 115.53 (d, ²J_{C-F} = 21.2 Hz), 115.48 (d, ²J_{C-F} = 22.0 Hz), 67.9, 63.9, 52.1, 52.0, 42.7, 41.9, 32.6, 31.8; $\nu_{\max}/\text{cm}^{-1}$ (thin film) 2997 br, 2952, 1702. Failed to ionise under high resolution mass spectrometry conditions.

Methyl 3-(4-fluorophenyl)-3-methoxycyclobutanecarboxylate 3.3.54

^1H NMR (400 MHz, CDCl_3) δ = 7.44 – 7.39 (m, 1H), 7.30 – 7.25 (m, 1H), 7.11 – 7.00 (m, 2H), 3.71 (s, 1.5H, Isomer 1) 3.66 (s, 1.5H, Isomer 2), 3.40 – 3.29 (m, 0.5H), 2.96 (s, 1.5H, Isomer 2), 2.92 (s, 1.5H, Isomer 1) 2.79 – 2.68 (m, 0.5H), 2.68 – 2.60 (m, 4H); ^{13}C NMR (101 MHz, CDCl_3) 175.5, 174.9, 162.2 (d, $^1J_{\text{C-F}}$ = 246.5 Hz), 162.1 (d, $^1J_{\text{C-F}}$ = 246.5 Hz), 138.3 (d, $^4J_{\text{C-F}}$ = 2.9 Hz), 137.6 (d, $^4J_{\text{C-F}}$ = 2.9 Hz), 128.1 (d, $^3J_{\text{C-F}}$ = 8.1 Hz), 127.8 (d, $^3J_{\text{C-F}}$ = 8.1 Hz), 115.3 (d, $^2J_{\text{C-F}}$ = 21.2 Hz), 115.2 (d, $^2J_{\text{C-F}}$ = 22.0 Hz), 79.4, 77.0, 51.9, 51.8, 50.8, 50.3, 36.8, 35.1, 31.9, 29.1; ^{19}F NMR (376 MHz, CDCl_3) δ = -114.9 (s, 1F), -115.0 (s, 1F); $\nu_{\text{max}}/\text{cm}^{-1}$ (thin film) 2994, 2950, 1732. Failed to ionise under high resolution mass spectrometry conditions.

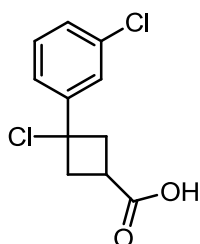
Methyl 3-chloro-3-(4-fluorophenyl)cyclobutanecarboxylate 3.3.53

To 3-chloro-3-(4-fluorophenyl)cyclobutanecarboxylic acid (482 mg, 2.108 mmol) and Et_3N (0.353 mL, 2.53 mmol) in CH_2Cl_2 (5 mL) was added SOCl_2 (0.185 mL, 2.53 mmol). The reaction mixture was stirred at ambient temperature for 3 h then MeOH (0.085 mL, 2.108 mmol) was added and stirred for a further 2 h. The reaction mixture was left unstirred for 16 h. The solvent was removed under reduced pressure

and then CH_2Cl_2 (5 mL) was added. This was also evaporated under reduced pressure and this was repeated a further 5 times. Water (5 mL) and CH_2Cl_2 (10 mL) was then added to the crude mixture and the layers were separated. The aqueous layer was extracted with CH_2Cl_2 (5 mL). The organics were then combined, filtered through a hydrophobic frit and evaporated under reduced pressure to give a crude product. This was purified using column chromatography eluting with a gradient of 0-20 cyclohexane: EtOAc. Fractions collected were evaporated under reduced pressure to give methyl 3-chloro-3-(4-fluorophenyl)cyclobutanecarboxylate (135 mg, 0.558 mmol, 26%) as an orange semi solid. (~2:1 mixture of diastereomers)

Data consistent with previous isolation.

3-Chloro-3-(3-chlorophenyl)cyclobutanecarboxylic acid 3.3.55

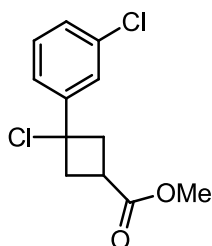


To 3-(3-chlorophenyl)-3-hydroxycyclobutanecarboxylic acid (3 g, 13.24 mmol) in PhMe (60 mL) was added $\text{HCl}_{(\text{aq})}$ (37.5%, 25 mL, 309 mmol). This was sonicated for 3 h. To the reaction mixture was added PhMe (50 mL). The layers were then separated and the aqueous layer was extracted with PhMe (3×20 mL). The organic layers were combined, filtered through a hydrophobic frit and evaporated under reduced pressure to give 3-chloro-3-(3-chlorophenyl)cyclobutanecarboxylic acid (3.26 g, 13.30 mmol, 100%) as an off white solid. (~2:1 mixture of diastereomers)

M.p. 75 – 77 °C; ^1H NMR (400 MHz, CDCl_3) δ = 7.52 – 7.18 (m, 4H), 3.79 – 3.67 (m, 0.7H, Isomer 1), 3.22 – 3.16 (m, 1.4H, Isomer 2), 3.10 – 2.97 (m, 2.6H, Isomer 1), 2.97 – 2.87 (m, 0.3H, Isomer 2) (1H not observed, exchangeable); ^{13}C NMR (101 MHz, CDCl_3) 180.0, 179.6, 146.5, 145.3, 134.7, 134.5, 130.00, 129.98, 128.4, 128.2, 126.3, 125.5, 124.0, 123.2 67.0, 63.6, 42.3, 41.5, 32.6, 31.8; $\nu_{\text{max}}/\text{cm}^{-1}$ (thin

film) 2940 br, 2755, 1693. Failed to ionise under high resolution mass spectrometry conditions.

Methyl 3-chloro-3-(3-chlorophenyl)cyclobutanecarboxylate 3.3.56



Method A:

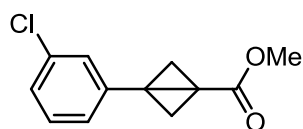
To 3-chloro-3-(3-chlorophenyl)cyclobutanecarboxylic acid (2.5 g, 10.20 mmol) in MeOH (10 mL) was added HCl (3.40 mL, 10.20 mmol). This was stirred at ambient temperature for 2 h. The solvent was then evaporated under reduced pressure to give methyl 3-chloro-3-(3-chlorophenyl)cyclobutanecarboxylate (2.597 g, 10.02 mmol, 98%) as an orange solid.

Method B:

To 3-chloro-3-(3-chlorophenyl)cyclobutanecarboxylic acid (130 mg, 0.530 mmol) in CH₂Cl₂ (2 mL) was added DIPEA (0.111 mL, 0.636 mmol) and SOCl₂ (0.046 mL, 0.636 mmol). The reaction mixture was stirred at ambient temperature for 4 h then MeOH (0.021 mL, 0.530 mmol) was added. This was stirred for a further 3 h. The solvent was then evaporated under reduced pressure. CH₂Cl₂ (5 mL) was added and then evaporated under reduced pressure. This was repeated a further 4 times. To the crude mixture was added water (5 mL) and CH₂Cl₂ (5 mL). The layers were separated and the aqueous layer was extracted with CH₂Cl₂ (3 × 2 mL). The combined organics were filtered through a hydrophobic frit and evaporated under reduced pressure to give methyl 3-chloro-3-(3-chlorophenyl)cyclobutanecarboxylate (116 mg, 0.448 mmol, 84%) as a black semi-solid. (~2:1 mixture of diastereomers)

M.p. 53 – 55 °C; LCMS (Method B, UV, ESI) $R_t = 1.28$ and 1.30 $[M-H]^-$ = No mass ion, 34 and 58%; 1H NMR (400 MHz, $CDCl_3$) $\delta = 7.50 - 7.19$ (m, 4H), 3.75 – 3.64 (m, 3.7H), 3.18 – 3.13 (m, 1.2H, Isomer 2), 3.06 – 2.93 (m, 2.8H, Isomer 1), 2.92 – 2.81 (m, 0.3H, Isomer 2); ^{13}C NMR (101 MHz, $CDCl_3$) 174.2, 173.7, 146.7, 145.5, 134.6, 134.5, 130.0, 129.9, 128.3, 128.2, 126.3, 125.5, 124.1, 123.2, 67.3, 63.6, 52.2, 52.0, 42.4, 41.6, 32.6, 31.8; ν_{max}/cm^{-1} (thin film) 3005, 2953, 1729. Failed to ionise under high resolution mass spectrometry conditions.

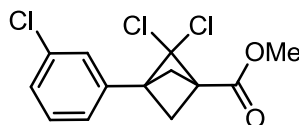
Methyl 3-(3-chlorophenyl)bicyclo[1.1.0]butane-1-carboxylate 3.3.57



To sodium hydride (0.730 g, 18.25 mmol) was added methyl 3-chloro-3-(3-chlorophenyl)cyclobutanecarboxylate (4.3 g, 16.59 mmol) in THF (80 mL). This was stirred for 16 h at ambient temperature.

EtOAc (50 mL) and water (50 mL) were added and the layers were separated. The organic layer was evaporated under reduced pressure to give 3.8 g crude material. EtOAc (50 mL) was added and this was washed with sat. $NaHCO_{3(aq)}$ (50 mL). The organic layer was filtered through a hydrophobic frit and evaporated under reduced pressure to give methyl 3-(3-chlorophenyl)bicyclo[1.1.0]butane-1-carboxylate (3.337 g, 14.99 mmol, 90%) as a yellow solid.

M.p. 49 – 51 °C; LCMS (Method B, UV, ESI) $R_t = 1.18$ $[M-H]^-$ = No mass ion, 92%; 1H NMR (400 MHz, $CDCl_3$): $\delta = 7.29 - 7.25$ (m, 1H), 7.23 – 7.20 (m, 2H), 7.18 – 7.13 (m, 1H), 3.52 (s, 3H), 2.89 (t, $J = 1.2$ Hz, 2H), 1.61 (t, $J = 1.2$ Hz, 2H); ^{13}C NMR (101 MHz, $CDCl_3$) 169.6, 136.1, 134.5, 129.7, 127.1, 126.2, 124.0, 51.9, 35.8, 31.8, 23.8; ν_{max}/cm^{-1} (thin film) 2954, 1709; HRMS: Calculated for $C_{12}H_{12}ClO_2$ 223.0526 Found $[M+H]^+$: 223.0532 (2.7 ppm).

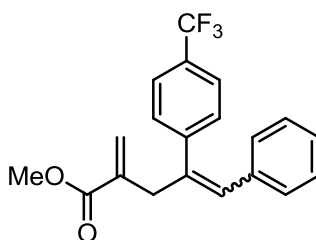
Methyl 2,2-dichloro-3-(3-chlorophenyl)bicyclo[1.1.1]pentane-1-carboxylate
3.3.58

Methyl 3-(3-chlorophenyl)bicyclo[1.1.0]butane-1-carboxylate (3 g, 13.47 mmol) was dissolved in diethylene glycol dimethyl ether (9 mL) and tetrachloroethylene (13 mL) and the reaction was heated to 120 °C. Sodium 2,2,2-trichloroacetate (12.49 g, 67.4 mmol) was added over 30 mins and the reaction was stirred at 140 °C for another 30 mins. Water (50 mL) and CH₂Cl₂ (100 mL) were added and the layers were separated. The organic layer was washed with 5% LiCl (8 × 50 mL). The organic layer was filtered through a hydrophobic frit and the solvent was removed under reduced pressure. Added CH₂Cl₂ (100 mL) and washed organics with 5% LiCl (5 × 50 mL). The organic layer was then filtered through a hydrophobic frit and evaporated under reduced pressure to give a crude product. This was purified using column chromatography eluting with a gradient of 0-15 cyclohexane: EtOAc loading in a mixture of cyclohexane and CH₂Cl₂. The collected fractions showed impure product so this was re-purified using column chromatography eluting with a gradient of 0-10 cyclohexane:TBME. First eluting fraction was evaporated under reduced pressure to give 600 mg of impure product. Second eluting fraction was evaporated under reduced pressure to give methyl 2,2-dichloro-3-(3-chlorophenyl)bicyclo[1.1.1]pentane-1-carboxylate (935 mg). First eluting fraction was purified again using column chromatography eluting with a gradient of 0-10 cyclohexane:TBME. The collected fractions gave methyl 2,2-dichloro-3-(3-chlorophenyl)bicyclo[1.1.1]pentane-1-carboxylate (344 mg). The two product fractions were combined to give methyl 2,2-dichloro-3-(3-chlorophenyl)bicyclo[1.1.1]pentane-1-carboxylate (1.28 g, 4.210 mmol, 31%) as an orange oil.

LCMS (Method B, UV, ESI) R_t = 1.35 [M-H]⁻ = No mass ion, 74%; ¹H NMR (400 MHz, CDCl₃): δ = 7.38 – 7.29 (m, 3H), 7.28 – 7.23 (m, 1H), 3.83 (s, 3H), 3.08 (d, J = 0.7 Hz, 2H), 2.42 (d, J = 1.0 Hz, 2H); ¹³C NMR (101 MHz, CDCl₃) 165.5,

134.6, 134.0, 129.9, 128.9, 127.4, 125.4, 94.1, 56.9, 52.4, 52.3, 49.3; $\nu_{\max}/\text{cm}^{-1}$ (thin film) 3028, 2955, 1736. Failed to ionise under high resolution mass spectrometry conditions.

Methyl 2-methylene-5-phenyl-4-(4-(trifluoromethyl)phenyl)pent-4-enoate 3.4.2

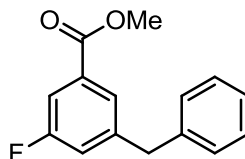


To palladium(II) acetate (37 mg, 0.164 mmol), RuPhos (153 mg, 0.328 mmol), methyl 2-chloro-3-(4-(trifluoromethyl)phenyl)bicyclo[1.1.1]pentane-1-carboxylate (50 mg, 0.164 mmol), phenylboronic acid (40.0 mg, 0.328 mmol) and potassium carbonate (68.0 mg, 0.492 mmol) was added PhMe (4 mL) and Water (0.4 mL) and this was heated in a sealed microwave vial at 110 °C for 16 h. The reaction mixture was filtered through Celite, washed with ethyl acetate (10 mL) and the solvent removed under reduced pressure. The crude material was purified using column chromatography eluting with 9:1 petroleum ether:EtOAc. Fractions containing product were evaporated under reduced pressure to give methyl 2-methylene-5-phenyl-4-(4-(trifluoromethyl)phenyl)pent-4-enoate (20 mg, 0.058 mmol, 35 % yield) as a yellow oil.

^1H NMR (400 MHz, CDCl_3) δ = 7.74 (s, 4H), 7.43 – 7.53 (m, 2H), 7.41 – 7.55 (m, 2H), 7.40 – 7.47 (m, 1H), 7.16 – 7.14 (m, 1H), 6.42 (d, J = 1.0 Hz, 1H), 5.66 – 5.74 (m, 1H), 3.93 (s, 3H), 3.91 (t, J = 1.6 Hz, 2H); ^{13}C NMR (101 MHz, CDCl_3) δ = 166.8, 145.0, 137.2, 136.4, 136.0, 132.3, 128.9 (q, $^2J_{\text{C-F}}$ = 32.0 Hz), 128.0, 127.9, 127.1, 126.0, 125.9, 125.0 (q, $^3J_{\text{C-F}}$ = 3.4 Hz), 51.6, 31.9 (1C not observed).

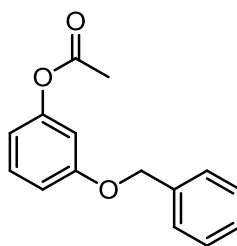
7.2 BET experimental

Methyl 3-benzyl-5-fluorobenzoate 5.1.6



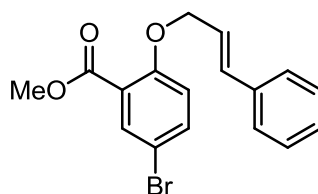
Palladium(II) acetate (0.095 g, 0.423 mmol), potassium benzyltrifluoroborate (1.12 g, 5.66 mmol), methyl 3-bromo-5-fluorobenzoate (0.95 g, 4.08 mmol), Cs₂CO₃ (4.16 g, 12.77 mmol) and cataCXium A (0.150 g, 0.418 mmol) were heated to 100 °C in THF (10 mL) and water (5 mL) for 6 h. To the reaction mixture was added EtOAc (100 mL) and water (50 mL). The layers were separated and the organic layer was washed with water (3 × 50 mL). The organic layer was filtered through hydrophobic frit and the solvent was evaporated under reduced pressure to give a crude product. This was purified using column chromatography eluting with 0-20 cyclohexane: EtOAc. The collected fractions were evaporated under reduced pressure to give a black liquid. This was dissolved in CH₂Cl₂ (50 mL) and activated charcoal (3 heaped spatulas) was added. This was stirred for 5 mins then filtered through Celite. The filtrate was evaporated under reduced pressure to give methyl 3-benzyl-5-fluorobenzoate (662 mg, 2.71 mmol, 67%) as a dark orange oil.

LCMS (Method A, UV, ESI) R_t = 1.24 [M+H]⁺ = 245.1, 100%; ¹H NMR (400 MHz, CDCl₃) δ = 7.71 – 7.69 (m, 1H), 7.57 – 7.52 (m, 1H), 7.33 – 7.27 (m, 2H), 7.25 – 7.20 (m, 1H), 7.19 – 7.15 (m, 2H), 7.05 (td, *J* = 2.0, 9.3 Hz, 1H), 4.01 (s, 2H), 3.90 (s, 3H); ¹³C NMR (101 MHz, CDCl₃) δ = 166.0 (d, ⁴*J*_{C-F} = 3.7 Hz), 162.7 (d, ¹*J*_{C-F} = 247.2 Hz), 144.0 (d, ³*J*_{C-F} = 7.3 Hz), 139.6, 132.2 (d, ³*J*_{C-F} = 8.1 Hz), 128.9, 128.7, 126.6, 125.8 (d, ⁴*J*_{C-F} = 2.9 Hz), 120.4 (d, ²*J*_{C-F} = 21.3 Hz), 114.3 (d, ²*J*_{C-F} = 22.7 Hz), 52.3, 41.5 (d, ⁴*J*_{C-F} = 1.5 Hz); ¹⁹F NMR (376 MHz, CDCl₃) δ = -121.7 (s, 1F); ν_{max}/cm⁻¹ (thin film) 3029, 2952, 1722; HRMS: Calculated for C₁₅H₁₄FO₂ 245.0978 Found [M+H]⁺: 245.0973 (- 2.0 ppm).

3-(Benzyloxy)phenyl acetate 5.1.8

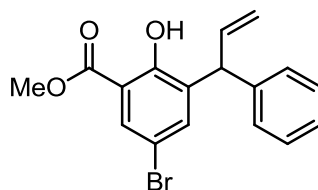
To potassium carbonate (200 mg, 1.446 mmol) and 3-hydroxyphenyl acetate (200 mg, 1.315 mmol) in DMF (1 mL) was added (bromomethyl)benzene (0.172 mL, 1.446 mmol) and this was heated to 100 °C for 16 h. Water (2 mL) and CH₂Cl₂ (4 mL) was added and the layers were separated. The organic layer was washed with 5% LiCl_(aq) (3 × 1 mL). The organic layer was then filtered through hydrophobic frit and evaporated under reduced pressure to give crude product. This was purified using column chromatography eluting with a gradient of 0-20 cyclohexane: EtOAc. Fractions collected contained impure product which was re-purified using column chromatography eluting with 0-10 cyclohexane:TBME. Fractions collected were evaporated under reduced pressure to give 3-(benzyloxy)phenyl acetate (41 mg, 0.169 mmol, 13%) as a white solid.

M.p. 87 – 89 °C; LCMS (Method B, UV, ESI) R_t = 1.21 [M+H]⁺ = 243.07, 94%; ¹H NMR (400 MHz, CDCl₃) δ = 7.45 – 7.26 (m, 6H), 6.85 (ddd, *J* = 0.7, 2.4, 8.3 Hz, 1H), 6.73 (t, *J* = 2.3 Hz, 1H), 6.72 – 6.69 (m, 1H), 5.04 (s, 2H), 2.28 (s, 3H); ¹³C NMR (101 MHz, CDCl₃) δ = 169.3, 159.7, 151.6, 136.6, 129.8, 128.6, 128.1, 127.5, 114.1, 112.5, 108.6, 70.2, 21.1; ν_{max}/cm⁻¹ (thin film) 3036, 2939, 1760. Failed to ionise under high resolution mass spectrometry conditions.

Methyl 5-bromo-2-(cinnamyloxy)benzoate 5.1.18

Methyl 5-bromo-2-hydroxybenzoate (11.88 g, 51.4 mmol), potassium carbonate (14.3 g, 103 mmol), potassium iodide (1.7 g, 10.24 mmol) and (*E*)-(3-chloroprop-1-en-1-yl)benzene (6 mL, 62.3 mmol) were heated under reflux in Acetone (110 mL) for 3 d. 2M HCl_(aq) (100 mL) was added portionwise (gas evolution) and then EtOAc (100 mL) was added. The layers were separated and the aqueous layer was extracted with EtOAc (3 × 50 mL). The combined organic layers were filtered through a hydrophobic frit and the solvent was then evaporated under reduced pressure to give a brown oil. MeOH (20 mL) was added and solid immediately precipitated. This was transferred to a pestle and mortar and the solid was ground up with further MeOH (50 mL). The solid was filtered off and washed with MeOH (50 mL) to give methyl 5-bromo-2-(cinnamyloxy)benzoate (12.012 g, 34.6 mmol, 67%) as a white solid.

M.p. 98 – 100 °C; LCMS (Method B, UV, ESI) $R_t = 1.41$ $[M-H]^- =$ No mass ion, 100%; 1H NMR (400 MHz, DMSO- d_6) $\delta = 7.79$ (d, $J = 2.7$ Hz, 1H), 7.70 (dd, $J = 2.7, 8.8$ Hz, 1H), 7.49 – 7.44 (m, 2H), 7.38 – 7.32 (m, 2H), 7.30 – 7.24 (m, 1H), 7.20 (d, $J = 8.8$ Hz, 1H), 6.84 – 6.77 (m, 1H), 6.47 (td, $J = 5.4, 16.1$ Hz, 1H), 4.81 (dd, $J = 1.5, 5.4$ Hz, 2H), 3.83 (s, 3H); ^{13}C NMR (101 MHz, DMSO- d_6) $\delta = 164.8, 156.3, 136.0, 135.7, 132.8, 132.1, 128.6, 127.8, 126.4, 124.2, 122.4, 116.5, 111.4, 69.0, 52.2$; ν_{max}/cm^{-1} (thin film) 3030, 2947, 1696. Failed to ionise under high resolution mass spectrometry conditions.

***rac*-Methyl 5-bromo-2-hydroxy-3-(1-phenylallyl)benzoate 5.1.16**

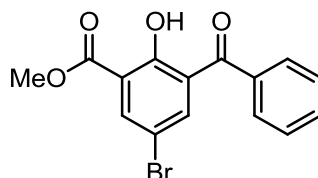
Methyl 5-bromo-2-(cinnamyloxy)benzoate (11.8 g, 34.0 mmol) was dissolved in *N,N*-dimethylaniline (100 mL) and heated at 200 °C for 20 h. The reaction mixture was allowed to cool and then Et₂O (100 mL) and cold HCl_(aq) (20% w/w, 100 mL) was added. The mixture was stirred vigorously. The layers were then separated and the aqueous layer was extracted with Et₂O (3 × 50 mL). The organics were combined, filtered through a hydrophobic frit and evaporated under reduced pressure to give a crude product. This was purified using column chromatography eluting with a gradient of 0-30 cyclohexane: EtOAc. Fractions collected contained impure product. This was re-purified using column chromatography eluting with a gradient of 0-20 cyclohexane: EtOAc. Fractions collected were evaporated under reduced pressure to give a product containing *N,N*-dimethylaniline. To this mixture was added HCl_(aq) (25%, 50 mL) and Et₂O (80 mL). The layers were separated and the aqueous layer was extracted with Et₂O (50 mL). The combined organic layers were filtered through a hydrophobic frit and evaporated under reduced pressure to give *rac*-methyl 5-bromo-2-hydroxy-3-(1-phenylallyl)benzoate (7.6 g, 21.89 mmol, 64%) as a grey liquid.

A sample (100 mg) was taken and purified using HpH MDAP (Method E) to give methyl 5-bromo-2-hydroxy-3-(1-phenylallyl)benzoate (46 mg) as a colourless oil.

LCMS (Method B, UV, ESI) R_t = 1.56 [M-H]⁻ = 345.0, 347.0, 100%; ¹H NMR (400 MHz, CDCl₃) δ = 11.05 (s, 1H), 7.87 (d, *J* = 2.4 Hz, 1H), 7.41 (d, *J* = 2.4 Hz, 1H), 7.33 – 7.26 (m, 2H), 7.24 – 7.16 (m, 3H), 6.29 – 6.20 (m, 1H), 5.26 (td, *J* = 1.3, 10.3 Hz, 1H), 5.17 (d, *J* = 6.6 Hz, 1H), 4.95 (td, *J* = 1.5, 17.1 Hz, 1H) 3.92 (s, 3H); ¹³C NMR (101 MHz, CDCl₃) δ = 169.8, 158.3, 141.5, 139.0, 137.8, 134.3, 130.5, 128.5, 128.4, 126.6, 117.1, 113.6, 110.7, 52.6, 47.1; ν_{max}/cm⁻¹ (thin film) 3085 br,

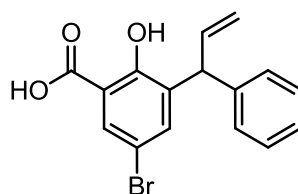
3027, 2953, 1674. Failed to ionise under high resolution mass spectrometry conditions.

Methyl 3-benzoyl-5-bromo-2-hydroxybenzoate 5.1.21



To ruthenium(III) chloride (8 mg, 0.039 mmol) and sodium periodate (252 mg, 1.178 mmol) was added methyl 5-bromo-2-hydroxy-3-(1-phenylallyl)benzoate (101 mg, 0.291 mmol) in MeCN (1 mL), EtOAc (1 mL) and Water (0.3 mL). This was stirred for 4 h at ambient temperature. To the reaction mixture was added sat. $\text{Na}_2\text{SO}_{3(\text{aq})}$ (10 mL) and EtOAc (10 mL). The layers were separated and the aqueous layer was extracted with EtOAc (3 x 20 mL). The organics were combined, filtered through a hydrophobic frit and evaporated under reduced pressure to give a crude product. This was purified using column chromatography eluting with a gradient of 0-30 cyclohexane:EtOAc. Collected fractions were evaporated under reduced pressure to give methyl 3-benzoyl-5-bromo-2-hydroxybenzoate (9 mg, 0.027 mmol, 9%) as a yellow solid.

M.p. 113 – 115 °C; LCMS (Method B, UV, ESI) $R_t = 1.27$ $[\text{M}+\text{H}]^+ = 334.9, 336.9, 94\%$; ^1H NMR (400 MHz, CDCl_3) $\delta = 11.19$ (s, 1H), 8.13 (d, $J = 2.7$ Hz, 1H), 7.84 – 7.79 (m, 2H), 7.71 (d, $J = 2.7$ Hz, 1H), 7.63 – 7.56 (m, 1H), 7.49 – 7.44 (m, 2H), 3.98 (s, 3H); ^{13}C NMR (101 MHz, CDCl_3) $\delta = 194.0, 168.8, 158.5, 138.3, 136.9, 135.1, 133.5, 129.9, 129.7, 128.5, 115.1, 110.7, 52.9$; $\nu_{\text{max}}/\text{cm}^{-1}$ (thin film) 3056 br, 2957, 1676, 1660; HRMS: Calculated for $\text{C}_{15}\text{H}_{12}\text{BrO}_4$ 334.9919 Found $[\text{M}+\text{H}]^+$: 334.9915 (– 1.2 ppm).

***rac*-5-Bromo-2-hydroxy-3-(1-phenylallyl)benzoic acid 5.1.22**

To methyl 5-bromo-2-hydroxy-3-(1-phenylallyl)benzoate (100 mg, 0.288 mmol) was added AD mix beta (700 mg, 0.288 mmol) in water (2 mL) and *tert*-Butanol (2 mL). This was stirred at 80 °C for 32 h. Water (10 mL) and EtOAc (10 mL) were added. The layers were separated and the aqueous layer was extracted with EtOAc (3 × 20 mL). The combined organics were filtered through a hydrophobic frit and then the solvent was evaporated under reduced pressure to give a crude product. This was purified using column chromatography eluting with a gradient of 0-50 cyclohexane: EtOAc with an EtOAc:MeOH 80:20 flush. Collected fractions were combined and evaporated under reduced pressure to give *rac*-5-bromo-2-hydroxy-3-(1-phenylallyl)benzoic acid (25 mg, 0.075 mmol, 26%) as a brown semi solid.

LCMS (Method B, UV, ESI) $R_t = 0.90$ $[M-H]^- = 331.0, 333.0, 100\%$; 1H NMR (400 MHz, DMSO- d_6) $\delta = 7.72$ (d, $J = 2.7$ Hz, 1H), 7.33 – 7.25 (m, 2H), 7.22 – 7.13 (m, 4H), 6.36 (ddd, $J = 17.2, 10.0, 7.4$ Hz, 1H), 5.16 (ddd, $J = 10.1, 1.9, 1.1$ Hz, 1H), 5.04 (d, $J = 7.4$ Hz, 1H), 4.94 (dt, $J = 17.0, 1.6$ Hz, 1H) (2H not observed, exchangeable); ^{13}C NMR (101 MHz, DMSO- d_6) $\delta = 170.4, 159.6, 142.6, 140.0, 133.2, 133.0, 130.3, 128.2, 128.1, 126.1, 120.6, 116.0, 107.0, 47.0$; ν_{max}/cm^{-1} (thin film) 3382 br, 3082, 1631.

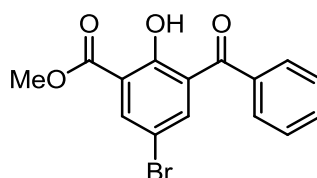
Methyl 5-bromo-2-hydroxy-3-(2-oxo-1-phenylethyl)benzoate 5.1.19 and *rac*-methyl 3-benzoyl-5-bromo-2-hydroxybenzoate 5.1.21

A solution of methyl 5-bromo-2-hydroxy-3-(1-phenylallyl)benzoate (1.5 g, 4.32 mmol) in acetone (15 mL) and water (15 mL) was treated with sodium periodate (3.70 g, 17.28 mmol) then osmium tetroxide (2 mL, 0.255 mmol) and was stirred at ambient temperature for 6 h. Sat. $Na_2SO_{3(aq)}$ (20 mL) and EtOAc (20 mL) was

added. The solid osmium residues were then filtered off. The layers were separated and the aqueous layer was extracted with EtOAc (3×20 mL). The organics were then combined, filtered through a hydrophobic frit and evaporated under reduced pressure to give a crude product. This was purified using column chromatography eluting with a gradient of 0-30 cyclohexane: EtOAc. First fraction collected was evaporated under reduced pressure to give methyl 3-benzoyl-5-bromo-2-hydroxybenzoate (151 mg, 0.452 mmol, 10%) as a yellow solid.

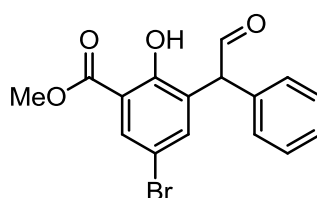
Second fraction collected was evaporated under reduced pressure to give *rac*-methyl 5-bromo-2-hydroxy-3-(2-oxo-1-phenylethyl)benzoate (438 mg, 1.259 mmol, 29%) as an off white solid.

Methyl 3-benzoyl-5-bromo-2-hydroxybenzoate 5.1.21

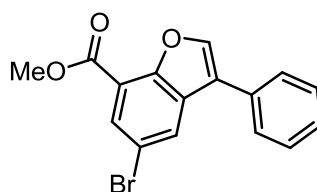


LCMS (Method B, UV, ESI) $R_t = 1.26$ $[M-H]^- = 333.0, 335.0, 100\%$, data consistent with previous isolation.

rac-Methyl 5-bromo-2-hydroxy-3-(2-oxo-1-phenylethyl)benzoate 5.1.19



M.p. 130 – 132 °C; LCMS (Method B, UV, ESI) $R_t = 1.21$ $[M-H]^- = 347.0, 349.0, 95\%$; 1H NMR (400 MHz, $CDCl_3$) $\delta = 11.19$ (s, 1H), 9.94 (d, $J = 1.0$ Hz, 1H), 7.98 – 7.90 (m, 1H), 7.44 – 7.23 (m, 6H), 5.25 (s, 1H), 3.95 (s, 3H); ^{13}C NMR (101 MHz, $CDCl_3$) $\delta = 197.6, 169.7, 158.2, 138.6, 134.4, 131.6, 129.6, 129.2, 128.5, 128.0, 113.8, 110.9, 57.7, 52.8$; ν_{max}/cm^{-1} (thin film) 3453, 2953, 1718, 1675; HRMS: Calculated for $C_{16}H_{14}BrO_4$ 349.0075 Found $[M+H]^+$: 349.0063 (– 3.4 ppm).

Methyl 5-bromo-3-phenylbenzofuran-7-carboxylate 5.1.23

Methyl 5-bromo-2-hydroxy-3-(2-oxo-1-phenylethyl)benzoate (400 mg, 1.146 mmol) and *p*-TsOH (218 mg, 1.146 mmol) were dissolved in PhMe (10 mL) and this was heated under reflux for 4 h. The reaction mixture was cooled to ambient temperature and EtOAc (15 mL) and sat. NaHCO_{3(aq)} (10 mL) was added. The layers were separated and the organic layer was filtered through a hydrophobic frit. The solvent was then evaporated under reduced pressure to give a crude product. This was purified using column chromatography eluting with a gradient of 0-20 cyclohexane: EtOAc. Collected fractions were evaporated under reduced pressure to give methyl 5-bromo-3-phenylbenzofuran-7-carboxylate (278 mg, 0.842 mmol, 73%) as an orange solid.

M.p. 118 – 120 °C; LCMS (Method B, UV, ESI) $R_t = 1.45$ [M+H]⁺ = No mass ion, 96%; ¹H NMR (400 MHz, CDCl₃) $\delta = 8.12 - 8.09$ (m, 2H), 7.88 (s, 1H), 7.58 – 7.54 (m, 2H), 7.52 – 7.46 (m, 2H), 7.43 – 7.38 (m, 1H), 4.03 (s, 3H); ¹³C NMR (101 MHz, CDCl₃) $\delta = 164.1, 152.9, 143.3, 130.5, 130.3, 129.7, 129.2, 128.1, 127.8, 127.7, 121.8, 116.6, 115.8, 52.5$; $\nu_{\max}/\text{cm}^{-1}$ (thin film) 3092, 2947, 1726; HRMS: Calculated for C₁₆H₁₂BrO₃ 330.9970 Found [M+H]⁺: 330.9966 (– 1.2 ppm).

Methyl 3-phenylbenzofuran-7-carboxylate 5.1.24

To Pd-C (96 mg, 0.045 mmol) was added methyl 5-bromo-3-phenylbenzofuran-7-carboxylate (153 mg, 0.462 mmol) in EtOAc (4 mL). This was stirred under an atmosphere of hydrogen for 7 d. The reaction mixture was filtered through Celite and the solvent was evaporated under reduced pressure. The crude product was transferred to COWare apparatus (400 mL):

Chamber 1 – Pd-C (400 mg), crude reaction mixture in EtOAc (8 mL)

Chamber 2 - Zinc (3.9 g), HCl_(aq) (14 mL, 25% w/v)

The reaction mixture was stirred for 16 h. It was then filtered through Celite and the solvent was evaporated under reduced pressure. The crude material was purified using column chromatography eluting with a gradient of 0-20 cyclohexane: EtOAc. Collected fractions were still impure so this was purified using HpH MDAP (Method D) to give methyl 3-phenylbenzofuran-7-carboxylate (20 mg, 0.079 mmol, 17%) as an orange solid.

LCMS (Method B, UV, ESI) $R_t = 1.29$ [M-H]⁻ = No mass ion, 96%; ¹H NMR (400 MHz, CDCl₃) $\delta = 8.02$ (d, $J = 7.8$ Hz, 2H), 7.90 (s, 1H), 7.64 – 7.60 (m, 2H), 7.51 – 7.46 (m, 2H), 7.42 – 7.36 (m, 2H), 4.03 (s, 3H); ¹³C NMR (101 MHz, CDCl₃) $\delta = 165.4, 154.1, 131.3, 129.0, 128.5, 128.3, 127.8, 127.7, 127.2, 125.4, 122.8, 122.2, 115.4, 52.2$; $\nu_{\max}/\text{cm}^{-1}$ (thin film) 3027, 1715; HRMS: Calculated for C₁₆H₁₃O₃ 253.0865 Found [M+H]⁺: 253.0864 (- 0.4 ppm).

***rac*-Methyl 3-phenyl-2,3-dihydrobenzofuran-7-carboxylate 5.1.9 and methyl 3-benzyl-2-hydroxybenzoate 5.1.25**

Methyl 5-bromo-3-phenylbenzofuran-7-carboxylate (250 mg, 0.755 mmol) was hydrogenated using COware apparatus (20 mL).

In chamber 1: methyl 5-bromo-3-phenylbenzofuran-7-carboxylate (250 mg, 0.755 mmol) in EtOAc (4 mL) was added to Pd-C (40.2 mg, 0.038 mmol)

In chamber 2: HCl_(aq) (25%, 0.734 mL, 6.04 mmol) was added to zinc (201 mg, 3.07 mmol).

The reaction mixture was stirred for 16 h. To chamber 2 was added zinc (207 mg) and a further HCl_(aq) (25%, 0.74 mL). This was stirred for a further 24 h. To chamber 1 was added 80 mg Pd/C. Chamber 2 was emptied and then zinc (204 mg) and HCl_(aq) (25%, 0.74 mL) was added. This was stirred for a further 72 h. The reaction mixture in chamber 1 was filtered through Celite and evaporated under reduced pressure to give a crude product. The crude mixture was then stirred under an atmosphere of hydrogen with Pd-C (215 mg) using hydrogenation suite apparatus for a further 5 d. Further Pd-C (210 mg) was added and the reaction mixture was stirred under an atmosphere of hydrogen using the hydrogenation suite apparatus for a further 2 d. The reaction mixture was filtered through Celite and evaporated under reduced pressure. The crude mixture was then transferred to COware apparatus (400 mL):

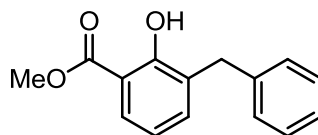
Chamber 1 – Pd-C (400 mg), crude reaction mixture, EtOAc (8 mL)

Chamber 2 - Zinc (4 g), HCl_(aq) (25%, 14 mL)

This was stirred for 3 d. The reaction mixture was filtered through Celite and evaporated under reduced pressure to give a crude orange liquid. This crude material was purified using column chromatography eluting with a gradient of 0-20 cyclohexane: EtOAc. Collected fraction 1 was evaporated under reduced pressure to give methyl 3-benzyl-2-hydroxybenzoate (61 mg, 0.252 mmol, 33%) as a colourless oil.

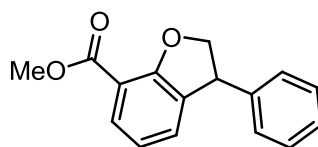
Collected fraction 2 was evaporated under reduced pressure to give methyl 3-phenyl-2,3-dihydrobenzofuran-7-carboxylate (20 mg, 0.079 mmol, 10%) as a white semi solid.

Methyl 3-benzyl-2-hydroxybenzoate 5.1.25

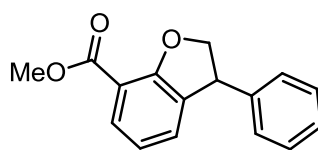


LCMS (Method B, UV, ESI) $R_t = 1.37$ $[M-H]^- = 241.2$, 94%; 1H NMR (400 MHz, $CDCl_3$) $\delta = 11.07$ (s, 1H), 7.72 (dd, $J = 1.7, 8.1$ Hz, 1H), 7.30 – 7.22 (m, 5H), 7.21 – 7.16 (m, 1H), 6.79 (t, $J = 7.7$ Hz, 1H), 4.02 (s, 2H), 3.93 (s, 3H); ^{13}C NMR (101 MHz, $CDCl_3$) $\delta = 170.9, 159.6, 140.3, 136.2, 129.7, 128.9, 128.4, 128.0, 126.0, 118.7, 112.1, 52.3, 35.4$; ν_{max}/cm^{-1} (thin film) 3086 br, 2954, 1670.

rac-Methyl 3-phenyl-2,3-dihydrobenzofuran-7-carboxylate 5.1.9



LCMS (Method B, UV, ESI) $R_t = 1.16$ $[M+H]^+ = 255.1$, 84%; 1H NMR (400 MHz, $CDCl_3$) $\delta = 7.80$ (d, $J = 7.8$ Hz, 1H), 7.35 – 7.29 (m, 2H), 7.28 – 7.23 (m, 1H), 7.21 – 7.18 (m, 2H), 7.15 (td, $J = 1.2, 7.3$ Hz, 1H), 6.88 (t, $J = 7.6$ Hz, 1H), 5.10 – 5.03 (m, 1H), 4.70 – 4.64 (m, 1H), 4.61 – 4.55 (m, 1H), 3.93 (s, 3H); ^{13}C NMR (101 MHz, $CDCl_3$) $\delta = 165.8, 160.5, 142.2, 133.1, 130.4, 129.9, 128.9, 127.8, 127.3, 120.6, 113.3, 80.2, 52.0, 47.7$; ν_{max}/cm^{-1} (thin film) 2950, 1709; HRMS: Calculated for $C_{16}H_{15}O_3$ 255.1021 Found $[M+H]^+$: 255.1018 (- 1.2 ppm).

***rac*-Methyl 3-phenyl-2,3-dihydrobenzofuran-7-carboxylate 5.1.9**

To Pd-C (Type 424) (386 mg, 0.181 mmol) was added methyl 5-bromo-3-phenylbenzofuran-7-carboxylate (200 mg, 0.604 mmol) in EtOAc (11 mL). This was stirred under an atmosphere of hydrogen for 24 h. The reaction mixture was then filtered through Celite and washed with EtOAc (10 mL). The combined organics were evaporated under reduced pressure to give a crude product. This was re-dissolved in ethanol (12 mL), added to Pd-C (Type 424) (381 mg) and stirred under an atmosphere of hydrogen for 16 h. The mixture was then filtered through Celite and washed with EtOAc (10 mL). The combined organics were evaporated under reduced pressure to give a crude product. This was then stirred in CH₂Cl₂ (4 mL) with activated charcoal (2 heaped spatulas). The mixture was filtered through Celite and the solvent evaporated under reduced pressure to give a brown semi solid. This was purified using a HpH MDAP (Method C) to give *rac*-methyl 3-phenyl-2,3-dihydrobenzofuran-7-carboxylate (81 mg, 0.319 mmol, 53%) as a yellow oil.

LCMS (Method B, UV, ESI) R_t = 1.17 [M+H]⁺ = 255.1, 99%; Data consistent with previous isolation.

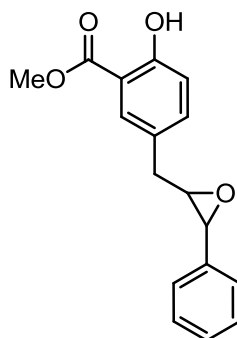
Methyl (*E*)-5-bromo-2-hydroxy-3-(3-hydroxy-1-phenylprop-1-en-1-yl)benzoate 5.1.35 and *rac*-methyl 2-hydroxy-5-((3-phenyloxiran-2-yl)methyl)benzoate 5.1.34

To *rac*-methyl 5-bromo-2-hydroxy-3-(1-phenylallyl)benzoate (500 mg, 1.440 mmol) in CH₂Cl₂ (10 mL) was added mCPBA (581 mg, 2.59 mmol). This was stirred at ambient temperature for 24 h. Sat. NaHCO_{3(aq)} (2 mL), sat. Na₂SO_{3(aq)} (2 mL) and CH₂Cl₂ (5 mL) was added and the layers were separated. The aqueous layer was extracted with CH₂Cl₂ (3 × 3 mL) and the combined organics were filtered through a hydrophobic frit. The solvent was evaporated under reduced pressure to give a crude

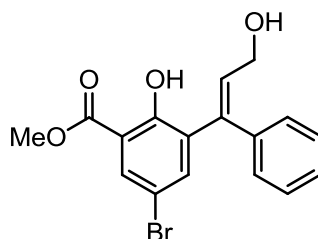
yellow solid. The crude mixture was dissolved in DMSO (5 mL), cooled using an ice bath and was slowly treated with KOH (162 mg, 2.88 mmol). The resulting solution was stirred ambient temperature for 16 h. Water (4 mL) and EtOAc (8 mL) were added and the layers were separated. The aqueous layer was extracted with EtOAc (3 × 5 mL). The combined organic layers were filtered through a hydrophobic frit and the solvent was evaporated under reduced pressure to give crude yellow oil. This was purified using column chromatography eluting with a gradient of 0-20 cyclohexane: EtOAc with 100% EtOAc flush. Collected fraction 1 was evaporated under reduced pressure to give *rac*-methyl 2-hydroxy-5-((3-phenyloxiran-2-yl)methyl)benzoate (17 mg, 0.060 mmol, 4%).

Collected fraction 2 was evaporated under reduced pressure to give methyl (*E*)-5-bromo-2-hydroxy-3-(3-hydroxy-1-phenylprop-1-en-1-yl)benzoate (16 mg, 0.044 mmol, 3%) as a yellow semi solid.

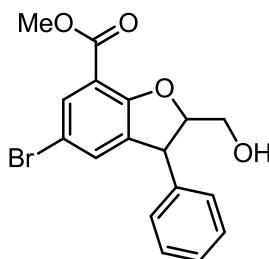
***rac*-Methyl 2-hydroxy-5-((3-phenyloxiran-2-yl)methyl)benzoate 5.1.34**



LCMS (Method B, UV, ESI) $R_t = 1.27$ $[M-H]^- = 283.1$, 83%; 1H NMR (400 MHz, $CDCl_3$) $\delta = 10.65$ (s, 1H), 7.76 (d, $J = 2.2$ Hz, 1H), 7.41 – 7.23 (m, 6H), 6.95 (d, $J = 8.6$ Hz, 1H), 3.95 (s, 3H), 3.66 (d, $J = 2.0$ Hz, 1H), 3.17 – 3.13 (m, 1H), 3.03 – 2.88 (m, 2H); ^{13}C NMR (101 MHz, $CDCl_3$) $\delta = 170.4$, 160.5, 137.2, 136.5, 130.0, 128.4, 128.1, 127.6, 125.5, 117.8, 112.3, 62.7, 58.3, 52.3, 37.5; ν_{max}/cm^{-1} (thin film) 3168 br, 2853, 1674, 1615; HRMS: Calculated for $C_{17}H_{17}O_4$ 285.1127 Found $[M+H]^+$: 285.1126 (– 0.4 ppm).

Methyl (E)-5-bromo-2-hydroxy-3-(3-hydroxy-1-phenylprop-1-en-1-yl)benzoate
5.1.35

LCMS (Method B, UV, ESI) $R_t = 1.23$ $[M-H]^- = 361.1, 363.1, 95\%$; 1H NMR (400 MHz, $CDCl_3$) $\delta = 11.07$ (br s, 1H), 7.99 (d, $J = 2.6$ Hz, 1H), 7.36 (d, $J = 2.6$ Hz, 1H), 7.26 (s, 2H), 7.32 - 7.19 (m, 3H), 6.43 (t, $J = 7.2$ Hz, 1H), 4.05 (d, $J = 7.2$ Hz, 2H), 3.97 (s, 3H) (1H not observed, exchangeable); ^{13}C NMR (101 MHz, $CDCl_3$) $\delta = 169.7, 157.9, 140.2, 139.7, 137.4, 132.0, 130.2, 129.7, 128.4, 127.9, 126.7, 114.1, 110.9, 60.9, 52.9$; ν_{max}/cm^{-1} (thin film) 3083 br, 2953, 2925, 1673.

Methyl 5-bromo-2-(hydroxymethyl)-3-phenyl-2,3-dihydrobenzofuran-7-carboxylate
5.1.41

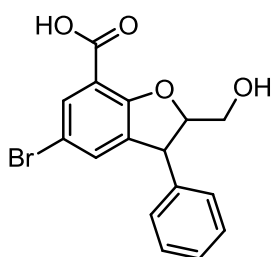
To *rac*-methyl 5-bromo-2-hydroxy-3-(1-phenylallyl)benzoate (100 mg, 0.288 mmol) in CH_2Cl_2 (2 mL) was added mCPBA (116 mg, 0.518 mmol). This was stirred at ambient temperature for 16 h. Sat. $NaHCO_{3(aq)}$ (2 mL) and sat. $Na_2SO_{3(aq)}$ (2 mL) was added. CH_2Cl_2 (5 mL) was added and the layers were separated. The aqueous layer was extracted with CH_2Cl_2 (3×3 mL) and the combined organics were filtered through a hydrophobic frit. The solvent was evaporated under reduced pressure to give crude methyl 5-bromo-2-hydroxy-3-(oxiran-2-yl(phenyl)methyl)benzoate (57 mg, 55%) as a yellow solid. The crude product (47 mg, 0.129 mmol) in DMSO

(1 mL) was cooled using a ice bath and was slowly treated with KOH (10 mg, 0.178 mmol) and the resulting solution was stirred at ambient temperature for 16 h. Water (3 mL) and EtOAc (3 mL) were added and the layers were separated. The aqueous layer was extracted with EtOAc (3 × 3 mL). The combined organics were then filtered through a hydrophobic frit and the solvent was evaporated under reduced pressure to give crude yellow product. This was purified using HpH MDAP (Method C) to give methyl 5-bromo-2-(hydroxymethyl)-3-phenyl-2,3-dihydrobenzofuran-7-carboxylate (8 mg, 0.022 mmol, 17%) as an orange semi solid. (~ 3:1 mixture of diastereomers, only major isomer signals reported)

LCMS (Method B, UV, ESI) $R_t = 1.19$ $[M-H]^- = 361.1, 363.1$, 69% (close running diastereomer $R_t = 1.17$, 23%); 1H NMR (400 MHz, DMSO- d_6) $\delta = 7.76 - 7.70$ (m, 1H), 7.38 – 7.33 (m, 2H), 7.30 – 7.26 (m, 3H), 7.24 – 7.19 (m, 2H), 4.83 – 4.78 (m, 1H), 4.63 (d, $J = 6.9$ Hz, 1H), 3.83 (s, 3H), 3.77 – 3.71 (m, 1H), 3.69 – 3.61 (m, 1H); ^{13}C NMR (101 MHz, DMSO- d_6) $\delta = 163.8, 159.0, 141.9, 136.7, 132.2, 131.5, 128.9, 127.8, 127.2, 113.9, 110.9, 93.2, 61.6, 52.1, 47.9$; ν_{max}/cm^{-1} (thin film) 3357 br, 2918, 1712, 1705; HRMS: Calculated for $C_{17}H_{16}BrO_4$ 363.0232 Found $[M+H]^+$: 363.0228 (– 1.1 ppm).

5-Bromo-2-(hydroxymethyl)-3-phenyl-2,3-dihydrobenzofuran-7-carboxylic acid

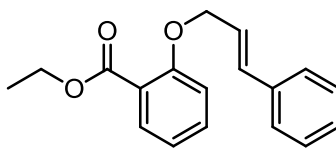
5.1.42



To *rac*-methyl 5-bromo-2-hydroxy-3-(1-phenylallyl)benzoate (200 mg, 0.576 mmol) in CH_2Cl_2 (3 mL) was added mCPBA (232 mg, 1.037 mmol). This was stirred at ambient temperature for 20 h. Further mCPBA (110 mg) was added and the reaction was stirred for a further 1 h. Sat. $NaHCO_{3(aq)}$ (3 mL), sat. $Na_2SO_{3(aq)}$ (4 mL) and CH_2Cl_2 (10 mL) was added and the layers were separated. The aqueous layer was

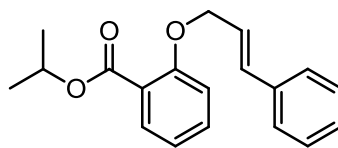
extracted with CH_2Cl_2 (3×5 mL) and filtered through a hydrophobic frit. The solvent was evaporated under reduced pressure to give a crude yellow oil. The crude oil was dissolved in DMSO (2 mL), cooled to 0°C and then KOH (42 mg, 0.749 mmol) in water (1 mL) was added. This was then allowed to warm to ambient temperature and stirred for 16 h. Further KOH (42 mg) was added and the reaction mixture was stirred for a further 6 h. 2M $\text{HCl}_{(\text{aq})}$ (5 mL) and EtOAc (5 mL) was then added. The layers were separated and the aqueous layer was extracted with EtOAc (3×5 mL). The combined organic layers were filtered through hydrophobic frit and the solvent evaporated under reduced pressure to give a crude product. 2M $\text{NaOH}_{(\text{aq})}$ (12 mL) and EtOAc (15 mL) was added to the crude product and the layers were separated. The organic layer was extracted with 2M $\text{NaOH}_{(\text{aq})}$ (3×5 mL). The combined aqueous layers were acidified with conc $\text{HCl}_{(\text{aq})}$ (25% w) and then EtOAc (15 mL) was added. The layers were separated and extracted aqueous with EtOAc (3×10 mL). The combined organics were filtered through a hydrophobic frit and evaporated under reduced pressure to give crude product. This was purified using HpH MDAP (Method A) to give 5-bromo-2-(hydroxymethyl)-3-phenyl-2,3-dihydrobenzofuran-7-carboxylic acid (69 mg, 0.198 mmol, 34%) as an orange solid. (*~ 3:1 mixture of diastereomers, only major isomer signals reported*)

M.p. $219 - 221^\circ\text{C}$; LCMS (Method B, UV, ESI) $R_t = 0.70$ $[\text{M}-\text{H}]^- = 347.1, 349.0, 91\%$; ^1H NMR (400 MHz, CDCl_3) $\delta = 7.63$ (d, $J = 2.2$ Hz, 1H), 7.38 – 7.33 (m, 2H), 7.33 – 7.24 (m, 1H), 7.24 – 7.19 (m, 2H), 7.16 - 7.13 (m, 1H), 7.01 (dd, $J = 1.2, 2.2$ Hz, 1H), 4.72 – 4.62 (m, 1H), 4.53 (d, $J = 7.3$ Hz, 1H), 3.76 – 3.61 (m, 2H); ^{13}C NMR (101 MHz, CDCl_3) $\delta = 166.3, 157.6, 142.4, 135.0, 132.2, 128.8, 128.6, 128.5, 127.9, 127.0, 110.5, 92.0, 61.7, 48.4$; $\nu_{\text{max}}/\text{cm}^{-1}$ (thin film) 3183 br, 3028, 1674, 1596; HRMS: Calculated for $\text{C}_{16}\text{H}_{14}\text{BrO}_4$ 349.0075 Found $[\text{M}+\text{H}]^+$: 349.0071 (-1.1 ppm).

Ethyl 2-(cinnamyloxy)benzoate 5.1.46

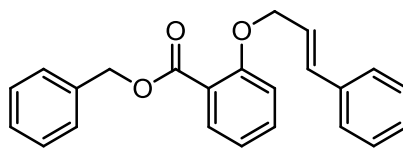
Ethyl 2-hydroxybenzoate (1.8 mL, 12.25 mmol), potassium carbonate (3.3 g, 23.88 mmol), potassium iodide (0.4 g, 2.410 mmol) and (*E*)-(3-chloroprop-1-en-1-yl)benzene (1.4 mL, 14.53 mmol) were refluxed in Acetone (22 mL) for 16 h. 2M HCl_(aq) (10 mL), water (10 mL) and EtOAc (10 mL) were added. The layers were separated and the aqueous layer was extracted with EtOAc (3 × 10 mL). The combined organics were filtered through a hydrophobic frit and evaporated under reduced pressure to give a crude product. This was purified using column chromatography eluting with a gradient of 0-20 cyclohexane: EtOAc. Collected fractions were evaporated under reduced pressure to give ethyl 2-(cinnamyloxy)benzoate (2.426 g, 8.599 mmol, 70%) as a yellow solid.

M.p. 67 – 69 °C; LCMS (Method B, UV, ESI) R_t = 1.36 [M-H]⁻ = No mass ion, 100%; ¹H NMR (400 MHz, DMSO-*d*₆) δ = 7.65 (dd, *J* = 1.7, 7.6 Hz, 1H), 7.56 – 7.50 (m, 1H), 7.47 (d, *J* = 7.6 Hz, 2H), 7.35 (t, *J* = 7.6 Hz, 2H), 7.30 – 7.24 (m, 1H), 7.21 (d, *J* = 8.3 Hz, 1H), 7.03 (t, *J* = 7.6 Hz, 1H), 6.82 (d, *J* = 15.9 Hz, 1H), 6.49 (td, *J* = 5.4, 16.1 Hz, 1H), 4.84 – 4.76 (m, 2H), 4.28 (q, *J* = 7.1 Hz, 2H), 1.29 (t, *J* = 7.1 Hz, 3H); ¹³C NMR (101 MHz, DMSO-*d*₆) δ = 165.8, 157.0, 136.2, 133.2, 131.8, 130.5, 128.6, 127.8, 126.3, 124.7, 120.9, 120.3, 114.0, 68.7, 60.4, 14.1; ν_{max}/cm⁻¹ (thin film) 2998, 2962, 1716. Failed to ionise under high resolution mass spectrometry conditions.

Isopropyl 2-(cinnamyloxy)benzoate 5.1.47

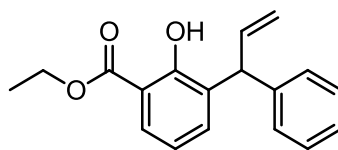
Isopropyl 2-hydroxybenzoate (4.6 mL, 27.8 mmol), potassium carbonate (7.67 g, 55.5 mmol), potassium iodide (0.9 g, 5.42 mmol) and (*E*)-(3-chloroprop-1-en-1-yl)benzene (3.22 mL, 33.4 mmol) were heated under reflux in Acetone (60 mL) for 88 h. 2M HCl_(aq) (75 mL) and EtOAc (100 mL) were added and the layers were separated. The aqueous layer was extracted with EtOAc (3 × 50 mL) and then the combined organics were filtered through a hydrophobic frit. The organics were washed with brine (50 mL) then filtered through a hydrophobic frit and evaporated under reduced pressure to give a crude product. This was purified using column chromatography eluting with a gradient of 0-20 cyclohexane: EtOAc. The collected fractions were evaporated under reduced pressure to give isopropyl 2-(cinnamyloxy)benzoate (6.373 g, 21.50 mmol, 77%) as a yellow oil.

LCMS (Method B, UV, ESI) $R_t = 1.40$ $[M-H]^- =$ No mass ion, 100%; 1H NMR (400 MHz, CDCl₃) $\delta = 7.75$ (dd, $J = 1.7, 7.6$ Hz, 1H), 7.44 – 7.38 (m, 3H), 7.34 – 7.29 (m, 2H), 7.27 – 7.22 (m, 1H), 7.02 – 6.95 (m, 2H), 6.81 – 6.75 (m, 1H), 6.41 (td, $J = 5.6, 16.0$ Hz, 1H), 5.31 – 5.21 (m, 1H), 4.77 (dd, $J = 1.5, 5.6$ Hz, 2H), 1.36 (d, $J = 6.4$ Hz, 6H); ^{13}C NMR (101 MHz, DMSO-*d*₆) $\delta = 165.5, 156.9, 136.2, 133.0, 131.8, 130.3, 128.6, 127.8, 126.3, 124.7, 121.5, 120.3, 114.0, 68.7, 67.7, 21.6$; ν_{max}/cm^{-1} (thin film) 2981, 1717, 1702. Failed to ionise under high resolution mass spectrometry conditions.

Benzyl 2-(cinnamyloxy)benzoate 5.1.48

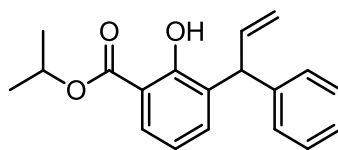
Benzyl 2-hydroxybenzoate (1.7 mL, 8.76 mmol), potassium carbonate (2.421 g, 17.52 mmol), potassium iodide (0.291 g, 1.752 mmol) and (*E*)-(3-chloroprop-1-en-1-yl)benzene (1 mL, 10.38 mmol) were heated under reflux in Acetone (22 mL) for 24 h. 2M HCl_(aq) (10 mL), water (10 mL) and EtOAc (10 mL) were added. The layers were separated and the aqueous layer was extracted with EtOAc (3 × 10 mL). The combined organics were filtered through a hydrophobic frit and evaporated under reduced pressure to give a crude product. This was purified using column chromatography eluting with a gradient of 0-20 cyclohexane: EtOAc. Collected fractions were evaporated under reduced pressure to give benzyl 2-(cinnamyloxy)benzoate (2.19 g, 6.364 mmol, 73%) as a yellow solid.

M.p. 63 – 65 °C; LCMS (Method B, UV, ESI) R_t = 1.47 [M-H]⁻ = No mass ion, 100%; ¹H NMR (400 MHz, DMSO-*d*₆) δ = 7.71 (dd, *J* = 1.8, 7.7 Hz, 1H), 7.58 – 7.52 (m, 1H), 7.48 – 7.40 (m, 4H), 7.38 – 7.21 (m, 7H), 7.04 (dt, *J* = 0.9, 7.5 Hz, 1H), 6.83 – 6.77 (m, 1H), 6.45 (td, *J* = 5.6, 15.9 Hz, 1H), 5.32 (s, 2H), 4.80 (dd, *J* = 1.2, 5.6 Hz, 2H); ¹³C NMR (101 MHz, DMSO-*d*₆) δ = 165.7, 157.2, 136.2, 136.1, 133.5, 132.3, 130.8, 128.6, 128.3, 127.8, 127.7, 126.4, 124.5, 120.4, 114.0, 68.8, 66.0 (2C not observed); ν_{max}/cm⁻¹ (thin film) 3062, 3034, 2938, 1696. Failed to ionise under high resolution mass spectrometry conditions.

***rac*-Ethyl 2-hydroxy-3-(1-phenylallyl)benzoate 5.1.49**

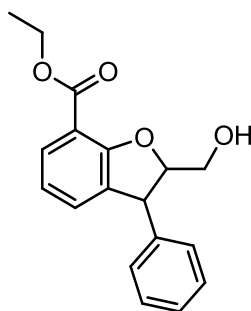
Ethyl 2-(cinnamyloxy)benzoate (2.3 g, 8.15 mmol) was dissolved in *N,N*-dimethylaniline (20 mL) and heated at 180 °C for 24 h. Et₂O (35 mL) and cold HCl_(aq) (25% w/w, 20 mL) were added. This was stirred vigorously and then the layers were separated. The aqueous layer was extracted with Et₂O (3 × 20 mL), filtered through a hydrophobic frit and then the solvent was evaporated under reduced pressure. HCl_(aq) (25% w/w, 20 mL) and Et₂O (20 mL) were then added and the layers separated. The aqueous layer was extracted with Et₂O (3 × 20 mL). The organic layers were combined, filtered through a hydrophobic frit and evaporated under reduced pressure to give a crude product. This was purified using column chromatography eluting with a gradient of 0-30 cyclohexane: EtOAc. The collected fractions were impure and so this was purified using column chromatography eluting with a gradient of 0-20 cyclohexane: EtOAc. Still some impurities remained in the collected fractions so this was purified again using column chromatography eluting with a gradient of 0-10 cyclohexane: EtOAc to give *rac*-ethyl 2-hydroxy-3-(1-phenylallyl)benzoate (1.493 g, 5.292 mmol, 65%) as an orange oil.

LCMS (Method B, UV, ESI) $R_t = 1.54$ $[M-H]^- = 281.2$, 84%; ¹H NMR (400 MHz, CDCl₃) $\delta = 11.20$ (s, 1H), 7.76 (dd, $J = 1.7, 8.1$ Hz, 1H), 7.37 – 7.25 (m, 3H), 7.24 – 7.17 (m, 3H), 6.84 (t, $J = 7.8$ Hz, 1H), 6.35 – 6.25 (m, 1H), 5.25 – 5.19 (m, 2H), 5.18 – 4.91 (m, 1H), 4.38 (q, $J = 7.3$ Hz, 2H), 1.39 (t, $J = 7.1$ Hz, 3H); ¹³C NMR (101 MHz, CDCl₃) $\delta = 170.5, 159.3, 142.4, 139.7, 135.2, 131.6, 128.6, 128.24, 128.17, 126.3, 118.5, 116.4, 112.4, 61.4, 47.5, 14.2$; ν_{max}/cm^{-1} (thin film) 3084 br, 2981, 1667; HRMS: Calculated for C₁₈H₁₉O₃ 283.1334 Found $[M+H]^+$: 283.1330 (– 1.4 ppm).

***rac*-Isopropyl 2-hydroxy-3-(1-phenylallyl)benzoate 5.1.50**

Isopropyl 2-(cinnamyloxy)benzoate (5.653 g, 19.07 mmol) was dissolved in *N,N*-dimethylaniline (40 mL) and heated at 180 °C for 30 h. Et₂O (50 mL) and cold HCl_(aq) (6M, 50 mL) was added and the solution was stirred vigorously. The layers were then separated and the organic layer was extracted cold HCl_(aq) (6M, 50 mL). The combined aqueous layers were then extracted with Et₂O (3 × 50 mL). The combined organics were then filtered through a hydrophobic frit and the solvent evaporated under reduced pressure to give a crude product. This was purified using column chromatography eluting with a gradient of 0-15 cyclohexane: EtOAc. The collected fractions were evaporated under reduced pressure to give *rac*-isopropyl 2-hydroxy-3-(1-phenylallyl)benzoate (5.065 g, 17.090 mmol, 90%) as a yellow oil.

LCMS (Method B, UV, ESI) $R_t = 1.59$ $[M-H]^- = 295.2$, 86%; ¹H NMR (400 MHz, CDCl₃) $\delta = 11.29$ (s, 1H), 7.75 (dd, $J = 1.6, 7.9$ Hz, 1H), 7.32 – 7.25 (m, 3H), 7.23 – 7.16 (m, 3H), 6.83 (t, $J = 7.7$ Hz, 1H), 6.36 – 6.25 (m, 1H), 5.32 – 5.20 (m, 3H), 4.98 – 4.94 (m, 1H), 1.39 – 1.34 (m, 6H); ¹³C NMR (101 MHz, CDCl₃) $\delta = 170.1, 159.4, 142.5, 139.8, 135.1, 131.6, 128.6, 128.24, 128.18, 126.3, 118.4, 116.4, 112.8, 69.2, 47.2, 21.8$; ν_{max}/cm^{-1} (thin film) 3028 br, 2982, 1662; HRMS: Calculated for C₁₉H₂₁O₃ 297.1491 Found $[M+H]^+$: 297.1484 (– 2.4 ppm).

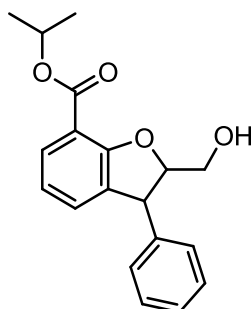
Ethyl 2-(hydroxymethyl)-3-phenyl-2,3-dihydrobenzofuran-7-carboxylate 5.1.52

To *rac*-ethyl 2-hydroxy-3-(1-phenylallyl)benzoate (202 mg, 0.715 mmol) in CH_2Cl_2 (3 mL) was added mCPBA (226 mg, 1.008 mmol). This was stirred for 16 h at ambient temperature. Further mCPBA (100 mg) was added and the reaction mixture was stirred for a further 6 h. 5% $\text{Na}_2\text{S}_2\text{O}_5(\text{aq})$ (2 mL), sat. $\text{NaHCO}_3(\text{aq})$ (5 mL) and CH_2Cl_2 (5 mL) was added. The layers were separated and the aqueous layer was extracted with CH_2Cl_2 (3×5 mL). The combined organics were filtered through hydrophobic frit and evaporated under reduced pressure. The crude product was dissolved in DMSO (5 mL). This was cooled to 0 °C and then KOH (63 mg, 1.123 mmol) in Water (3 mL) was added. This was allowed to warm to ambient temperature and stirred for 16 h. 2M $\text{HCl}(\text{aq})$ (10 mL), water (10 mL) and EtOAc (20 mL) were added. The layers were separated and the aqueous layer was extracted with EtOAc (3×10 mL). The combined organics were filtered through a hydrophobic frit and the solvent evaporated under reduced pressure to give a crude product. 2M $\text{NaOH}(\text{aq})$ (12 mL) and EtOAc (15 mL) were added. The layers were separated and the organic layer was extracted with 2M $\text{NaOH}(\text{aq})$ (3×5 mL). The organic layer was evaporated under reduced pressure to give ethyl 2-(hydroxymethyl)-3-phenyl-2,3-dihydrobenzofuran-7-carboxylate (145 mg, 68%, 85% purity by LCMS).

This crude product was purified using a HpH MDAP (Method C) in two portions to give ethyl 2-(hydroxymethyl)-3-phenyl-2,3-dihydrobenzofuran-7-carboxylate (61 mg, 0.204 mmol, 29%) as a yellow semi solid. (~ 1.5:1 mixture of diastereomers)

LCMS (Method B, UV, ESI) $R_t = 1.10$ and 1.11 $[M+H]^+ = 299.1$, 56 and 44%; 1H NMR (400 MHz, $CDCl_3$) $\delta = 7.84 - 7.80$ (m, 0.6H), $7.78 - 7.75$ (m, 0.4H), $7.34 - 7.26$ (m, 3H), $7.23 - 7.18$ (m, 1.6H), 7.11 (td, $J = 1.2, 7.3$ Hz, 0.4H), $7.06 - 7.01$ (m, 1H), 6.92 (t, $J = 7.6$ Hz, 0.6H), 6.88 (t, $J = 7.6$ Hz, 0.4H), $5.19 - 5.13$ (m, 0.6H), 4.84 (m, 0.4H), 4.76 (d, $J = 9.5$ Hz, 0.6H), 4.54 (d, $J = 8.3$ Hz, 0.4H), $4.42 - 4.32$ (m, 2H), 4.05 (dd, $J = 2.9, 12.5$ Hz, 0.4H), 3.83 (dd, $J = 4.9, 12.5$ Hz, 0.4H), 3.51 (dd, $J = 8.3, 12.5$ Hz, 0.6H), 3.32 (dd, $J = 4.0, 12.3$ Hz, 0.6H), 2.14 (br. s, 1H), 1.39 (t, $J = 7.1$ Hz, 3H); ^{13}C NMR (101 MHz, $CDCl_3$) $\delta = 165.24, 165.16, 160.1, 141.7, 137.7, 133.2, 132.6, 130.4, 130.2, 130.1, 129.9, 128.9, 128.6, 128.2, 127.6, 127.4, 120.8, 120.7, 113.7, 113.5, 93.1, 87.8, 63.0, 62.9, 60.83, 60.80, 49.1, 49.0, 14.3$ (3C not observed); ν_{max}/cm^{-1} (thin film) 3450 br, 2929, 1700; HRMS: Calculated for $C_{18}H_{19}O_4$ 299.1283 Found $[M+H]^+$: 299.1287 (1.3 ppm).

Isopropyl 2-(hydroxymethyl)-3-phenyl-2,3-dihydrobenzofuran-7-carboxylate
5.1.53

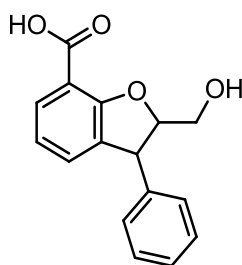


To *rac*-isopropyl 2-hydroxy-3-(1-phenylallyl)benzoate (202 mg, 0.682 mmol) in CH_2Cl_2 (3 mL) was added mCPBA (217 mg, 0.968 mmol). The reaction mixture was stirred for 16 h. Further mCPBA (100 mg) was added and the reaction mixture was stirred for a further 6 h. 5% $Na_2S_2O_5(aq)$ (2 mL), sat. $NaHCO_3(aq)$ (5 mL) and CH_2Cl_2 (5 mL) was added. The aqueous layer was extracted with CH_2Cl_2 (3×5 mL). The combined organic layers were filtered through a hydrophobic frit and evaporated under reduced pressure. The crude product was dissolved in DMSO (5 mL). This was cooled to $0^\circ C$ and then KOH (61 mg, 1.087 mmol) in water (3 mL) was added. This

was allowed to warm to ambient temperature and stirred for 16 h. 2M HCl_(aq) (10 mL), water (10 mL) and EtOAc (20 mL) were added. The layers were separated and the aqueous was extracted with EtOAc (3 × 10 mL). The combined organics were filtered through a hydrophobic frit and the solvent evaporated under reduced pressure to give a isopropyl 2-(hydroxymethyl)-3-phenyl-2,3-dihydrobenzofuran-7-carboxylate (160 mg, 0.512 mmol, 75%, 88% purity by LCMS).

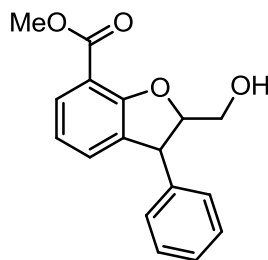
An 80 mg portion was purified by HpH MDAP (Method C) to give isopropyl 2-(hydroxymethyl)-3-phenyl-2,3-dihydrobenzofuran-7-carboxylate (27 mg) as an orange oil. (~ 1.5:1 mixture of diastereomers)

LCMS (Method B, UV, ESI) R_t = 1.18 and 1.19 [M+H]⁺ = 313.1, 55 and 45%; ¹H NMR (400 MHz, CDCl₃) δ = 7.82 – 7.78 (m, 0.6H), 7.77 – 7.73 (m, 0.4H), 7.34 – 7.23 (m, 3H), 7.22 – 7.18 (m, 1.6H), 7.10 (td, *J* = 1.2, 7.3 Hz, 0.4H), 7.03 (dd, *J* = 1.8, 7.5 Hz, 1H), 6.91 (t, *J* = 7.7 Hz, 0.6H), 6.86 (t, *J* = 7.6 Hz, 0.4H), 5.27 – 5.19 (m, 1H), 5.19 – 5.12 (m, 0.6H), 4.86 – 4.81 (m, 0.4H), 4.75 (d, *J* = 9.3 Hz, 0.6H), 4.54 (d, *J* = 8.1 Hz, 0.4H), 4.04 (dd, *J* = 3.2, 12.5 Hz, 0.4H), 3.83 (dd, *J* = 4.9, 12.5 Hz, 0.4H), 3.51 (dd, *J* = 8.4, 12.3 Hz, 0.6H), 3.31 (dd, *J* = 3.9, 12.5 Hz, 0.6H), 1.42 (s, 1H), 1.39 – 1.33 (m, 6H); ¹³C NMR (101 MHz, CDCl₃) δ = 164.7, 164.6, 160.24, 160.21, 141.7, 137.7, 133.1, 132.6, 130.3, 130.1, 130.0, 129.8, 128.93, 128.90, 128.5, 128.2, 127.5, 127.3, 120.7, 120.6, 114.0, 113.8, 93.0, 87.8, 68.3, 68.2, 63.0, 62.9, 49.1, 49.0, 21.9 (1C not observed); ν_{max}/cm⁻¹ (thin film) 3446 br, 2980, 2935, 1698; HRMS: Calculated for C₁₉H₂₁O₄ 313.1440 Found [M+H]⁺: 313.1443 (1.0 ppm).

2-(Hydroxymethyl)-3-phenyl-2,3-dihydrobenzofuran-7-carboxylic acid 5.1.54

To isopropyl 2-(hydroxymethyl)-3-phenyl-2,3-dihydrobenzofuran-7-carboxylate (80 mg, 0.256 mmol) in 1,4-dioxane (2 mL) was added LiOH (0.256 mL, 0.512 mmol). This was heated at 60 °C for 16 h. 2M HCl_(aq) (4 mL) and EtOAc (8 mL) were added and the layers were separated. The aqueous layer was extracted with EtOAc (3 × 3 mL). The combined organic layers were filtered through a hydrophobic frit and the solvent was evaporated under reduced pressure to give a crude product. This was purified using high pH MDAP (Method A) to give 2-(hydroxymethyl)-3-phenyl-2,3-dihydrobenzofuran-7-carboxylic acid (40 mg, 0.148 mmol, 58%) as an off white solid. (~ 1.5:1 mixture of diastereomers)

M.p. 145 – 147 °C; LCMS (Method B, UV, ESI) $R_t = 0.60$ $[M-H]^- = 269.1$, 100%; 1H NMR (400 MHz, DMSO- d_6) $\delta = 7.70 - 7.62$ (m, 1H), 7.38 – 7.32 (m, 1H), 7.30 – 7.18 (m, 3.4H), 7.12 (d, $J = 7.3$ Hz, 0.6H), 6.99 – 6.95 (m, 1H), 6.94 – 6.85 (m, 1H), 5.00 – 4.93 (m, 0.4H), 4.74 (d, $J = 8.8$ Hz, 0.4H), 4.71 – 4.66 (m, 0.6H), 4.58 (d, $J = 7.3$ Hz, 0.6H), 3.77 – 3.63 (m, 1H), 3.21 (d, $J = 6.4$ Hz, 1H) (2H not observed, exchangeable); ^{13}C NMR (101 MHz, DMSO- d_6) $\delta = 166.07$, 166.05, 159.70, 159.69, 142.6, 138.9, 133.6, 133.1, 130.1, 129.9, 129.7, 129.4, 128.8, 128.7, 128.2, 127.9, 126.9, 120.5, 120.1, 114.0, 113.7, 92.4, 87.9, 61.7, 61.3, 48.3, 48.1 (1C not observed); ν_{max}/cm^{-1} (thin film) 3425 br, 2920 br, 1687; HRMS: Calculated for C₁₆H₁₅O₄ 271.0970 Found $[M+H]^+$: 271.0975 (1.8 ppm).

Methyl 2-(hydroxymethyl)-3-phenyl-2,3-dihydrobenzofuran-7-carboxylate
5.1.33

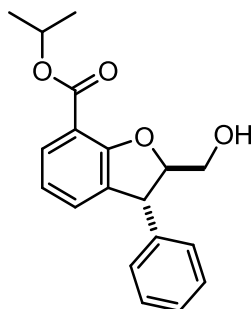
To 2-(hydroxymethyl)-3-phenyl-2,3-dihydrobenzofuran-7-carboxylic acid (23 mg, 0.085 mmol) in MeOH (0.5 mL) was added HCl (4M in 1,4-dioxane) (0.043 mL, 0.170 mmol). This was stirred for 16 h at ambient temperature. Further MeOH (0.5 mL) was added and stirred for 16 h. HCl (4M in 1,4-dioxane) (0.1 mL) was added and stirred for a further 16 h. The solvent was evaporated under a stream of nitrogen on a Radleys blowdown unit to give methyl 2-(hydroxymethyl)-3-phenyl-2,3-dihydrobenzofuran-7-carboxylate (16 mg, 0.056 mmol, 66%) as a yellow oil. (~ 1.5:1 mixture of diastereomers)

LCMS (Method B, UV, ESI) $R_t = 1.01$ and 1.03 $[M-H]^- = 283.1$, 41 and 55%; 1H NMR (400 MHz, $CDCl_3$) $\delta = 7.83$ (d, $J = 7.6$ Hz, 0.4H), 7.77 (d, $J = 7.8$ Hz, 0.6H), 7.36 – 7.27 (m, 3H), 7.25 – 7.18 (m, 1.4H), 7.14 – 7.11 (m, 0.6H), 7.06 – 7.02 (m, 1H), 6.94 (t, $J = 7.6$ Hz, 0.4H), 6.89 (t, $J = 7.6$ Hz, 0.6H), 5.20 – 5.12 (m, 0.4H), 4.87 – 4.81 (m, 0.6H), 4.79 – 4.74 (m, 0.4H), 4.56 (d, $J = 7.8$ Hz, 0.6H), 4.06 (dd, $J = 2.7$, 12.5 Hz, 0.6H), 3.91 (m, 3H), 3.84 (dd, $J = 4.6$, 12.5 Hz, 0.6H), 3.52 (dd, $J = 8.2$, 11.9 Hz, 0.4H), 3.37 – 3.31 (m, 0.4H) (1H not observed, exchangeable); ^{13}C NMR (101 MHz, $CDCl_3$) $\delta = 165.8$, 165.7, 160.0, 141.6, 137.6, 133.2, 132.6, 130.6, 130.4, 130.2, 130.0, 128.94, 128.92, 128.6, 128.2, 127.6, 127.4, 120.9, 120.7, 113.3, 113.0, 93.1, 87.9, 63.0, 62.9, 52.0, 49.0 (3C not observed); ν_{max}/cm^{-1} (thin film) 3443 br, 2951, 1705; HRMS: Calculated for $C_{17}H_{17}O_4$ 285.1127 Found $[M+H]^+$: 285.1125 (– 0.7 ppm).

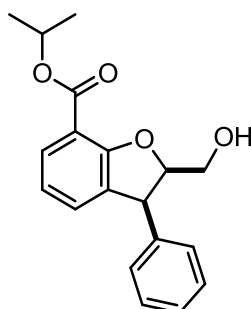
***rel*-(2*R*,3*R*) Isopropyl 2-(hydroxymethyl)-3-phenyl-2,3-dihydrobenzofuran-7-carboxylate 5.1.55 and *rel*-(2*R*,3*S*)-isopropyl 2-(hydroxymethyl)-3-phenyl-2,3-dihydrobenzofuran-7-carboxylate 5.1.56**

To *rac*-isopropyl 2-hydroxy-3-(1-phenylallyl)benzoate (300 mg, 1.012 mmol) in CH₂Cl₂ (3 mL) was added mCPBA (408 mg, 1.822 mmol). This was stirred at ambient temperature for 24 h. 5% Na₂S₂O_{5(aq)} (4 mL), CH₂Cl₂ (10 mL) and water (2 mL) was added. The layers were separated and the aqueous layer was extracted with CH₂Cl₂ (3 × 5 mL). The combined organics were filtered through a hydrophobic frit and the solvent evaporated under reduced pressure. The crude oil was dissolved in DMSO (8 mL). This was cooled to 0 °C and then KOH (85 mg, 1.518 mmol) in water (3 mL) was added. This was then allowed to warm to ambient temperature and stirred for 16 h. 2M HCl_(aq) (10 mL), water (5 mL) and EtOAc (20 mL) were added. The layers were separated and the aqueous layer was extracted with EtOAc (3 × 10 mL). The combined organics were filtered through a hydrophobic frit and the solvent evaporated under reduced pressure to give a crude product. This was purified using column chromatography eluting with a gradient of 0-30 cyclohexane: EtOAc. Collected fraction 1 was evaporated under reduced pressure to give *rel*-(2*R*,3*R*)-isopropyl 2-(hydroxymethyl)-3-phenyl-2,3-dihydrobenzofuran-7-carboxylate (80 mg, 0.256 mmol, 25%) as a yellow semi solid.

Collected fraction 2 was evaporated under reduced pressure to give *rel*-(2*R*,3*S*)-isopropyl 2-(hydroxymethyl)-3-phenyl-2,3-dihydrobenzofuran-7-carboxylate (113 mg, 0.362 mmol, 36%) as a yellow semi solid.

rel-(2R,3R)-Isopropyl 2-(hydroxymethyl)-3-phenyl-2,3-dihydrobenzofuran-7-carboxylate 5.1.55

LCMS (Method B, UV, ESI) $R_t = 1.19$ $[M-H]^- = 311.2$, 92%; 1H NMR (400 MHz, $CDCl_3$) $\delta = 7.75$ (d, $J = 8.1$ Hz, 1H), 7.43 – 7.23 (m, 4H), 7.22 – 7.17 (m, 2H), 7.10 (d, $J = 7.3$ Hz, 1H), 6.87 (t, $J = 7.6$ Hz, 1H), 5.26 – 5.19 (m, 1H), 4.83 (m, 1H), 4.53 (d, $J = 8.1$ Hz, 1H), 4.06 – 4.00 (m, 1H), 3.82 (dd, $J = 5.0, 12.6$ Hz, 1H), 1.36 (d, $J = 6.4$ Hz, 6H); ^{13}C NMR (101 MHz, $CDCl_3$) $\delta = 164.7, 160.2, 141.7, 133.1, 130.0, 129.8, 128.9, 128.2, 127.3, 120.6, 113.8, 93.1, 68.3, 63.1, 49.1, 21.9$; ν_{max}/cm^{-1} (thin film) 3445 br, 2980, 1698; HRMS: Calculated for $C_{19}H_{21}O_4$ 313.1440 Found $[M+H]^+$: 313.1440 (0.0 ppm).

rel-(2R,3S)-Isopropyl 2-(hydroxymethyl)-3-phenyl-2,3-dihydrobenzofuran-7-carboxylate 5.1.56

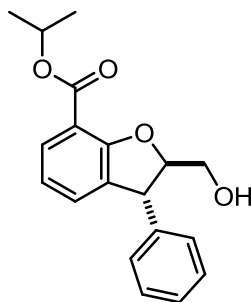
LCMS (Method B, UV, ESI) $R_t = 1.18$ $[M-H]^- = 311.1$, 100%; 1H NMR (400 MHz, $CDCl_3$) $\delta = 7.80$ (d, $J = 7.8$ Hz, 1H), 7.34 – 7.24 (m, 3H), 7.23 – 7.17 (m, 1H), 7.04 (dd, $J = 1.6, 7.5$ Hz, 2H), 6.91 (t, $J = 7.7$ Hz, 1H), 5.28 – 5.20 (m, 1H), 5.19 – 5.12 (m, 1H), 4.76 (d, $J = 9.5$ Hz, 1H), 3.51 (dd, $J = 8.4, 12.3$ Hz, 1H), 3.30 (dd, $J = 3.9, 12.5$ Hz, 1H), 1.37 (dd, $J = 3.3, 6.2$ Hz, 6H) (1H not observed, exchangeable); ^{13}C NMR (101 MHz, $CDCl_3$) $\delta = 164.6, 160.2, 137.7, 132.6, 130.3, 130.1, 128.9, 128.6$,

127.5, 120.7, 114.0, 87.8, 68.3, 62.9, 49.0, 21.9; $\nu_{\max}/\text{cm}^{-1}$ (thin film) 3461 br, 2980, 1698; HRMS: Calculated for $\text{C}_{19}\text{H}_{21}\text{O}_4$ 313.1440 Found $[\text{M}+\text{H}]^+$: 313.1436 (– 1.3 ppm).

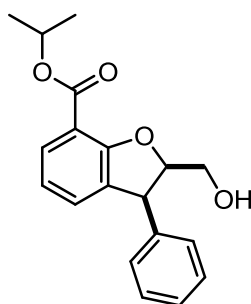
***rel*-(2*R*,3*R*)-Isopropyl 2-(hydroxymethyl)-3-phenyl-2,3-dihydrobenzofuran-7-carboxylate 5.1.55, *rel*-(2*R*,3*S*)-isopropyl 2-(hydroxymethyl)-3-phenyl-2,3-dihydrobenzofuran-7-carboxylate 5.1.56, *rel*-(2*R*,3*R*)-methyl 2-(hydroxymethyl)-3-phenyl-2,3-dihydrobenzofuran-7-carboxylate 5.1.57 and *rel*-(2*R*,3*S*)-methyl 2-(hydroxymethyl)-3-phenyl-2,3-dihydrobenzofuran-7-carboxylate 5.1.58**

To *rac*-isopropyl 2-hydroxy-3-(1-phenylallyl)benzoate (496 mg, 1.674 mmol) in CH_2Cl_2 (5 mL) was added mCPBA (675 mg, 3.01 mmol). This was stirred at ambient temperature for 24 h. Sat. $\text{Na}_2\text{SO}_{3(\text{aq})}$ (10 mL) and CH_2Cl_2 (10 mL) were added. The layers were separated and the aqueous layer was extracted with CH_2Cl_2 (3×10 mL). The combined organic layers were filtered through a hydrophobic frit and the solvent was evaporated under reduced pressure. The crude solid was dissolved in DMSO (10 mL) and cooled to 0 °C. KOH (141 mg, 2.51 mmol) in water (5 mL) was then added. This was then allowed to warm to ambient temperature and stirred for 16 h. 2M $\text{HCl}_{(\text{aq})}$ (10 mL) and EtOAc (30 mL) were then added. 2M $\text{NaOH}_{(\text{aq})}$ (15 mL) was added and the layers were separated. The organic layer was extracted with 2M $\text{NaOH}_{(\text{aq})}$ (3×5 mL). The organic layer was filtered through a hydrophobic frit and evaporated under reduced pressure to give a crude product. This was purified using column chromatography eluting with a gradient of 0-40 cyclohexane: EtOAc. First eluting fraction was evaporated under reduced pressure to give *rel*-(2*R*,3*R*)-isopropyl 2-(hydroxymethyl)-3-phenyl-2,3-dihydrobenzofuran-7-carboxylate (127 mg, 0.407 mmol, 24%) as a yellow semi solid.

Second eluting fraction was evaporated under reduced pressure to give *rel*-(2*R*,3*S*)-isopropyl 2-(hydroxymethyl)-3-phenyl-2,3-dihydrobenzofuran-7-carboxylate (146 mg, 0.467 mmol, 28%) as a yellow semi solid.

***rel*-(2*R*,3*R*)-Isopropyl 2-(hydroxymethyl)-3-phenyl-2,3-dihydrobenzofuran-7-carboxylate 5.1.55**

LCMS (Method B, UV, ESI) $R_t = 1.19$ $[M-H]^- = 311.1$, 94%; Data consistent with previous preparation

***rel*-(2*R*,3*S*)-Isopropyl 2-(hydroxymethyl)-3-phenyl-2,3-dihydrobenzofuran-7-carboxylate 5.1.56**

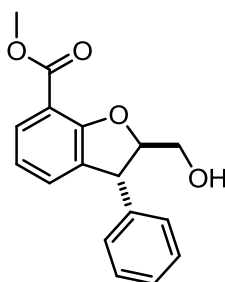
LCMS (Method B, UV, ESI) $R_t = 1.18$ $[M+H]^+ = 313.1$, 95% (17:1 mix of diastereomers); Data consistent with previous preparation

The aqueous layer was acidified with $HCl_{(aq)}$ (37% w) and then EtOAc (40 mL) was added. The layers were separated and the aqueous layer was extracted with EtOAc (3×40 mL). The combined organic layers were filtered through a hydrophobic frit and the solvent was evaporated under reduced pressure. HCl (4M in 1,4-dioxane) (0.5 mL, 2.00 mmol) and MeOH (3 mL). This was stirred for 16 h. The solvent was then evaporated under reduced pressure to give a crude product. This was purified using column chromatography eluting with a gradient of 0-40 cyclohexane: EtOAc. First eluting fraction was evaporated under reduced pressure to give *rel*-(2*R*,3*R*)-

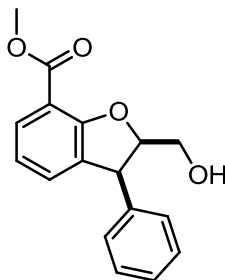
methyl 2-(hydroxymethyl)-3-phenyl-2,3-dihydrobenzofuran-7-carboxylate (54 mg, 0.190 mmol, 11%) as a white semi solid. (~ 7:1 mixture of diastereomers)

Second eluting fraction was evaporated under reduced pressure to give *rel*-(2*R*,3*S*)-methyl 2-(hydroxymethyl)-3-phenyl-2,3-dihydrobenzofuran-7-carboxylate (52 mg, 0.183 mmol, 11%) as a white semi solid.

***rel*-(2*R*,3*R*)-Methyl 2-(hydroxymethyl)-3-phenyl-2,3-dihydrobenzofuran-7-carboxylate 5.1.57**



LCMS (Method B, UV, ESI) $R_t = 1.03$ $[M-H]^- = 283.1$, 89% (7:1 mixture of diastereomers, $R_t = 1.01$ $[M-H]^- = 283.1$, 10%); 1H NMR (400 MHz, $CDCl_3$) $\delta = 7.76$ (td, $J = 1.2, 7.9$ Hz, 1H), 7.35 – 7.24 (m, 3H), 7.21 – 7.17 (m, 2H), 7.11 (td, $J = 1.3, 7.3$ Hz, 1H), 6.87 (t, $J = 7.6$ Hz, 1H), 4.83 (ddd, $J = 3.2, 4.9, 8.1$ Hz, 1H), 4.54 (d, $J = 8.1$ Hz, 1H), 4.05 (dd, $J = 3.1, 12.6$ Hz, 1H), 3.89 (s, 3H), 3.83 (dd, $J = 4.9, 12.5$ Hz, 1H) (1H not observed, exchangeable); ^{13}C NMR (101 MHz, $CDCl_3$) $\delta = 165.8, 160.1, 141.6, 133.2, 130.2, 130.0, 128.9, 128.2, 127.4, 120.7, 113.0, 93.1, 63.0, 52.0, 49.0$; ν_{max}/cm^{-1} (thin film) 3446 br, 2950, 1706; HRMS: Calculated for $C_{17}H_{17}O_4$ 285.1127 Found $[M+H]^+$: 285.1136 (3.2 ppm).

***rel*-(2*R*,3*S*)-Methyl 2-(hydroxymethyl)-3-phenyl-2,3-dihydrobenzofuran-7-carboxylate 5.1.58**

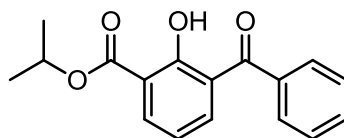
LCMS (Method B, UV, ESI) $R_t = 1.01$ $[M-H]^- = 283.2$, 100%; 1H NMR (400 MHz, $CDCl_3$) $\delta = 7.85 - 7.81$ (m, 1H), 7.32 – 7.25 (m, 3H), 7.23 (td, $J = 1.1, 7.3$ Hz, 1H), 7.07 – 7.03 (m, 2H), 6.94 (t, $J = 7.7$ Hz, 1H), 5.17 (ddd, $J = 3.9, 8.3, 9.4$ Hz, 1H), 4.77 (d, $J = 9.5$ Hz, 1H), 3.91 (s, 3H), 3.53 (dd, $J = 8.2, 12.3$ Hz, 1H), 3.35 (dd, $J = 4.2, 12.5$ Hz, 1H) (1H not observed, exchangeable); ^{13}C NMR (101 MHz, $CDCl_3$) $\delta = 165.7, 160.1, 137.7, 132.7, 130.5, 130.4, 128.9, 128.6, 127.6, 120.9, 113.3, 87.9, 62.9, 52.0, 49.0$; ν_{max}/cm^{-1} (thin film) 3557 br, 2924, 1712; HRMS: Calculated for $C_{17}H_{17}O_4$ 285.1127 Found $[M+H]^+$: 285.1130 (1.1 ppm).

Isopropyl 3-benzoyl-2-hydroxybenzoate 5.1.59 and *rac*-isopropyl 2-hydroxy-3-(2-oxo-1-phenylethyl)benzoate 5.1.60

A solution of *rac*-isopropyl 2-hydroxy-3-(1-phenylallyl)benzoate (5.01 g, 16.90 mmol) in acetone (50 mL) and water (50 mL) at ambient temperature was treated with sodium periodate (14.6 g, 68.3 mmol) then osmium tetroxide (4% w, 5 mL, 0.637 mmol) and the resulting mixture was stirred at ambient temperature for 3 h. Sat $Na_2SO_{3(aq)}$ (100 mL) and EtOAc (100 mL) were added and then filtered through Celite. The layers were separated and the aqueous layer was extracted with EtOAc (3 \times 50 mL). The combined organics were filtered through a hydrophobic frit and the solvent evaporated under reduced pressure to give a black liquid. This was purified using column chromatography eluting with a gradient of 0-30 cyclohexane: EtOAc. Collected fraction 1 was evaporated under reduced pressure to give isopropyl 3-benzoyl-2-hydroxybenzoate (514 mg, 1.808 mmol, 11%) as a brown solid.

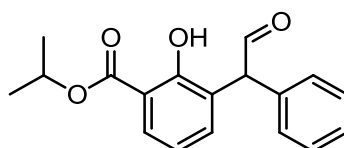
Collected fraction 2 was evaporated under reduced pressure to give *rac*-isopropyl 2-hydroxy-3-(2-oxo-1-phenylethyl)benzoate (1.677 g, 5.621 mmol, 33%) as a yellow oil.

Isopropyl 3-benzoyl-2-hydroxybenzoate 5.1.60

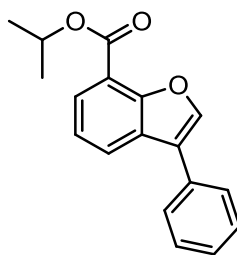


M.p. 71 – 73 °C; LCMS (Method B, UV, ESI) $R_t = 1.34$ $[M-H]^- = 283.1$, 97%; 1H NMR (400 MHz, $CDCl_3$) $\delta = 11.43$ (s, 1H), 8.02 (dd, $J = 1.7, 7.8$ Hz, 1H), 7.85 – 7.82 (m, 2H), 7.61 (dd, $J = 1.7, 7.6$ Hz, 1H), 7.59 – 7.55 (m, 1H), 7.48 – 7.42 (m, 2H), 6.98 (t, $J = 7.7$ Hz, 1H), 5.36 – 5.25 (m, 1H), 1.40 (d, $J = 6.1$ Hz, 6H); ^{13}C NMR (101 MHz, $CDCl_3$) $\delta = 195.7, 169.1, 159.8, 137.5, 135.8, 133.1, 133.0, 129.7, 128.3, 128.0, 118.7, 114.1, 69.7, 21.8$; ν_{max}/cm^{-1} (thin film) 3081 br, 2984, 1660; HRMS: Calculated for $C_{17}H_{17}O_4$ 285.1127 Found $[M+H]^+$: 285.1131 (1.4 ppm).

***rac*-Isopropyl 2-hydroxy-3-(2-oxo-1-phenylethyl)benzoate 5.1.59**

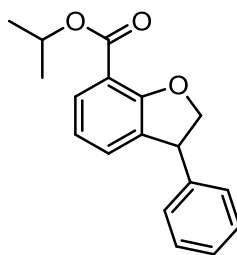


LCMS (Method B, UV, ESI) $R_t = 1.24$ $[M-H]^- = 297.2$, 86%; 1H NMR (400 MHz, $CDCl_3$) $\delta = 11.43$ (s, 1H), 9.98 (d, $J = 1.2$ Hz, 1H), 7.81 (dd, $J = 1.6, 7.9$ Hz, 1H), 7.40 – 7.34 (m, 2H), 7.33 – 7.20 (m, 4H), 6.85 (t, $J = 7.7$ Hz, 1H), 5.33 – 5.21 (m, 2H), 1.41 – 1.36 (m, 6H); ^{13}C NMR (101 MHz, $CDCl_3$) $\delta = 198.7, 169.9, 159.3, 135.8, 135.5, 129.5, 129.3, 128.9, 127.6, 125.9, 118.8, 113.1, 69.5, 58.0, 21.8$; ν_{max}/cm^{-1} (thin film) 3447, 2982, 1702, 1662; HRMS: Calculated for $C_{18}H_{19}O_4$ 299.1283 Found $[M+H]^+$: 299.1287 (1.3 ppm).

Isopropyl 3-phenylbenzofuran-7-carboxylate 5.1.61

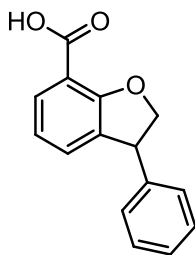
rac-Isopropyl 2-hydroxy-3-(2-oxo-1-phenylethyl)benzoate (1.587 g, 5.32 mmol) and *p*-TsOH (1.012 g, 5.32 mmol) were dissolved in PhMe (50 mL) and this was heated under reflux for 3 h. The reaction was then cooled to ambient temperature and sat. NaHCO_{3(aq)} (50 mL) and EtOAc (50 mL) were added. The layers were separated and the aqueous layer was extracted with EtOAc (3 × 50 mL). The combined organic layers were filtered through a hydrophobic frit and evaporated under reduced pressure to give a crude product. This was purified using column chromatography eluting with a gradient of 0-20 cyclohexane: EtOAc. Collected fractions were evaporated under reduced pressure to give isopropyl 3-phenylbenzofuran-7-carboxylate (1.117 g, 3.98 mmol, 75%) as yellow oil.

LCMS (Method B, UV, ESI) $R_t = 1.44$ [M-H]⁻ = No mass ion, 96%; ¹H NMR (400 MHz, CDCl₃) $\delta = 7.99$ (d, $J = 7.6$ Hz, 2H), 7.90 (s, 1H), 7.63 – 7.59 (m, 2H), 7.50 – 7.45 (m, 2H), 7.39 (td, $J = 1.7, 7.5$ Hz, 1H), 7.37 – 7.32 (m, 1H), 5.42 – 5.31 (m, 1H), 1.44 (d, $J = 6.4$ Hz, 6H); ¹³C NMR (101 MHz, CDCl₃) $\delta = 164.3, 154.3, 142.3, 131.4, 129.0, 128.3, 127.7, 126.9, 125.1, 122.7, 122.0, 116.3, 68.7, 22.0$ (1C not observed); $\nu_{\max}/\text{cm}^{-1}$ (thin film) 2980, 1709; HRMS: Calculated for C₁₈H₁₇O₃ 281.1178 Found [M+H]⁺: 281.1177 (-0.4 ppm).

***rac*-Isopropyl 3-phenyl-2,3-dihydrobenzofuran-7-carboxylate 5.1.27**

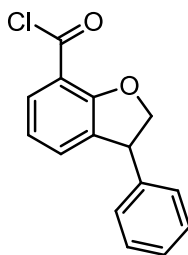
To Pd-C (Type 424) (0.729 g, 0.342 mmol) was added isopropyl 3-phenylbenzofuran-7-carboxylate (0.96 g, 3.42 mmol) in ethanol (50 mL). This was stirred under an atmosphere of hydrogen for 24 h using the hydrogenation suite apparatus. The reaction mixture was filtered through Celite and washed with EtOAc (20 mL). The filtrate was evaporated under reduced pressure to give *rac*-isopropyl 3-phenyl-2,3-dihydrobenzofuran-7-carboxylate (0.941 g, 3.33 mmol, 97%) as a yellow oil.

LCMS (Method B, UV, ESI) $R_t = 1.33$ $[M+H]^+ = 283.1$, 93%; ^1H NMR (400 MHz, CDCl_3) $\delta = 7.78 - 7.74$ (m, 1H), 7.33 – 7.29 (m, 2H), 7.28 – 7.23 (m, 1H), 7.21 – 7.18 (m, 2H), 7.13 (td, $J = 1.3, 7.2$ Hz, 1H), 6.86 (t, $J = 7.7$ Hz, 1H), 5.32 – 5.22 (m, 1H), 5.10 – 5.03 (m, 1H), 4.69 – 4.62 (m, 1H), 4.61 – 4.54 (m, 1H), 1.38 (d, $J = 6.4$ Hz, 6H); ^{13}C NMR (101 MHz, CDCl_3) $\delta = 164.6, 160.8, 142.3, 133.1, 130.1, 129.5, 128.9, 127.8, 127.2, 120.4, 114.1, 80.2, 68.1, 47.7, 22.0$; $\nu_{\text{max}}/\text{cm}^{-1}$ (thin film) 2979, 1714, 1701. Failed to ionise under high resolution mass spectrometry conditions.

***rac*-3-Phenyl-2,3-dihydrobenzofuran-7-carboxylic acid 5.1.62**

To *rac*-isopropyl 3-phenyl-2,3-dihydrobenzofuran-7-carboxylate (887 mg, 3.14 mmol) in 1,4-dioxane (15 mL) was added 2M LiOH_(aq) (4 mL, 8.00 mmol). This was stirred at 80 °C for 5 h. The reaction mixture was allowed to cool then 2M HCl_(aq) (40 mL) and EtOAc (40 mL) was added. The layers were separated and the aqueous layer was extracted with EtOAc (3 × 15 mL). The organic layers were combined, filtered through a hydrophobic frit and evaporated under reduced pressure to give an impure product. This was dissolved in EtOAc (50 mL) and MeOH (10 mL) and extracted with 2M NaOH_(aq) (3 × 25 mL). The aqueous layers were combined and extracted with EtOAc (25 mL). The aqueous layer was then acidified with HCl_(aq) (37.5%) and extracted with CH₂Cl₂ (4 × 50 mL). The organics were combined and filtered through a hydrophobic frit. The original organic layer still contained acid. This was extracted with 2M NaOH_(aq) (2 × 25 mL). These aqueous layers were combined and acidified using HCl_(aq) (37.5%). They were extracted with CH₂Cl₂ (4 × 25 mL). The organics were combined and filtered through a hydrophobic frit. This was then combined with the previous extraction and evaporated under reduced pressure to give *rac*-3-phenyl-2,3-dihydrobenzofuran-7-carboxylic acid (671 mg, 2.79 mmol, 89%) as a white solid.

M.p. 160 – 162 °C; LCMS (Method B, UV, ESI) R_t = 0.61 [M+H]⁺ = 241.2, 100%; ¹H NMR (400 MHz, CDCl₃) δ = 7.91 – 7.87 (m, 1H), 7.37 – 7.31 (m, 2H), 7.31 – 7.25 (m, 1H), 7.24 – 7.18 (m, 3H), 6.96 (t, *J* = 7.6 Hz, 1H), 5.13 (dd, *J* = 8.6, 9.3 Hz, 1H), 4.75 – 4.68 (m, 1H), 4.68 – 4.62 (m, 1H) (1H not observed, exchangeable); ¹³C NMR (101 MHz, CDCl₃) δ = 168.2, 160.3, 141.7, 132.7, 131.1, 130.8, 129.0, 127.8, 127.5, 121.3, 112.5, 80.7, 47.6; ν_{max}/cm⁻¹ (thin film) 2922, 2545 br, 1689, 1670; HRMS: Calculated for C₁₅H₁₃O₃ 241.0865 Found [M+H]⁺: 241.0863 (– 0.8 ppm).

***rac*-3-Phenyl-2,3-dihydrobenzofuran-7-carbonyl chloride 5.1.63**

To *rac*-3-phenyl-2,3-dihydrobenzofuran-7-carboxylic acid (600 mg, 2.497 mmol) dissolved in CH₂Cl₂ (10 mL) was added SOCl₂ (0.274 mL, 3.75 mmol). The reaction mixture was stirred for 6 h. The solvent was then evaporated off under reduced pressure. CH₂Cl₂ (5 mL) was then added and this was evaporated under reduced pressure to give crude *rac*-3-phenyl-2,3-dihydrobenzofuran-7-carbonyl chloride which was used directly in the subsequent esterifications.

LCMS (Method B, UV, ESI) R_t = 1.16 [M+H]⁺ = 255.2, 99%. Mass ion of methyl ester (LCMS sample dissolved in methanol)

***rac*-Methyl 3-phenyl-2,3-dihydrobenzofuran-7-carboxylate 5.1.9, *rac*-ethyl 3-phenyl-2,3-dihydrobenzofuran-7-carboxylate 5.1.26, *rac*-cyclobutyl 3-phenyl-2,3-dihydrobenzofuran-7-carboxylate 5.1.28, *rac*-1,1,1,3,3,3-hexafluoropropan-2-yl 3-phenyl-2,3-dihydrobenzofuran-7-carboxylate 5.1.30 and *rac*-2,2,2-trifluoroethyl 3-phenyl-2,3-dihydrobenzofuran-7-carboxylate 5.1.31**

Crude *rac*-3-phenyl-2,3-dihydrobenzofuran-7-carbonyl chloride (646 mg, 2.497 mmol) was dissolved in CH₂Cl₂ (6 mL) and partitioned into 6 equal fractions. To each reaction was added a different alcohol and was stirred for 16 h at ambient temperature:

Reaction 1: MeOH (0.101 mL, 2.497 mmol)

Reaction 2: EtOH (0.146 mL, 2.497 mmol)

Reaction 3: cyclobutanol (0.196 mL, 2.497 mmol).

Reaction 4: 1-methylcyclopropan-1-ol (0.142 mL, 2.497 mmol).

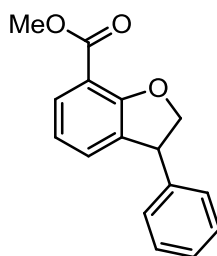
Reaction 5: HFIP (0.263 mL, 2.497 mmol).

Reaction 6: TFE (0.182 mL, 2.497 mmol).

Each reaction had the solvent removed under a stream of nitrogen and reaction 1 – 3 and 5 were purified using high pH MDAP (Reactions 1-3 using Method C, Reaction 5 using Method D). Reaction 4 produced no desired product.

Reaction 1: Gave *rac*-methyl 3-phenyl-2,3-dihydrobenzofuran-7-carboxylate (47 mg, 0.185 mmol, 44%) as a colourless oil.

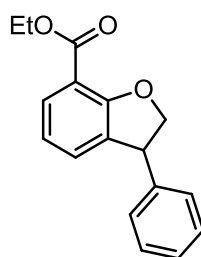
***rac*-Methyl 3-phenyl-2,3-dihydrobenzofuran-7-carboxylate 5.1.9**



LCMS (Method B, UV, ESI) $R_t = 1.17$ $[M+H]^+ = 255.1$, 100%; Data consistent with previous isolation.

Reaction 2: Gave *rac*-ethyl 3-phenyl-2,3-dihydrobenzofuran-7-carboxylate (68 mg, 0.253 mmol, 61%) as a colourless oil.

***rac*-Ethyl 3-phenyl-2,3-dihydrobenzofuran-7-carboxylate 5.1.26**

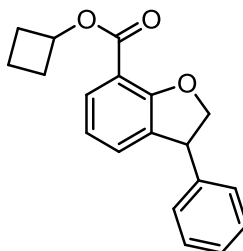


LCMS (Method B, UV, ESI) $R_t = 1.25$ $[M+H]^+ = 269.1$, 96%; $^1\text{H NMR}$ (400 MHz, CDCl_3) $\delta = 7.81 - 7.76$ (m, 1H), $7.34 - 7.29$ (m, 2H), $7.28 - 7.23$ (m, 1H), $7.21 - 7.17$ (m, 2H), 7.14 (td, $J = 1.2, 7.3$ Hz, 1H), 6.87 (t, $J = 7.6$ Hz, 1H), 5.06 (t, $J =$

9.0 Hz, 1H), 4.69 – 4.63 (m, 1H), 4.61 – 4.55 (m, 1H), 4.44 – 4.36 (m, 2H), 1.40 (t, $J = 7.1$ Hz, 3H); ^{13}C NMR (101 MHz, CDCl_3) $\delta = 165.2, 160.7, 142.2, 133.1, 130.2, 129.7, 128.9, 127.8, 127.2, 120.5, 113.7, 80.2, 60.8, 47.7, 14.4$; $\nu_{\text{max}}/\text{cm}^{-1}$ (thin film) 2981, 2898, 1704; HRMS: Calculated for $\text{C}_{17}\text{H}_{17}\text{O}_3$ 269.1178 Found $[\text{M}+\text{H}]^+$: 269.1186 (3.0 ppm).

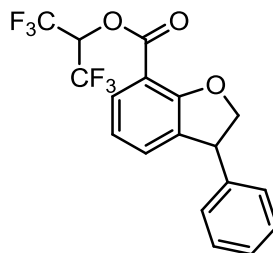
Reaction 3: Gave *rac*-cyclobutyl 3-phenyl-2,3-dihydrobenzofuran-7-carboxylate (80 mg, 0.272 mmol, 66%) as a colourless oil.

rac-Cyclobutyl 3-phenyl-2,3-dihydrobenzofuran-7-carboxylate 5.1.28



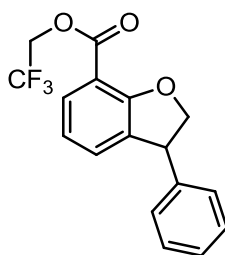
LCMS (Method B, UV, ESI) $R_t = 1.37$ $[\text{M}+\text{H}]^+ = 295.1$, 97%; ^1H NMR (400 MHz, CDCl_3) $\delta = 7.81 - 7.76$ (m, 1H), 7.34 – 7.29 (m, 2H), 7.28 – 7.23 (m, 1H), 7.21 – 7.17 (m, 2H), 7.14 (td, $J = 1.2, 7.3$ Hz, 1H), 6.87 (t, $J = 7.6$ Hz, 1H), 5.27 – 5.17 (m, 1H), 5.10 – 5.03 (m, 1H), 4.69 – 4.63 (m, 1H), 4.61 – 4.55 (m, 1H), 2.52 – 2.42 (m, 2H), 2.30 – 2.16 (m, 2H), 1.92 – 1.80 (m, 1H), 1.73 – 1.63 (m, 1H); ^{13}C NMR (101 MHz, CDCl_3) $\delta = 164.5, 160.8, 142.3, 133.1, 130.2, 129.7, 128.9, 127.8, 127.2, 120.4, 113.6, 80.2, 69.3, 47.7, 30.5, 30.4, 13.7$; $\nu_{\text{max}}/\text{cm}^{-1}$ (thin film) 2987, 2947, 1701; HRMS: Calculated for $\text{C}_{19}\text{H}_{19}\text{O}_3$ 295.1334 Found $[\text{M}+\text{H}]^+$: 295.1340 (2.0 ppm).

Reaction 5: Gave *rac*-1,1,1,3,3,3-hexafluoropropan-2-yl 3-phenyl-2,3-dihydrobenzofuran-7-carboxylate (47 mg, 0.120 mmol, 29%) as a yellow semi solid.

***rac*-1,1,1,3,3,3-Hexafluoropropan-2-yl 3-phenyl-2,3-dihydrobenzofuran-7-carboxylate 5.1.30**

LCMS (Method B, UV, ESI) $R_t = 1.46$ $[M-H]^- = 389.1$, 100%; 1H NMR (400 MHz, $CDCl_3$) $\delta = 7.84$ (d, $J = 7.8$ Hz, 1H), 7.37 – 7.31 (m, 2H), 7.31 – 7.24 (m, 2H), 7.23 – 7.18 (m, 2H), 6.94 (t, $J = 7.6$ Hz, 1H), 6.04 (spt, $J = 6.2$ Hz, 1H), 5.13 (t, $J = 8.7$ Hz, 1H), 4.74 – 4.61 (m, 2H); ^{13}C NMR (101 MHz, $CDCl_3$) $\delta = 162.2$, 161.1, 141.8, 133.8, 131.7, 130.3, 129.0, 127.8, 127.5, 120.9, 120.6 (q, $^1J_{C-F} = 282.4$ Hz), 109.8, 80.7, 66.5 (spt, $^2J_{C-F} = 34.5$ Hz), 47.6; ^{19}F NMR (376 MHz, $CDCl_3$) $\delta = -73.1$ (s, 6F); ν_{max}/cm^{-1} (thin film) 2967, 1744, 1193, 1105. Failed to ionise under high resolution mass spectrometry conditions.

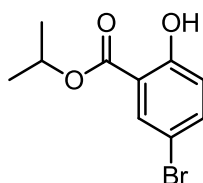
To reaction 6 was added CH_2Cl_2 (4 mL) and $NaHCO_3$ (2 mL). The layers were separated and the organic layer was filtered through a hydrophobic frit and the solvent evaporated under reduced pressure. This was then purified using high pH MDAP (Method C) to give *rac*-2,2,2-trifluoroethyl 3-phenyl-2,3-dihydrobenzofuran-7-carboxylate (70 mg, 0.217 mmol, 52%) as a yellow solid.

***rac*-2,2,2-Trifluoroethyl 3-phenyl-2,3-dihydrobenzofuran-7-carboxylate 5.1.31**

M.p. 72 – 74 °C; LCMS (Method B, UV, ESI) $R_t = 1.32$ $[M-H]^- =$ No mass ion, 91%; 1H NMR (400 MHz, $CDCl_3$) $\delta = 7.84$ – 7.78 (m, 1H), 7.36 – 7.30 (m, 2H), 7.29 – 7.24 (m, 1H), 7.23 – 7.17 (m, 3H), 6.93 – 6.88 (m, 1H), 5.13 – 5.06 (m, 1H), 4.75 –

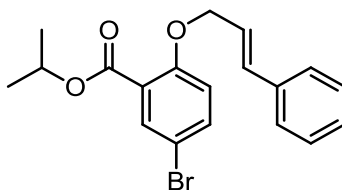
4.67 (m, 3H), 4.64 – 4.59 (m, 1H); ^{13}C NMR (101 MHz, CDCl_3) δ = 163.2, 161.4, 142.0, 133.5, 130.8, 130.3, 129.0, 127.8, 127.4, 123.2 (q, $^1J_{\text{C-F}}$ = 277.3 Hz), 120.7, 111.5, 80.5, 60.5 (q, $^2J_{\text{C-F}}$ = 36.7 Hz), 47.6; ^{19}F NMR (376 MHz, CDCl_3) δ = -73.5 (s, 3F); $\nu_{\text{max}}/\text{cm}^{-1}$ (thin film) 2972, 1732, 1153; HRMS: Calculated for $\text{C}_{17}\text{H}_{14}\text{F}_3\text{O}_3$ 323.0895 Found $[\text{M}+\text{H}]^+$: 323.0892 (- 0.9 ppm).

Isopropyl 5-bromo-2-hydroxybenzoate 5.1.65



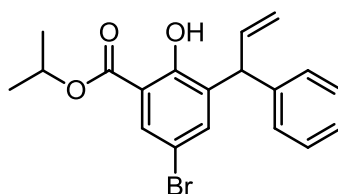
To methyl 5-bromo-2-hydroxybenzoate (5.035 g, 21.79 mmol) in isopropanol (30 mL) and 2-MeTHF (20 mL) was added TBD (0.903 g, 6.49 mmol). The reaction mixture was stirred at 80 °C for 4 h. 2M $\text{HCl}_{(\text{aq})}$ (20 mL) and EtOAc (50 mL) were added. The layers were separated and the aqueous layer was extracted with EtOAc (3×25 mL). The combined organic layers were filtered through a hydrophobic frit and evaporated under reduced pressure to give isopropyl 5-bromo-2-hydroxybenzoate (5.450 g, 21.03 mmol, 97%) as a white solid.

M.p. 61 – 63 °C; LCMS (Method B, UV, ESI) R_t = 1.39 $[\text{M}-\text{H}]^-$ = 257.0, 259.1, 94%; ^1H NMR (400 MHz, $\text{DMSO}-d_6$) δ = 10.61 (s, 1H), 7.82 (d, J = 2.5 Hz, 1H), 7.64 (dd, J = 2.5, 8.8 Hz, 1H), 6.95 (d, J = 8.8 Hz, 1H), 5.23 – 5.12 (m, 1H), 1.33 (d, J = 6.3 Hz, 6H); ^{13}C NMR (101 MHz, $\text{DMSO}-d_6$) δ = 166.9, 159.1, 137.7, 131.7, 119.8, 115.6, 110.0, 69.6, 21.4; $\nu_{\text{max}}/\text{cm}^{-1}$ (thin film) 3205 br, 2982, 1691.

Isopropyl 5-bromo-2-(cinnamyloxy)benzoate 5.1.66

Isopropyl 5-bromo-2-hydroxybenzoate (3.07 g, 11.85 mmol), potassium carbonate (3.26 g, 23.59 mmol), potassium iodide (0.200 g, 1.205 mmol) and (E)-(3-chloroprop-1-en-1-yl)benzene (2 mL, 14.36 mmol) were refluxed in acetone (70 mL) for 16 h. 2M HCl_(aq) (75 mL) and EtOAc (100 mL) were added. The layers were separated and the aqueous layer was extracted with EtOAc (3 × 50 mL). The combined organic layers were filtered through a hydrophobic frit and the solvent evaporated under reduced pressure to give crude product. Brine (50 mL) and EtOAc (50 mL) were added, the layers separated and the aqueous layer was extracted with EtOAc (50 mL). The combined organics were filtered through a hydrophobic frit and the solvent evaporated under reduced pressure to give crude product. This was purified using column chromatography eluting with a gradient of 0-20 cyclohexane: EtOAc. Collected fractions were evaporated under reduced pressure to give isopropyl 5-bromo-2-(cinnamyloxy)benzoate (4.201 g, 11.19 mmol, 94%) as a yellow oil.

LCMS (Method B, UV, ESI) $R_t = 1.53$ [M-H]⁻ = No mass ion, 94%; ¹H NMR (400 MHz, CDCl₃) $\delta = 7.86$ (d, $J = 2.7$ Hz, 1H), 7.51 (dd, $J = 2.6, 8.9$ Hz, 1H), 7.41 – 7.37 (m, 2H), 7.35 – 7.30 (m, 2H), 7.28 – 7.23 (m, 1H), 6.89 (d, $J = 9.0$ Hz, 1H), 6.80 – 6.74 (m, 1H), 6.39 (td, $J = 5.6, 16.0$ Hz, 1H), 5.25 (m, 1H), 4.75 (dd, $J = 1.6, 5.5$ Hz, 2H), 1.36 (d, $J = 6.1$ Hz, 6H); ¹³C NMR (101 MHz, CDCl₃) $\delta = 164.5, 157.1, 136.3, 135.5, 133.9, 133.2, 128.6, 128.0, 126.6, 123.7, 123.5, 115.8, 112.7, 69.9, 68.8, 21.9$; $\nu_{\max}/\text{cm}^{-1}$ (thin film) 2980, 2916, 1702. Failed to ionise under high resolution mass spectrometry conditions.

***rac*-Isopropyl 5-bromo-2-hydroxy-3-(1-phenylallyl)benzoate 5.1.67**

Isopropyl 5-bromo-2-(cinnamyloxy)benzoate (1.554 g, 4.14 mmol) was dissolved in *N,N*-dimethylaniline (20 mL) and heated at 200 °C. Solution turned black after reaching 200 °C, reduced to 180 °C and heated for 30 h. Et₂O (35 mL) and cold HCl_(aq) (25% w/w, 20 mL) were added. The solution was stirred vigorously and then the layers were separated. The aqueous layer was extracted with Et₂O (3 × 20 mL). The combined organic layers were filtered through a hydrophobic frit then the solvent evaporated under reduced pressure. HCl_(aq) (25% w/w, 20 mL) and Et₂O (20 mL) were added and the layers were separated. The aqueous layer was extracted with Et₂O (3 × 20 mL). The organic layers were combined, filtered through a hydrophobic frit and the solvent was evaporated under reduced pressure to give a crude product. This was purified using column chromatography eluting with a gradient of 0-20 cyclohexane: EtOAc. Collected fractions were evaporated under reduced pressure to give *rac*-isopropyl 5-bromo-2-hydroxy-3-(1-phenylallyl)benzoate (1.289 g, 3.435 mmol, 83%) as a colourless oil.

LCMS (Method B, UV, ESI) R_t = 1.70 [M-H]⁻ = 373.1, 375.2, 83%; ¹H NMR (400 MHz, CDCl₃) δ = 11.25 (s, 1H), 7.85 (d, *J* = 2.4 Hz, 1H), 7.40 (d, *J* = 2.4 Hz, 1H), 7.33 – 7.27 (m, 2H), 7.24 – 7.17 (m, 3H), 6.30 – 6.21 (m, 1H), 5.31 – 5.22 (m, 2H), 5.19 – 5.15 (m, 1H), 4.95 (td, *J* = 1.5, 17.1 Hz, 1H), 1.40 – 1.35 (m, 6H); ¹³C NMR (101 MHz, CDCl₃) δ = 169.0, 158.4, 141.6, 139.0, 137.6, 134.2, 130.4, 128.6, 128.4, 126.6, 117.1, 114.2, 110.5, 69.9, 47.1, 21.8; ν_{max}/cm⁻¹ (thin film) 3085 br, 2982, 1667.

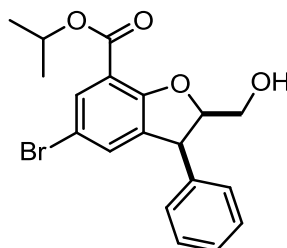
***rel*-(2*R*,3*S*)-Isopropyl 5-bromo-2-(hydroxymethyl)-3-phenyl-2,3-dihydrobenzofuran-7-carboxylate 5.1.68, *rel*-(2*R*,3*R*)-methyl 5-bromo-2-(hydroxymethyl)-3-phenyl-2,3-dihydrobenzofuran-7-carboxylate 5.1.70 and *rel*-(2*R*,3*S*)-methyl 5-bromo-2-(hydroxymethyl)-3-phenyl-2,3-dihydrobenzofuran-7-carboxylate 5.1.71**

To *rac*-isopropyl 5-bromo-2-hydroxy-3-(1-phenylallyl)benzoate (4.027 g, 10.73 mmol) in CH₂Cl₂ (50 mL) was added mCPBA (4.3 g, 19.19 mmol). This was stirred at ambient temperature for 24 h. 5% Na₂S₂O_{5(aq)} (50 mL), and CH₂Cl₂ (50 mL) were added. The layers were separated and the aqueous layer was extracted with CH₂Cl₂ (3 × 50 mL). The combined organic layers were filtered through a hydrophobic frit and evaporated under reduced pressure to give a crude product. The crude solid was dissolved in DMSO (35 mL). This was cooled to 0 °C and then KOH (0.925 g, 16.49 mmol) in water (10 mL) was added. This was allowed to warm to ambient temperature and stirred for 16 h. 2M HCl_(aq) (40 mL), and EtOAc (80 mL) were added and the layers were separated. The aqueous layer was extracted with EtOAc (3 × 30 mL). The combined organics were filtered through a hydrophobic frit and the solvent evaporated under reduced pressure to give a crude product. This was purified using column chromatography eluting with a gradient of 0-50 cyclohexane: EtOAc. Collected fraction 1 was impure and purified further. Collected fraction 2 was evaporated under reduced pressure to give *rel*-(2*R*,3*S*)-isopropyl 5-bromo-2-(hydroxymethyl)-3-phenyl-2,3-dihydrobenzofuran-7-carboxylate (332 mg, 0.849 mmol, 8%) as a yellow semi solid.

rel-(2*R*,3*S*)-Isopropyl

5-bromo-2-(hydroxymethyl)-3-phenyl-2,3-

dihydrobenzofuran-7-carboxylate 5.1.68

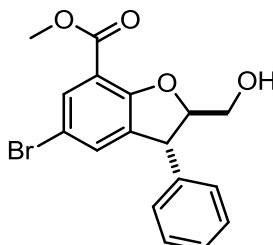


LCMS (Method B, UV, ESI) $R_t = 1.32$ $[M-H]^- = 389.2, 391.2, 95\%$; 1H NMR (400 MHz, $CDCl_3$) $\delta = 7.90$ (dd, $J = 0.7, 2.2$ Hz, 1H), 7.34 – 7.27 (m, 4H), 7.06 – 7.02 (m, 2H), 5.24 (td, $J = 6.2, 12.5$ Hz, 1H), 5.17 (ddd, $J = 3.9, 8.3, 9.4$ Hz, 1H), 4.75 (d, $J = 9.3$ Hz, 1H), 3.56 – 3.49 (m, 1H), 3.32 (dd, $J = 3.9, 12.5$ Hz, 1H), 2.66 (br. s., 1H), 1.38 (dd, $J = 2.9, 6.1$ Hz, 6H); ^{13}C NMR (101 MHz, $CDCl_3$) $\delta = 163.3, 159.4, 136.9, 135.2, 132.8, 132.7, 128.9, 128.7, 127.8, 115.4, 112.3, 88.5, 68.9, 62.7, 48.9, 21.9$; ν_{max}/cm^{-1} (thin film) 3469 br, 2980, 2935, 1702; HRMS: Calculated for $C_{19}H_{20}BrO_4$ 391.0545 Found $[M+H]^+$: 391.0547 (0.5 ppm).

Fraction 1 was purified using column chromatography eluting with a gradient of 30-50 cyclohexane: EtOAc. Collected fractions still contained impurity. 1,4-Dioxane (30 mL) and 2M $LiOH_{(aq)}$ (10 mL) was added to the crude material. This was heated at 60 °C for 16 h. 2M $HCl_{(aq)}$ (20 mL) and EtOAc (40 mL) were added and the layers were separated. The aqueous layer was extracted with EtOAc (3 × 20 mL). The combined organic layers were filtered through a hydrophobic frit and the solvent evaporated under reduced pressure. MeOH (30 mL) and HCl (3M in MeOH) (10 mL) was added and stirred for 16 h at ambient temperature. The solvent was evaporated under reduced pressure to give a crude product. This was purified using column chromatography eluting with a gradient of 40-60 cyclohexane: EtOAc. Collected fraction 3 was evaporated under reduced pressure to give *rel*-(2*R*,3*R*)-methyl 5-bromo-2-(hydroxymethyl)-3-phenyl-2,3-dihydrobenzofuran-7-carboxylate (580 mg, 1.597 mmol, 15%) as a white semi solid.

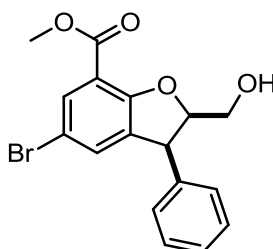
Collected fraction 4 was evaporated under reduced pressure to give *rel*-(2*R*,3*S*)-methyl 5-bromo-2-(hydroxymethyl)-3-phenyl-2,3-dihydrobenzofuran-7-carboxylate (47 mg, 0.129 mmol, 1%) as a white solid.

***rel*-(2*R*,3*R*)-Methyl 5-bromo-2-(hydroxymethyl)-3-phenyl-2,3-dihydrobenzofuran-7-carboxylate 5.1.70**



LCMS (Method B, UV, ESI) $R_t = 1.18$ $[M-H]^- = 361.0, 363.1, 88\%$; 1H NMR (400 MHz, $CDCl_3$) $\delta = 7.87$ (d, $J = 1.5$ Hz, 1H), 7.40 – 7.26 (m, 3H), 7.22 – 7.08 (m, 3H), 4.84 (td, $J = 3.8, 7.9$ Hz, 1H), 4.55 (d, $J = 8.3$ Hz, 1H), 4.05 (dd, $J = 2.7, 12.7$ Hz, 1H), 3.90 (s, 3H), 3.84 – 3.76 (m, 1H) (1H not observed, exchangeable); ^{13}C NMR (101 MHz, $CDCl_3$) $\delta = 164.5, 159.2, 140.7, 135.8, 132.7, 132.6, 129.1, 128.2, 127.7, 114.3, 112.4, 93.7, 62.7, 52.2, 48.8$; ν_{max}/cm^{-1} (thin film) 3445 br, 2950, 1710; HRMS: Calculated for $C_{17}H_{16}BrO_4$ 363.0232 Found $[M+H]^+$: 363.0237 (1.4 ppm).

***rel*-(2*R*,3*S*)-Methyl 5-bromo-2-(hydroxymethyl)-3-phenyl-2,3-dihydrobenzofuran-7-carboxylate 5.1.71**



M.p. 94 – 96 °C; LCMS (Method B, UV, ESI) $R_t = 1.16$ $[M-H]^- = 361.0, 363.1, 91\%$; 1H NMR (400 MHz, $CDCl_3$) $\delta = 7.95 - 7.92$ (m, 1H), 7.37 – 7.27 (m, 4H), 7.06 – 7.02 (m, 2H), 5.17 (ddd, $J = 4.0, 8.1, 9.4$ Hz, 1H), 4.75 (d, $J = 9.5$ Hz, 1H), 3.93 – 3.88 (m, 3H), 3.53 (dd, $J = 8.1, 12.5$ Hz, 1H), 3.35 (dd, $J = 3.9, 12.5$ Hz, 1H) (1H not

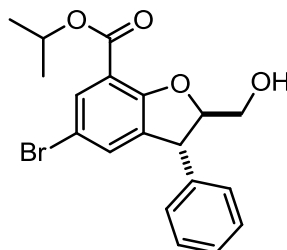
observed, exchangeable); ^{13}C NMR (101 MHz, CDCl_3) δ = 164.4, 159.2, 136.9, 135.2, 133.0, 132.9, 128.84, 128.75, 127.9, 114.6, 112.5, 88.5, 62.6, 52.2, 48.9; $\nu_{\text{max}}/\text{cm}^{-1}$ (thin film) 3536 br, 3372 br, 3195 br, 2962, 2850, 1712; HRMS: Calculated for $\text{C}_{17}\text{H}_{16}\text{BrO}_4$ 363.0232 Found $[\text{M}+\text{H}]^+$: 363.0240 (2.2 ppm).

***rel*-(2*R*,3*R*)-Isopropyl 5-bromo-2-(hydroxymethyl)-3-phenyl-2,3-dihydrobenzofuran-7-carboxylate 5.1.72 and *rel*-(2*R*,3*S*)-isopropyl 5-bromo-2-(hydroxymethyl)-3-phenyl-2,3-dihydrobenzofuran-7-carboxylate 5.1.68**

To *rac*-isopropyl 5-bromo-2-hydroxy-3-(1-phenylallyl)benzoate (2.131 g, 5.68 mmol) in CH_2Cl_2 (30 mL) was added mCPBA (2.291 g, 10.22 mmol). This was stirred for 18 h at ambient temperature. Further mCPBA (350 mg) was added and the reaction mixture was stirred for a further 4 h. 5% $\text{Na}_2\text{S}_2\text{O}_5(\text{aq})$ (30 mL) and CH_2Cl_2 (50 mL) were added. The layers were separated and the aqueous layer was extracted with CH_2Cl_2 (3×50 mL). The combined organic layers were filtered through a hydrophobic frit and the solvent evaporated under reduced pressure. The crude solid was dissolved in DMSO (50 mL) and then KOH (0.478 g, 8.52 mmol) in water (15 mL) was added. This was stirred for 4 h at ambient temperature. Further KOH (392 mg) was added and then stirred for 72 h. 2M $\text{HCl}(\text{aq})$ (20 mL) and EtOAc (100 mL) were added. The layers were separated and the organic layer was extracted with 5% $\text{LiCl}(\text{aq})$ (50 mL). The aqueous layer was then extracted with EtOAc (50 mL) and this organic was then extracted with 5% $\text{LiCl}(\text{aq})$ (50 mL). The two organic layers were combined and filtered through a hydrophobic frit. The organic layer was then washed with sat. $\text{NaHCO}_3(\text{aq})$ (3×50 mL). The organic layer was then filtered through a hydrophobic frit and evaporated under reduced pressure to give a crude yellow oil. This was purified using column chromatography eluting with a gradient of 40-60 cyclohexane: EtOAc. Collected fraction 1 was evaporated under reduced pressure to give *rel*-(2*R*,3*R*)-isopropyl 5-bromo-2-(hydroxymethyl)-3-phenyl-2,3-dihydrobenzofuran-7-carboxylate (741 mg, 1.894 mmol, 33%) as a yellow semi solid.

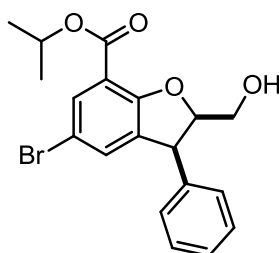
Collected fraction 2 was evaporated under reduced pressure to give *rel*-(2*R*,3*S*)-isopropyl 5-bromo-2-(hydroxymethyl)-3-phenyl-2,3-dihydrobenzofuran-7-carboxylate (806 mg, 2.060 mmol, 36%) as a yellow semi solid.

***rel*-(2*R*,3*R*)-Isopropyl 5-bromo-2-(hydroxymethyl)-3-phenyl-2,3-dihydrobenzofuran-7-carboxylate 5.1.72**

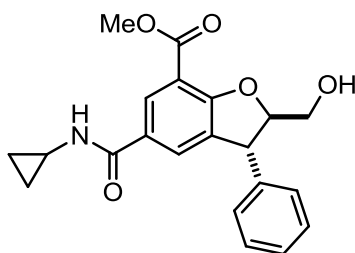


LCMS (Method B, UV, ESI) $R_t = 1.34$ $[M-H]^- = 389.1, 391.1, 91\%$; 1H NMR (400 MHz, $CDCl_3$) $\delta = 7.86 - 7.84$ (m, 1H), $7.43 - 7.27$ (m, 3H), $7.22 - 7.17$ (m, 3H), 5.24 (m, 1H), 4.86 (ddd, $J = 2.9, 4.6, 8.1$ Hz, 1H), 4.55 (d, $J = 8.3$ Hz, 1H), 4.05 (dd, $J = 2.9, 12.7$ Hz, 1H), 3.81 (dd, $J = 4.6, 12.7$ Hz, 1H), 3.48 (s, 1H), 1.38 (d, $J = 6.4$ Hz, 6H); ^{13}C NMR (101 MHz, $CDCl_3$) $\delta = 163.5, 159.4, 140.8, 135.7, 132.5, 132.3, 129.1, 128.2, 127.7, 115.1, 112.3, 93.7, 68.9, 62.8, 48.8, 21.9$; ν_{max}/cm^{-1} (thin film) 3451 br, 2980, 2935, 1702; HRMS: Calculated for $C_{19}H_{20}BrO_4$ 391.0545 Found $[M+H]^+$: 391.0547 (0.5 ppm).

***rel*-(2*R*,3*S*)-Isopropyl 5-bromo-2-(hydroxymethyl)-3-phenyl-2,3-dihydrobenzofuran-7-carboxylate 5.1.68**



LCMS (Method B, UV, ESI) $R_t = 1.32$ $[M-H]^- = 389.1, 391.0, 100\%$; Consistent with previous isolation

***rel*-(2*R*,3*R*)-Methyl 5-(cyclopropylcarbamoyl)-2-(hydroxymethyl)-3-phenyl-2,3-dihydrobenzofuran-7-carboxylate 5.1.73**

rel-(2*R*,3*R*)-Methyl 5-bromo-2-(hydroxymethyl)-3-phenyl-2,3-dihydrobenzofuran-7-carboxylate (300 mg, 0.826 mmol), XantPhos Pd G3 (50 mg, 0.053 mmol), and 2,6-dimethylpyridine (0.192 mL, 1.652 mmol) were dissolved in cyclopropylamine (8 mL) and heated at 50 °C for 20 h under a carbon monoxide atmosphere. The reaction mixture was filtered through a hydrophobic frit and the solvent evaporated under reduced pressure to give a crude product. The crude material was purified using column chromatography eluting with 0-100 cyclohexane:ethyl acetate. Impure fractions containing product were combined and purified using a high pH MDAP (Method B) to give *rel*-(2*R*,3*R*)-methyl 5-(cyclopropylcarbamoyl)-2-(hydroxymethyl)-3-phenyl-2,3-dihydrobenzofuran-7-carboxylate (19 mg, 0.052 mmol, 6%) as a yellow solid.

M.p. 99 – 101 °C; LCMS (Method B, UV, ESI) $R_t = 0.87$ $[M+H]^+ = 368.1$, 100%; ^1H NMR (400 MHz, CDCl_3) $\delta = 8.06$ (d, $J = 1.5$ Hz, 1H), 7.54 – 7.51 (m, 1H), 7.36 – 7.24 (m, 3H), 7.16 – 7.12 (m, 2H), 6.44 (br. s., 1H), 4.86 (ddd, $J = 3.2, 4.3, 7.7$ Hz, 1H), 4.52 (d, $J = 8.1$ Hz, 1H), 4.07 (dd, $J = 2.2, 12.5$ Hz, 1H), 3.91 (s, 3H), 3.79 (dd, $J = 2.9, 12.7$ Hz, 1H), 3.25 (br. s., 1H), 2.83 (dt, $J = 3.4, 7.1$ Hz, 1H), 0.85 – 0.76 (m, 2H), 0.62 – 0.55 (m, 2H); ^{13}C NMR (101 MHz, CDCl_3) $\delta = 167.5, 165.2, 162.3, 141.0, 134.2, 129.4, 129.1, 128.9, 128.2, 127.6, 127.4, 112.3, 94.1, 62.7, 52.2, 48.5, 23.2, 6.60, 6.57$; $\nu_{\text{max}}/\text{cm}^{-1}$ (thin film) 3302 br, 2951, 1710, 1635; HRMS: Calculated for $\text{C}_{21}\text{H}_{22}\text{NO}_5$ 368.1498 Found $[M+H]^+$: 368.1494 (– 1.1 ppm).

8.0 Assay protocols

8.1 Lp-PLA₂ and PLA₂-VIIB Biological Assay Information

1-*O*-Hexadecyl-2-deoxy-2-thio-*S*-acetyl-*sn*-glyceryl-3-phosphorylcholine (2-thio-PAF) is a substrate for PAF-hydrolases (PAF-AH) commercially available from Cayman Chemical. Upon cleavage with PAF-AH, the free thiol is released at the *sn*-2 position and can then react with 7-diethylamino-3-(4'-maleimidylphenyl)-4-methylcoumarin (CPM) a thiol-reactive coumarin. This reaction (Michael addition) results in an increase in fluorescence. Inhibitors of PLA₂ therefore prevent this cleavage and no fluorescent increase is observed.

8.2 Lipoprotein-associated phospholipase A₂ (Lp-PLA₂) Human Plasma

The human plasma assay utilizes the same thioester analog of PAF as described in the HR thioPAF assay. This assay may detect the activity of Lp-PLA₂ in human plasma, as determined by specific inhibition by Lp-PLA₂ inhibitors.

The thio-PAF assay was run as a quenched 20 µL assay. The compounds source plate was prepared by making 1:3 (by volume) serial dilution of the compounds into pure DMSO on a 96-well microplate. 5 µL of compounds on the compound source plate were transferred to 96-well Corning 3686 (black) low-volume plates by a STAR+ (Hamilton) liquid dispenser. 10 µL pooled human plasma, which was previously aliquoted and frozen, was added. Plates were centrifuged for 30 sec at 1000 rpm. After 15 minutes preincubation at room temperature, 5 µL of the substrate solution comprising 2 mM 2-thio-PAF [from ethanol stock], 52 µM CPM [from a DMSO stock] and 2.5 mM NEM (*N*-ethylmaleimide) [made fresh daily in DMSO] in assay buffer (50mM HEPES, pH 7.4, 150 mM NaCl, 1 mM CHAPS) was added to 96-well Corning 3686 (black) low-volume plates. After 3 mins, the reaction was quenched with 10 µL of 5% aqueous trifluoroacetic acid (TFA). The plates were centrifuged 30 sec at 1000 rpm, covered to protect from light and incubated for 10 min at room temperature. Plates were read at ex: 380 nm / em: 485 nm using an Envision plate reader (Perkin Elmer). Raw data were transferred to Excel software

and pIC₅₀ data, curve, and QC analysis was conducted by using the XL fit module in Excel.

IC₅₀ values quoted correspond to the IC₅₀ value after 20 minutes unless otherwise indicated.

8.3 CLND Solubility

Solubility was determined by precipitation of 10 mM DMSO stock concentration to 5% DMSO pH7.4 phosphate buffered saline, with quantification by ChemiLuminescent Nitrogen Detection.

8.4 FaSSIF solubility

Compounds were dissolved in DMSO at 2.5 mg/mL and then diluted in Fast State Simulated Intestinal Fluid (FaSSIF pH 6.5) at 125 µg/mL (final DMSO concentration is 5%). After 16h of incubation at 25°C, the suspension was filtered. The concentration of the compound was determined by a fast HPLC gradient. The ratio of the peak areas obtained from the standards and the sample filtrate was used to calculate the solubility of the compound.

8.5 ChromLogD_{7.4}

Carried out according to literature protocols,²⁴³ using a Waters Aquity UPLC System, Phenomenex Gemini NX 50x2 mm, 3 µm HPLC column, 0-100% pH 7.40 ammonium acetate buffer/acetonitrile gradient. Retention time was compared to standards of known pH to derive Chromatographic Hydrophobicity Index (CHI).
ChromLogD = 0.0857CHI – 2.

8.6 Artificial membrane permeability measurement.

Permeability across a lipid membrane was measured using the published protocol.²⁴⁴

8.7 BET Assays

BET proteins were produced using protocols given in the literature.²⁰³ Compounds were screened against either 6H-Thr Brd4 (1-477) (Y390A) (Brd4 BD2 mutation to monitor compound binding to BD1) or 6H-Thr Brd4 (1-477) (Y97A) (Brd4 BD1

mutation to monitor compound binding to BD2) in a dose-response format in a TR-FRET assay measuring competition between test compound and an Alexa Fluor 647 derivative of I-BET762.1 Compounds were titrated from 10 mM in 100% DMSO and 50 nL transferred to a low volume black 384 well micro titre plate using a Labcyte Echo 555. A Thermo Scientific Multidrop Combi was used to dispense 5 μ L of 20 nM protein in an assay buffer of 50 mM HEPES, 150 mM NaCl, 5% glycerol, 1 mM DTT and 1 mM CHAPS, pH 7.4, and in the presence of 100 nM fluorescent ligand ($\sim Kd$ concentration for the interaction between Brd4 BD1 and ligand). After equilibrating for 30 min in the dark at rt, the bromodomain protein:fluorescent ligand interaction was detected using TR-FRET following a 5 μ L addition of 3 nM europium chelate labelled anti-6His antibody (Perkin Elmer, W1024, AD0111) in assay buffer. Time resolved fluorescence (TRF) was then detected on a TRF laser equipped Perkin Elmer Envision multimode plate reader (excitation = 337 nm; emission 1 = 615 nm; emission 2 = 665 nm; 317 dual wavelength bias dichroic = 400 nm, 630 nm). TR-FRET ratio was calculated using the following equation: Ratio = ((Acceptor fluorescence at 665 nm) / (Donor fluorescence at 615 nm)) * 1000. TR-FRET ratio data was normalised to high (DMSO) and low (compound control derivative of I-BET762) controls and IC_{50} values determined for each of the compounds tested by fitting the fluorescence ratio data to a four parameter model: $y = a + ((b - a) / (1 + (10^x / 10^c)^d))$ where 'a' is the minimum, 'b' is the Hill slope, 'c' is the IC_{50} and 'd' is the maximum.

8.8 X-ray crystallography

Materials and methods

Lp-PLA₂ (residues 46-428 with a C-terminal His6 tag) was expressed, purified and crystallised essentially as previously described²⁴⁵ though the purified protein was concentrated to 15mg/mL for crystallisation. To obtain the protein complex structure with **analogue-5**, a crystal was soaked in 30% PEG3350, 0.1 M HEPES pH 7.3, 0.2 M NaCl, 0.04% pluronic F68, 10 mM CHAPS and 2mM compound dissolved in DMSO for ~1 day.

The crystal was cryoprotected by briefly soaking in well buffer with 10% glycerol. A diffraction dataset was acquired at 100 K at the ESRF (station ID29) using a Pilatus 6M detector, and processed by the synchrotron autoprocessing suite (XDS_PARALLELPROC)²⁴⁶ using XDS.²⁴⁷ Data were merged using AIMLESS²⁴⁸ within the CCP4 programming suite.²⁴⁹

The crystal structure was solved by Fourier Synthesis using REFMAC²⁵⁰ and a previously determined in-house Lp-PLA₂ crystal structure as the starting model. Refinement was carried out with REFMAC and model building using COOT.²⁵¹ The final R_{factor} (and R_{free}) achieved were 16.2% (and 19.2%) and the structure was deposited into the PDB as entry 5LP1.

Table of Statistics

Lp-PLA ₂	Analogue 5
PARAMETER^a	
DATA COLLECTION	
Space Group	C2
Cell Dimensions	
a,b,c (Å)	100.28,91.56,51.65
α, β, γ (°)	90.00,111.88, 90.00
Resolution (Å)	1.91 (1.98)
R_{merge}^b	0.094 (0.624)
Average $I/\sigma I$	7.8 (1.7)
Completeness (%)	98.7 (92.5)
Redundancy	3.4 (3.2)
No. Reflections	112961 (9618)
No. Unique Reflections	33162 (3045)
REFINEMENT	
Resolution (Å)	20.00-1.91
$R_{\text{work}}/R_{\text{free}}$	0.162/0.192
No. Reflections	31474
No. atoms	
Protein (chain A)	3040
Cmpd (L)	46
Water (W)	332
Cl (C)	2
B-factors [Å²]	
Protein (chain A)	35.3
Cmpd (L)	37.0
Water (W)	47.4
Cl (C)	36.5
R.m.s deviations	
Bond lengths (Å)	0.007
Bond angles (°)	1.386

^a Data for the highest resolution shell are given in parentheses.

^b $R_{\text{merge}} = \sum |I_j - \langle I_j \rangle| / \sum \langle I_j \rangle$.

9.0 References

- (1) Rosenson, R. S.; Stafforini, D. M. *J. Lipid Res.* **2012**, *53* (9), 1767–1782.
- (2) Libby, P. *Circulation* **2002**, *105* (9), 1135–1143.
- (3) Gu, L.; Okada, Y.; Clinton, S. K.; Gerard, C.; Sukhova, G. K.; Libby, P.; Rollins, B. J. *Mol. Cell* **1998**, *2* (2), 275–281.
- (4) Burke, J. E.; Dennis, E. A. *Cardiovasc Drugs Ther.* **2009**, *23* (1), 49–71.
- (5) Schaloske, R. H.; Dennis, E. A. *Biochim. Biophys. Acta - Mol. Cell Biol. Lipids* **2006**, *1761* (11), 1246–1259.
- (6) Samanta, U.; Bahnson, B. J. *J. Biol. Chem.* **2008**, *283* (46), 31617–31624.
- (7) Kriska, T.; Marathe, G. K.; Schmidt, J. C.; McIntyre, T. M.; Girotti, A. W. *J. Biol. Chem.* **2007**, *282* (1), 100–108.
- (8) Stafforini, D. M.; Sheller, J. R.; Blackwell, T. S.; Sapirstein, A.; Yull, F. E.; McIntyre, T. M.; Bonventre, J. V.; Prescott, S. M.; Roberts, L. J. *J. Biol. Chem.* **2006**, *281* (8), 4616–4623.
- (9) Stafforini, D. M.; McIntyre, T. M.; Carter, M. E.; Prescott, S. M. *J. Biol. Chem.* **1987**, *262* (9), 4215–4222.
- (10) Stremmler, K. E.; Stafforini, D. M.; Prescott, S. M.; McIntyre, T. M. *J. Biol. Chem.* **1991**, *266* (17), 11095–11103.
- (11) Steinbrecher, U. P.; Pritchard, P. H. *J. Lipid Res.* **1989**, *30* (3), 305–315.
- (12) Marathe, G. K.; Harrison, K. A.; Murphy, R. C.; Prescott, S. M.; Zimmerman, G. A.; McIntyre, T. M. *Free Radic. Biol. Med.* **2000**, *28* (12), 1762–1770.
- (13) Stafforini, D. M.; Prescott, S. M.; McIntyre, T. M.; Zimmerman, G. A. *J. Biol. Chem.* **1990**, *265* (17), 9682–9687.
- (14) Olofsson, K. E.; Andersson, L.; Nilsson, J.; Björkbacka, H. *Biochem. Biophys. Res. Commun.* **2008**, *370* (2), 348–352.
- (15) White, H. *Curr. Opin. Cardiol.* **2010**, *25* (4), 299–301.
- (16) The LpPLA2 Studies Collaboration. *Lancet* **2010**, *375* (9725), 1536–1544.
- (17) Kiechl, S.; Willeit, J.; Mayr, M.; Viehweider, B.; Oberhollenzer, M.; Kronenberg, F.; Wiedermann, C. J.; Oberthaler, S.; Xu, Q.; Witztum, J. L.; Tsimikas, S. *Arterioscler. Thromb. Vasc. Biol.* **2007**, *27* (8), 1788–1795.
- (18) Tsimikas, S.; Mallat, Z.; Talmud, P. J.; Kastelein, J. J. P.; Wareham, N. J.; Sandhu, M. S.; Miller, E. R.; Benessiano, J.; Tedgui, A.; Witztum, J. L.; Khaw, K.-T.; Boekholdt, S. M. *J. Am. Coll. Cardiol.* **2010**, *56* (12), 946–955.
- (19) Ryu, S. K.; Mallat, Z.; Benessiano, J.; Tedgui, A.; Olsson, A. G.; Bao, W.; Schwartz, G. G.; Tsimikas, S. *Circulation* **2012**, *125* (6), 757–766.
- (20) Mallat, Z.; Lambeau, G.; Tedgui, A. *Circulation* **2010**, *122* (21), 2183–2200.
- (21) Koenig, W. *Arterioscler. Thromb. Vasc. Biol.* **2006**, *26* (7), 1586–1593.
- (22) Sabatine, M. S.; Morrow, D. A.; O’Donoghue, M.; Jablonksi, K. A.; Rice, M. M.; Solomon, S.; Rosenberg, Y.; Domanski, M. J.; Hsia, J. *Arterioscler. Thromb. Vasc. Biol.* **2007**, *27* (11), 2463–2469.
- (23) Brilakis, E. S. *Eur. Heart J.* **2004**, *26* (2), 137–144.
- (24) Stafforini, D. M.; Satoh, K.; Atkinson, D. L.; Tjoelker, L. W.; Eberhardt, C.; Yoshida, H.; Imaizumi, T.; Takamatsu, S.; Zimmerman, G. A.; McIntyre, T. M.; Gray, P. W.; Prescott, S. M. *J. Clin. Invest.* **1996**, *97* (12), 2784–2791.
- (25) Miwa, M.; Miyake, T.; Yamanaka, T.; Sugatani, J.; Suzuki, Y.; Sakata, S.; Araki, Y.; Matsumoto, M. *J. Clin. Invest.* **1988**, *82* (6), 1983–1991.

- (26) Yamada, Y.; Yoshida, H.; Ichihara, S.; Imaizumi, T.; Satoh, K.; Yokota, M. *Atherosclerosis* **2000**, *150* (1), 209–216.
- (27) Yamada, Y.; Ichihara, S.; Fujimura, T.; Yokota, M. *Metabolism*. **1998**, *47* (2), 177–181.
- (28) Yamada, Y.; Izawa, H.; Ichihara, S.; Takatsu, F.; Ishihara, H.; Hirayama, H.; Sone, T.; Tanaka, M.; Yokota, M. *N. Engl. J. Med.* **2002**, *347* (24), 1916–1923.
- (29) Unno, N.; Nakamura, T.; Kaneko, H.; Uchiyama, T.; Yamamoto, N.; Sugatani, J.; Miwa, M.; Nakamura, S. *J. Vasc. Surg.* **2000**, *32* (2), 263–267.
- (30) Hiramoto, M.; Yoshida, H.; Imaizumi, T.; Yoshimizu, N.; Satoh, K. *Stroke* **1997**, *28* (12), 2417–2420.
- (31) Jang, Y.; Kim, O. Y.; Koh, S. J.; Chae, J. S.; Ko, Y. G.; Kim, J. Y.; Cho, H.; Jeong, T.-S.; Lee, W. S.; Ordovas, J. M.; Lee, J. H. *J. Clin. Endocrinol. Metab.* **2006**, *91* (9), 3521–3527.
- (32) Jang, Y.; Waterworth, D.; Lee, J.-E.; Song, K.; Kim, S.; Kim, H.-S.; Park, K. W.; Cho, H.-J.; Oh, I.-Y.; Park, J. E.; Lee, B.-S.; Ku, H. J.; Shin, D.-J.; Lee, J. H.; Jee, S. H.; Han, B.-G.; Jang, H.-Y.; Cho, E.-Y.; Vallance, P.; Whittaker, J.; Cardon, L.; Mooser, V. *PLoS One* **2011**, *6* (4), 18208–18214.
- (33) The Stability Investigators. *N. Engl. J. Med.* **2014**, *370* (18), 1702–1711.
- (34) Blackie, J. A.; Bloomer, J. C.; Brown, M. J. B.; Cheng, H.-Y.; Hammond, B.; Hickey, D. M. B.; Ife, R. J.; Leach, C. A.; Lewis, V. A.; Macphee, C. H.; Milliner, K. J.; Moores, K. E.; Pinto, I. L.; Smith, S. A.; Stansfield, I. G.; Stanway, S. J.; Taylor, M. A.; Theobald, C. J. *Bioorg. Med. Chem. Lett.* **2003**, *13* (6), 1067–1070.
- (35) Steen, D. L.; O'Donoghue, M. L. *Cardiol. Ther.* **2013**, *2* (2), 125–134.
- (36) Wilensky, R. L.; Shi, Y.; Mohler, E. R.; Hamamdziec, D.; Burgert, M. E.; Li, J.; Postle, A.; Fenning, R. S.; Bollinger, J. G.; Hoffman, B. E.; Pelchovitz, D. J.; Yang, J.; Mirabile, R. C.; Webb, C. L.; Zhang, L.; Zhang, P.; Gelb, M. H.; Walker, M. C.; Zalewski, A.; Macphee, C. H. *Nat. Med.* **2008**, *14* (10), 1059–1066.
- (37) Serruys, P. W.; García-García, H. M.; Buszman, P.; Erne, P.; Verheye, S.; Aschermann, M.; Duckers, H.; Bleie, O.; Dudek, D.; Bøtker, H. E.; Von Birgelen, C.; D'Amico, D.; Hutchinson, T.; Zambanini, A.; Mastik, F.; Van Es, G. A.; Van Der Steen, A. F. W.; Vince, D. G.; Ganz, P.; Hamm, C. W.; Wijns, W.; Zalewski, A. *Circulation* **2008**, *118* (11), 1172–1182.
- (38) Mohler, E. R.; Ballantyne, C. M.; Davidson, M. H.; Hanefeld, M.; Ruilope, L. M.; Johnson, J. L.; Zalewski, A. *J. Am. Coll. Cardiol.* **2008**, *51* (17), 1632–1641.
- (39) O'Donoghue, M. L.; Braunwald, E.; White, H. D.; Steen, D. P.; Lukas, M. A.; Tarka, E.; Steg, P. G.; Hochman, J. S.; Bode, C.; Maggioni, A. P.; Im, K.; Shannon, J. B.; Davies, R. Y.; Murphy, S. A.; Crugnale, S. E.; Wiviott, S. D.; Bonaca, M. P.; Watson, D. F.; Weaver, W. D.; Serruys, P. W.; Cannon, C. P. *Jama* **2014**, *312* (10), 1006.
- (40) GlaxoSmithKline. GSK announces phase III study with darapladib did not meet primary endpoint in patients following an acute coronary syndrome <https://us.gsk.com/en-us/media/press-releases/2014/gsk-announces-phase-iii-study-with-darapladib-did-not-meet-primary-endpoint-in-patients-following-an-acute-coronary-syndrome/>.

- (41) Maher-Edwards, G.; De’Ath, J.; Barnett, C.; Lavrov, A.; Lockhart, A. *Alzheimer’s Dement. Transl. Res. Clin. Interv.* **2015**, *1* (2), 131–140.
- (42) Acharya, N. K.; Levin, E. C.; Clifford, P. M.; Han, M.; Tourtellotte, R.; Chamberlain, D.; Pollaro, M.; Coretti, N. J.; Kosciuk, M. C.; Nagele, E. P.; Demarshall, C.; Freeman, T.; Shi, Y.; Guan, C.; MacPhee, C. H.; Wilensky, R. L.; Nagele, R. G. *J. Alzheimer’s Dis.* **2013**, *35* (1), 179–198.
- (43) Liu, Q.; Chen, X.; Chen, W.; Yuan, X.; Su, H.; Shen, J.; Xu, Y. *J. Med. Chem.* **2016**, acs.jmedchem.6b00282.
- (44) Shaddinger, B. C.; Xu, Y.; Roger, J. H.; Macphee, C. H.; Handel, M.; Baidoo, C. A.; Magee, M.; Lepore, J. J.; Sprecher, D. L. *PLoS One* **2014**, *9* (1), e83094.
- (45) Young, R. J.; Green, D. V. S.; Luscombe, C. N.; Hill, A. P. *Drug Discov. Today* **2011**, *16* (17–18), 822–830.
- (46) Jambhekar, S. S.; Breen, P. J. *Drug Discov. Today* **2013**, *18* (23–24), 1173–1184.
- (47) Leeson, P. D.; Springthorpe, B. *Nat. Rev. Drug Discov.* **2007**, *6* (11), 881–890.
- (48) Valko, K.; Butler, J.; Eddershaw, P. *Expert Opin. Drug Discov.* **2013**, *8* (10), 1225–1238.
- (49) Lipinski, C. A.; Lombardo, F.; Dominy, B. W.; Feeney, P. J. *Adv. Drug Deliv. Rev.* **2001**, *46* (1–3), 3–26.
- (50) Veber, D. F.; Johnson, S. R.; Cheng, H.; Smith, B. R.; Ward, K. W.; Kopple, K. D. *J. Med. Chem.* **2002**, *45* (12), 2615–2623.
- (51) Meanwell, N. A. *Chem. Res. Toxicol.* **2011**, *24* (9), 1420–1456.
- (52) Bhal, S. K.; Kassam, K.; Peirson, I. G.; Pearl, G. M. *Mol. Pharm.* **2007**, *4* (4), 556–560.
- (53) Johnson, T. W.; Dress, K. R.; Edwards, M. *Bioorg. Med. Chem. Lett.* **2009**, *19* (19), 5560–5564.
- (54) Hughes, J. D.; Blagg, J.; Price, D. A.; Bailey, S.; DeCrescenzo, G. A.; Devraj, R. V.; Ellsworth, E.; Fobian, Y. M.; Gibbs, M. E.; Gilles, R. W.; Greene, N.; Huang, E.; Krieger-Burke, T.; Loesel, J.; Wager, T.; Whiteley, L.; Zhang, Y. *Bioorg. Med. Chem. Lett.* **2008**, *18* (17), 4872–4875.
- (55) Sutherland, J. J.; Raymond, J. W.; Stevens, J. L.; Baker, T. K.; Watson, D. E. *J. Med. Chem.* **2012**, *55* (14), 6455–6466.
- (56) Lovering, F.; Bikker, J.; Humblet, C. *J. Med. Chem.* **2009**, *52* (21), 6752–6756.
- (57) Tyrchan, C.; Blomberg, N.; Engkvist, O.; Kogej, T.; Muresan, S. *Bioorg. Med. Chem. Lett.* **2009**, *19* (24), 6943–6947.
- (58) Leeson, P. D.; Empfield, J. R. *Reducing the Risk of Drug Attrition Associated with Physicochemical Properties*, Edition Ed.; Elsevier Inc., 2010; Vol. 45.
- (59) Waring, M. J.; Arrowsmith, J.; Leach, A. R.; Leeson, P. D.; Mandrell, S.; Owen, R. M.; Pairedeau, G.; Pennie, W. D.; Pickett, S. D.; Wang, J.; Wallace, O.; Weir, A. *Nat Rev Drug Discov* **2015**, *14* (7), 475–486.
- (60) Langmuir, I. *J. Am. Chem. Soc.* **1919**, *41* (10), 1543–1559.
- (61) Erlenmeyer, H.; Berger, E. *Biochem. Z.* **1932**, *252*, 22–36.
- (62) Erlenmeyer, H.; Berger, E.; Leo, M. *Helv. Chim. Acta* **1933**, *16*, 733–738.
- (63) Meanwell, N. A. *J. Med. Chem.* **2011**, *54* (8), 2529–2591.
- (64) Friedman, H. L. In *First symposium on Chemical-Biological correlation*; 1951; pp 295–358.

- (65) Burger, A. *Prog. Drug Res.* **1991**, *37*, 288–392.
- (66) Patani, G. A.; LaVoie, E. J. *Chem. Rev.* **1996**, *96* (8), 3147–3176.
- (67) Turowski, M.; Yamakawa, N.; Meller, J.; Kimata, K.; Ikegami, T.; Hosoya, K.; Tanaka, N.; Thornton, E. R. *J. Am. Chem. Soc.* **2003**, *125* (45), 13836–13849.
- (68) Tayar, N. El; van de Waterbeemd, H.; Gryllaki, M.; Testa, B.; Trager, W. F. *Int. J. Pharm.* **1984**, *19* (3), 271–281.
- (69) Perrin, C. L.; Ohta, B. K.; Kuperman, J. *J. Am. Chem. Soc.* **2003**, *125* (49), 15008–15009.
- (70) Perrin, C. L.; Dong, Y. *J. Am. Chem. Soc.* **2008**, *130* (33), 11143–11148.
- (71) Perrin, C. L.; Dong, Y. *J. Am. Chem. Soc.* **2007**, *129* (14), 4490–4497.
- (72) Perrin, C. L.; Ohta, B. K.; Kuperman, J. *J. Am. Chem. Soc.* **2003**, *125* (49), 15008–15009.
- (73) Gant, T. G.; Sarshar, S. Substituted phenethylamines with serotonergic and/or norepinephrinergic activity. US7456317 B2, 2008.
- (74) Mutlib, A. E. *Chem. Res. Toxicol.* **2008**, *21* (9), 1672–1689.
- (75) Nelson, S. D. *Drug Metab. Dispos.* **2003**, *31* (12), 1481–1497.
- (76) Mutlib, A. E.; Gerson, R. J.; Meunier, P. C.; Haley, P. J.; Chen, H.; Gan, L. S.; Davies, M. H.; Gemzik, B.; Christ, D. D.; Krahn, D. F.; Markwalder, J. A.; Seitz, S. P.; Robertson, R. T.; Miwa, G. T. *Toxicol. Appl. Pharmacol.* **2000**, *169* (1), 102–113.
- (77) Maltais, F.; Jung, Y. C.; Chen, M.; Tanoury, J.; Perni, R. B.; Mani, N.; Laitinen, L.; Huang, H.; Liao, S.; Gao, H.; Tsao, H.; Block, E.; Ma, C.; Shawgo, R. S.; Town, C.; Brummel, C. L.; Howe, D.; Pazhanisamy, S.; Raybuck, S.; Namchuk, M.; Bennani, Y. L. *J. Med. Chem.* **2009**, *52* (24), 7993–8001.
- (78) Tung, R. Novel Benzo-[d][1,3]-dioxol derivatives. WO 2007/016431 A2, 2007.
- (79) Uttamsingh, V.; Gallegos, R.; Liu, J. F.; Harbeson, S. L.; Bridson, G. W.; Cheng, C.; Wells, D. S.; Graham, P. B.; Zelle, R.; Tung, R. *J. Pharmacol. Exp. Ther.* **2015**, *354* (1), 43–54.
- (80) Böhm, H.-J.; Banner, D.; Bendels, S.; Kansy, M.; Kuhn, B.; Müller, K.; Obst-Sander, U.; Stahl, M. *ChemBioChem* **2004**, *5* (5), 637–643.
- (81) Clader, J. W. *J. Med. Chem.* **2004**, *47* (1), 1–9.
- (82) Hagmann, W. K. *J. Med. Chem.* **2008**, *51* (15), 4359–4369.
- (83) Cox, C. D.; Coleman, P. J.; Breslin, M. J.; Whitman, D. B.; Garbaccio, R. M.; Fraley, M. E.; Buser, C. A.; Walsh, E. S.; Hamilton, K.; Schaber, M. D.; Lobell, R. B.; Tao, W.; Davide, J. P.; Diehl, R. E.; Abrams, M. T.; South, V. J.; Huber, H. E.; Torrent, M.; Prueksaritanont, T.; Li, C.; Slaughter, D. E.; Mahan, E.; Fernandez-Metzler, C.; Yan, Y.; Kuo, L. C.; Kohl, N. E.; Hartman, G. D. *J. Med. Chem.* **2008**, *51* (14), 4239–4252.
- (84) Deniau, G.; Slawin, A. M. Z.; Lebl, T.; Chorki, F.; Issberner, J. P.; van Mourik, T.; Heygate, J. M.; Lambert, J. J.; Etherington, L.-A.; Sillar, K. T.; O’Hagan, D. *ChemBioChem* **2007**, *8* (18), 2265–2274.
- (85) Pinto, D. J. P.; Orwat, M. J.; Koch, S.; Rossi, K. A.; Alexander, R. S.; Smallwood, A.; Wong, P. C.; Rendina, A. R.; Luetgen, J. M.; Knabb, R. M.; He, K.; Xin, B.; Wexler, R. R.; Lam, P. Y. S. *J. Med. Chem.* **2007**, *50* (22), 5339–5356.

- (86) Quan, M. L.; Lam, P. Y. S.; Han, Q.; Pinto, D. J. P.; He, M. Y.; Li, R.; Ellis, C. D.; Clark, C. G.; Teleha, C. A.; Sun, J.; Alexander, R. S.; Bai, S.; Luetzgen, J. M.; Knabb, R. M.; Wong, P. C.; Wexler, R. R. *J. Med. Chem.* **2005**, *48* (6), 1729–1744.
- (87) Meanwell, N. A.; Wallace, O. B.; Fang, H.; Wang, H.; Deshpande, M.; Wang, T.; Yin, Z.; Zhang, Z.; Pearce, B. C.; James, J.; Yeung, K.-S.; Qiu, Z.; Kim Wright, J. J.; Yang, Z.; Zadjura, L.; Tweedie, D. L.; Yeola, S.; Zhao, F.; Ranadive, S.; Robinson, B. A.; Gong, Y.-F.; Wang, H.-G. H.; Blair, W. S.; Shi, P.-Y.; Colonna, R. J.; Lin, P. *Bioorg. Med. Chem. Lett.* **2009**, *19* (7), 1977–1981.
- (88) Bégué, J. P.; Bonnet-Delpon, D. *Bioorganic and Medicinal Chemistry of Fluorine*; John Wiley & Sons: Hoboken, NJ, 2008.
- (89) Domagala, J. M.; Hanna, L. D.; Heifetz, C. L.; Hutt, M. P.; Mich, T. F.; Sanchez, J. P.; Solomon, M. *J. Med. Chem.* **1986**, *29* (3), 394–404.
- (90) Barbachyn, M. R.; Ford, C. W. *Angew. Chemie Int. Ed.* **2003**, *42* (18), 2010–2023.
- (91) Sliskovic, D. R.; Picard, J. A.; Krause, B. R. In *Progress in Medicinal Chemistry*; 2002; Vol. 39, pp 121–171.
- (92) Oswald, S.; König, J.; Lütjohann, D.; Giessmann, T.; Kroemer, H. K.; Rimmbach, C.; Roskopf, D.; Fromm, M. F.; Siegmund, W. *Pharmacogenet. Genomics* **2008**, *18* (7), 559–568.
- (93) Rose, W. C.; Marathe, P. H.; Jang, G. R.; Monticello, T. M.; Balasubramanian, B. N.; Long, B.; Fairchild, C. R.; Wall, M. E.; Wani, M. C. *Cancer Chemother. Pharmacol.* **2006**, *58* (1), 73–85.
- (94) Wall, M. E.; Wani, M. C.; Cook, C. E.; Palmer, K. H.; McPhail, A. T.; Sim, G. A. *J. Am. Chem. Soc.* **1966**, *88* (16), 3888–3890.
- (95) Cawello, W.; Schweer, H.; Müller, R.; Bonn, R.; Seyberth, H. W. *Eur. J. Clin. Pharmacol.* **1994**, *46* (3), 275–277.
- (96) Iseki, K.; Kanayama, T.; Hayasi, Y.; Shibasaki, M. *Chem. Pharm. Bull. (Tokyo)*. **1990**, *38* (6), 1769–1771.
- (97) Meanwell, N. A.; Rosenfeld, M. J.; Trehan, A. K.; Wright, J. J. K.; Brassard, C. L.; Buchanan, J. O.; Federici, M. E.; Fleming, J. S.; Gamberdella, M.; Zavoico, G. B.; Seiler, S. M. *J. Med. Chem.* **1992**, *35* (19), 3483–3497.
- (98) Gareau, Y.; Labelle, M.; Sturino, C. F.; Sawyer, N.; Denis, D.; Tremblay, N.; Lamontagne, S.; Carrie, M.; Metters, K. M. *Bioorg. Med. Chem.* **2001**, *9*, 1977–1984.
- (99) Wuitschik, G.; Rogers-Evans, M.; Müller, K.; Fischer, H.; Wagner, B.; Schuler, F.; Polonchuk, L.; Carreira, E. M. *Angew. Chemie Int. Ed.* **2006**, *45* (46), 7736–7739.
- (100) Wuitschik, G.; Carreira, E. M.; Wagner, B.; Fischer, H.; Parrilla, I.; Schuler, F.; Rogers-Evans, M.; Müller, K. *J. Med. Chem.* **2010**, *53* (8), 3227–3246.
- (101) Burkhard, J. A.; Wuitschik, G.; Rogers-Evans, M.; Müller, K.; Carreira, E. M. *Angew. Chemie Int. Ed.* **2010**, *49* (48), 9052–9067.
- (102) Wuitschik, G.; Rogers-Evans, M.; Buckl, A.; Bernasconi, M.; Märki, M.; Godel, T.; Fischer, H.; Wagner, B.; Parrilla, I.; Schuler, F.; Schneider, J.; Alker, A.; Schweizer, W. B.; Müller, K.; Carreira, E. M. *Angew. Chemie Int. Ed.* **2008**, *47* (24), 4512–4515.
- (103) Brown, N. *Bioisosteres in Medicinal Chemistry*; Brown, N., Folkers, G.,

- Kubinyi, H., Mannhold, R., Eds.; Wiley-VCH Verlag & Co., 2012.
- (104) Vandyck, K.; Cummings, M. D.; Nyanguile, O.; Boutton, C. W.; Vendeville, S.; McGowan, D.; Devogelaere, B.; Amssoms, K.; Last, S.; Rombauts, K.; Tahri, A.; Lory, P.; Hu, L.; Beauchamp, D. A.; Simmen, K.; Raboisson, P. *J. Med. Chem.* **2009**, *52* (14), 4099–4102.
- (105) Saunders, J.; Cassidy, M.; Freedman, S. B.; Harley, E. A.; Iversen, L. L.; Kneen, C.; MacLeod, A. M.; Merchant, K. J.; Snow, R. J.; Baker, R. *J. Med. Chem.* **1990**, *33* (4), 1128–1138.
- (106) Watjen, F.; Baker, R.; Engelstoff, M.; Herbert, R.; MacLeod, A.; Knight, A.; Merchant, K.; Moseley, J.; Saunders, J. *J. Med. Chem.* **1989**, *32* (10), 2282–2291.
- (107) Black, W. C.; Bayly, C. I.; Davis, D. E.; Desmarais, S.; Falguyret, J.-P.; Léger, S.; Li, C. S.; Massé, F.; McKay, D. J.; Palmer, J. T.; Percival, M. D.; Robichaud, J.; Tsou, N.; Zamboni, R. *Bioorg. Med. Chem. Lett.* **2005**, *15* (21), 4741–4744.
- (108) Gauthier, J. Y.; Chauret, N.; Cromlish, W.; Desmarais, S.; Duong, L. T.; Falguyret, J.-P.; Kimmel, D. B.; Lamontagne, S.; Léger, S.; LeRiche, T.; Li, C. S.; Massé, F.; McKay, D. J.; Nicoll-Griffith, D. A.; Oballa, R. M.; Palmer, J. T.; Percival, M. D.; Riendeau, D.; Robichaud, J.; Rodan, G. A.; Rodan, S. B.; Seto, C.; Thérien, M.; Truong, V.-L.; Venuti, M. C.; Wesolowski, G.; Young, R. N.; Zamboni, R.; Black, W. C. *Bioorg. Med. Chem. Lett.* **2008**, *18* (3), 923–928.
- (109) Ballatore, C.; Huryn, D. M.; Smith, A. B. *ChemMedChem* **2013**, *8* (3), 385–395.
- (110) Drysdale, M. J.; Pritchard, M. C.; Horwell, D. C. *J. Med. Chem.* **1992**, *35* (14), 2573–2581.
- (111) Duncia, J. V.; Chiu, A. T.; Carini, D. J.; Gregory, G. B.; Johnson, A. L.; Price, W. a; Wells, G. J.; Wong, P. C.; Calabrese, J. C.; Timmermans, P. B. M. W. *M. J. Med. Chem.* **1990**, *33* (5), 1312–1329.
- (112) Carini, D. J.; Duncia, J. V.; Johnson, A. L.; Chiu, A. T.; Price, W. A.; Wong, P. C.; Timmermans, P. B. *J Med Chem* **1990**, *33* (5), 1330–1336.
- (113) Carini, D. J.; Duncia, J. V.; Aldrich, P. E.; Chiu, a T.; Johnson, a L.; Pierce, M. E.; Price, W. a; Santella, J. B.; Wells, G. J.; Wexler, R. R. *J. Med. Chem.* **1991**, *34* (8), 2525–2547.
- (114) Aulakh, G. K.; Sodhi, R. K.; Singh, M. *Life Sci.* **2007**, *81* (8), 615–639.
- (115) Herr, R. J. *Bioorganic Med. Chem.* **2002**, *10* (11), 3379–3393.
- (116) Marshall, W. S.; Goodson, T.; Cullinan, G. J.; Swanson-Bean, D.; Haisch, K. D.; Rinkema, L. E.; Fleisch, J. H. *J. Med. Chem.* **1987**, *30* (4), 682–689.
- (117) Fleisch, J. H.; Rinkema, L. E.; Haisch, K. D.; Swanson-Bean, D.; Goodson, T.; Ho, P. P.; Marshall, W. S. *J. Pharmacol. Exp. Ther.* **1985**, *233* (1), 148–157.
- (118) Kinney, W. A.; Abou-Gharbia, M.; Garrison, D. T.; Schmid, J.; Kowal, D. M.; Bramlett, D. R.; Miller, T. L.; Tasse, R. P.; Zaleska, M. M.; Moyer, J. A. *J. Med. Chem.* **1998**, *41* (2), 236–246.
- (119) Nicolaou, I.; Zika, C.; Demopoulos, V. J. *J. Med. Chem.* **2004**, *47* (10), 2706–2709.
- (120) Ballatore, C.; Gay, B.; Huang, L.; Robinson, K. H.; James, M. J.; Trojanowski, J. Q.; Lee, V. M.-Y.; Brunden, K. R.; Smith, A. B. *Bioorg. Med.*

- Chem. Lett.* **2014**.
- (121) Cai, J.; Fradera, X.; van Zeeland, M.; Dempster, M.; Cameron, K. S.; Bennett, D. J.; Robinson, J.; Popplestone, L.; Baugh, M.; Westwood, P.; Bruin, J.; Hamilton, W.; Kinghorn, E.; Long, C.; Uitdehaag, J. C. M. *Bioorg. Med. Chem. Lett.* **2010**, *20* (15), 4507–4510.
- (122) Pierce, A. C.; ter Haar, E.; Binch, H. M.; Kay, D. P.; Patel, S. R.; Li, P. J. *Med. Chem.* **2005**, *48* (4), 1278–1281.
- (123) Wang, T.; Zhang, Z.; Wallace, O. B.; Deshpande, M.; Fang, H.; Yang, Z.; Zadjura, L. M.; Tweedie, D. L.; Huang, S.; Zhao, F.; Ranadive, S.; Robinson, B. S.; Gong, Y. F.; Ricarrdi, K.; Spicer, T. P.; Deminie, C.; Rose, R.; Wang, H. G. H.; Blair, W. S.; Shi, P. Y.; Lin, P. F.; Colonno, R. J.; Meanwell, N. A. *J. Med. Chem.* **2003**, *46* (20), 4236–4239.
- (124) Wang, T.; Yin, Z.; Zhang, Z.; Bender, J. A.; Yang, Z.; Johnson, G.; Yang, Z.; Zadjura, L. M.; D'Arienzo, C. J.; DiGiugno Parker, D.; Gesenberg, C.; Yamanaka, G. A.; Gong, Y.-F.; Ho, H.-T.; Fang, H.; Zhou, N.; McAuliffe, B. V.; Eggers, B. J.; Fan, L.; Nowicka-Sans, B.; Dicker, I. B.; Gao, Q.; Colonno, R. J.; Lin, P.-F.; Meanwell, N. A.; Kadow, J. F. *J. Med. Chem.* **2009**, *52* (23), 7778–7787.
- (125) Hanna, G. J.; Lalezari, J.; Hellinger, J. A.; Wohl, D. A.; Nettles, R.; Persson, A.; Krystal, M.; Lin, P.; Colonno, R.; Grasela, D. M. *Antimicrob. Agents Chemother.* **2011**, *55* (2), 722–728.
- (126) Yu, K.-L.; Sin, N.; Civiello, R. L.; Wang, X. A.; Combrink, K. D.; Gulgeze, H. B.; Venables, B. L.; Wright, J. J. K.; Dalterio, R. A.; Zadjura, L.; Marino, A.; Dando, S.; D'Arienzo, C.; Kadow, K. F.; Cianci, C. W.; Li, Z.; Clarke, J.; Genovesi, E. V.; Medina, I.; Lamb, L.; Colonno, R. J.; Yang, Z.; Krystal, M.; Meanwell, N. A. *Bioorg. Med. Chem. Lett.* **2007**, *17* (4), 895–901.
- (127) Kalgutkar, A. S.; Griffith, D. A.; Ryder, T.; Sun, H.; Miao, Z.; Bauman, J. N.; Didiuk, M. T.; Frederick, K. S.; Zhao, S. X.; Prakash, C.; Soglia, J. R.; Bagley, S. W.; Bechle, B. M.; Kelley, R. M.; Dirico, K.; Zawistoski, M.; Li, J.; Oliver, R.; Guzman-Perez, A.; Liu, K. K. C.; Walker, D. P.; Benbow, J. W.; Morris, J. *Chem. Res. Toxicol.* **2010**, *23* (6), 1115–1126.
- (128) Qiao, J. X.; Cheney, D. L.; Alexander, R. S.; Smallwood, A. M.; King, S. R.; He, K.; Rendina, A. R.; Luettgen, J. M.; Knabb, R. M.; Wexler, R. R.; Lam, P. Y. S. *Bioorg. Med. Chem. Lett.* **2008**, *18* (14), 4118–4123.
- (129) Chalmers, B. A.; Xing, H.; Houston, S.; Clark, C.; Ghassabian, S.; Kuo, A.; Cao, B.; Reitsma, A.; Murray, C.-E. P.; Stok, J. E.; Boyle, G. M.; Pierce, C. J.; Littler, S. W.; Winkler, D. A.; Bernhardt, P. V.; Pasay, C.; De Voss, J. J.; McCarthy, J.; Parsons, P. G.; Walter, G. H.; Smith, M. T.; Cooper, H. M.; Nilsson, S. K.; Tsanaktsidis, J.; Savage, G. P.; Williams, C. M. *Angew. Chemie Int. Ed.* **2016**, *55* (11), 3580–3585.
- (130) Pellicciari, R.; Raimondo, M.; Marinozzi, M.; Natalini, B.; Costantino, G.; Thomsen, C. *J. Med. Chem.* **1996**, *39* (15), 2874–2876.
- (131) Costantino, G.; Maltoni, K.; Marinozzi, M.; Camaioni, E.; Prezeau, L.; Pin, J.-P.; Pellicciari, R. *Bioorg. Med. Chem.* **2001**, *9* (2), 221–227.
- (132) Pellicciari, R.; Filosa, R.; Fulco, M. C.; Marinozzi, M.; Macchiarulo, A.; Novak, C.; Natalini, B.; Hermit, M. B.; Nielsen, S.; Sager, T. N.; Stensbøl, T. B.; Thomsen, C. *ChemMedChem* **2006**, *1* (3), 358–365.
- (133) Eaton, S. A.; Jane, D. E.; Jones, P. L.; Porter, R. H.; Pook, P. C.; Sunter, D.

- C.; Udvarhelyi, P. M.; Roberts, P. J.; Salt, T. E.; Watkins, J. C. *Eur. J. Pharmacol.* **1993**, *244* (2), 195–197.
- (134) Stepan, A. F.; Subramanyam, C.; Efremov, I. V.; Dutra, J. K.; O’Sullivan, T. J.; DiRico, K. J.; McDonald, W. S.; Won, A.; Dorff, P. H.; Nolan, C. E.; Becker, S. L.; Pustilnik, L. R.; Riddell, D. R.; Kauffman, G. W.; Kormos, B. L.; Zhang, L.; Lu, Y.; Capetta, S. H.; Green, M. E.; Karki, K.; Sibley, E.; Atchison, K. P.; Hallgren, A. J.; Oborski, C. E.; Robshaw, A. E.; Sneed, B.; O’Donnell, C. J. *J. Med. Chem.* **2012**, *55* (7), 3414–3424.
- (135) Nicolaou, K. C.; Vourloumis, D.; Totokotsopoulos, S.; Papakyriakou, A.; Karsunky, H.; Fernando, H.; Gavriluk, J.; Webb, D.; Stepan, A. F. *ChemMedChem* **2016**, *11* (1), 31–37.
- (136) Hunter, T. *J. Clin. Invest.* **2007**, *117* (8), 2036–2043.
- (137) Wiberg, K. B.; Connor, D. S. *J. Am. Chem. Soc.* **1966**, *88* (19), 4437–4441.
- (138) Wiberg, K. B.; Williams, V. Z. *J. Org. Chem.* **1970**, *35* (2), 369–373.
- (139) Semmler, K.; Szeimies, G.; Belzner, J. *J. Am. Chem. Soc.* **1985**, *107* (22), 6410–6411.
- (140) Belzner, J.; Bunz, U.; Semmler, K.; Szeimies, G.; Opitz, K.; Schlüter, A.-D. *Chem. Ber.* **1989**, *122* (2), 397–398.
- (141) Kaszynski, P.; Michl, J. *J. Org. Chem.* **1988**, *53* (19), 4593–4594.
- (142) Wiberg, K. B.; Waddell, S. T. *J. Am. Chem. Soc.* **1990**, *112* (6), 2194–2216.
- (143) Screttas, C. G.; Micha-Screttas, M. *J. Org. Chem.* **1978**, *43* (6), 1064–1071.
- (144) Eaton, P. E.; Xiong, Y.; Zhou, J. P. *J. Org. Chem.* **1992**, *57* (15), 4277–4281.
- (145) Della, E. W.; Taylor, D. K. *J. Org. Chem.* **1994**, *59* (11), 2986–2996.
- (146) Wiberg, K. B.; McMurdie, N. *J. Am. Chem. Soc.* **1994**, *116* (26), 11990–11998.
- (147) Messner, M.; Kozhushkov, S. I.; de Meijere, A. *European J. Org. Chem.* **2000**, *2000* (7), 1137–1155.
- (148) Goh, Y. L.; Tam, E. K. W.; Bernardo, P. H.; Cheong, C. B.; Johannes, C. W.; William, A. D.; Adsool, V. A. *Org. Lett.* **2014**, *16* (7), 1884–1887.
- (149) Gianatassio, R.; Lopchuk, J. M.; Wang, J.; Pan, C.-M.; Malins, L. R.; Prieto, L.; Brandt, T. A.; Collins, M. R.; Gallego, G. M.; Sach, N. W.; Spangler, J. E.; Zhu, H.; Zhu, J.; Baran, P. S. *Science (80-.)*. **2016**, *351* (6270), 241–246.
- (150) Applequist, D. E.; Renken, T. L.; Wheeler, J. W. *J. Org. Chem.* **1982**, *47* (25), 4985–4995.
- (151) Wiberg, K. B.; Dailey, W. P.; Walker, F. H.; Waddell, S. T.; Crocker, L. S.; Newton, M. *J. Am. Chem. Soc.* **1985**, *107* (25), 7247–7257.
- (152) Manas, E. S. Unpublished Work 2014.
- (153) Labute, P. *J. Comput. Chem.* **2008**, *29* (10), 1693–1698.
- (154) Jakalian, A.; Jack, D. B.; Bayly, C. I. *J. Comput. Chem.* **2002**, *23* (16), 1623–1641.
- (155) Li-Yuan Bao, R.; Zhao, R.; Shi, L. *Chem. Commun.* **2015**, *51* (32), 6884–6900.
- (156) Yasuda, M.; Yamasaki, S.; Onishi, Y.; Baba, A. *J. Am. Chem. Soc.* **2004**, *126* (23), 7186–7187.
- (157) Helmkamp, G. K.; Rickborn, B. F. *J. Org. Chem.* **1957**, *22* (5), 479–482.
- (158) Hall, H. K.; Smith, C. D.; Blanchard, E. P.; Cherkofsky, S. C.; Sieja, J. B. *J. Am. Chem. Soc.* **1971**, *93* (1), 121–130.
- (159) Irigineni, R. Synthesis run externally at GVK Bio - Unpublished work 2014.

- (160) Furukawa, J.; Kawabata, N.; Nishimura, J. *Tetrahedron* **1968**, *24* (1), 53–58.
- (161) Simmons, H. E.; Smith, R. D. *J. Am. Chem. Soc.* **1959**, *81* (16), 4256–4264.
- (162) Takakis, I. M.; Rhodes, Y. E. *J. Org. Chem.* **1978**, *43* (18), 3496–3500.
- (163) Gassman, P. G.; Greenlee, M. L.; Dixon, D. A.; Richtsmeier, S.; Gougoutas, J. *Z. J. Am. Chem. Soc.* **1983**, *105* (18), 5865–5874.
- (164) Newton, M. D.; Schulman, J. M. *J. Am. Chem. Soc.* **1972**, *94* (3), 767–773.
- (165) Whitman, D. R.; Chiang, J. F. *J. Am. Chem. Soc.* **1972**, *94* (4), 1126–1129.
- (166) Pomerantz, M.; Abrahamson, E. W. *J. Am. Chem. Soc.* **1966**, *88* (17), 3970–3972.
- (167) Azran, C.; Hoz, S. *Tetrahedron* **1995**, *51* (42), 11421–11430.
- (168) Luong, H.; Luss-Lusis, E.; Tanoury, G. J.; Nugent, W. A. *European J. Org. Chem.* **2013**, *2013* (20), 4238–4241.
- (169) Doyle, M. P.; Griffin, J. H.; Bagheri, V.; Dorow, R. L. *Organometallics* **1984**, *3* (1), 53–61.
- (170) Horner, L.; Schläfer, L.; Kämmerer, H. *Chem. Ber.* **1959**, *92* (7), 1700–1705.
- (171) Doyle, M. P.; McOsker, C. C.; West, C. T. *J. Org. Chem.* **1976**, *41* (8), 1393–1396.
- (172) Chatgililoglu, C.; Griller, D.; Lesage, M. *J. Org. Chem.* **1988**, *53* (15), 3641–3642.
- (173) Postigo, A.; Kopssov, S.; Zlotzky, S. S.; Ferreri, C.; Chatgililoglu, C. *Organometallics* **2009**, *28* (11), 3282–3287.
- (174) Das, S.; Li, Y.; Bornschein, C.; Pisiewicz, S.; Kiersch, K.; Michalik, D.; Gallou, F.; Junge, K.; Beller, M. *Angew. Chemie Int. Ed.* **2015**, *54* (42), 12389–12393.
- (175) Cheng, C.; Brookhart, M. *J. Am. Chem. Soc.* **2012**, *134* (28), 11304–11307.
- (176) Pelletier, G.; Bechara, W. S.; Charette, A. B. *J. Am. Chem. Soc.* **2010**, *132* (37), 12817–12819.
- (177) Limited, G. G. Novel compounds. WO2003/87088 A2, 2003.
- (178) Boymond, L.; Rotländer, M.; Cahiez, G.; Knochel, P. *Angew. Chemie Int. Ed.* **1998**, *37* (12), 1701–1703.
- (179) Heaney, H. *Chem. Rev.* **1962**, *62* (2), 81–97.
- (180) Sapountzis, I.; Knochel, P. *Angew. Chemie Int. Ed.* **2002**, *41* (9), 1610–1611.
- (181) Ricci, A.; Fochi, M. *Angew. Chemie Int. Ed.* **2003**, *42* (13), 1444–1446.
- (182) Bartoli, G.; Palmieri, G.; Bosco, M.; Dalpozzo, R. *Tetrahedron Lett.* **1989**, *30* (16), 2129–2132.
- (183) Kambe, N.; Iwasaki, T.; Terao, J. *Chem. Soc. Rev.* **2011**, *40* (10), 4937.
- (184) Cárdenas, D. J. *Angew. Chemie Int. Ed.* **2003**, *42* (4), 384–387.
- (185) Netherton, M. R.; Fu, G. C. *Angew. Chemie Int. Ed.* **2002**, *41* (20), 3910–3912.
- (186) Kirchhoff, J. H.; Dai, C.; Fu, G. C. *Angew. Chemie Int. Ed.* **2002**, *41* (11), 1945.
- (187) Netherton, M. R.; Dai, C.; Neuschütz, K.; Fu, G. C. *J. Am. Chem. Soc.* **2001**, *123* (41), 10099–10100.
- (188) Tasker, S. Z.; Standley, E. A.; Jamison, T. F. *Nature* **2014**, *509* (7500), 299–309.
- (189) González-Bobes, F.; Fu, G. C. *J. Am. Chem. Soc.* **2006**, *128* (16), 5360–5361.
- (190) Bodor, N.; Buchwald, P. *Med. Res. Rev.* **2000**, *20* (1), 58.
- (191) Bodor, N.; Kaminski, J. J.; Selk, S. *J. Med. Chem.* **1980**, *23* (5), 469–474.

- (192) Bodor, N.; Kaminski, J. J. *J. Med. Chem.* **1980**, *23* (5), 566–569.
- (193) Bodor, N.; Woods, R.; Raper, C.; Kearney, P.; Kaminski, J. J. *J. Med. Chem.* **1980**, *23* (5), 474–480.
- (194) Wiest, D. *Clin. Pharmacokinet.* **1995**, *28* (3), 190–202.
- (195) Blake, C. M.; Kharasch, E. D.; Schwab, M.; Nagele, P. *Clin. Pharmacol. Ther.* **2013**, *94* (3), 394–399.
- (196) Hospira. Labetalol Hydrochloride <https://www.drugs.com/pro/labetalol.html>.
- (197) Benfield, P.; Sorkin, E. M. *Drugs* **1987**, *33* (4), 392–412.
- (198) Stout, D. M.; Black, L. A.; Barcelon-Yang, C.; Matier, W. L.; Brown, B. S.; Quon, C. Y.; Stampfli, H. F. *J. Med. Chem.* **1989**, *32* (8), 1910–1913.
- (199) Brown, B. S.; Calzadilla, S. V.; Diemer, M. J.; Hartman, J. C.; Reynolds, R. D. *J. Pharmacol. Exp. Ther.* **1987**, *243* (3), 1225–1234.
- (200) Chorvat, R. J.; Black, L. A.; Ranade, V. V.; Barcelon-Yang, C.; Stout, D. M.; Brown, B. S.; Stampfli, H. F.; Quon, C. Y. *J. Med. Chem.* **1993**, *36* (17), 2494–2498.
- (201) Larkin, J.; Goh, X. Y.; Vetter, M.; Pickering, L.; Swanton, C. *Nat. Rev. Urol.* **2012**, *9* (3), 147–155.
- (202) Jones, P. A.; Archer, T. K.; Baylin, S. B.; Beck, S.; Berger, S.; Bernstein, B. E.; Carpten, J. D.; Clark, S. J.; Costello, J. F.; Doerge, R. W.; Esteller, M.; Feinberg, A. P.; Gingeras, T. R.; Grealley, J. M.; Henikoff, S.; Herman, J. G.; Jackson-Grusby, L.; Jenuwein, T.; Jirtle, R. L.; Kim, Y.-J.; Laird, P. W.; Lim, B.; Martienssen, R.; Polyak, K.; Stunnenberg, H.; Tlsty, T. D.; Tycko, B.; Ushijima, T.; Zhu, J.; Pirrotta, V.; Allis, C. D.; Elgin, S. C.; Jones, P. A.; Martienssen, R.; Rine, J.; Wu, C. *Nature* **2008**, *454* (7205), 711–715.
- (203) Chung, C.-W.; Coste, H.; White, J. H.; Mirguet, O.; Wilde, J.; Gosmini, R. L.; Delves, C.; Magny, S. M.; Woodward, R.; Hughes, S. A.; Boursier, E. V.; Flynn, H.; Bouillot, A. M.; Bamborough, P.; Brusq, J.-M. G.; Gellibert, F. J.; Jones, E. J.; Riou, A. M.; Homes, P.; Martin, S. L.; Uings, I. J.; Toum, J.; Clément, C. A.; Boullay, A.-B.; Grimley, R. L.; Blandel, F. M.; Prinjha, R. K.; Lee, K.; Kirilovsky, J.; Nicodeme, E. *J. Med. Chem.* **2011**, *54* (11), 3827–3838.
- (204) Smith, S. G.; Zhou, M.-M. *ACS Chem. Biol.* **2016**, *11* (3), 598–608.
- (205) Brand, M.; Measures, A. M.; Wilson, B. G.; Cortopassi, W. A.; Alexander, R.; Höss, M.; Hewings, D. S.; Rooney, T. P. C.; Paton, R. S.; Conway, S. J. *ACS Chem. Biol.* **2015**, *10* (1), 22–39.
- (206) Filippakopoulos, P.; Knapp, S. *Nat. Rev. Drug Discov.* **2014**, *13* (5), 337–356.
- (207) Filippakopoulos, P.; Qi, J.; Picaud, S.; Shen, Y.; Smith, W. B.; Fedorov, O.; Morse, E. M.; Keates, T.; Hickman, T. T.; Felletar, I.; Philpott, M.; Munro, S.; McKeown, M. R.; Wang, Y.; Christie, A. L.; West, N.; Cameron, M. J.; Schwartz, B.; Heightman, T. D.; La Thangue, N.; French, C. a; Wiest, O.; Kung, A. L.; Knapp, S.; Bradner, J. E. *Nature* **2010**, *468* (7327), 1067–1073.
- (208) Filippakopoulos, P.; Picaud, S.; Mangos, M.; Keates, T.; Lambert, J.-P.; Barsyte-Lovejoy, D.; Felletar, I.; Volkmer, R.; Müller, S.; Pawson, T.; Gingras, A.-C.; Arrowsmith, C. H.; Knapp, S. *Cell* **2012**, *149* (1), 214–231.
- (209) Muller, S.; Filippakopoulos, P.; Knapp, S. *Expert Rev. Mol. Med.* **2011**, *13* (September), e29.
- (210) Bamborough, P. Unpublished Work 2014.
- (211) Shi, J.; Vakoc, C. R. *Mol. Cell* **2014**, *54* (5), 728–736.

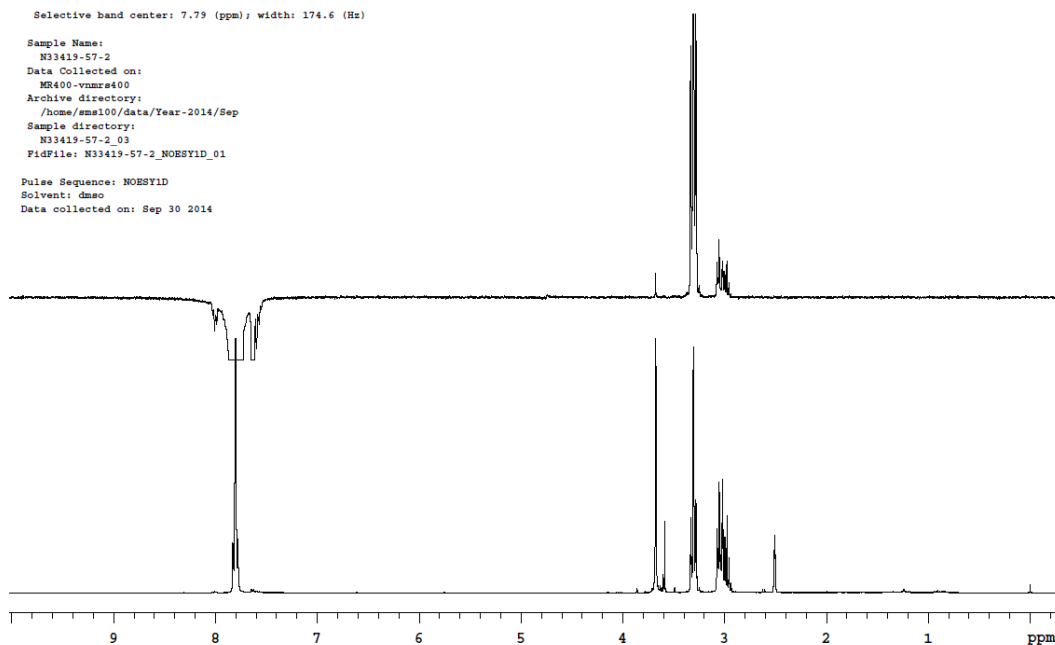
- (212) McLure, K. G.; Gesner, E. M.; Tsujikawa, L.; Kharenko, O. A.; Attwell, S.; Campeau, E.; Wasiak, S.; Stein, A.; White, A.; Fontano, E.; Suto, R. K.; Wong, N. C. W.; Wagner, G. S.; Hansen, H. C.; Young, P. R. *PLoS One* **2013**, *8* (12), e83190.
- (213) Nakamura, Y.; Umehara, T.; Nakano, K.; Jang, M. K.; Shirouzu, M.; Morita, S.; Uda-Tochio, H.; Hamana, H.; Terada, T.; Adachi, N.; Matsumoto, T.; Tanaka, A.; Horikoshi, M.; Ozato, K.; Padmanabhan, B.; Yokoyama, S. *J. Biol. Chem.* **2006**, *282* (6), 4193–4201.
- (214) Zhou, M.-M.; Dhalluin, C.; Carlson, J. E.; Zeng, L.; He, C.; Aggarwal, A. K.; Zhou, M.-M. *Nature* **1999**, *399* (6735), 491–496.
- (215) Vollmuth, F.; Blankenfeldt, W.; Geyer, M. *J. Biol. Chem.* **2009**, *284* (52), 36547–36556.
- (216) Mujtaba, S.; Zeng, L.; Zhou, M.-M. *Oncogene* **2007**, *26* (37), 5521–5527.
- (217) Nicodeme, E.; Jeffrey, K. L.; Schaefer, U.; Beinke, S.; Dewell, S.; Chung, C.; Chandwani, R.; Marazzi, I.; Wilson, P.; Coste, H.; White, J.; Kirilovsky, J.; Rice, C. M.; Lora, J. M.; Prinjha, R. K.; Lee, K.; Tarakhovsky, A. *Nature* **2010**, *468* (7327), 1119–1123.
- (218) Mirguet, O.; Gosmini, R.; Toum, J.; Clément, C. A.; Barnathan, M.; Brusq, J.-M.; Mordaunt, J. E.; Grimes, R. M.; Crowe, M.; Pineau, O.; Ajakane, M.; Daugan, A.; Jeffrey, P.; Cutler, L.; Haynes, A. C.; Smithers, N. N.; Chung, C.; Bamborough, P.; Uings, I. J.; Lewis, A.; Witherington, J.; Parr, N.; Prinjha, R. K.; Nicodème, E. *J. Med. Chem.* **2013**, *56* (19), 7501–7515.
- (219) Mertz, J. A.; Conery, A. R.; Bryant, B. M.; Sandy, P.; Balasubramanian, S.; Mele, D. A.; Bergeron, L.; Sims, R. J. *Proc. Natl. Acad. Sci.* **2011**, *108* (40), 16669–16674.
- (220) Delmore, J. E.; Issa, G. C.; Lemieux, M. E.; Rahl, P. B.; Shi, J.; Jacobs, H. M.; Kastritis, E.; Gilpatrick, T.; Paranal, R. M.; Qi, J.; Chesi, M.; Schinzel, A. C.; McKeown, M. R.; Heffernan, T. P.; Vakoc, C. R.; Bergsagel, P. L.; Ghobrial, I. M.; Richardson, P. G.; Young, R. A.; Hahn, W. C.; Anderson, K. C.; Kung, A. L.; Bradner, J. E.; Mitsiades, C. S. *Cell* **2011**, *146* (6), 904–917.
- (221) Lockwood, W. W.; Zejnullahu, K.; Bradner, J. E.; Varmus, H. *Proc. Natl. Acad. Sci.* **2012**, *109* (47), 19408–19413.
- (222) Mumby, S.; Gambaryan, N.; Meng, C.; Perros, F.; Humbert, M.; Wort, S. J.; Adcock, I. M. *Respirology* **2016**, 1–8.
- (223) Poghosyan, A.; Patel, J. K.; Clifford, R. L.; Knox, A. J. *Biochem. Biophys. Res. Commun.* **2016**, *476* (4), 431–437.
- (224) Chen, K.; Campfield, B. T.; Wenzel, S. E.; McAleer, J. P.; Kreindler, J. L.; Kurland, G.; Gopal, R.; Wang, T.; Chen, W.; Eddens, T.; Quinn, K. M.; Myerburg, M. M.; Horne, W. T.; Lora, J. M.; Albrecht, B. K.; Pilewski, J. M.; Kolls, J. K. *JCI Insight* **2016**, *1* (11), 1–10.
- (225) Nguyen, T. H.; Maltby, S.; Eyers, F.; Foster, P. S.; Yang, M. *PLoS One* **2016**, *11* (9), e0163392.
- (226) Bolden, J. E.; Tasdemir, N.; Dow, L. E.; van Es, J. H.; Wilkinson, J. E.; Zhao, Z.; Clevers, H.; Lowe, S. W. *Cell Rep.* **2014**, *8* (6), 1919–1929.
- (227) Vanam, N. Unpublished Work 2014.
- (228) Watson, R. Unpublished Work 2015.
- (229) Li, X. Unpublished Work 2012.
- (230) Epigenetics DPU. Unpublished Work 2015 - 2017.

- (231) Demont, E. Unpublished Work 2015.
- (232) Xing, D.; Guan, B.; Cai, G.; Fang, Z.; Yang, L.; Shi, Z. *Org. Lett.* **2006**, 8 (4), 693–696.
- (233) Plietker, B.; Niggemann, M. *Org. Lett.* **2003**, 5 (18), 3353–3356.
- (234) Sharpless, K. B.; Amberg, W.; Bennani, Y. L.; Crispino, G. a; Hartung, J.; Jeong, K. S.; Kwong, H. L.; Morikawa, K.; Wang, Z. M. *J. Org. Chem.* **1992**, 57 (10), 2768–2771.
- (235) Friis, S. D.; Lindhardt, A. T.; Skrydstrup, T. *Acc. Chem. Res.* **2016**, 49 (4), 594–605.
- (236) Preston, A.; Wheelhouse, K. Unpublished Work 2016.
- (237) Stables, S. J.; Gregory, R. Unpublished Work 2016.
- (238) Thesmar, P.; Watson, R.; Demont, E. Unpublished Work 2015.
- (239) Weiberth, F. J.; Yu, Y.; Subotkowski, W.; Pemberton, C. *Org. Process Res. Dev.* **2012**, 16 (12), 1967–1969.
- (240) Kiesewetter, M. K.; Scholten, M. D.; Kirn, N.; Weber, R. L.; Hedrick, J. L.; Waymouth, R. M. *J. Org. Chem.* **2009**, 74 (24), 9490–9496.
- (241) Pratt, R. C.; Lohmeijer, B. G. G.; Long, D. A.; Waymouth, R. M.; Hedrick, J. L. *J. Am. Chem. Soc.* **2006**, 128 (14), 4556–4557.
- (242) Friis, S. D.; Skrydstrup, T.; Buchwald, S. L. *Org. Lett.* **2014**, 16 (16), 4296–4299.
- (243) Valko, K.; Nunhuck, S.; Bevan, C.; Abraham, M. H.; Reynolds, D. P. *J. Pharm. Sci.* **2003**, 92 (11), 2236–2248.
- (244) Ballell, L.; Bates, R. H.; Young, R. J.; Alvarez-Gomez, D.; Alvarez-Ruiz, E.; Barroso, V.; Blanco, D.; Crespo, B.; Escribano, J.; González, R.; Lozano, S.; Huss, S.; Santos-Villarejo, A.; Martín-Plaza, J. J.; Mendoza, A.; Rebollo-Lopez, M. J.; Remuiñan-Blanco, M.; Lavandera, J. L.; Pérez-Herran, E.; Gamo-Benito, F. J.; García-Bustos, J. F.; Barros, D.; Castro, J. P.; Cammack, N. *ChemMedChem* **2013**, 8 (2), 313–321.
- (245) Woolford, A. J.-A.; Pero, J. E.; Aravapalli, S.; Berdini, V.; Coyle, J. E.; Day, P. J.; Dodson, A. M.; Grondin, P.; Holding, F. P.; Lee, L. Y. W.; Li, P.; Manas, E. S.; Marino, J.; Martin, A. C. L.; McClelland, B. W.; McMenamín, R. L.; Murray, C. W.; Neipp, C. E.; Page, L. W.; Patel, V. K.; Potvain, F.; Rich, S.; Rivero, R. A.; Smith, K.; Somers, D. O.; Trotter, L.; Velagaleti, R.; Williams, G.; Xie, R. *J. Med. Chem.* **2016**, 59 (11), 5356–5367.
- (246) Monaco, S.; Gordon, E.; Bowler, M. W.; Delagenière, S.; Guijarro, M.; Spruce, D.; Svensson, O.; McSweeney, S. M.; McCarthy, A. A.; Leonard, G.; Nanao, M. H. *J. Appl. Crystallogr.* **2013**, 46 (Pt 3), 804–810.
- (247) Kabsch, W. *Acta Crystallogr. D. Biol. Crystallogr.* **2010**, 66 (Pt 2), 125–132.
- (248) Evans, P. R.; Murshudov, G. N. *Acta Crystallogr. D. Biol. Crystallogr.* **2013**, 69 (Pt 7), 1204–1214.
- (249) Winn, M. D.; Ballard, C. C.; Cowtan, K. D.; Dodson, E. J.; Emsley, P.; Evans, P. R.; Keegan, R. M.; Krissinel, E. B.; Leslie, A. G. W.; McCoy, A.; McNicholas, S. J.; Murshudov, G. N.; Pannu, N. S.; Potterton, E. A.; Powell, H. R.; Read, R. J.; Vagin, A.; Wilson, K. S. *Acta Crystallogr. D. Biol. Crystallogr.* **2011**, 67 (Pt 4), 235–242.
- (250) Murshudov, G. N.; Vagin, A. A.; Dodson, E. J. *Acta Crystallogr. D. Biol. Crystallogr.* **1997**, 53 (Pt 3), 240–255.
- (251) Emsley, P.; Cowtan, K. *Acta Crystallogr. Sect. D Biol. Crystallogr.* **2004**, 60

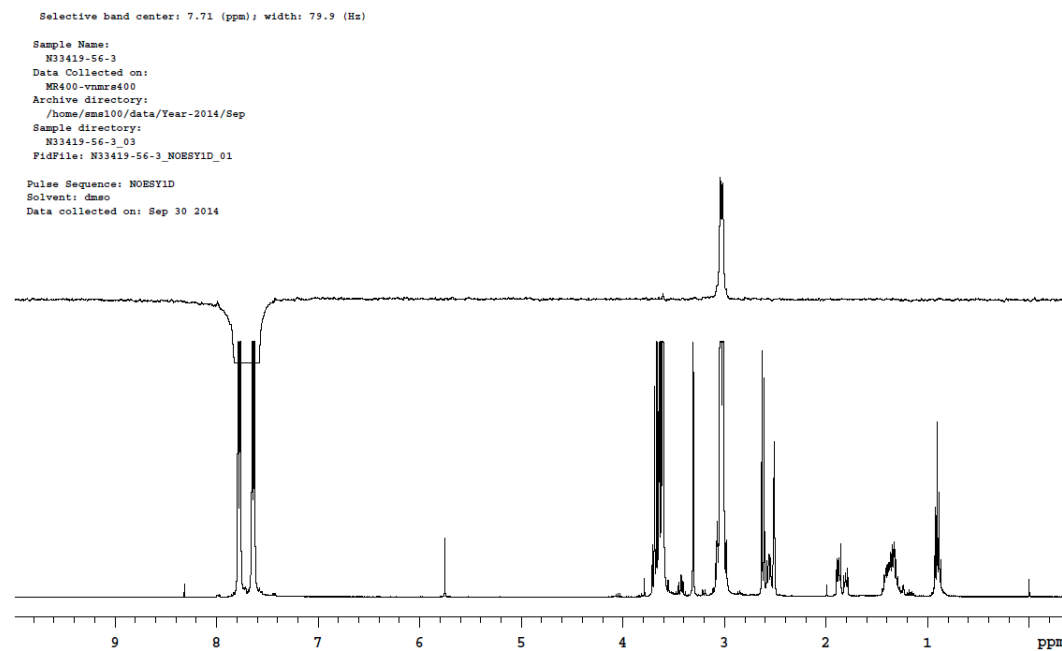
(12), 2126–2132.

10.0 Appendix

3.1.12 1D NOESY

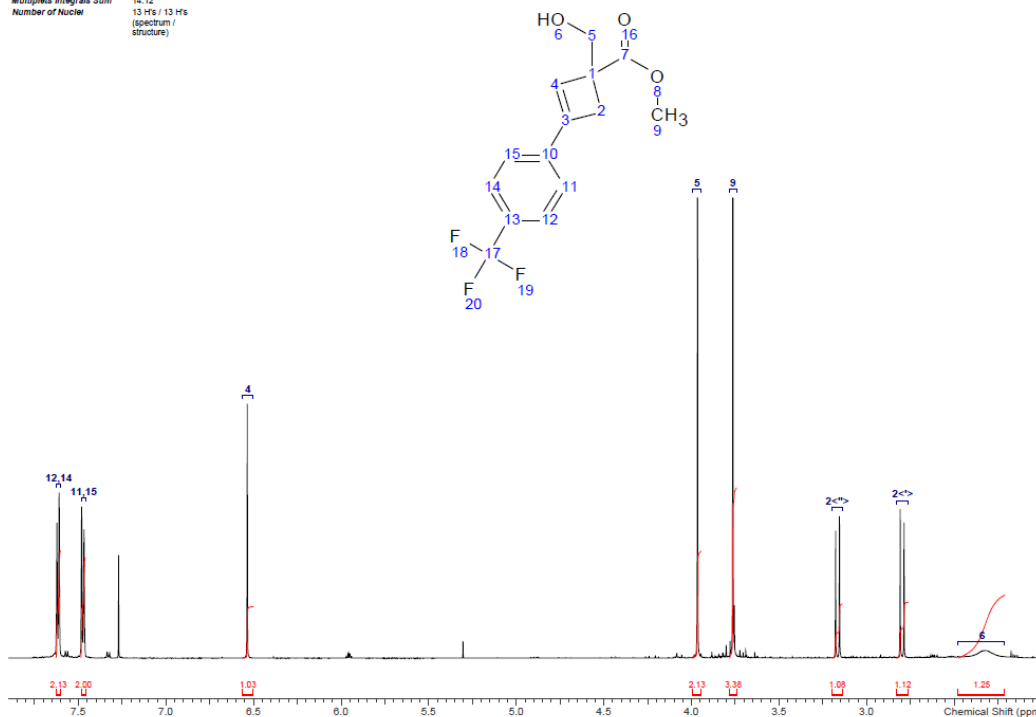


3.1.13 1D NOESY



3.1.14 ¹H

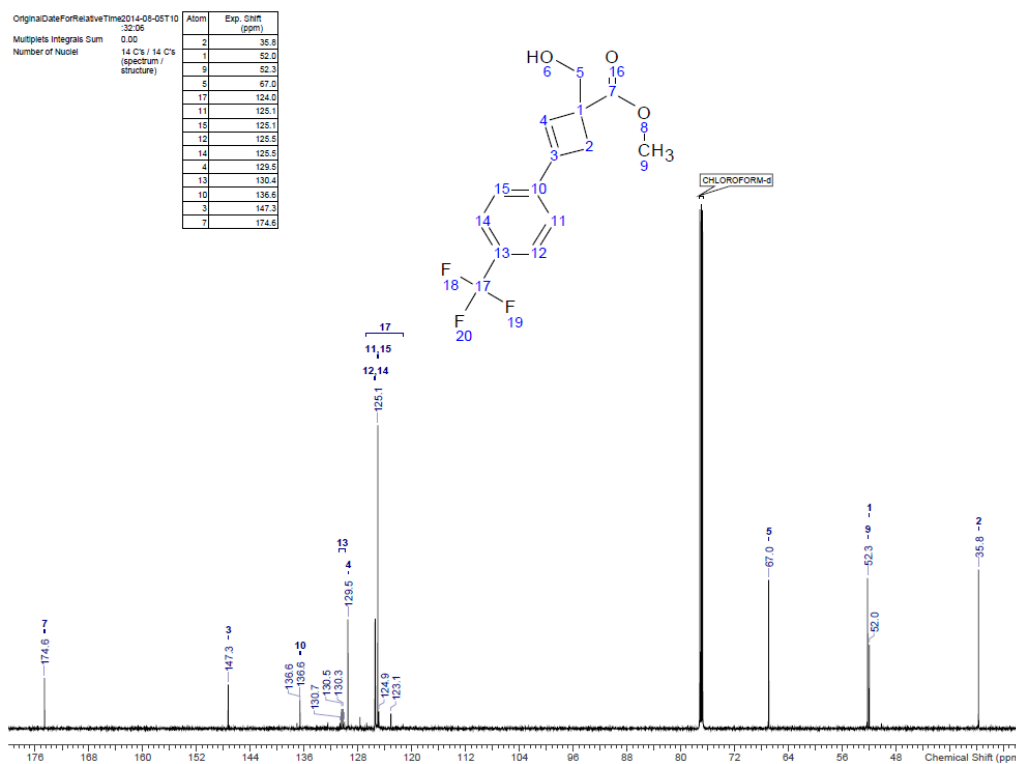
OriginalDateForRelativeTime 2014-08-05T10:32:36
 Multiplets Integrals Sum 14.12
 Number of Nuclei 13 H's / 13 H's
 (Spectrum / Structure)



¹H NMR (CHLOROFORM-d, 600MHz): δ (ppm) 7.62 (d, $J=8.1$ Hz, 2H, (H-12, 14)), 7.47 (d, $J=8.1$ Hz, 2H, (H-11, 15)), 6.54 (s, 1H, (H-4)), 3.97 (s, 2H, (H-5)), 3.76 (s, 3H, (H-9)), 3.17 (d, $J=13.0$ Hz, 1H, (H-2^{exo})), 2.80 (d, $J=13.0$ Hz, 1H, (H-2^{endo})), 2.32 (br s, 1H, (H-6))

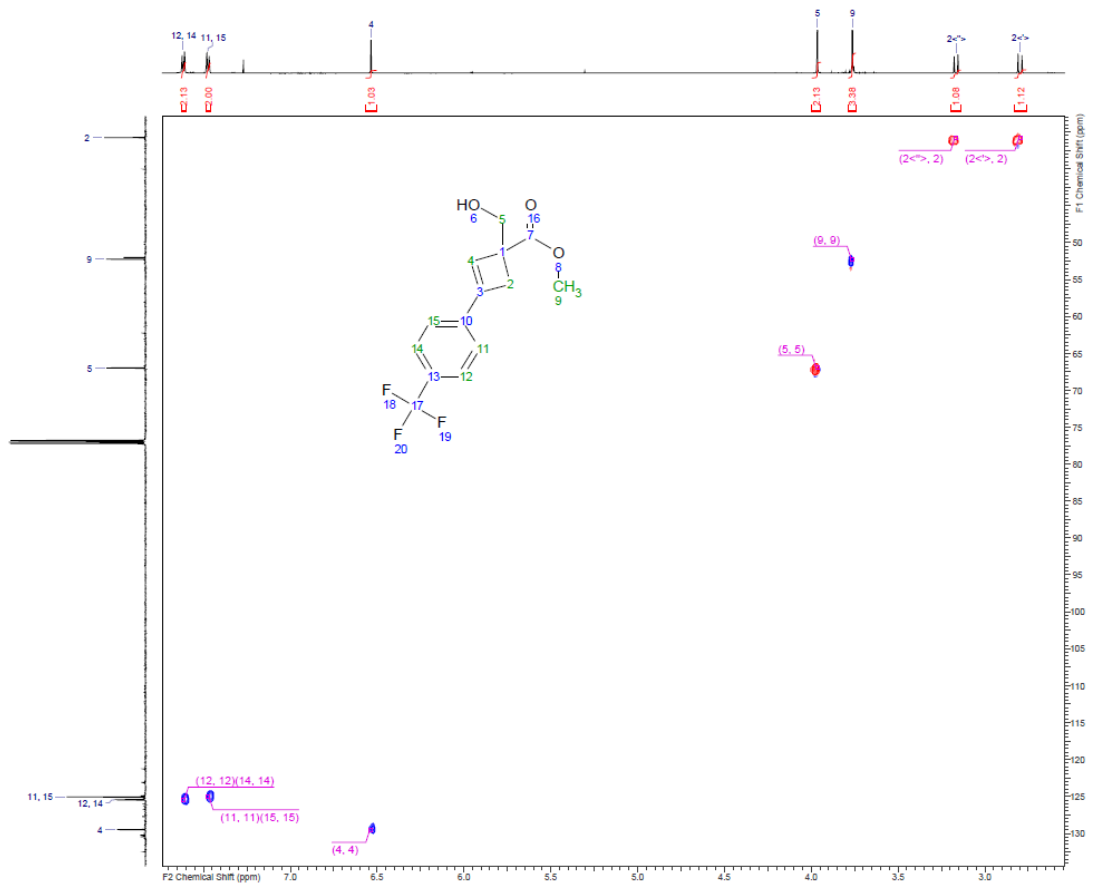
3.1.14 ¹³C

OriginalDateForRelativeTime 2014-08-05T10:32:36
 Multiplets Integrals Sum 0.00
 Number of Nuclei 14 C's / 14 C's
 (Spectrum / Structure)

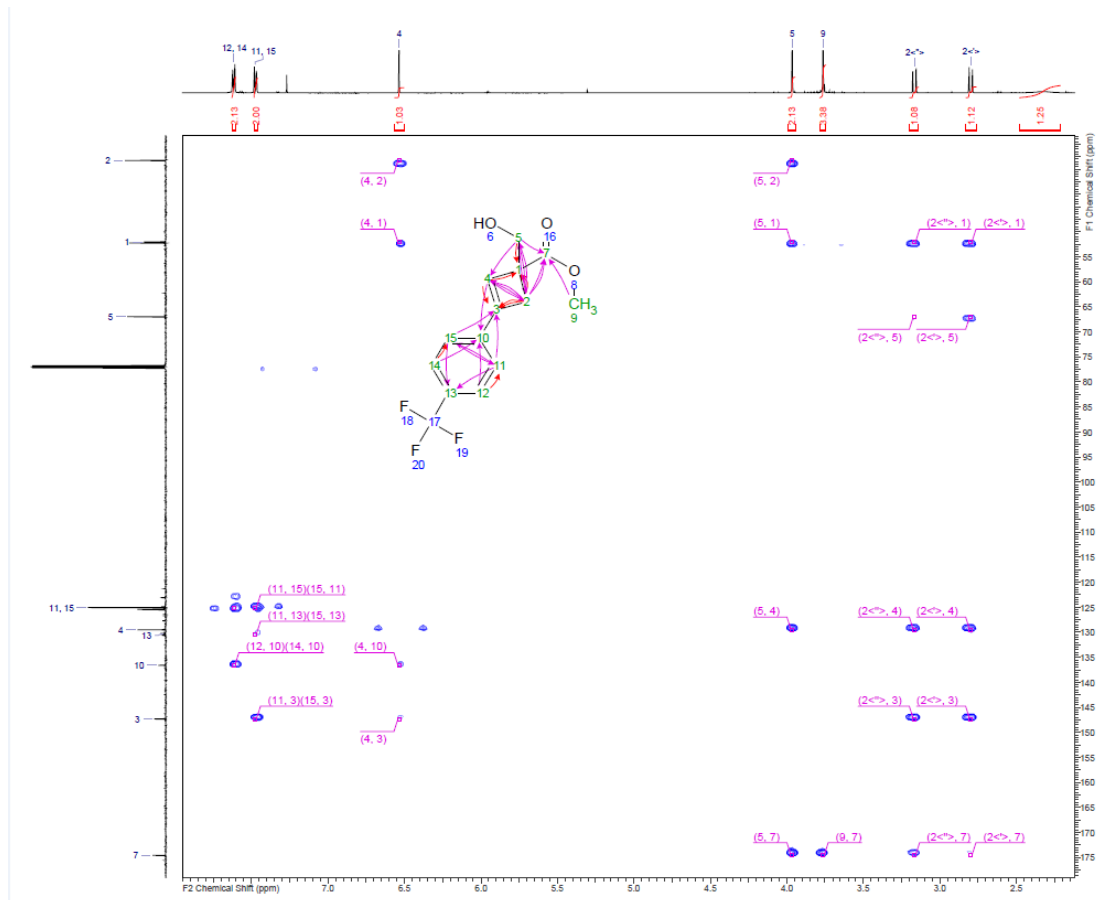


¹³C NMR (CHLOROFORM-d, 151MHz): δ (ppm) 174.6 (s, 1C, (C-7)), 147.3 (s, 1C, (C-3)), 136.6 (q, $J=1.7$ Hz, 1C, (C-10)), 130.4 (q, $J=32.6$ Hz, 1C, (C-13)), 129.5 (s, 1C, (C-4)), 125.5 (q, $J=3.9$ Hz, 2C, (C-12, 14)), 125.1 (s, 2C, (C-11, 15)), 124.0 (q, $J=272.0$ Hz, 1C, (C-17)), 67.0 (s, 1C, (C-5)), 52.3 (s, 1C, (C-9)), 52.0 (s, 1C, (C-1)), 35.8 (s, 1C, (C-2))

3.1.14 HSQC

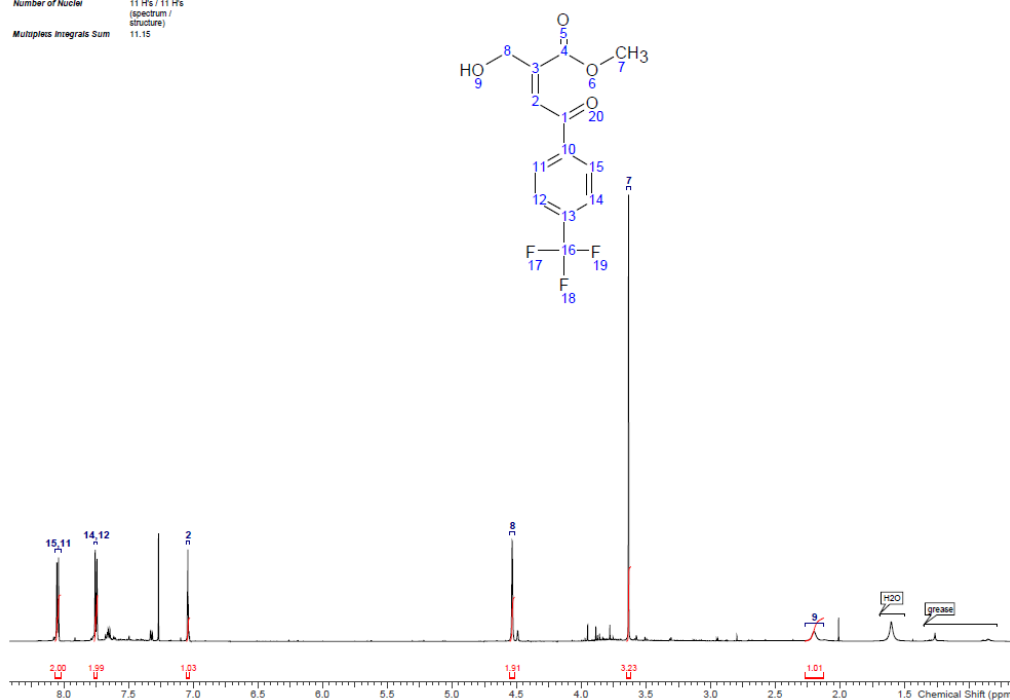


3.1.14 HMBC



3.1.15 ¹H

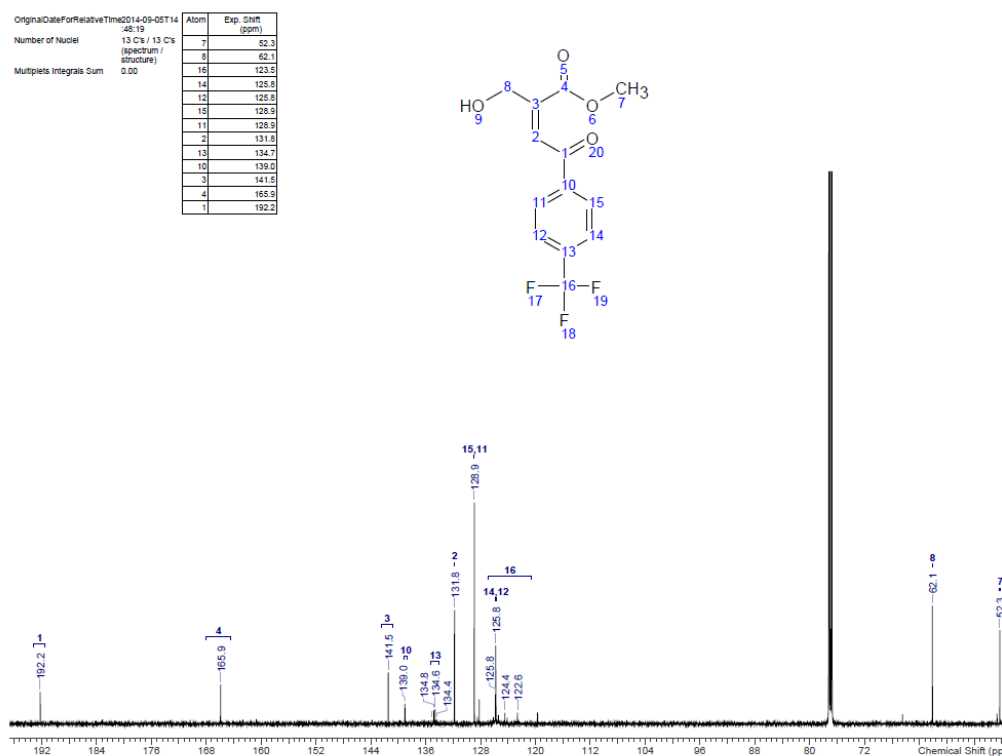
OriginalDateForRelativeTime 2014-09-05T14:45:37
 Number of Nuclei 11 Hs / 11 Hs (spectrum / structure)
 Multiplets Integrals Sum 11.15



¹H NMR (CHLOROFORM-d, 600MHz): δ (ppm) 8.05 (d, $J=8.1$ Hz, 2H, (H-15, 11)), 7.75 (d, $J=8.3$ Hz, 2H, (H-14, 12)), 7.04 (t, $J=1.7$ Hz, 1H, (H-2)), 4.53 (d, $J=1.7$ Hz, 2H, (H-8)), 3.63 (s, 3H, (H-7)), 2.20 (br s, 1H, (H-9))

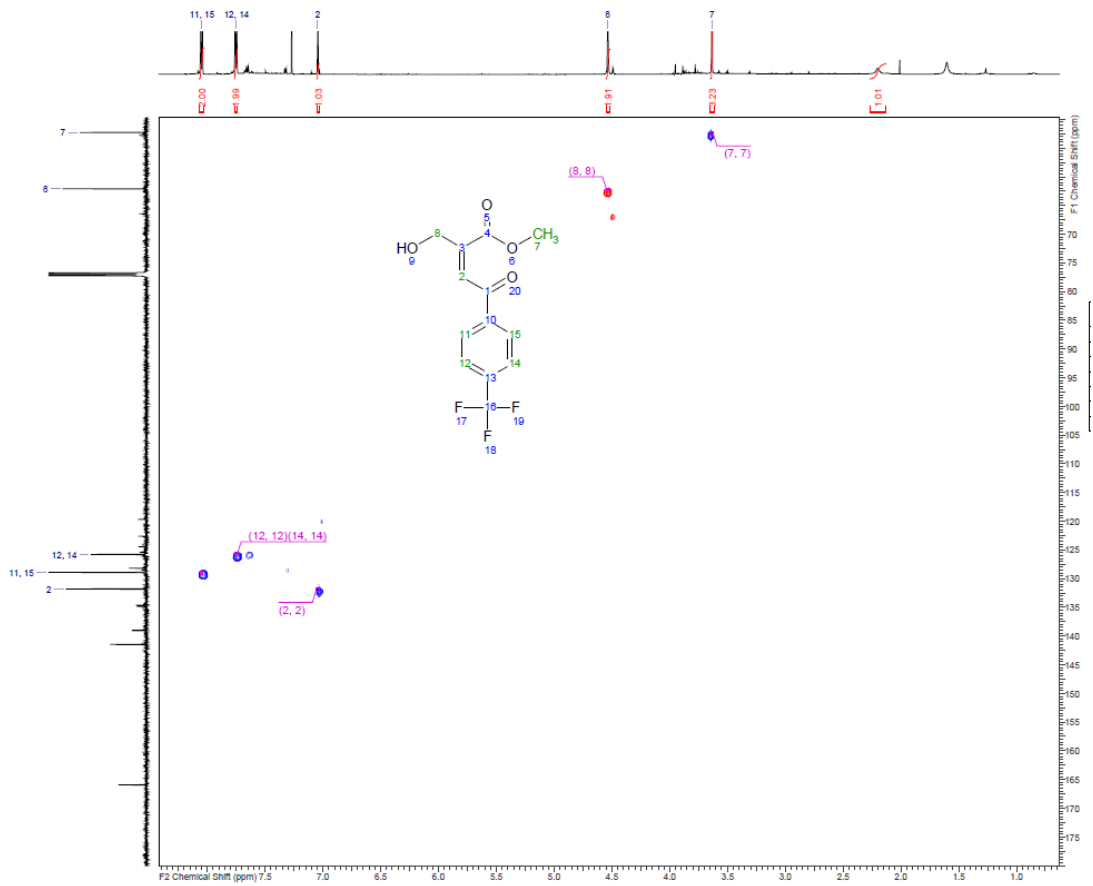
3.1.15 ¹³C

Atom	Exp. Shift (ppm)
7	52.3
8	62.1
16	123.5
14	125.8
12	125.8
15	125.9
11	125.9
3	131.8
13	134.7
10	139.0
3	141.5
4	165.9
1	192.2

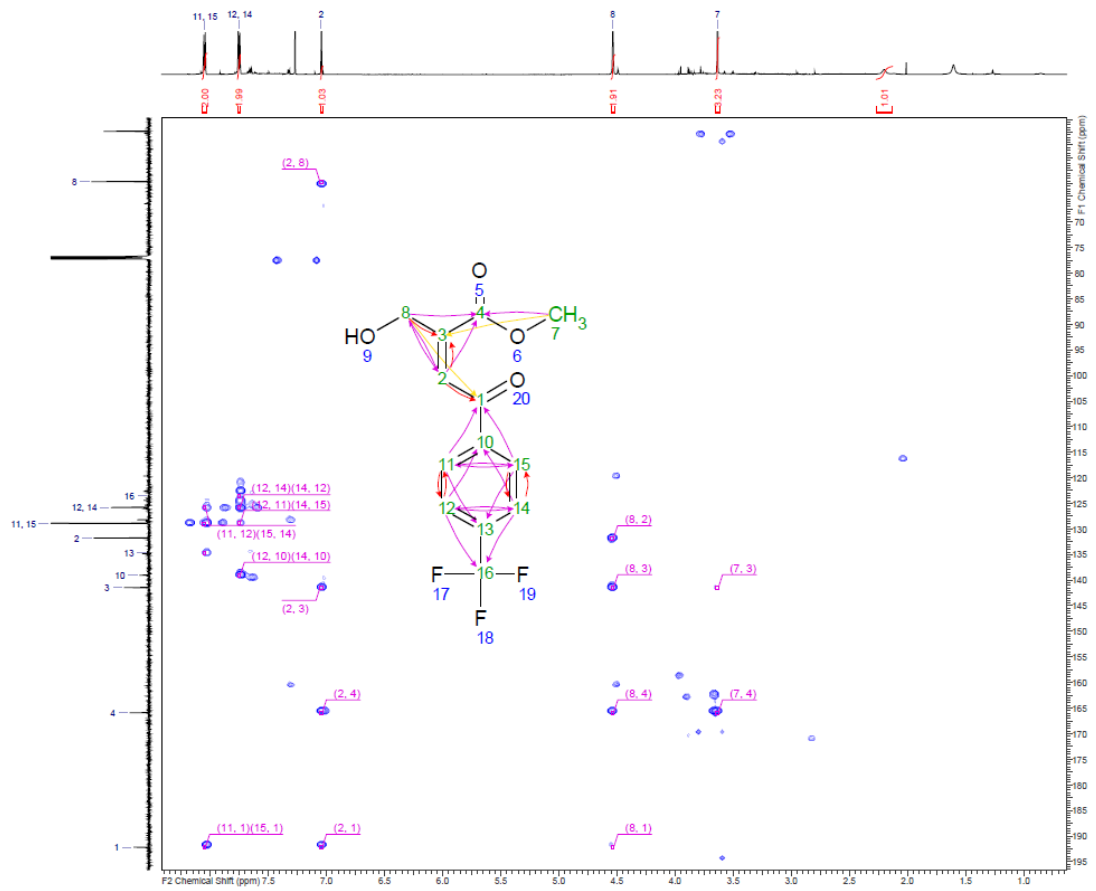


¹³C NMR (CHLOROFORM-d, 151MHz): δ (ppm) 192.2 (s, 1C, (C-1)), 165.9 (s, 1C, (C-4)), 141.5 (s, 1C, (C-3)), 139.0 (s, 1C, (C-10)), 134.7 (q, $J=32.6$ Hz, 1C, (C-13)), 131.8 (s, 1C, (C-2)), 128.9 (s, 2C, (C-15, 11)), 125.8 (q, $J=3.9$ Hz, 2C, (C-14, 12)), 123.5 (q, $J=272.8$ Hz, 1C, (C-16)), 62.1 (s, 1C, (C-8)), 52.3 (s, 1C, (C-7))

3.1.15 HSQC

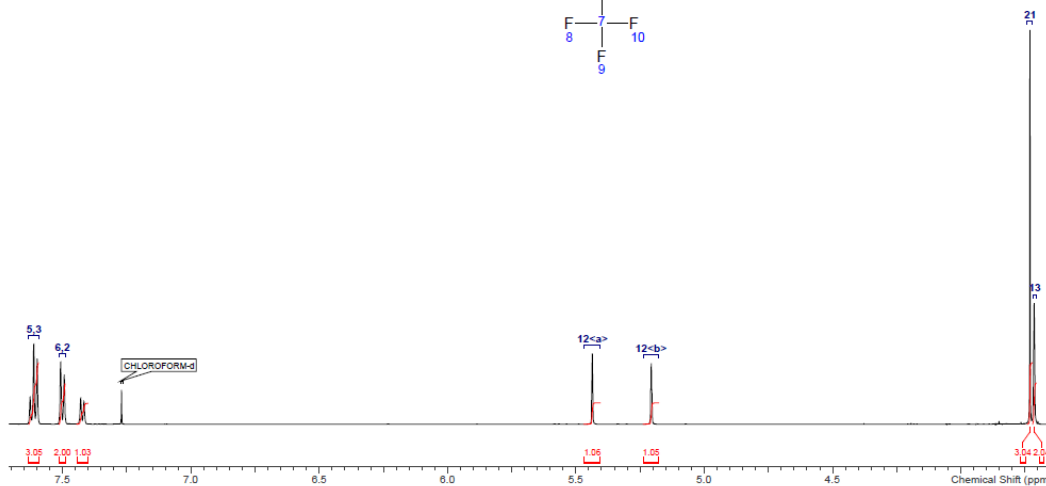
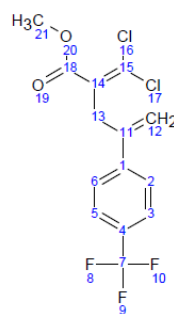


3.1.15 HMBC



3.1.19 ¹H

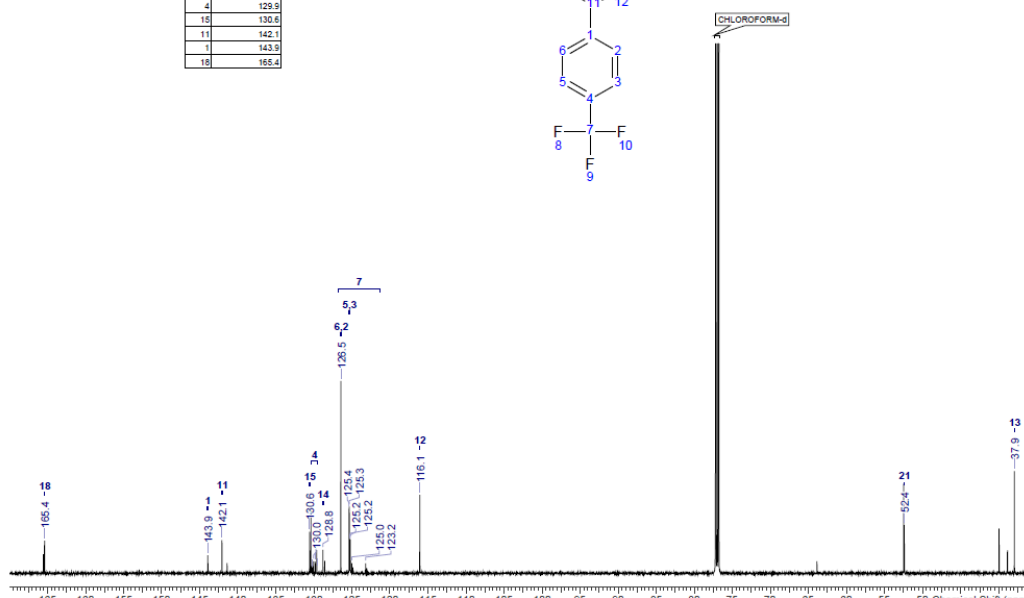
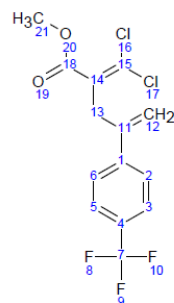
OriginalDateForRelativeTime 2014-11-28T13
2:47:32
Multiplets Integrals Sum
Number of Nuclei 11 Hs / 11 Hs
(spectrum /
structure)



¹H NMR (CHLOROFORM-d, 600MHz): δ (ppm) 7.59 - 7.63 (m, 2H, (H-5, 3)), 7.50 (d, $J=8.1$ Hz, 2H, (H-6, 2)), 5.44 (s, 1H, (H-12-a)), 5.21 (s, 1H, (H-12-b)), 3.73 (s, 3H, (H-21)), 3.71 (s, 2H, (H-13))

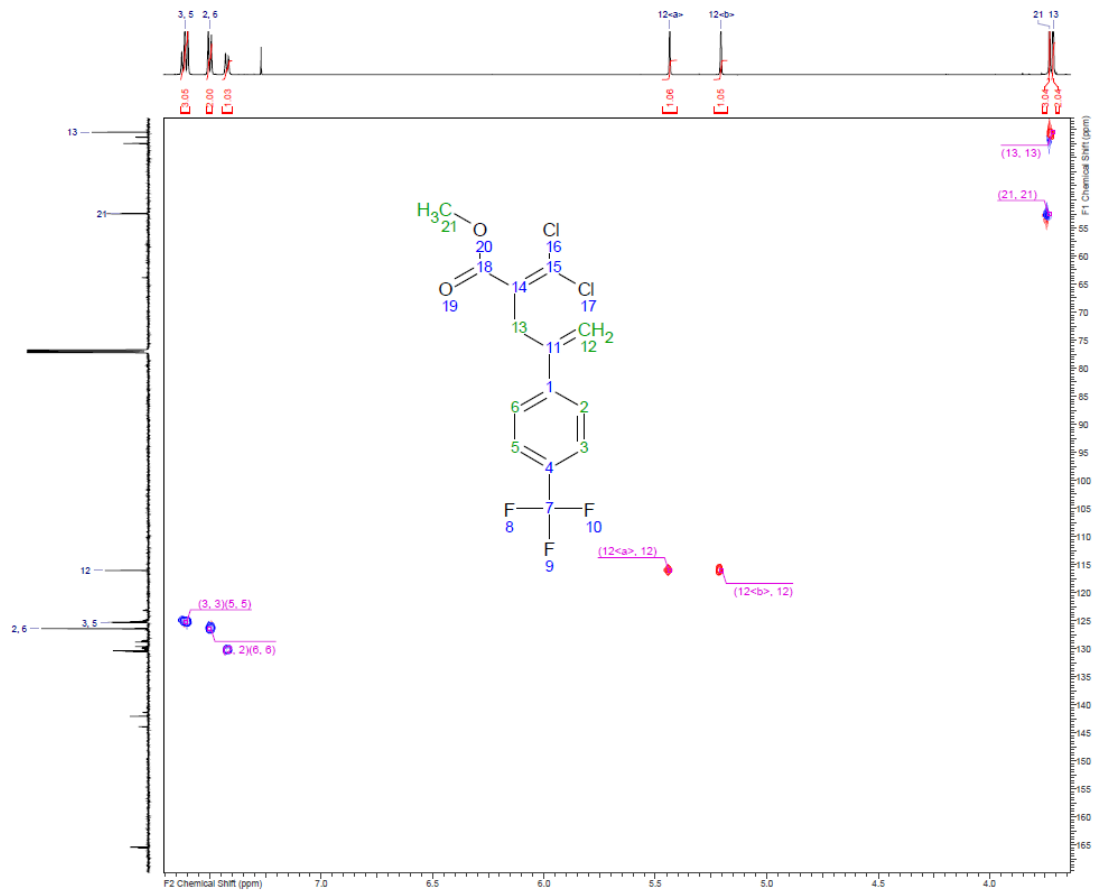
3.1.19 ¹³C

OriginalDateForRelativeTime 2014-11-28T13
11:01
Multiplets Integrals Sum
Number of Nuclei 14 Cs / 14 Cs
(spectrum /
structure)

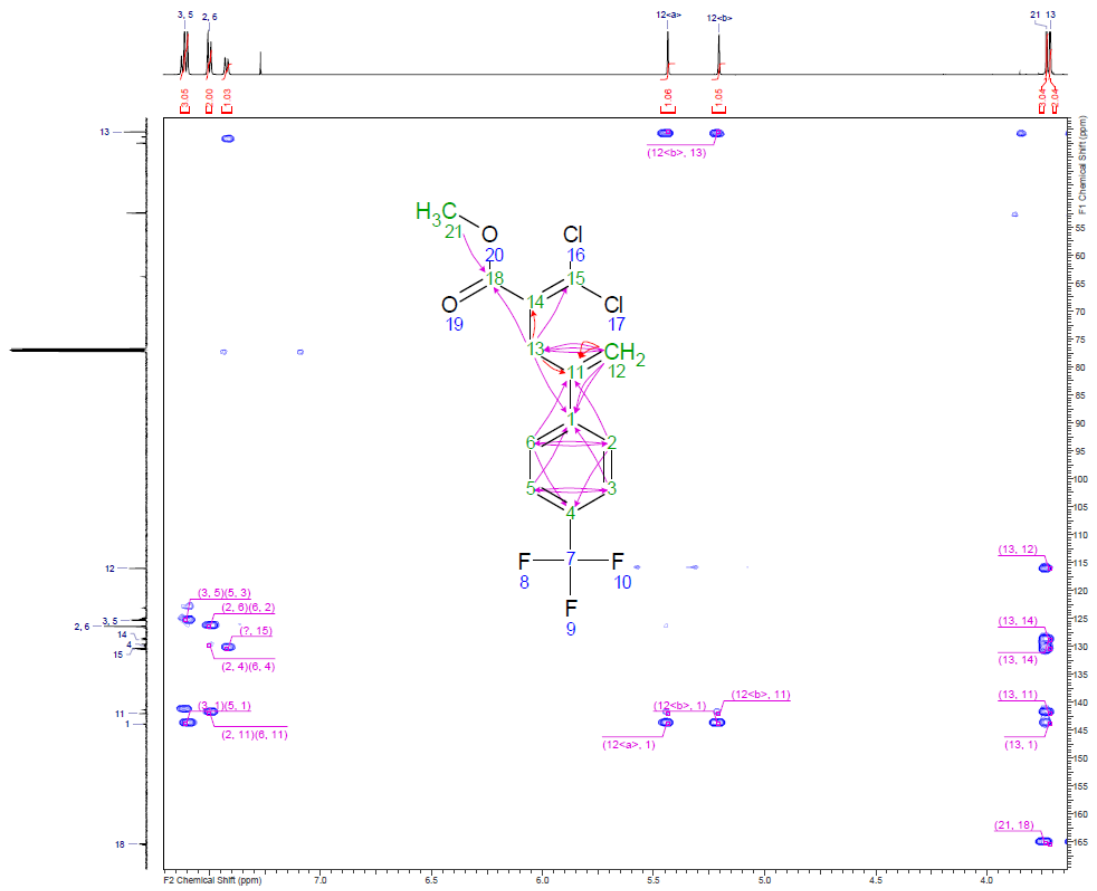


¹³C NMR (CHLOROFORM-d, 151MHz): δ (ppm) 165.4 (s, 1C, (C-18)), 143.9 (q, $J=1.1$ Hz, 1C, (C-1)), 142.1 (s, 1C, (C-11)), 130.6 (s, 1C, (C-15)), 129.9 (q, $J=32.4$ Hz, 1C, (C-4)), 128.8 (s, 1C, (C-14)), 126.5 (s, 2C, (C-6, 2)), 125.3 (q, $J=3.8$ Hz, 2C, (C-5, 3)), 124.1 (q, $J=272.0$ Hz, 1C, (C-7)), 116.1 (s, 1C, (C-12)), 52.4 (s, 1C, (C-21)), 37.9 (s, 1C, (C-13))

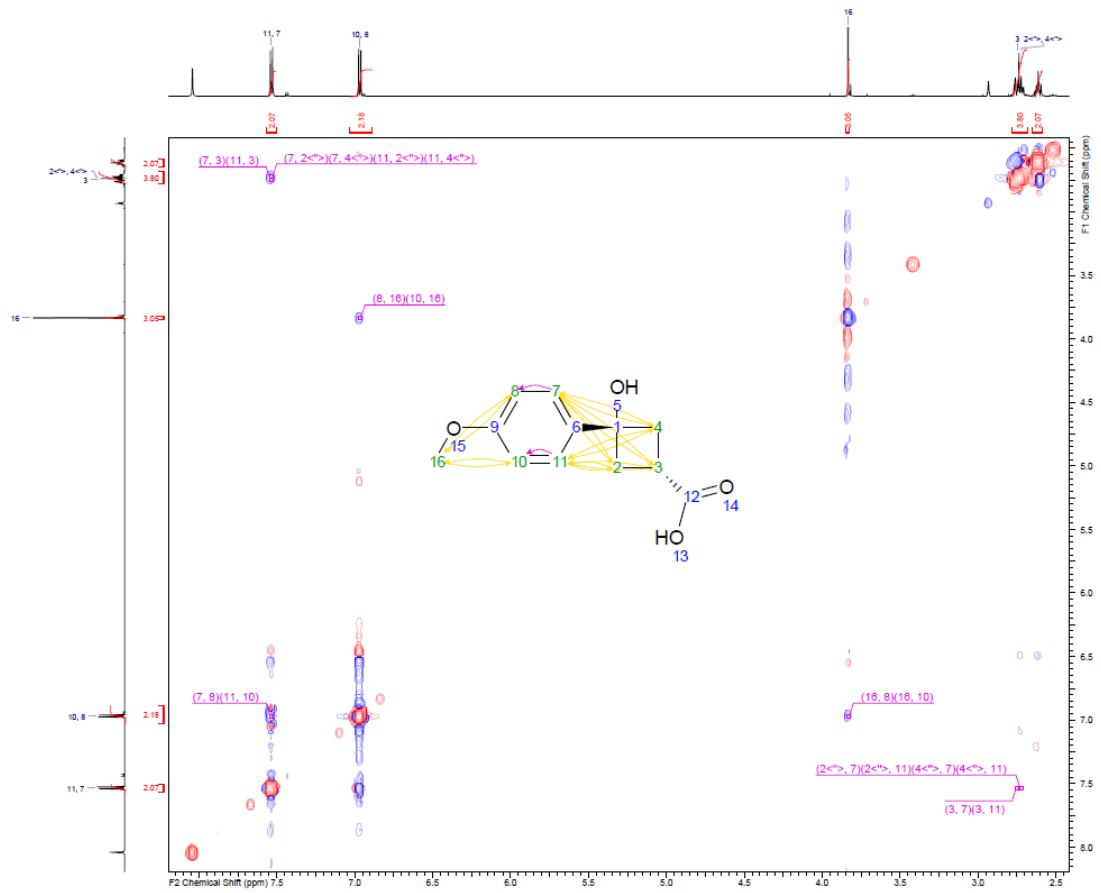
3.1.19 HSQC



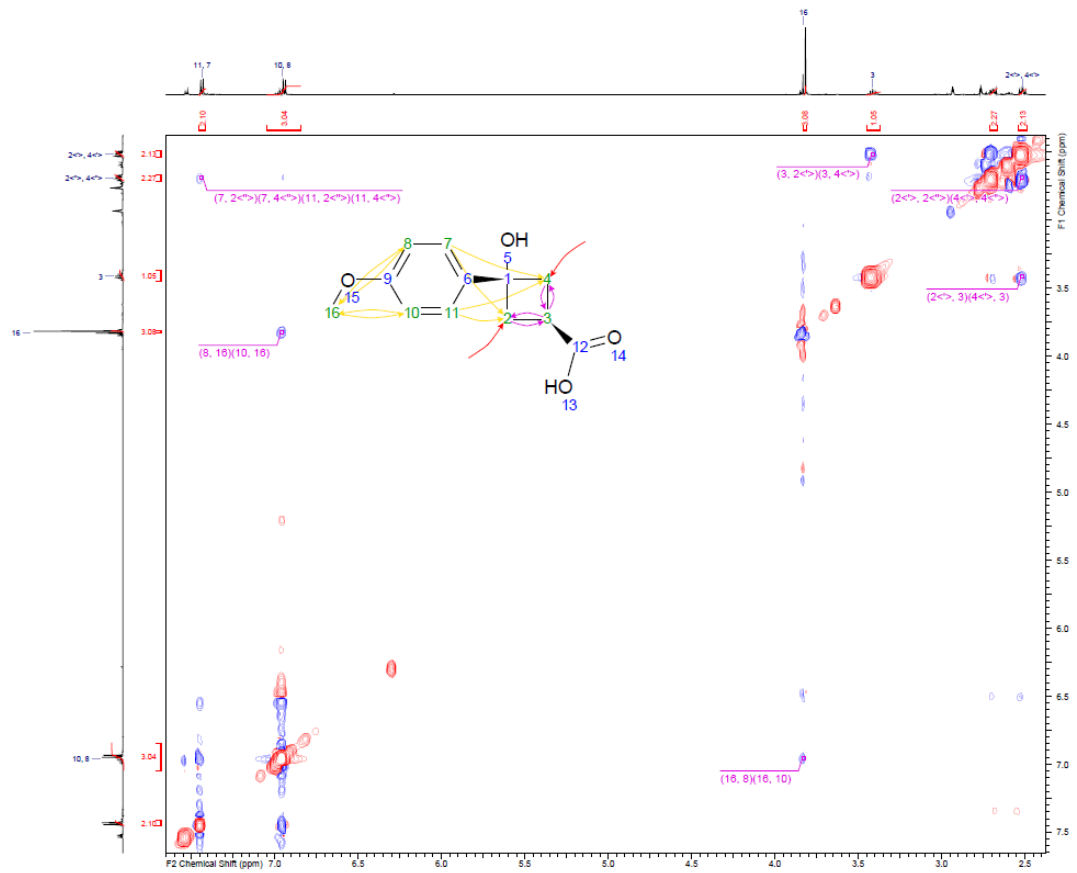
3.1.19 HMBC



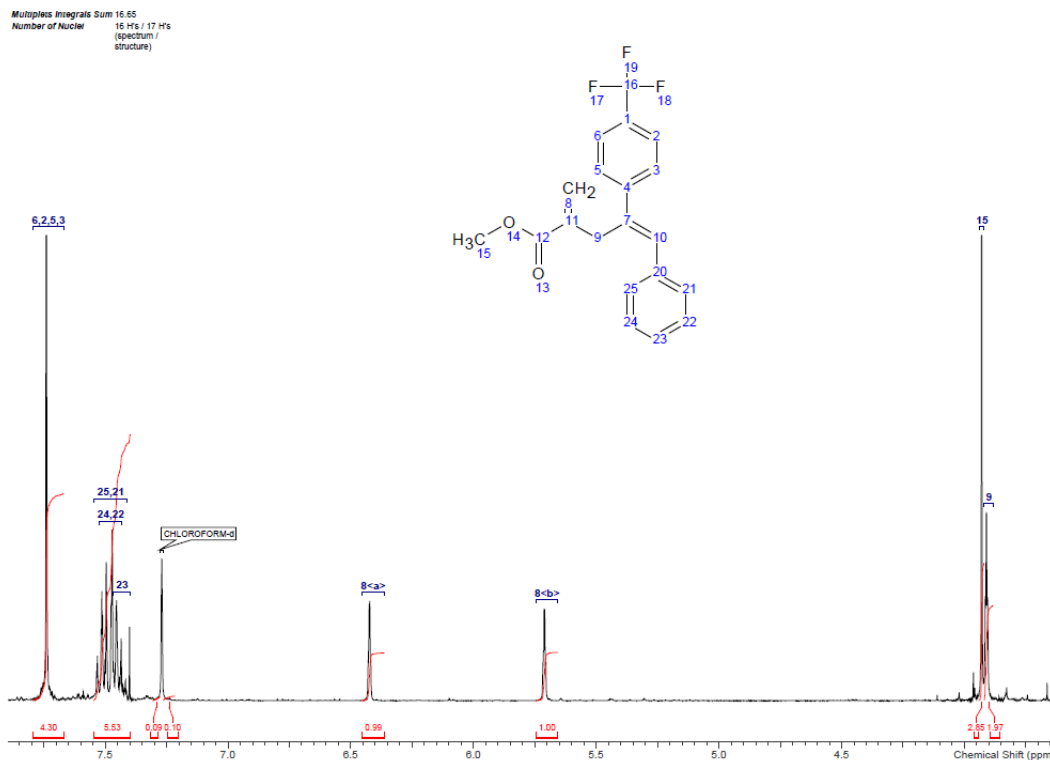
3.3.20 ROESY



3.3.21 ROESY

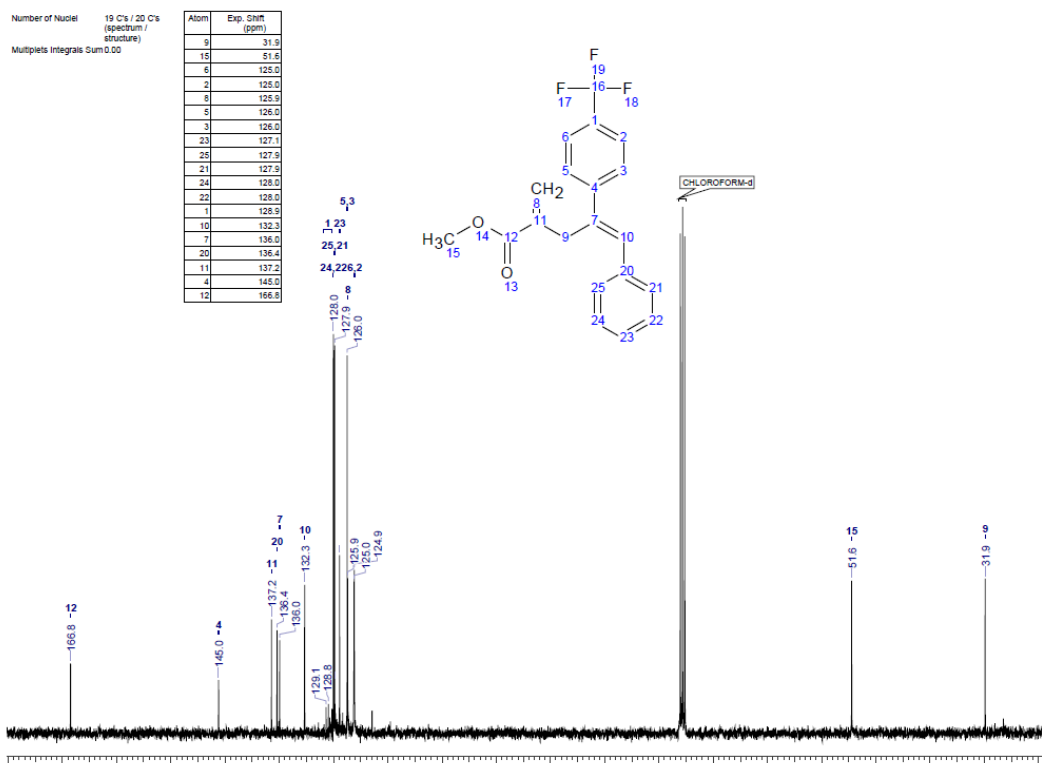


3.4.2 ¹H



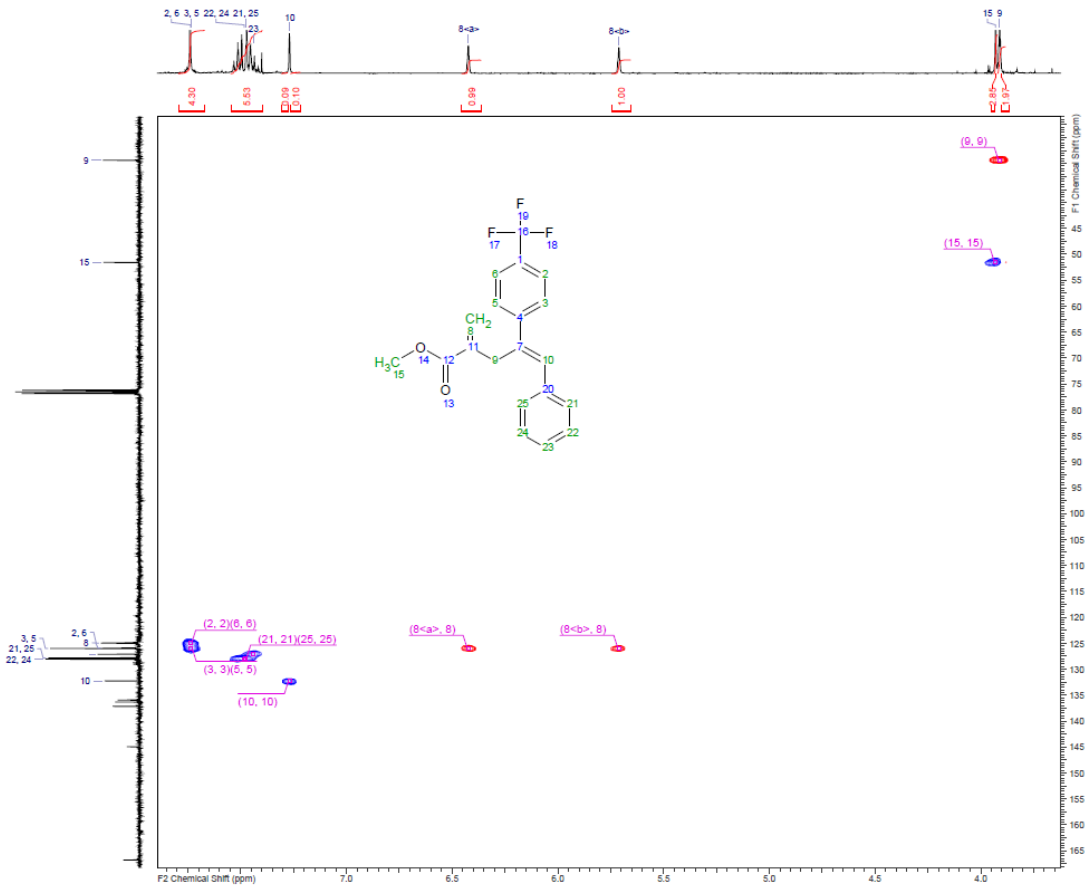
¹H NMR (CHLOROFORM-d, 400MHz): δ (ppm) 7.74 (s, 4H, (H-6, 2, 5, 3)), 7.43 - 7.53 (m, 2H, (H-24, 22)), 7.41 - 7.55 (m, 2H, (H-25, 21)), 7.40 - 7.47 (m, 1H, (H-23)), 6.42 (d, *J*=1.0 Hz, 1H, (H-8-a->)), 5.66 - 5.74 (m, 1H, (H-8-b->)), 3.93 (s, 3H, (H-15)), 3.91 (t, *J*=1.6 Hz, 2H, (H-9))

3.4.2 ¹³C

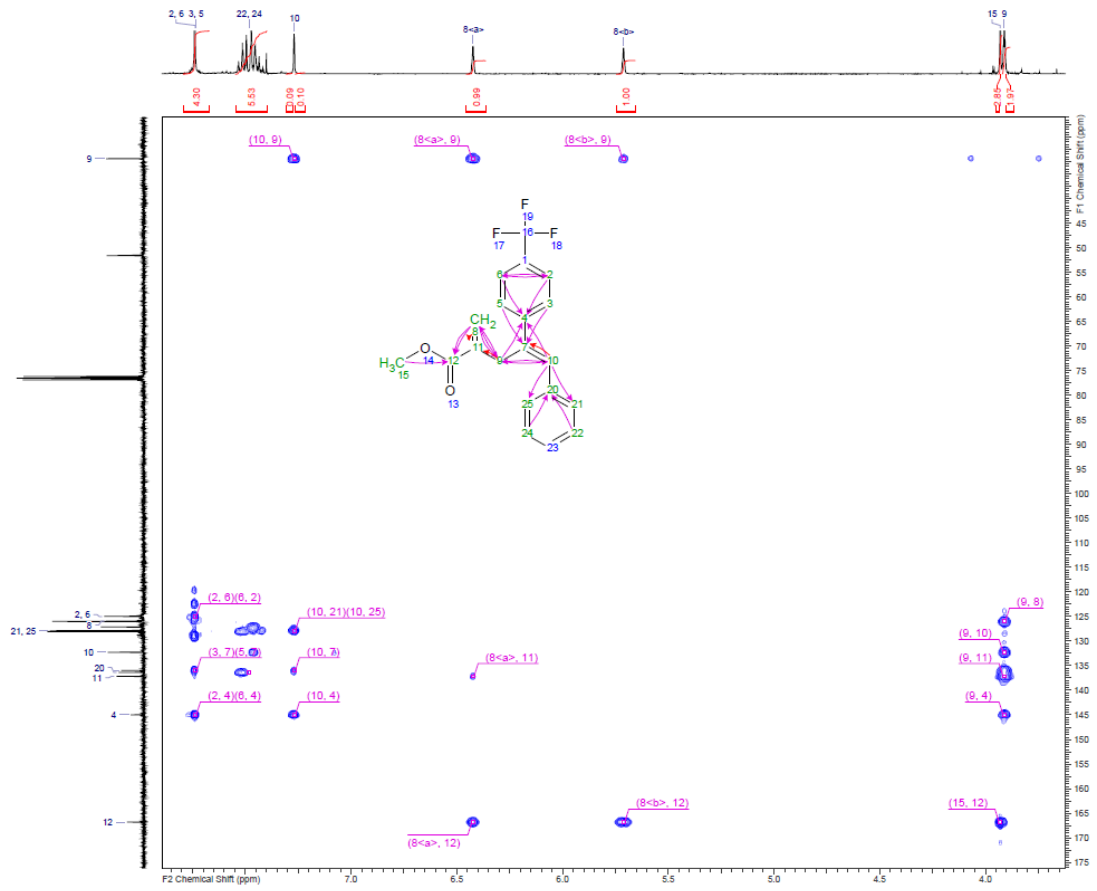


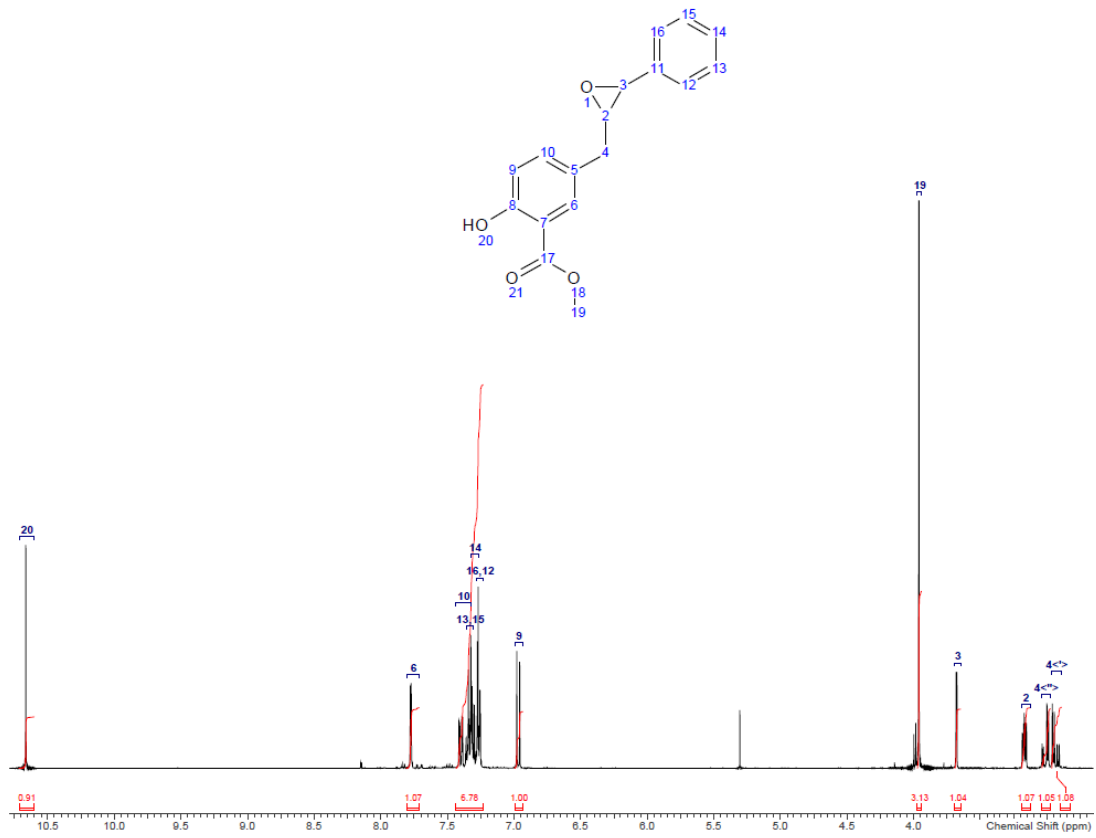
¹³C NMR (CHLOROFORM-d, 101MHz): δ (ppm) 166.8 (s, 1C, (C-12)), 145.0 (s, 1C, (C-4)), 137.2 (s, 1C, (C-11)), 136.4 (s, 1C, (C-20)), 136.0 (s, 1C, (C-7)), 132.3 (s, 1C, (C-10)), 128.9 (q, *J*=32.0 Hz, 1C, (C-1)), 128.0 (s, 2C, (C-24, 22)), 127.9 (s, 2C, (C-25, 21)), 127.1 (s, 1C, (C-23)), 126.0 (s, 2C, (C-5, 3)), 125.9 (s, 1C, (C-8)), 125.0 (q, *J*=3.4 Hz, 2C, (C-6, 2)), 51.6 (s, 1C, (C-15)), 31.9 (s, 1C, (C-9))

3.4.2 HSQC

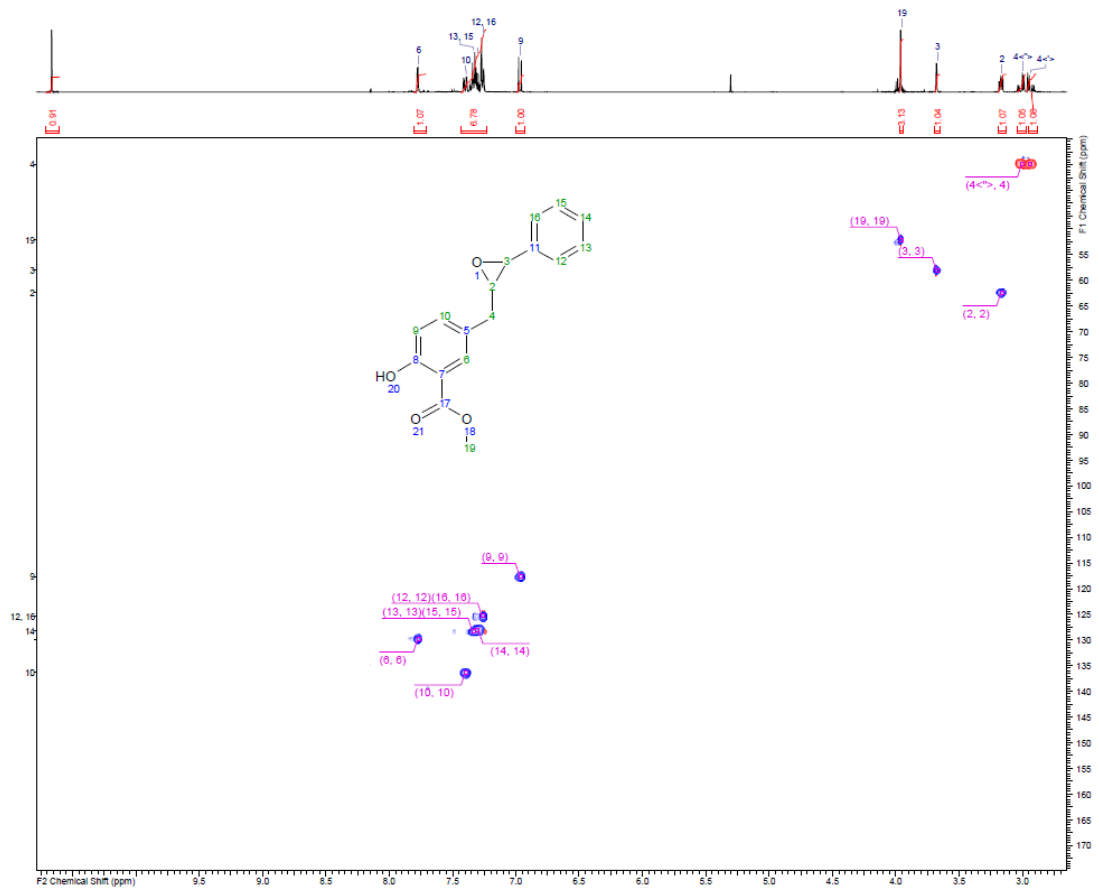


3.4.2 HMBC

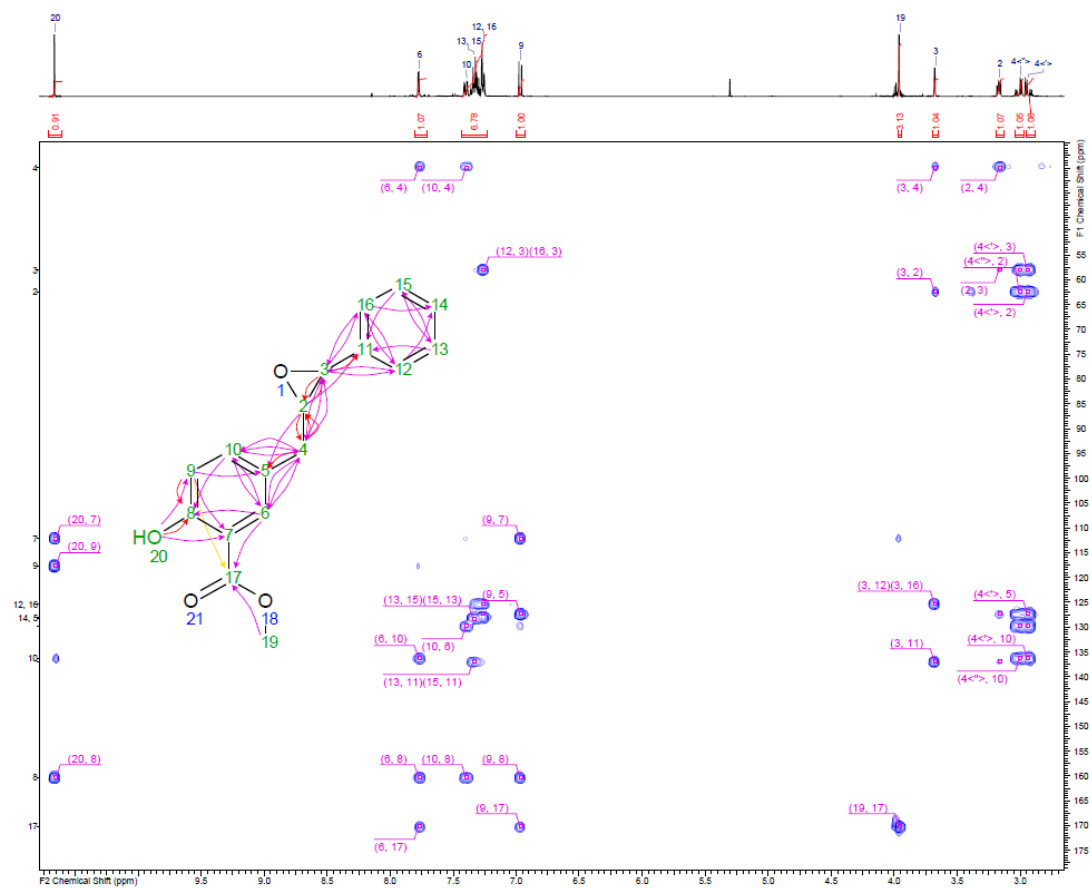


5.1.34 ^1H 

5.1.34 HSQC

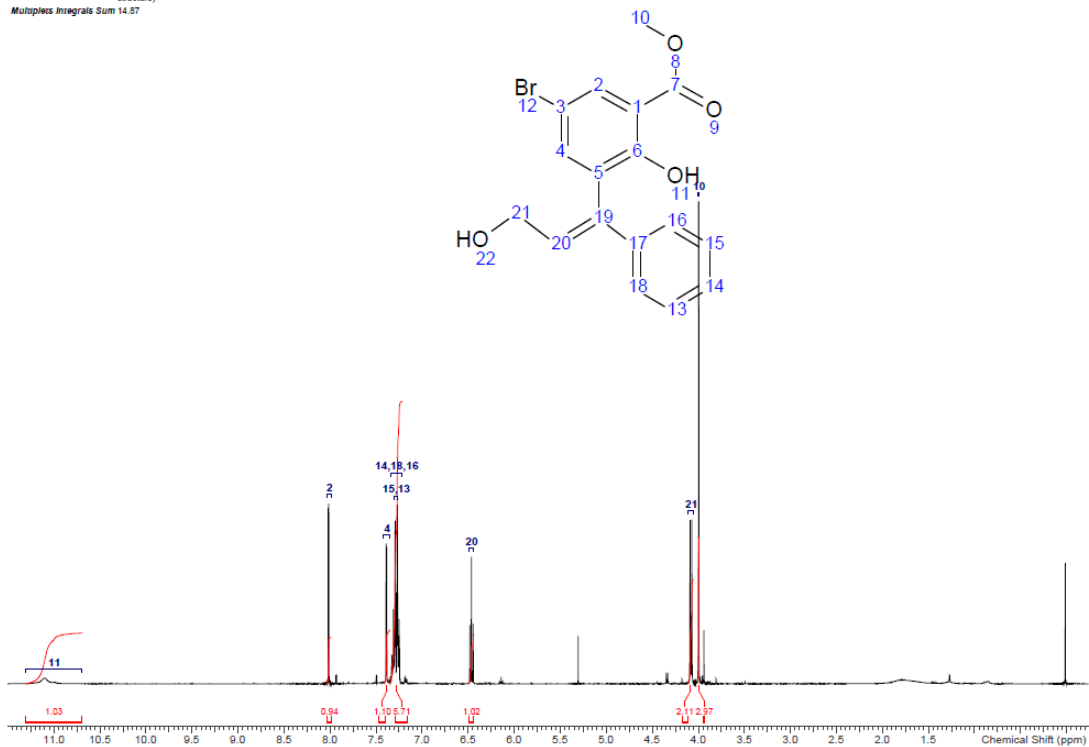


5.1.34 HMBC



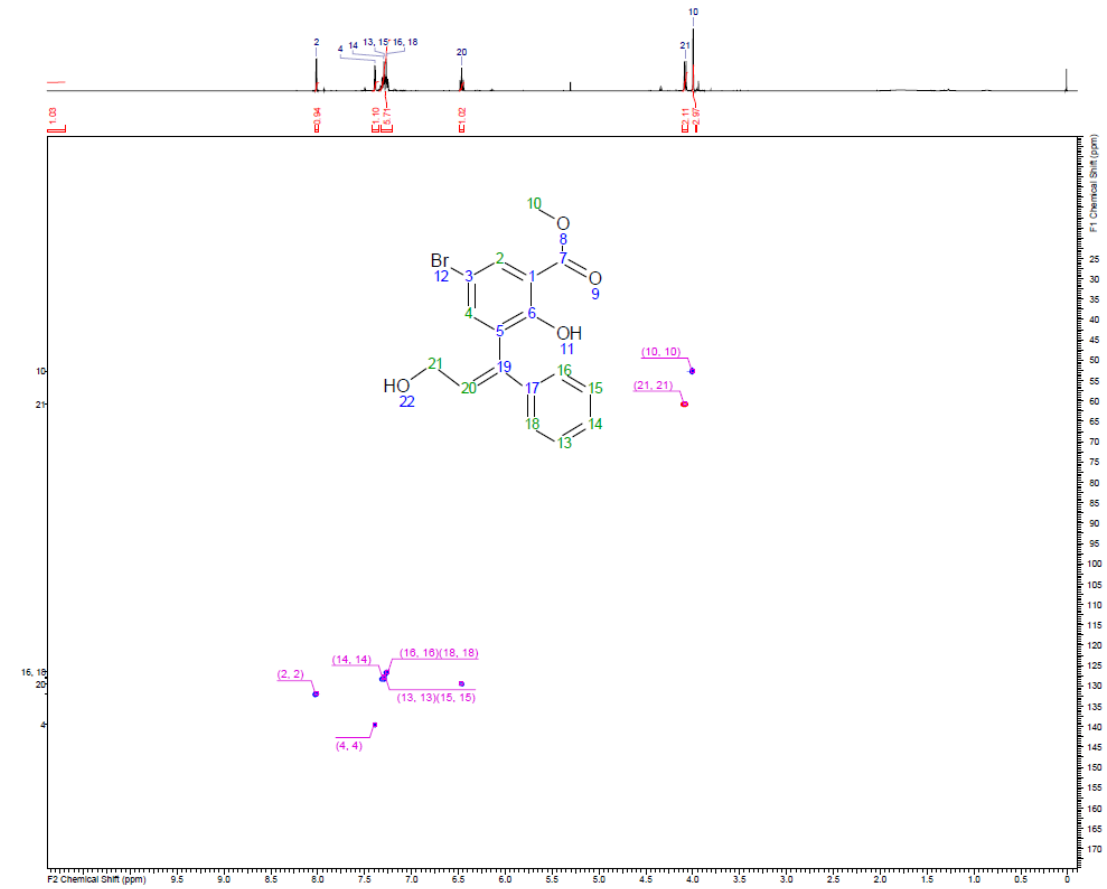
5.1.35 ^1H

Number of Nuclei 14 H's / 15 H's
(spectrum /
structure)
Multiplex Integrals Sum 14.87

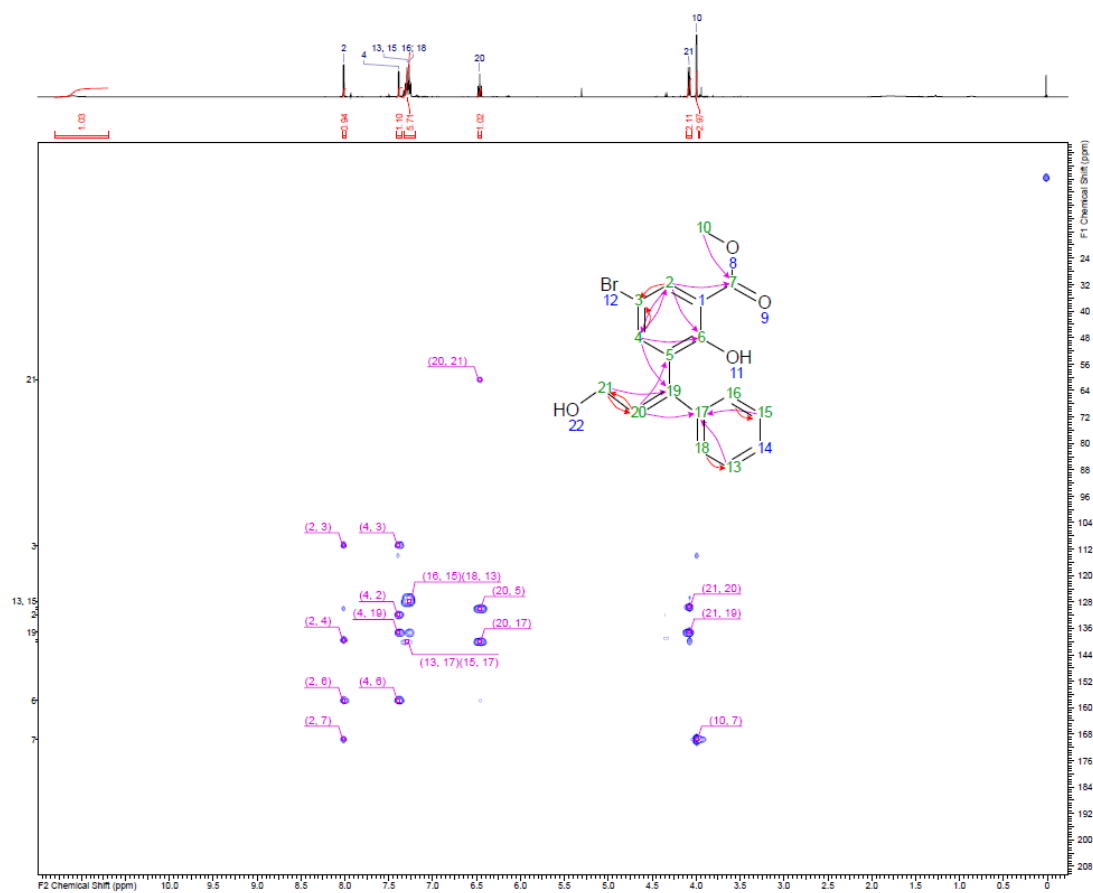


^1H NMR (CHLOROFORM- d , 400MHz): d (ppm) 11.10 (br s, 1H, (H-11)), 8.02 (d, $J=2.6$ Hz, 1H, (H-2)), 7.39 (d, $J=2.6$ Hz, 1H, (H-4)), 7.22 - 7.35 (m, 3H, (H-14, 18, 16)), 6.46 (t, $J=7.2$ Hz, 1H, (H-20)), 4.08 (d, $J=7.2$ Hz, 2H, (H-21)), 4.00 (s, 3H, (H-10))

5.1.35 HSQC

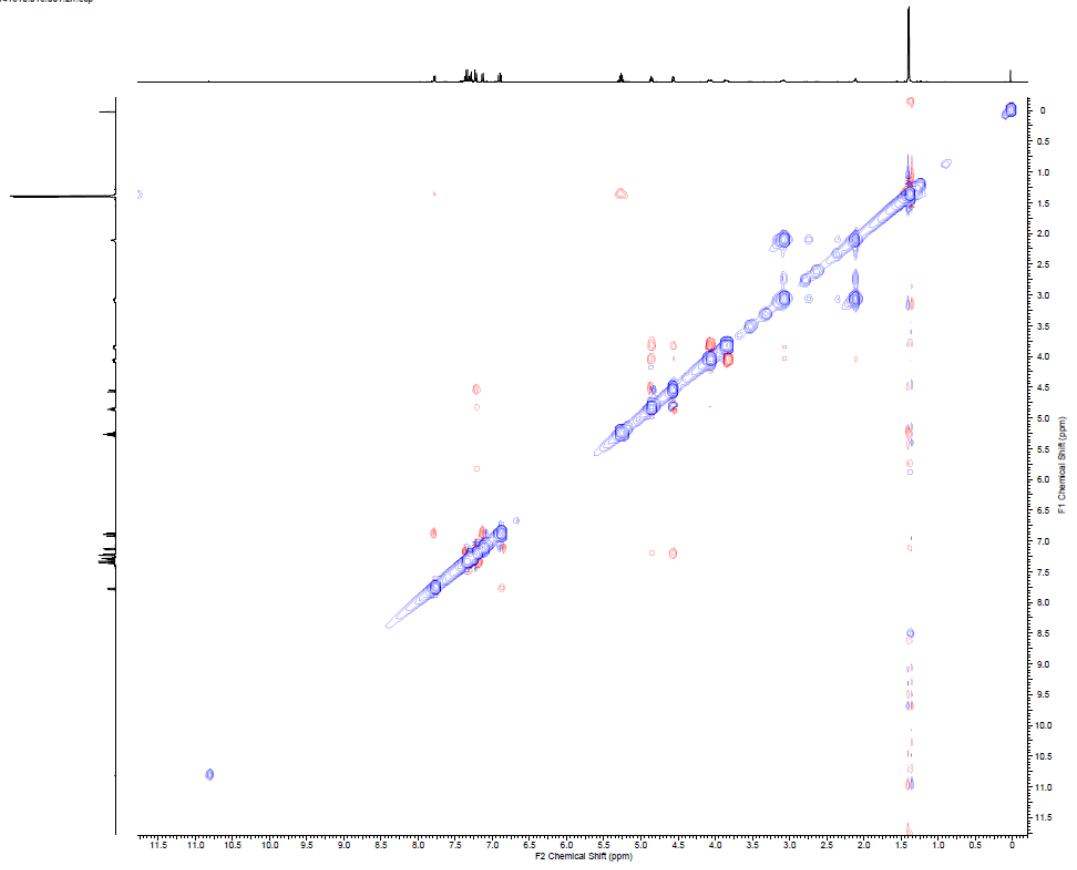


5.1.35 HMBC



5.1.55 ROESY

M141510.015.001.2tr.esp



5.1.56 ROESY

